Membrane – Solute – Cleaning agent interaction during the ultrafiltration of black tea liquor

Evans, Philip

Award date:
2008

Awarding institution:
University of Bath

Membrane – Solute – Cleaning agent interaction during the ultrafiltration of black tea liquor

Submitted by Philip John Evans

For the degree of Ph.D

At the University of Bath
Department of Chemical Engineering

April 2008

Acknowledgements

Dr Mike Bird, my supervisor has always been extremely approachable, helpful and generous with his time throughout my studies here in Bath. I would like to thank you for your strong support and inspiration during my time here.

The chemical engineering department has greatly aided the development of my project. Without the help of the technicians Fernando, Richard, Robert, Merv and Olivier, my work here would have been very difficult, I would like to thank them for their continued friendliness and abilities to transfer ideas into a reality. I would also like to thank Dan Wu for all her help and advice throughout the project.

I would like to thank Dr's Jacek Obuchowicz and Francois-Xavier Pierre of *Unilever R&D Colworth* for their invaluable help and guidance with this project. I also thank *Unilever R&D Colworth* for supplying the tea powders used in experimentation and for their help in carrying out the FTIR and HPLC analyses.

I would also like to thank Dr Frank Lipnizki of *Alfa Laval Copenhagen* for the generous donation of fluoropolymer membranes and Dr Jens Lipnizki of *Microdyn Nadir* for the kind donation of regenerated cellulose membranes.

A big thanks goes to Professor. Marianne Nyström and Dr Arto Pihlajamäki for allowing me to visit Lappeenranta University of Technology, Finalnd, to perform numerous zeta potential experiments and contact angle measurements. They provided a warm welcome, even during the freezing winter months.

I would like to thank Dr Chris Wright and Dale Rogers from the chemical engineering department at Swansea University for allowing me to return to sunny Wales to perform atomic force microscope work.

I am also grateful to Dr Tom Arnot and Dr Robert Field for all their help and advice regarding the flux decline modelling work.

I am very thankful to my colleagues, Ian "fluffy" Benzeval, Ian "crouch" Gillard and Chris "has to be real coffee" Campbell for all their help, advice and amusing discussions during my time in the postgrad room.

Finally, I would like to thank *Unilever R&D Colworth* and the BBSRC for providing financial support.

Abstract

Ultrafiltration technology has been successfully demonstrated in ready to drink (RTD) tea processing to yield beverages with a significantly reduced degree of haze. This study reports experimental results concerning the ultrafiltration of hot tea extract reconstituted from tea powder using regenerated cellulose (RC) and fluoropolymer (FP) membrane materials.

The work described in this thesis can be split into four distinctive parts; filtration (fouling) optimisation, cleaning optimisation, membrane surface science and foulant adhesion investigations.

Specific fouling resistances, apparent membrane rejections and cleaning efficiencies were analysed for variations in feed concentration, transmembrane pressure (TMP), temperature, ionic-strength and calcium content.

Concentration polarisation contributed predominantly to the increased total fouling resistance of both membranes as feed concentration was increased, although there was no extra effect upon deposit formation on the RC membrane, whereas rinsable fouling deposit did increase on the FP membrane due to slightly stronger interaction of foulant with the membrane surface.

Increasing the ionic strength increased the total fouling resistance, thus reducing performance, while decreasing the severity of deposition fouling due to increased concentration polarisation. Addition of calcium to the feed stream caused a significant increase in irreversible fouling deposition due to polar group - calcium complexation (bridging). This deposition could not be adequately removed using standard sodium hydroxide cleaning protocols, or by the addition of surfactants and chelating agents.

The optimum cleaning conditions for the FP membrane were found to be: 0.5 wt% NaOH, 60°C feed temperature, 0.5 bar TMP and 1.15ms^{-1} cross-flow velocity (CFV). The optimum cleaning conditions for the RC membrane were found to be: 0.01wt% NaOH, 45°C feed temperature, 0.5 bar TMP and 1.15ms^{-1} cross flow velocity. These results will increase the efficiency of cleaning processes by reducing cleaning times, chemical waste and the energy consumption required during black tea ultrafiltration.

Experiments were concentrated on two main materials (i) regenerated cellulose (RC) and (ii) fluoropolymer (FP) membranes of different nominal molar mass cut-off values were investigated. Changes during filtration in the hydrophobicity, surface charge on the pore walls, surface roughness and chemical properties were investigated. Results indicate that both of the membrane materials studied produced clarified tea liquors with polyphenol transmission rates of *ca* 90%.

Increased fouling was present on rougher, more hydrophobic FP surfaces. When roughness, charge and hydrophobicity were similar (i.e. for the RC membrane), variation in pore size was not found to affect the filtration properties significantly over the range investigated. Porous structures with isoelectric points at the pH of the liquor being filtered were linked to an increased fouling tendency.

All RC and FP 100 kg mol^{-1} membranes were cleaned relatively easily. FP 10 kg mol^{-1} and FP 30 kg mol^{-1} membranes were found to have undergone surface modification, including increased negative charge and changes in hydrophobicity.

The dominant fouling mechanism during all ultrafiltration experiments was found to be cake filtration. The cake formed on RC membranes is thought to dominate filtration properties due to similar transmissions detected through varied pore sizes.

Atomic Force Microscopy (AFM) surface interaction measurements were performed for a model polyphenol present in tea (theaflavin-3-gallate) with a regenerated cellulose ultrafiltration membrane. This study has investigated the influence of multiple (200x) measurements of force curves at different points on the membrane surface. Force data on approach to the membrane surface is reported as well as the more frequently published pull-off force measurements. Differently treated membranes from throughout the fouling cleaning cycle were investigated.

The pull-off force of the foulant from the virgin and the fouled once / cleaned once (F1C1) membrane surface was stronger than that recorded for foulant – foulant interactions. Interestingly, NaOH cleaning of the virgin conditioned membrane reduced foulant – membrane adhesion compared to the virgin or F1C1 surface. This technique can be used as an aid to understanding the nature of fouling and cleaning mechanisms in protein / polyphenol systems.

Contents

List of Figures

List of Tables

Nomenclature

Abbreviations	Description
ACN	Acetonitrile
AFM	Atomic force microscopy
Ag	Silver
ATR	Attenuated total reflection
BSA	Bovine Serum Albumin
C	Carbon
Ca	Calcium
Ca^{2+}	Calcium ion
$CaCO_3$	Calcium Carbonate
CFV	Cross-Flow Velocity (ms^{-1})
CIP	Cleaning in place
Cl	Chlorine
CP	Concentration Polarisation
CTAB	Cetyl-trimethyl-ammonium
Cu^{2+}	Copper ion
D	Photodiode array,
Da	Dalton (1000Da – 1 kDa)
DVO	Direct Visual Observation
DSS	Danish separation systems
EDTA	Ethylendiaminetetraacetic acid
F	Flow cell.
F1C1	Fouled once then cleaned once
FESEM	Field Emission Electron Scanning Microscopy
FP	Fluoropolymer
FTIR	Fourier transform infrared
IR	Infrared
H	Hydrogen
HPLC	High performance liquid chromatography
Hz	Hertz (cycles per second, unit of frequency)
IEP	Iso-electric point
IRE	Internal reflectance element

K	Potassium
L	Light source
LMH	Litres m^{-2} h^{-1}
M	Molar Concentration (moles $litre^{-1}$)
MF	Microfiltration
Mg^{2+}	Magnesium ion
MW	Molecular Weight (Da)
MWCO	Molecular Weight Cut Off (Da)
N	Nitrogen
NaOH	Sodium Hydroxide
NaCl	Sodium Chloride
NF	Nanofiltration
NMWCO	Nominal Molecular Weight Cut Off (Da)
MMCO –	Molecular Mass Cut Off (kg mol^{-1})
NMMCO	Nominal Molecular Mass Cut Off (kg mol^{-1})
NOM	Natural Organic Matter
O	Oxygen
P	Prism
P1	Inlet pressure (bar)
P2	Outlet pressure (bar)
PAN	polyacrylonitrile
PD	Piezodialysis
PES	Polyethersulfone
pH	Measure of acidity / alkalinity at 25°C
PT	Pressure tranducer
PS	Polysulphone
PVDF	Polyvinylidene Difluoride
PVP	Polyvinyl pyrrolidone
PVPP	polyvinylpolypyrrolidone
PWF	Pure Water Flux
R & D	Research and Design
Re	Reynolds Number
RC	Regenerated Cellulose
RO	Reverse Osmosis

RTD	Ready-To-Drink
S	Sensor surface
SDS	sodium dodecyl sulphate
SEM	Scanning Electron Microscope
TEM	Transmission electron microscope
TF	Theaflavin
TF3G	Theaflain-3-Gallate
TF3'G	Theaflain-3'-Gallate
TFDG	Theaflavin Digallate
TMP	Transmembrane Pressure (bar)
TPP	Total Polyphenols
TT	Thermocouple
UF	Ultrafiltration
UV – VIS	Ultraviolet to Visible
wt%	Weight Percentage (% w/w)
XRD	X-ray detector
ZP	Zeta potential

Symbols	Description	Units
$\mathbf{A_m}$	Membrane surface area	(m^2)
$\mathbf{A_0}$	Area of clean membrane and cake when formed	(m^2)
a	Channel height	(m)
$\mathbf{a^H}$	Hunter colour redness	(-)
a* (Δa)	CIE colour redness	(-)
b	Channel width	(m)
$\mathbf{b^H}$	Hunter colour yellowness	(-)
b* (Δb)	CIE colour yellowness	(-)
C	Concentration	(wt%)
$\mathbf{C_B}$	Tea solids concentration in bulk feed stream	(wt%)
$\mathbf{C_{BS}}$	Concentration of component within bulk feed dehydrated tea solids fraction (Equation 4.14)	(wt%)
$\mathbf{C_g}$	Gel layer concentration	(wt%)
$\mathbf{C_M}$	Membrane surface concentration	(wt%)
$\mathbf{C_P}$	Tea solids concentration in permeate stream	(wt%)
$\mathbf{C_{PS}}$	Concentration of component within permeate dehydrated tea solids fraction (Equation 4.14)	(wt%)
d	diameter of channel	(m)
$\mathbf{d_e}$	Equivalent diameter	(m)
dh	hydraulic channel diameter	(m)
D	Diffusion coefficient	(m^2s^{-1})
E	Streaming Potential	mV
$\mathbf{E_Q}$ **(**$\Delta\mathbf{E_Q}$**)**	Total colour quality	(-)
F	Force acting on the membrane surface	(Nm^{-2})
$\mathbf{J_0}$	Initial virgin filtrate (fouling) flux	(litres $h^{-1}m^{-2}$)
J	Overall membrane flux	(ms^{-1})
J*	Flux at "steady state"	(litres h^{-1} m^{-2})
$\mathbf{J_F}$	Filtrate (Fouling) Flux	(litres $h^{-1}m^{-2}$)
$\mathbf{J_{FC}}$	Pure water flux of fouled then cleaned membrane	(litres $h^{-1}m^{-2}$)
$\mathbf{J_{lim}}$	Limiting flux	(ms^{-1})
$\mathbf{J_N}$	Normalised pure water flux	(-)
$\mathbf{J_r}$	Flux recovery	(%)

$\mathbf{J_U}$	Pure water flux of virgin membrane	(litres $h^{-1}m^{-2}$)
$\mathbf{J_V}$	Volumetric Permeate flux (steady state)	(ms^{-1})
$\mathbf{J_W}$	Pure water flux	(litres $h^{-1}m^{-2}$)
$\mathbf{K_A}$	Blocked surface area of membrane per unit area	(m^{-1})
$\mathbf{K_B}$	decrease in the cross-sectional area of the pores per unit of permeate volume	(m^{-1})
$\mathbf{K_C}$	Area of the cake per unit of permeate volume	(m^{-1})
k	Mass transfer coefficient	(ms^{-1})
kc	Spring constant of cantilever	(Nm^{-3})
$\mathbf{k_e}$	Conductivity of electrolyte in the pores	(ohm)
$\mathbf{k_f}$	Fouling potential	(m^{-4})
$\mathbf{k_g}$	Mass transfer coefficient (Limiting flux region)	(ms^{-1})
$\mathbf{k_H}$	Fouling mechanism rate constant in Hermia relationship, Equation 2.15	(vary with n)
$\mathbf{k_J}$	Fouling mechanism rate constant, cross flow filtration	(vary with n)
l	Channel length	(m)
$\mathbf{L^H}$	Hunter colour lightness	
L	Litre	(m^3)
L* (ΔL)	Lightness	(-)
$\mathbf{M_{conc}}$	Concentration of tea	
$\mathbf{M_{tea}}$	Mass of tea powder	(kg)
$\mathbf{M_{RO}}$	Mass of reverse osmosis water	(kg)
$\mathbf{M_{V0}}$	Mass of virgin cleaned vial	(kg)
$\mathbf{M_{VT0}}$	Total mass of vial and wet sample	(kg)
$\mathbf{M_{VT1}}$	Total mass of vial and dried sample	(kg)
n	Fouling mechanism power constant	(-)
N	Number of channels	(-)
$\mathbf{OD_{Intercept}}$	Intercept with y axis in figure 7.8	(-)
$\mathbf{OD_{Sample}}$	Sample absorbance	(-)
Pa	Pascal	(Nm^{-2})
ΔP	Transmembrane Pressure	(bar or Nm^{-2})
Q	Volumetric flow rate	(m^3/s)
$\mathbf{R_{coeff}}$	Apparent Rejection Coefficient	(-)

$\mathbf{R_A}$	Resistance due to adsorption on membrane surface	(m^{-1})
$\mathbf{R_{bl}}$	Boundary layer resistance	(m^{-1})
$\mathbf{R_C}$	Resistance due to Cake layer	(m^{-1})
$\mathbf{R_{CP}}$	Resistance due to Concentration Polarisation	(m^{-1})
$\mathbf{R_F}$	Total Fouling Resistance	(m^{-1})
$\mathbf{R_g}$	Resistance due to gel layer	(m^{-1})
$\mathbf{R_{IR}}$	Irreversible Fouling Resistance	(m^{-1})
$\mathbf{R_{Max}}$	Maximum true rejection coefficient	(-)
$\mathbf{R_M}$	Virgin or Cleaned Membrane Resistance	(m^{-1})
$\mathbf{R_P}$	Resistance due to pore plugging	(m^{-1})
$\mathbf{R_r}$	Ratio of cake to clean membrane resistance	(-)
$\mathbf{R_{REV}}$	Reversible Fouling Resistance	(m^{-1})
$\mathbf{R_T}$	Total Fouling Resistance	(m^{-1})
$\mathbf{Slope_{std}}$	gradient of line in figure 7.8	(-)
$\mathbf{t}$	time	(s)
$\mathbf{u}$	average linear fluid velocity	(ms^{-1})
$\mathbf{U_0}$	Initial mean velocity of fluid through membrane	(ms^{-1})
$\mathbf{V}$	Volume of fluid	(m^3)
$\mathbf{W_a}$	Adhesion per unit area between the two phases	(Nm^{-1})

Greek Symbols

ε_0	permittivity of a vacuum	($C^2\ N^{-1}\ m^{-2}$)
ε_r	The relative dielectric constant of the electrolyte	(-)
δ	Concentration polarisation Boundary layer thickness	(m^{-1})
$\prod$	Osmotic pressure	(bar)
ρ	Fluid density	(kgm^{-3}) (Nm^{-1})
μ_{E_1}	Viscosity of the electrolyte	(Pa s)
μ_F	Viscosity of black tea feed solution	(Pa s)
μ_P	Viscosity of permeate solution	(Pa s)
μ_W	Viscosity of RO water	(Pas)
γ_{lv}	Interfacial energies of the liquid / vapour (Surface tension)	(Nm^{-1})
γ_{sv}	Interfacial energies of the solid / vapour interface	(Nm^{-1})
γ_s	Interfacial energies of the solid / liquid interface	(Nm^{-1})
θ	Contact angle of liquid drop with solid surface	(°)
ς	Apparent Zeta Potential	(mV)
δ_C	Cantilever deflection	(m)

Chapter 1 Introduction

1.1 Preface

In all of its various forms (green, black and Oolong) tea is an ubiquitous beverage, one of the most widely consumed beverages in the world second only to water (Harbowy and Balentine 1997). Tea is largely characterised by its high polyphenol content and their attendant antioxidant properties. These antioxidant properties are attributed by its ability to inhibit free radical generation, to scavenge existing free radicals and chelate transition metals (Luczaj and Skrzydlewska 2005). There have been numerous studies linking drinking tea with reduction of risk of health problems, (Satoh et al. 2001) such as cancer in humans (Leone et al. 2003) and even certain effects caused by alcohol intoxication and smoking (Luczaj and Skrzydlewska 2004) although the evidence is still insufficient to allow any clear statements to be made. These proposed health benefits have increased the popularity of tea beverages throughout the world.

1.2 Ready to drink tea (Iced Tea)

Ready to drink (RTD) tea or iced tea is responsible for about 75% of all tea consumption within the USA and is increasingly consumed throughout the world, especially in Japan and China due to it's potential health benefits (Weisburger 1997).
Black iced tea manufacture begins with the extraction of the tea liquor from black fermented leaves, followed by removal of the redundant leaves and successive concentration of the tea extract.
Upon cooling of hot black tea infusions of RTD tea is produced usually giving the beverage a muddy or hazy appearance. This problem associated with RTD tea production is a phenomena known as "tea creaming". Tea cream is the precipitation of solids from the tea solution which is affected by concentration, pH and time-temperature history of the tea infusion (Tolstoguzov 2002). Tea cream contains many of the compounds that provide taste and colour in black tea thus giving rise to a loss of both of these properties during the production of RTD tea (Jobstl et al. 2005). Consequently a decreaming stage is required to remove this insoluble matter. Usually this is achieved by the partially concentrated black tea extract being centrifuged,

removing this insoluble matter before further concentration. Usually the concentrated extract is then spray dried for easier transportation from the country of origin to the bottling plant, where the powder can be reconstituted into the final product.

The shelf life of RTD tea products is generally 6 – 12 months and the stability of the tea infusions during storage is of great importance. Bee et al. 1987 and Liang and Xu 2003 have confirmed an increase in black tea cream particle volume concentration by up to 45% during 12 days of storage at 4°C. It is worth noting that RTD tea is consumed at fridge temperature < 5°C and could potentially be stored at this temperature for up to 6 – 12 months.

1.3 Possible application of membrane process

Liang and Xu 2001 examined the size of black tea cream using light scattering techniques, and found that within the range 0.1- 100μm, 84.8% of tea cream particles were below 1.03μm and 7.5% of particles were above 5.07μm. This suggests that potentially a physical barrier could be used to separate some polyphenolic containing thearubigins from the larger tea cream aggregates.

Todisco et al. 2002 showed that haze reduction and polyphenol content remained constant in the final product for up to 2 months using a 40 kDa molecular weight cut-off (NMWCO) ceramic membrane in a cross flow mode. This facilitated the permeation of the most important polyphenols in the molecular mass range of 290 - 458 Da, whilst maintaining the essential properties of tea (Todisco et al. 2002).

1.4 Issues due to fouling and cleaning

The nature of complex feeds and membrane filtration generally causes a progressive flux decline which has a marked effect on the economic benefit of the process. This area although very well understood is still being heavily researched to understand the intricate nature of membrane fouling and inevitable flux decline at practical industrially relevant flux values. Cleaning of membranes is inevitable and the frequency of cleaning can be reduced due to advanced fouling knowledge. The membrane surface parameters; hydrophobicity, charge, morphology and roughness (Weis et al. 2003, Weis et al. 2005) and defined molecular mass cut-off can all critical to the mechanism of fouling and cleaning which will affect product quality and performance.

1.5 Project aims and objectives

The initial aim of the project was the utilisation of ultrafiltration technology in ready to drink (RTD) tea processing to potentially yield beverages with reduced levels of haze and impact significantly on the formation of tea cream. Subsequently the main objectives were as follows:

- To evaluate the mechanisms involved in fouling and cleaning ultrafiltration membranes used in polyphenol / protein based mixtures.

- To investigate the variables affecting permeate flux and quality for polyphenol / protein based mixtures.

- To understand and characterise the physical and chemical interactions between membranes and tea components.

- To investigate the interaction between individual polyphenols, proteins, alkaloids, amino acids and ultrafiltration membranes.

- To model membrane transport processes in order to establish generic polyphenol transmission mechanisms for application to a range of tea based beverage products.

1.6 The outline of the thesis

Chapter 2 examines the current knowledge of tea chemistry and the nature of tea cream (aggregate) formation. Ultrafiltration is also critically appraised as a process and examination of the previous literature on fouling and cleaning mechanisms are reviewed. Analysis techniques are also discussed alongside their potential to obtain information.

Chapter 3 describes all the raw materials and physical equipment used in this study including the ultrafiltration module, rig and analytical tools required.

Chapter 4 presents all the results obtained during experimentation including fouling and cleaning experiments, fluid analysis and membrane surface science analysis techniques.

Chapter 5 concludes all the findings of this study and discusses the potential recommendations for future work.

Figure 1.1 displays a summary of all the work performed in this study.

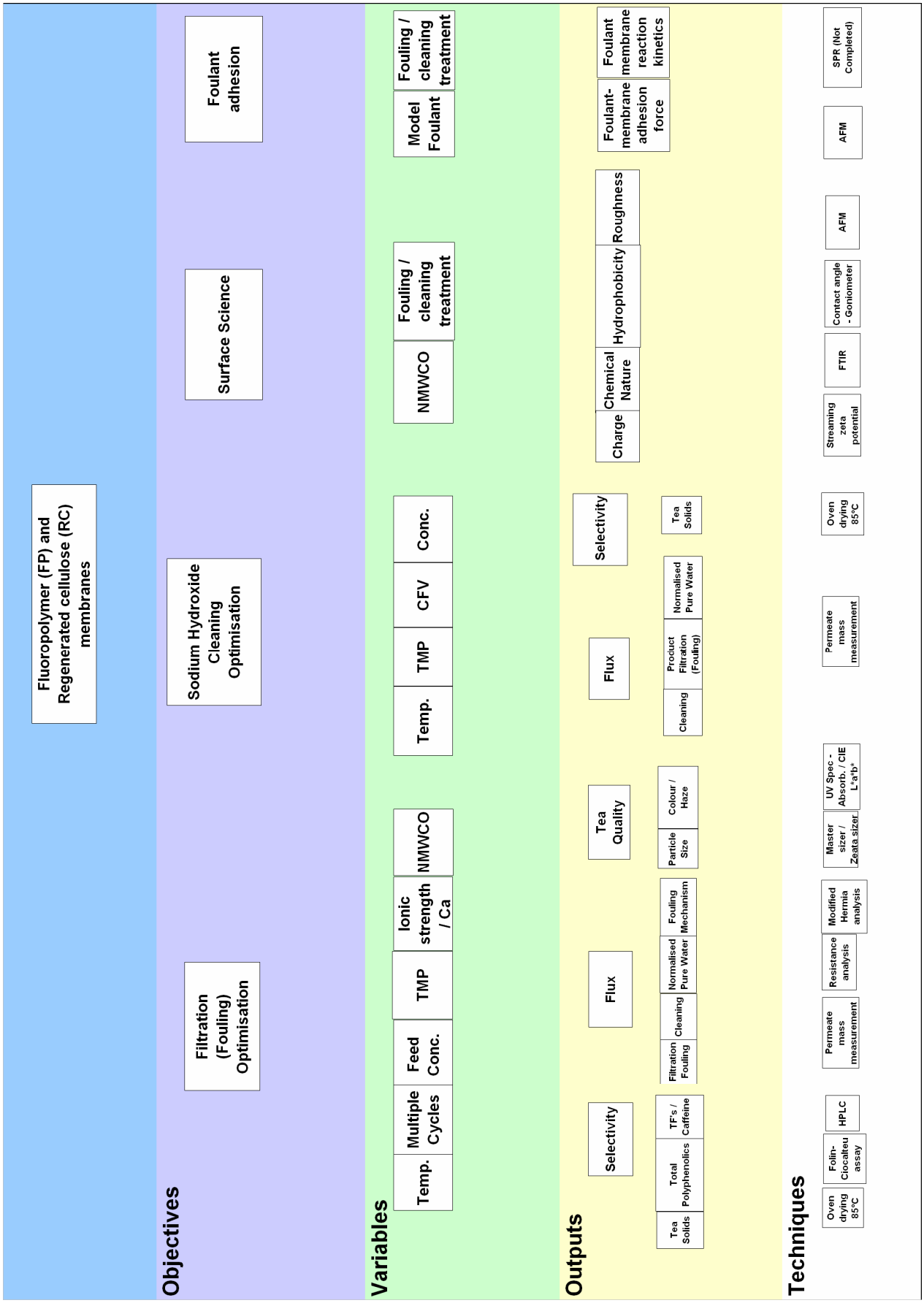

Figure 1.1: Overview of the work performed within this study

1.7 List of publications arising from thesis

1.7.1 Refereed Journal papers

Evans, P. J. and Bird. M. R. (2006). "Solute - Membrane Fouling Interactions during the Ultrafiltration of Black Tea Liquor." Food and Bioproducts Processing 84: 292 - 301.

Evans, P. J. and Bird. M. R. (2008). "The influence of hydrophobicity, roughness and charge upon the performance of (UF) membranes for the clarification of black tea." Journal of Membrane Science, 313: 250-262

Evans, P. J. and M. R. Bird (2008). "The influence of black tea feed conditions on ultrafiltration performance during membrane fouling and cleaning." Accepted subject to minor changes, Journal of Food Process Engineering, DOI:10.111/j.1745-4530.2008.00276.x

Philip J. Evans, Michael R. Bird, Dale Rogers and Christopher Wright (2008). "Polyphenol – membrane retraction and removal force measurement during the ultrafiltration of black tea liquor." Submitted to Journal of Membrane Science.

Philip J. Evans, Michael R Bird (2008). "Tea quality indicators during the ultrafiltration of black tea" Awaiting approval from Unilever.

1.7.2 Conference papers

Bird, MR, Evans, P and Wu, D, 2007, "The application of UF membranes to the filtration of model tea component solutions and reconstituted black tea powder' /International membrane science and technology conference" (IMSTEC'07)/, Sydney, Australia, 5- 9 November 2007, p. 104. ISBN 978 0 7334 2561 5.

Evans, P. J. and Bird. M. R. “The fouling and cleaning of ultrafiltration membranes for black tea liquor clarification.” European Congress of Chemical Engineering (ECCE – 6), Copenhagen, 16 – 20th September 2007. ISBN 978-87-91435-56-0

Evans, P. J. and Bird. M. R. "Solute - Membrane Fouling Interactions during the Ultrafiltration of Black Tea Liquor.” Fouling and Cleaning Conference, Cambridge, 23 – 26th March 2006. ISBN 0-9542483-1-7

Chapter 2 Literature Review

2.1 What is Tea?

2.1.1 Introduction

The tea plant, *Camellia sinensis*, is an evergreen tree belonging to the family of Theaceae. The leaves can be harvested by hand or by special machining equipment (Weisburger 1997). The following manufacturing process of the leaves determines the type of tea produced, in general there are three different types: green tea (unferemented), Oolong tea (partially fermented) and black tea (fully fermented) (Balentine 1992). The subsequent leaves are dried and when infused in hot boiling water produce the hot beverage known as tea.

Tea is one of the most widely consumed beverages in the world other than water with an annual production of 1.8×10^6 tonnes of dry leaves and approximate 40 litres (L) intake per capita worldwide per year. (Harbowy and Balentine 1997). It is estimated that $(18\text{-}20) \times 10^6$ cups (6oz) of tea are drunk on a daily basis in the world (Fernandez-Caceres et al. 2001).

Tea is largely characterised by its high polyphenol (antioxidant) properties. Lunder reports that the approximate amounts of polyphenol (antioxidant) in fresh leaf, green and black teas are in the range 30 – 35%, 10-25% and 8 – 21% respectively (Lunder 1992). These antioxidant properties are credited to its ability to inhibit free radical generation, to scavenge existing free radicals and chelate transition metals (Luczaj and Skrzydlewska 2005) There have been numerous studies linking drinking tea with reduction of risk of health problems, (Satoh et al. 2001) cancer in humans (Leone et al. 2003) and even certain effects caused by alcohol intoxication and smoking (Luczaj and Skrzydlewska 2004) although the evidence is still insufficient to allow for any clear statements to be made.

2.1.2 The composition of Tea

2.1.2.1 Fresh / Green Tea Leaf

The composition of fresh tea leaf is made up of; fibre, proteins, carbohydrates, minerals, pigments, amino acids, caffeine, phenolic and organic acids with the remainder being polyphenols. Table 2.1 below shows some approximations of the content of dried fresh tea leaf based on different studies (Balentine 1992, Lunder 1992, Astill et al. 2001). Due to diverse tea leaf varieties, growing conditions and locations precise content quantities are difficult to ascertain.

The fresh leaf is largely characterised by the simple monomeric polyphenols, catechins. The chemical structures of these catechins are shown below in Figure 2.1 obtained from Balentine 1992, the molecular weight (M.W.) of catechins range from 290 – 458Da.

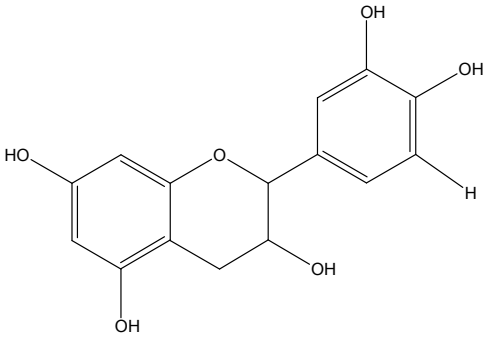

(a) (M.W. 290)

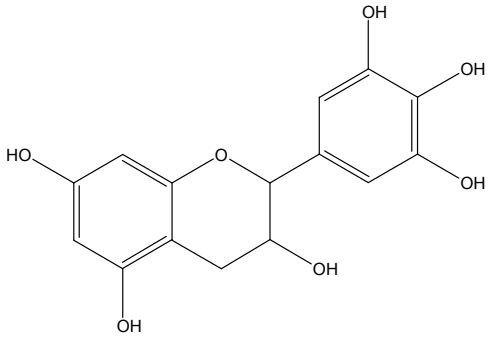

(b) (M.W. 306)

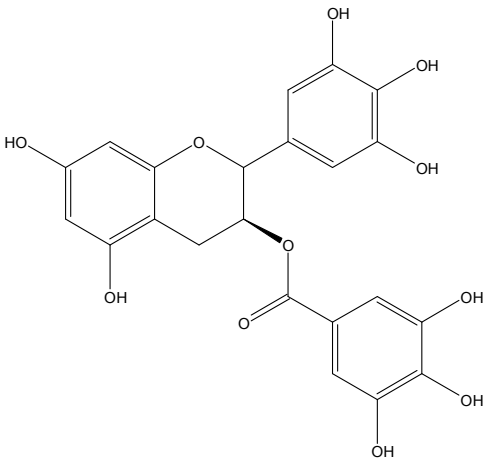

(c) (M.W. 458)

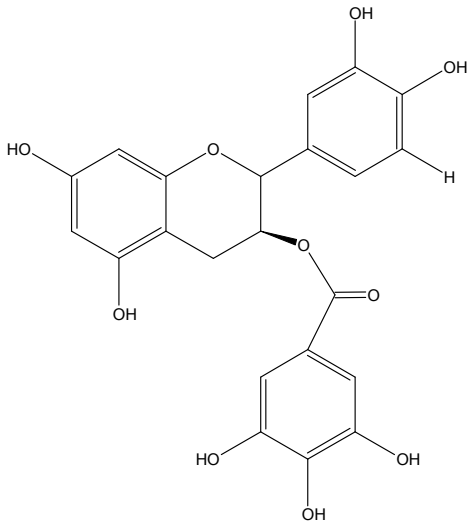

(d) (M.W. 442)

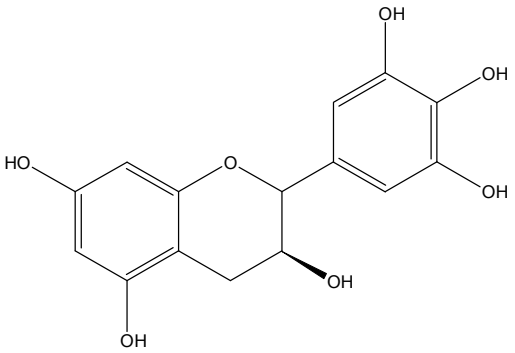

(e) (M.W. 306)

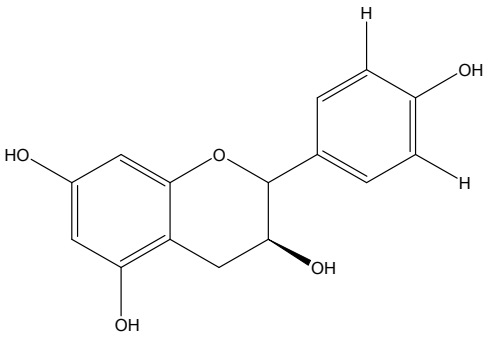

(f) (M.W. 290)

Figure 2.1: Chemical structures of green tea monomeric polyphenols; (a) catechin, (b) gallocatechin, (c)epigallocatechin gallate, (d) epicatechin gallate, (e) epigallocatechin, (f) epicatechin (Balentine 1992).

In green tea production the enzymatic reaction or fermentation is prevented by rapid steaming or pan firing of the fresh leaves. This inhibits any significant oxidation of catechin or flavanol polyphenols as shown in Table 2.2 where Catechins are initially 21.34 (wt%) and are 22.76 (wt%) after manufacturing demonstrating that no oxidation has occurred.

Constituents	Balentine, 1992	Lunder, 1992	Personal Communication, Jacek Obuchowicz, Unilever, Colworth.	Astill et al, 2001
Total Polyphenolics	**39**	**30 - 35**	**30 - 40**	**11.9 - 25.2**
Catechins (Flavanols, Flavan-3-ols)	10.1	17 - 30	18 - 32	7.1 - 20.8
catechin	0.1	0.35	1 - 2	
epicatechin	0.9	0.63	1 - 3	
epicatechin gallate	0.8	2.75	3 - 6	
gallocatechin	3.5	0.37	1 - 2	
epigallocatechin	4.4	2.35	3 - 6	
epigallocatechin gallate	3.9	10.55	9 - 13	
Other Flavanols and Favonol glycosides	1.676	3 - 4	3 - 4	
Caffeine	3.5	4	3 - 4	1.18 - 3.66
Amino Acids	4	4	2	
Carbohydrates	25	7	18 - 21	
Phenolic / Organic acids	1.5	5	4.5	
Volatiles		0.01 - 0.02	0.01	
Proteins	15	15	15	
Minerals (Ash)	5	10	5	
Fiber	9	30	16	

Table 2.1: Composition of dry fresh tea leaf (wt%) based on information from various authors.

2.1.2.2 Fermented Black Tea Leaf

Black tea is manufactured through fermentation of fresh tea leaves by encouraging the enzymatic polymerisation of simple polyphenols (Catechin monomers, Figure 2.1), principally the catalyst polyphenol oxidase and atmospheric oxygen.

Fermentation is encouraged by allowing the leaves to wither and then continual rolling and crushing of the tea leaves whilst warm air is blown through. (Balentine 1992). Table 2.2 demonstrates this process, Astill et al. 2001 measured the catechins

content of leaves during black tea manufacturing. The catechins content decreases from an initial 21.34 to 1.79 (wt%) following the fermentation process.

Stage in manufacturing process	% Catechin	% TPP	% Caffeine
(a) Black tea			
Freshly plucked tea shoots	21.34	23.69	3.18
Withered leaf	22.17	25.16	3.57
CTC rolled leaf	22.62	24.85	3.75
Leaf after 60 mins fermentation	4.78	19.53	3.65
Leaf after 120 mins fermentation	2.08	18.39	3.69
Fired leaf (60mins fermentation)	3.35	18.83	3.58
Fired leaf (120mins fermentation)	1.79	17.13	3.6
(b) Green tea			
Freshly plucked tea shoots	21.34	23.69	3.18
Short withered leaf	24.2	24.9	3.82
Pan fired green leaf	22	24.82	3.77
Shaped green leaf	21.63	25.05	3.74
fired green leaf	22.76	24.81	3.77

Table 2.2: Changes in composition (% w/w) of leaf during the manufacture of black and green teas from the same fresh Assam (C. sinensis Var. assamica) tea. (Astill et al. *2001)*

Following fermentation of the simple polyphenols in green tea leaf (catechins, flavanol glycosides and flavanols) 15% remain unchanged and around 10% are oxidised to theaflavins and other oligomers with molecular weights of 500 – 3000Da (Balentine 1992). Approximately 75% of the monomeric catechins are converted to deeply coloured compounds known as thearubigins (Todisco et al. 2002). This mixture of polymeric polyphenolic compounds have recently generated a great deal of interest, many theaflavins have been characterised having molecular weights ranging 564 – 868 Da (Figure 2.2), although thearubigins less so (Haslam 2003; Menet et al. 2004). The term 'thearubigin' is used to define a wide variety of compounds whose chemical identity has not been traced to any specific chemical group. There are some reports on the size of the thearubigins ranging from 700 – 40,000Da, although others have stated no reliable size could be measured (Haslam 2003). Table 2.3 shows some approximations of the fermented black tea content based on different studies (Balentine 1992, Lunder 1992, Astill et al. 2001) confirming the conversion of catechins to more complex theaflavins and thearubigins.

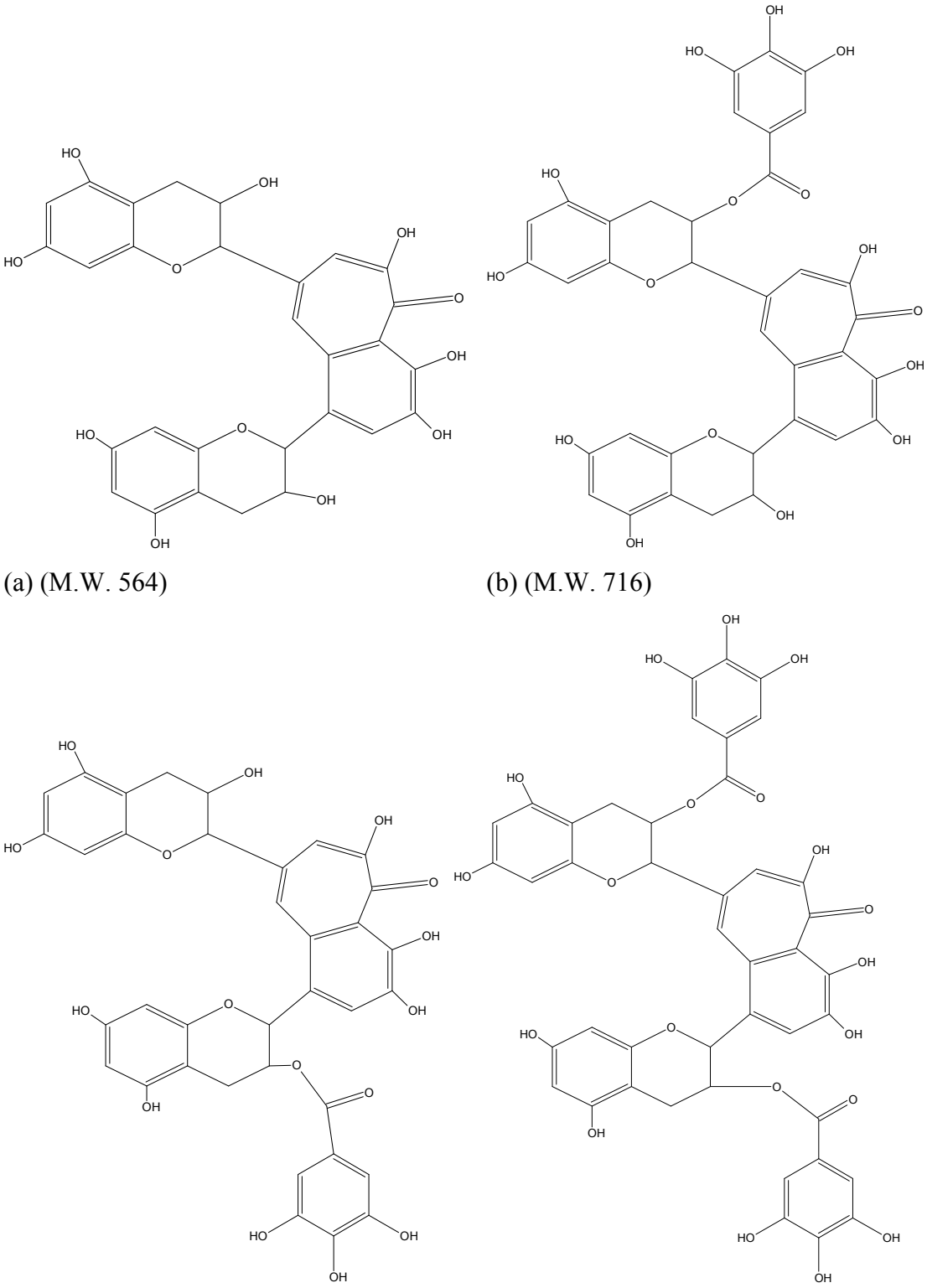

Figure 2.2: Chemical structure of theaflavins structures; (a) Theaflavin (TF), (b) Theaflavin – 3 gallate(TF3G), (c) Theaflavin – 3' gallate(TF3'G), (d) Thaflavin – 3-3' digallate(TFDG).

Constituents	Balentine, 1992	Lunder, 1992	Personal Communication, Jacek Obuchowicz, Unilever, Colworth.	Astill et al, 2001
Total Polyphenolics	**11.38**	**30 - 35**	**30 - 40**	**7.3 - 21.9**
Catechins (Flavanols, Flavan-3-ols)	4.15	5	5 - 10	0.7 - 8.8
catechin	0.23			
epicatechin	0.41			
epicatechin gallate	0.8			
gallocatechin	ND			
epigallocatechin	1.05			
epigallocatechin gallate	1.66			
Other Flavanols and Favonol glycosides	0.379	4 - 7		
Theaflavins	0.91	1 - 2	2 - 4	
theaflavin (TF)	0.25			
theaflavin-3-gallate (TF3G)	0.17			
theaflavin-3'-gallate (TF3'G)	0.24			
theaflavin digallate (TFDG)	0.25			
Thearubigins	5.94	15 - 20	15 - 20	
Caffeine	4	4	3 - 4	2.21 - 3.97
Amino Acids	4	4	2	
Carbohydrates	7	7	18 - 21	
Phenolic / Organic acids			4.5	
Volatiles			0.01	
Proteins	15	15	15	
Minerals (Ash)	5	10	5	
Fiber	30	30	16	

Table 2.3: Composition of fermented black tea leaf (wt%) according to various authors.

2.1.2.3 Black Tea Extract

The manufactured black tea leaves are now ready to be extracted, this process involves adding the leaves to hot boiling water and allowing constituents to transfer from the leaf to the water. The extraction process can be significantly varied itself by differences in brew time, water/leaf ratio, temperature, water quality, mechanical agitation and multiple extract possibilities. It is difficult to state a reliable composition of solids extract of black tea infusions due to the variations of growing conditions and production processes. Based on Astill *et al.* 2001**,** 18.8 – 29.6% of leaf solids can be extracted to water producing soluble solids concentrations of 2.637 – 3.933 g/L with the most popular UK brands. Approximations of the dry powder black tea extract content are shown in Table 2.4 below based on results from several authors. (Balentine 1992, Astill *et al*. 2001, Harbowy and Balentine 1997, Jobstl *et al*. 2005)

2.1.2.4 Catechins

Approximately 24 – 50 wt% of the water soluble solids are polyphenolic in nature. Catechins are water soluble and present in black tea extract (3 – 11 wt%) although in lower quantities than green tea as a large proportion of the catechins have been oxidised as previously discussed (Table 2.2).

2.1.2.5 Theaflavins and Thearubigins

Theaflavins and thearubigins are also water soluble and are found in the black tea extract in significant quantities 1 – 6 and 12 – 36 (wt%) respectively. Liang and Xu 2001, showed that theaflavins make a greater contribution to the brightness of black tea infusion than theaflavin gallates. However theaflavin gallates have a stronger ability to form tea cream than theaflavin. Liang[b] et al. 2003 report that tea colour shows positive values of Δa (redness) and Δb (yellowness) suggesting that tea infusions are red and yellow in colour and these qualities including ΔE_Q (total colour quality) were positively correlated with black tea appearance, infused leaf and total quality respectively. Individual compounds of (a) theaflavin, (b) theaflavin-3-gallate, (c) theaflavin-3'-gallate and (d) theaflavin-3,3'-digallate (figure 2.2) and total theaflavins [including (a) – (d)] were also positively correlated with of Δa and Δb and ΔE_Q. This suggests that high quality black tea may have a high concentration of red and yellow tea pigments, among which theaflavins (TF's) are an important group. Liang[b] et al. 2003, also demonstrated that a lower lightness, ΔL was associated with a higher quality black tea and a higher content of total theaflavins. No mention was made of the higher molecular weight thearubigins by Liang[b] et al. 2003. However, these compounds have been described by Scharbert and Hofmann 2005, as the orange low molecular weight theaflavins and red-brown polymeric thearubigins..

As well as colour, these oxidised polyphenols have generally been thought to impart flavour, astringency, acidity, body and delightful aromatics of black tea (Liang and Xu 2001; Todisco et al. 2002).

2.1.2.6 Caffeine

Caffeine, shown in Figure 2.3 is a colourless water soluble molecule with a molecular mass of 238 Da, which is present in black tea extract at concentrations of 4 – 11 (wt%). Caffeine is an alkaloid of the methylxianthine family and is a pharmacologically active bitter tasting substance and dose dependent, a stimulant of the central nervous system (Mumin et al. 2006). The average black tea contains 241mg/L of caffeine, (56.7mg in 235ml cup) (Astill et al. 2001).

2.1.2.7 Carbohydrates

Carbohydrates including many polysaccharides such as starch contribute to 4 – 15% of the extracted solids. Pectin is the main polysaccharide in tea leaves (Tolstoguzov 2002). Siebert[b] et al. 1996 indicates upon stabilization of beer haze that carbohydrate is found in beer haze in substantial quantities, as much as 80%, but is not involved in the haze formation process (Siebert[b] et al. 1996).

2.1.2.8 Amino Acids

There are many common free amino acids in black tea extract making up approximately 5 – 15% of the solids. Theanine is a unique amino acid only found in tea (ς-N-ethyl glutamine, Figure 2.4) and is believed to be the major amino acid present in tea extract, 3 (% w/w). (Harbowy and Balentine 1997). Theanine can cross the blood brain barrier and because of this theanine has psychoactive properties occurring through central neurotransmission (Yamada et al. 2005). Recent research has demonstrated effects of theanine such as reducing blood pressure in hypertensive rats, inhibiting caffeine-induced excitatory stimulation and protection of neuronal death in the brain. Theanine has clearly been linked with human condition and emotional function of the brain suggesting that theanine has a calming effect on neurotransmission and mood, although mechanistic function is still unclear (Yamada et al. 2005). Consequently marketing campaigns from tea companies such as "*PG Tips*" have been emphasising the natural presence of theanine in their product demonstrating that "when theanine is absorbed by the body, it can help to bring about a relaxed yet alert state of mind" and "drinking 2 – 3 cups of *PG Tips* can help you to focus" (www.pgtips.co.uk/theaninefacts/).

2.1.2.9 Proteins

Tea proteins are partially soluble in water, from 1 – 10 w/w% of the solid extract depending on the information source (Table 2.4). The reason for this variation is likely to be based on the definition of proteins and the fact that amino acids are the building blocks of proteins. The most important protein, ribuosediphosphate

carboxylase, an oligomeric protein, is about 25% of the water-soluble extracted proteins.

2.1.2.10 Nutrition

The nutritional significance of black tea derives from its vitamins and minerals. Vitamin C is found in the fresh green leaf, although as a consequence of the drying process its amount is largely reduced in black tea (Lunder 1992). The tea plant has been shown to be rich in minerals such as potassium, calcium and magnesium as well as small amounts of manganese, iron, phosphorous, copper, nickel and sodium (Lunder 1992 and Harbowy and Balentine 1997).

2.1.2.11 Insolubles

Fibres such as ligand, cellulose and lipids are not significantly water soluble and therefore not found in tea extract.

Constituents	Balentine, 1992	Harold and Graham, 1992	Harbowy, 1997	Astill et al, 2001	Jobstl, 2005
Total Polyphenolics	**24.43**	**24 - 42**	**40**	**32 - 33**	**50**
Catechins (Flavanols, Flavan-3-ols)	4.2	3 - 10	9		11
Other Flavanols and Favonol glycosides	1.4	6 - 8	4		
Theaflavins	1.83	3 - 6	4		3
theaflavin (TF)	0.68				
theafavin-3-gallate (TF3G)	0.83				
theafavin-3'-gallate (TF3'G)	0.25				
theaflavin digallate (TFDG)	0.07				
Thearubigins	17	12 - 18	23		36
Caffeine	7.1	8 - 11	4	7.1 - 9.5	ND
Amino Acids	4.8	13 - 15	6		7
Carbohydrates	13.5	15	14		4
Phenolic / Organic acids	11	10 - 12	2		2
Volatiles		< 0.1	trace		
Proteins	10.7	1	6		6
Minerals (Ash)		10	10		10
Fiber					

Table 2.4:Composition of fermented black tea extract dried powder (wt%) according to various authors.

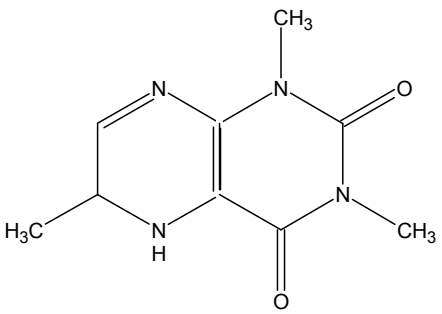

(M.W. 238)

Figure 2.3: Chemical structure of Caffeine

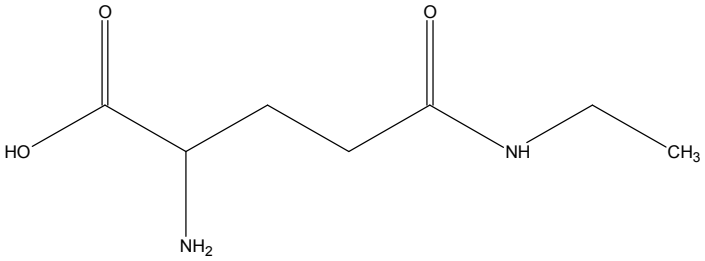

(M.W. 174)

Figure 2.4: Chemical structure of Theanine

2.1.3 Sensory Quality of Tea

Liang[b] et al. 2003 describe how sensory quality of tea samples are generally assessed in China. The grading system was based on a total score of 100, of which 10% is given for the appearance of the dry tea, 30% for the tea aroma, 15% for the infusion colour, 35% for the taste and 10% for the infused leaves.

Scharbert and Hofmann 2005 have performed an interesting study attempting to correlate the key components within tea to taste by comparing model solutions with actual infused tea. They found that there are 12 key components to tea taste, with catechins, caffeine, epigallocatechin-3-gallate and flavanol-3-glycosides being mainly responsible for the taste qualities, and that theaflavins were not crucial in taste. In addition flavanol-3-glycosides were found not only to impart a velvety astringent taste, but also contributed to the bitter taste of tea by amplifying the inherent bitterness of caffeine.

2.1.4 Production Process of Black Ready to Drink (RTD) Tea

Ready to drink (RTD) tea or iced tea is widely consumed throughout the world responsible for approximately 75% of all tea consumption within the USA (Weisburger 1997)

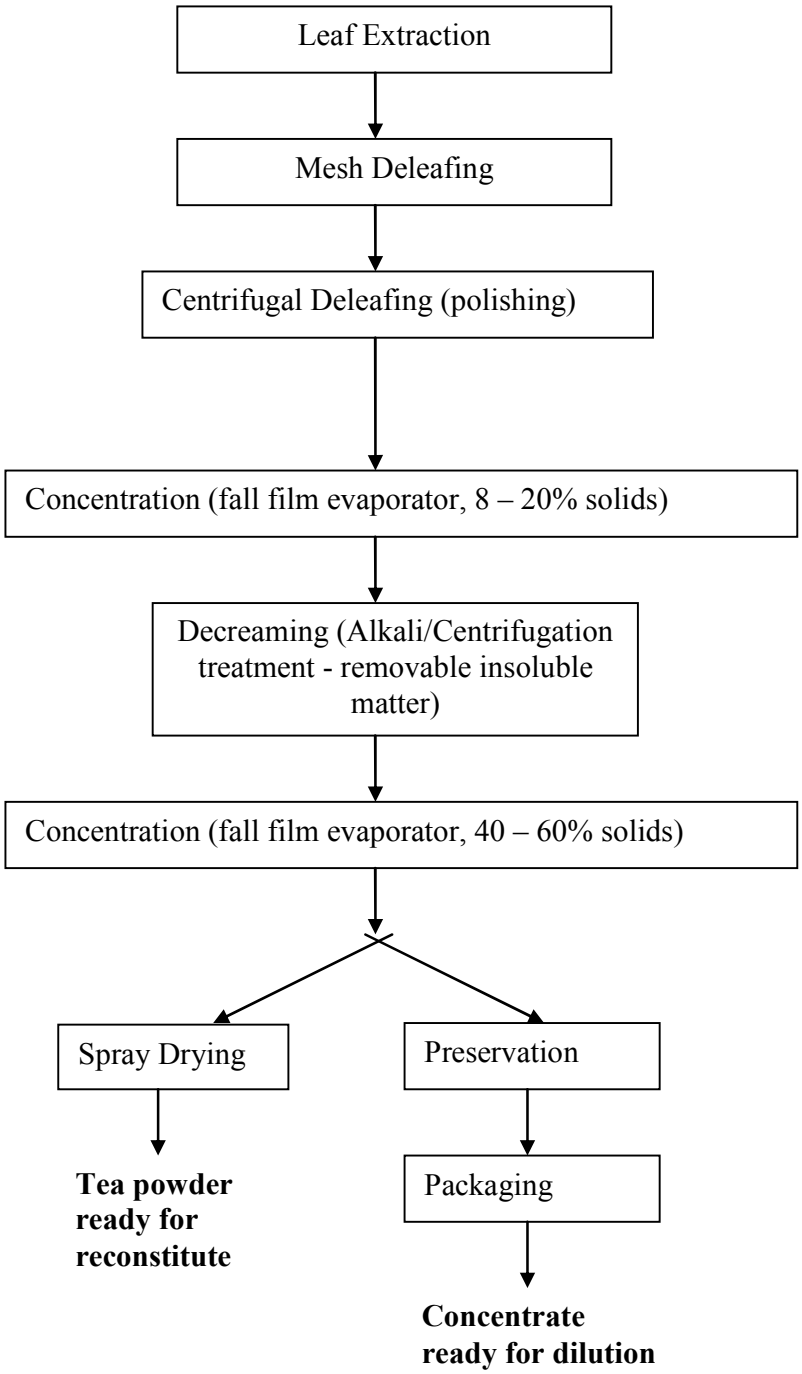

Figure 2.5: Flowsheet for current RTD tea production process (After Unilever 2004)

The current manufacturing of RTD tea, as shown in Figure 2.5, starts with the hot extraction from fermented black tea leaves. On completion of the extraction process the coarser leaves are first separated from the extract solution using a mesh and then the smaller fines by centrifugation. Next the solution is concentrated to approximately 8 – 20 wt% solids using a falling film evaporator after which the decreaming stage takes place using centrifugation to separate the insoluble precipitates. This is followed by acidification to re-dissolve the insoluble matter of which a small quantity can be used in the final product. Following this stage a further concentration stage occurs using a falling film evaporator, increasing the solids concentration to 40-60 wt%. The concentrate can then either be spray dried into a powder or preserved and packaged ready for sending to desired final product. Generally, sweeteners and citric acid are added to modify the flavour and also helps to stabilise the final product. Currently "*Lipton Ice Tea*" contains a solids concentration of black tea extract of 0.14 wt% whereas a normal 3 minute brewed cup (235ml) of *PG tips* tea bag (UK) would could have a concentration of 0.39 wt%, (3.933g/L) (Astill et al. 2001) nearly three times that of the RTD tea. The potential insertion of a membrane process in accordance with the objective of this study could be placed before or after the first concentration stage with the aim of removing the alkali/centrifugal decreaming stage.

2.2 Issues with Black RTD Tea

2.2.1 Tea Cream

A problem associated with RTD tea is a phenomenon known as "tea creaming". Tea cream is the precipitation of solids from the tea solution that causes visible haze and sediment formation, which can be affected by concentration, pH and time-temperature history of the tea infusion (Tolstoguzov 2002). Tea cream does not favour RTD tea production because it gives the bottled solution a hazy or muddy appearance (Liang and Xu 2003) which can limit the shelf life of the product and consumer expectation of the RTD tea being clear. Tea cream can contribute to the fouling of process equipment surfaces with deposits that are difficult to remove by cleaning-in-place (Siebert[a] et al. 1996). The majority of tea cream dissolves above 40°C although complete dissolution does not occur until 90°C. The molecular weight and solubility of polyphenol polymers are changed due to the formation of larger complexes with other components like proteins, polysaccharides, lipids and metal cations (Tolstoguzov 2002).

2.2.2 Protein - Polyphenol Interactions

Protein and polyphenol compounds can combine to form soluble complexes which can then grow to colloidal size. Colloidal size complexes scatter light (haze) and if the complexes grow further sediment is formed (Siebert[a] et al. 1996). Siebert 1999 reports that polyphenols interact mostly with proteins to form tea cream (Siebert 1999). Analogous interactions have also been reported in other polyphenol – protein containing beverages such as lager beer, wine and fruit juices (McMurrough et al. 1991; Siebert[b] et al. 1996).

Siebert[b] et al. 1996 investigated the amount of haze active proteins and polyphenols in different beverages by adding different amounts of haze active proteins and polyphenols and measuring the haze produced. The results indicate that commercial beers have a considerable amount of haze active protein and almost no haze active

polyphenol, while commercial apple juices are the opposite. Grape juices and wines were intermediate but resembled apple juice more than beer (Siebert[b] et al. 1996).

Siebert[a] et al. 1996 put forward a model for the protein – polyphenol interactions (Figure 2.6) observed when the ratio of gelatin and tannic acid was varied and haze produced recorded. The results demonstrated that there was an optimum ratio required for maximum haze production suggesting that proteins had a fixed number of peptide – polyphenol binding sites and polyphenols the same. Saturation of either proteins or polyphenols compared to available binding sites resulted in smaller complexes being produced, as represented in Figure 2.6 below.

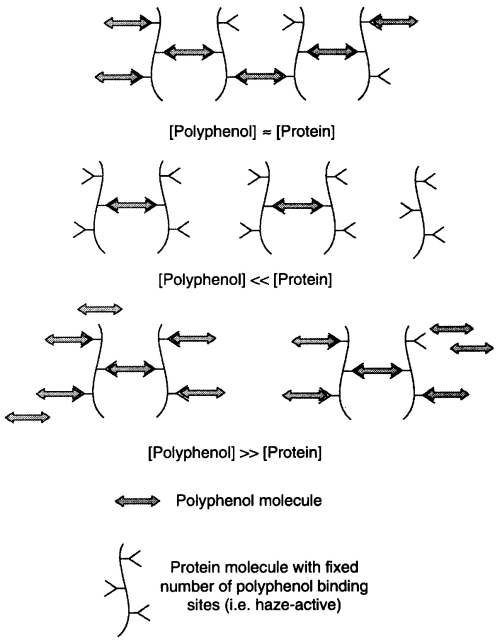

Figure 2.6: Conceptual mechanism of protein – polyphenol interaction (After Siebert[a] et al. 1996)

Siebert[a] et al. 1996 report that peptides and proteins that contain proline formed haze in the presence of polyphenolic compounds and that when peptides and proteins lacking in proline were used no haze was formed. Generally peptides with larger amounts of proline formed more haze.

Isolates of protein from apple juice sediment indicated that the percentage of proline ranged from 15.9 – 31.7wt% (Johnson et al. 1968). A large amount of proline (21.8 – 39.8 wt% depending on growing conditions) was found in green tea protein by Hu et al. 2001 during their study on the effect of selenium on green tea preservation.

Siebert 2006 discusses the nature of haze active polyphenols; for a phenol to bind to a protein a dependence on the location and number of hydroxyl groups on an aromatic

ring is of importance. Flavanols including catechins and procyanidins have the strongest haze-forming activity being demonstrated in model systems and actual beverages. The catechins shown in Figure 2.1, are large enough to encompass two attachment sites, an aromatic ring with at least two hydroxyl groups. These catechins are present in this form or more complicated dimers and trimers, namely procyanidins (e.g catechin – catechin dimer). Haze activity has also been shown to increase with molecular complexity (Siebert 2006).

A great deal of work has been performed regarding protein – polyphenol interaction, it is known that the initial reaction is not covalent bonding as most haze can be removed by partially warming (Siebert 1999). Harbowy and Balentine 1997 discuss the mechanism of polyphenol / protein binding, initially caused by hydrogen bonding or hydrophobic interactions between the polyphenol and protein. After binding there is a reduction in the hydrophilic surface area and the hydrophobic side chains are reoriented outward into the aqueous solution resulting in further interactions and thus precipitation. In addition binding of the hydrophobic polyphenol with the hydrophobic portion of the protein may cause the hydrophilic portions of the protein to turn inwards, denaturing the protein causing precipitation (Harbowy and Balentine 1997).

Black tea extract clearly has a large proportion of reactive complex polyphenols and many proline rich proteins both potentially haze active and are likely to be one of the main causes of haze formation in black tea.

The reactivity of polyphenols with salivary proteins (rather than product based) is responsible for the characteristic astringent taste of tea (Cheynier 2005). Charlton et al. 2002 proposed a mechanism for the binding and precipitation of polyphenols by proline-rich proteins. Initially polyphenols are thought to bind reversibly and weakly to the hydrophobic peptide of the protein surface forming a soluble complex. The number of polyphenols adhering to the surface then reaches a critical amount so that there is enough polyphenol on the peptide to act as a link between two peptide molecules causing the complex to become insoluble. Further aggregation is caused by further polyphenol addition (Charlton et al. 2002).

2.2.3 Water quality – Calcium interactions

It is thought that highly heterogeneous protein-Ca-polyphenol complexes are formed stabilised by the presence of cations, hydrogen bonds and hydrophobic interactions (Tolstoguzov 2002). The concentration of calcium ions within tea infusions is relatively high (0.045% w/w) and when the tea cream phase is formed a significant proportion of the cream is Calcium (Ca) cations (Jobstl et al. 2005). Chao and Chiang 1999 demonstrated that 66% of the calcium in the original infusion are participated in cream formation in semi-fermented teas. The amount of tea cream formed in this study did not depend on water quality as tap water and deionised water were not significantly different. This suggests that the calcium from the tea infusions, not the water is largely responsible for tea cream formation (Chao and Chiang 1999). Calcium is thought to enhance the self-association of polyphenols and caffeine by bridging polar groups (Jobstl et al. 2005). Therefore adding chelating agents such as ethylendiaminetetraacetic acid (EDTA) has been shown to decrease cream formation by up to 50% (Jobstl et al. 2005). Tanizawa et al. 2007 performed an interesting study on tea stain formation on porcelain tiles and initially theorised that calcium was integral to the formation of tea stains by calcium bridging of polyphenolic constituents (Tanizawa et al. 2007). This theory was confirmed in a follow up study by Yamada et al. 2007 where the addition of extra calcium ions enhanced the calcium bridging of polar hydroxyl groups causing increased tea stain formation. EDTA was also used in this study and was found to break up black tea stains formed on the surface of porcelain tiles (Yamada et al. 2007).

2.2.4 Caffeine complex

The solubility of tea in solution is enhanced by the absence of caffeine (Penders[a] et al. 1998) and/or gallate esters despite theaflavins and other high molecular weight polyphenols are preferential to caffeine to partition into the cream phase (Penders[b] et al. 1998). Caffeine has also been shown to associate with theaflavin (Charlton et al. 2000), which further demonstrates the complexity of tea cream formation. The association of caffeine and theaflavins cause causes a depletion of caffeine and theaflavin by complexation with each other and constituents such as proteins. This

can cause tea taste to be affected and the reduction of the well documented stimulatory effect of caffeine and its bitter taste.

Jobstl et al. 2005, demonstrated that caffeine causes a reduction in creaming temperature, although is not required to initiate tea cream formation. Caffeine has been shown to bind weakly with cream components increasing the bulk and decreasing the solubility of tea cream by effectively filling in the vacant binding sites (Jobstl et al. 2005).

2.2.5 Extraction Temperature

Extraction of solids into infusion from leaf has been shown to be critical in cream formation at constant solids concentration. The extraction of black tea at temperatures below 35°C would produce an infusion incapable of creaming (Chao and Chiang 1999). However, low temperature extraction leads to a poor extraction of tea solids.

Liang and Xu 2003 demonstrated that increasing extraction temperature increased dry weight of tea cream, particle volume concentration of tea cream and the amount of haze formed. As the extraction temperature increased the lightness (L^H) decreased and the redness (a^H) increased whereas the yellowness (b^H) increased until 40°C before starting to decline. The change in all parameters was most significant between 50 and 60°C suggesting a possibility of reducing extraction temperature to below 50°C so that in RTD tea production less tea cream is formed and haze stability is increased (Liang[a] and Xu 2003). Siebert[a] et al. 1996 also demonstrated advantages in low temperature production within a model protein(gliadin) / polyphenol(tannic acid) system. By initially heating the protein sample a large increase in haze production was found in the presence of the polyphenol, indicating that more hydrophobic binding sites were exposed within the protein due to the unfolding via heating. This hydrophobic interaction is thought to play a greater role in polyphenol / protein interaction than hydrogen bonding (Siebert[a] et al. 1996).

2.2.6 pH of tea infusion

Extreme pH has been reported to increase solid extraction from leaf, particularly at low acidic pH levels where a significant increase in extraction is noticed. Extreme pH also encourages increased tea cream formation, however this may be more closely

related to the increased concentration that exists due the increased extraction at these pH's (Liang and Xu 2001). Liang and Xu 2001 also noted that increased particle size was found under alkali conditions, although at more acidic conditions (pH 3 -7) the particle size distribution showed a single peak where 90% of particles had diameters below 1.0μm. When infusion pH was above pH 7 or below pH 3 there was a bimodal distribution with colloidal particles (3 - 70μm) present suggesting increased precipitation and increased haze.

Jhoo et al. 2005 analysed the stability of theaflavin in varying pH conditions as a means of understanding what may happen in a gastric juice environment and found that theaflavin was most unstable in alkali conditions whilst being stable in acidic conditions.

2.2.7 Storage duration

The shelf life of RTD tea products is generally 6 – 12 months and the stability of the tea infusions in this time is of great importance. Storage duration will affect tea cream formation Bee et al. 1987 and Liang and Xu 2003 have confirmed an increase in tea cream particle volume concentration of up to 45% during 12 days of storage at 4°C. It is worth noting that RTD tea is consumed at fridge temperature < 5°C and could potentially be stored at this temperature for 6 – 12 months.

2.2.8 Other natural polyphenol / protein containing beverage

There are many natural polyphenol/protein containing beverages which have issues with clarity and stability. Apple juice, beer and wine require different stabilization methods usually by encouraging either protein or polyphenol removal. Polyphenol is usually removed by adsorption to polyvinylpolypyrrolidone (PVPP) or protein fining, usually gelatin. Removal of proteins by adsorption on bentonite or silica gels are often used and ultrafiltration is commonly used in wine and apple juice clarification for removal of proteins (Siebert[b] et al. 1996). Membrane separation processes have increasingly been used to clarify and stabilise many fruit beverages such as apple juice, (Mangas et al. 1997; Borneman et al. 2001; Tajchakavit et al. 2001; Brujin et al.

2002; Vladisavljevic' et al. 2003; Youn et al. 2004) pineapple juice, (Barros et al. 2003) beer, wine and milk (Daufin et al. 2001).

2.2.9 Potential use of size exclusion separation process

Liang and Xu 2001 examined the size of black tea cream using light scattering techniques, and found that within the range 0.1- 100 μm, 84.8% of tea cream particles were below 1.03μm and 7.5% of particles were above 5.07 μm. This suggests that potentially a physical barrier could be used to separate some polyphenolic containing thearubigins from the larger tea cream aggregates.

2.2.10 Use of a membrane separation process for tea clarification

Todisco et al. 2002 has shown ultrafiltration to remove relatively large suspended solid complexes, proteins and enzymes to increase product stability and thus reduce haze, whilst maintaining the smaller polyphenols that largely determine the tea's taste and character. Their paper shows that haze reduction and polyphenol content remained constant in the final product for up to 2 months using 40,000 Da Molecular weight cut-off (MWCO) ceramic membrane in a cross flow mode. This facilitated the permeation of the most important polyphenols in the molecular mass range of 290 - 458 Da, whilst maintaining the essential nutritional properties of tea. (Todisco et al. 2002).

Wu and Bird 2007 investigated the relative importance of individual black tea components in the fouling process of 30 kDa MWCO polysulfone ultrafiltration membranes in dead end mode. Also a comparison of sodium hydroxide (NaOH) cleaning characteristics were determined for differently fouled membranes. The model solutions consisted of proteins, theaflavins, thearubigins, caffeine and mixtures of each. Generally, the smaller molecular weight theaflavins and caffeine transmitted the membrane with higher fluxes and lower rejection coefficients than the higher molecular weight proteins and thearubigins. Investigation of binary mixtures of all the polyphenols (25mg/L) with protein (25mg/L) demonstrated a higher rejection of the polyphenols, but interestingly the transmission of proteins increased. This demonstrated that a membrane that completely rejects a pure protein solution can be

made to transmit protein in the presence of small molecular weight polyphenols. The cleanability of the membranes fouled by different model tea components demonstrated pure water flux recoveries of more than 62%, although membranes fouled by binary mixtures generally showed poor cleanabilities because of the comparatively severe fouling present. There were exceptions to this, membranes fouled by a mixture of TF-3-G / TF-3'-G with protein demonstrating over 90% pure water flux recovery.

2.3 Membrane Separation Processes

2.3.1 Introduction

Effective separation is crucial throughout the process industries and membrane technology has increased significantly especially with the onset of the newer biotechnological industries and increasingly sophisticated processing in the food and beverage industries (Coulson et al. 1997).

Membrane separation is essentially the use of a selective barrier between two phases in solution or suspension. The material which passes through the membrane is generally called the permeate and the material which is retained by the selective barrier is called the retentate. The driving force for passing the permeate through the membrane is usually a pressure driven process where a pressure gradient exists between the retentate side and the permeate side. Other driving forces can be used including concentration gradient (dialysis), electric field gradient (Electrodialysis, Electrophoresis) and even temperature gradient (Coulson et al. 1997). In this study the focus is on pressure driven processes.

2.3.2 Classification

There are many different pressure driven membrane processes including Microfiltration (MF), Ultrafiltration (UF), Nanofiltration (UF), Reverse Osmosis, (RO) and Piezodialysis (PD) (Mulder 2000). MF, UF, NF and RO are the most common industrial processes used and typical criteria for these processes are summarised in Table 2.5 below.

Microfiltration (MF)	**Ultrafiltration (UF)**	**Nanofiltration/Reverse Osmosis**
Separation of Particles (Bacteria, yeasts etc - Pore size: 0.05 - 10μm)	Separation of macromolecules(Proteins etc - Pore size: 100nm - 1nm)	Separation of low MW solutes (salts, glucose, lactose, micropollutants Pore size: < 2nm)
Osmotic pressure negligible*	Osmotic pressure negligible*	Osmotic pressure high (≈1 - 25bar)
Applied pressure low (<2bar)	Applied pressure low (≈1 - 10 bar)	Applied pressure high (≈10 - 60bar)
Symmetric structure Assymmetric structure	Asymmetric structure	Asymmetric structure
Thickness of separating layer: Symmetric ≈ 10 - 150μm Asymmetric layer ≈1 μm	Thickness of actual separating layer (active layer) ≈ 0.1 - 1.0 μm	Thickness of actual separating layer (active layer) ≈ 0.1 - 1.0 μm
Separation based on particle size	Separation based on particle size	Separation based on differecnes in solubility and diffusivity

* In absence of concentration polarisation

Table 2.5: Comparison of various pressure driven membrane processes – (after Mulder 2000)

MF and UF membranes are generally quite similar as demonstrated in Table 2. Essentially UF membranes have smaller pore sizes requiring larger applied pressures to separate smaller solutes from solution than MF. NF and RO separate using different mechanisms than MF and UF. They are used to separate low molecular weight solutions or small organic molecules which require denser membranes with a much higher hydrodynamic resistance. Higher pressures are required to overcome the higher resistances caused by these membranes and must also overcome the higher osmotic pressures (Mulder 2000).

2.3.3 Ultrafiltration Membranes

Ultrafiltration has been applied industrially in many diverse applications from demulsifying oil-in-water emulsions in the chemical industry (Hlavacek 1995) to separations of linguosulphonates in the paper industry (Weis et al. 2003) and clarification of honey in the food industry (Barhate et al. 2003).

The solutes retained by ultrafiltration membranes are those with molecular weights of 1000 or greater and depend on the nature of the molecular weight cut off (MWCO) membrane used. There are many types of membrane material including organic and

inorganic polymer materials. The material used can be of great importance due to the thermal / chemical stability. Material choice can also influence permeability and contribute to any detrimental fouling that may occur during the process due to adsorption. There are many organic polymeric materials from which membranes can be made by usually using a phase inversion technique. Several of these materials are listed below:-

Polysulphone/Polyethersulphone/Sulfonated polysulphone (PS)

Poly(vinylidene fluoride) (PVDF)

Polyacrylonitrile

Cellulosics (e.g. Cellulose acetate) (CA)

Polyimide/poly(ether imide)

Polyetheretherketone

(Mulder 2000)

As well as these organic polymeric membranes there are also inorganic ceramic materials being used for UF membranes (Mulder 2000) which have high thermal capacity and are very chemically stable. In addition stainless steel materials have been proposed as UF membrane materials (Shallo et al. 2001).

Ultrafiltration is often applied for the concentration or clarification of macromolecular solutions where large molecules have to be retained by the membrane while small molecules and the solvent can pass through the membrane as permeate (Mulder 2000)

Manufacture's characterise their membranes mainly by material and Nominal Molecular Weight Cut-Off (NMWCO), but as has been reported by some authors (Gekas and Zhang 1989; Gekas et al. 1990) this data should be reviewed critically as the methods used to estimate this value have drawbacks.

The definition of the MWCO is the nominal molecular weight (MW) of a solute for which 95% of that solute is retained by the membrane (Coulson et al. 1997). Even if a consistent approach was used with similar solutes/proteins for each membrane; due to the different properties of every membrane material there would be different interactions between the solutes and the membrane, which can alter the results obtained (Gekas and Zhang 1989; Gekas et al. 1990). The size of these membrane pores are difficult to calculate or observe, a concept to be discussed in detail later in section 2.4.9.7.

2.3.4 Dead End Configuration

Traditionally, membranes are used in the dead-end mode whereby the suspension to be separated is fed to a barrier with pressure as the driving force that allows smaller solute, but not larger solute above the MWCO of membrane to pass through. This is basically a sieving operation and as expected there can be a build-up of particles at the filter to form a cake (Figure 2.7). This cake then acts as an additional barrier to the flow of particles and the liquid, acting as an additional resistance to the flow through the filter decreasing the flux (volume flow per unit area of membrane) with time as the cake layer thickness/resistance increases (Mulder 2000). A representation of this is shown in Figure 2.8. Dead end configurations are now used more often where solute concentrations are very low or at bench scale for research purposes.

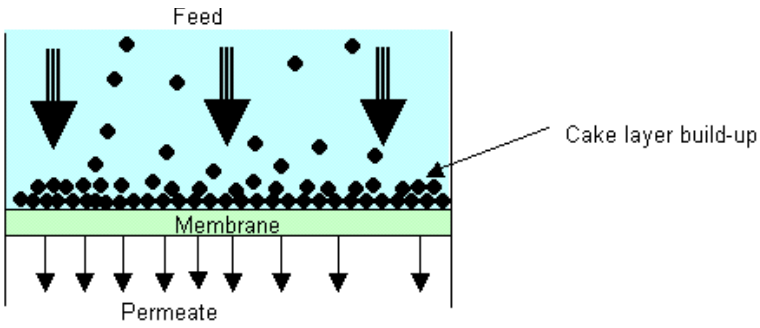

Figure 2.7: Classical dead end mode schematic

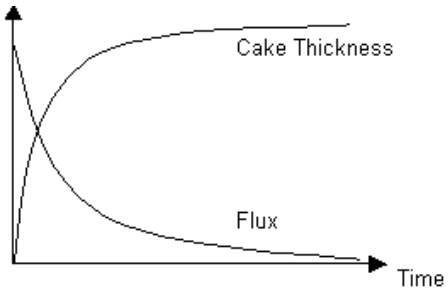

Figure 2.8: Representation of decrease in flux as cake layer thickness (resistance) is increased in dead-end mode

Dead end filtration can be performed with a stirrer (usually magnetic) on top of the memrbane, which then becomes a hybrid of a dead – end and a cross flow system. The cross – flow shear on the surface of membrane will be non linear with a greater shear on the outer edge of the membrane surface.

2.3.5 Cross – Flow Configuration

There are many different configurations used in industry to minimise the build up of a cake layer As discussed in Ripperger and Altmann 2002, the filtration of colloidal and very fine suspensions using a parallel flow to the filter medium increases the permeate volume before the filter medium is blocked. This was the invention of cross flow filtration. Cross flow UF is successfully used in industry especially where higher concentrations of solute are present within a system and generally with the use of cross-flow mode the onset of fouling tends to be less due to the flow across the membrane slowing the formation of any filter cake being formed.

Figure 2.9 shows the basic principle behind cross flow filtration where the retentate flows along the surface of the membrane as shown below and the permeate passes through the membrane. The movement of the retentate prevents to a large extent the build up of the cake layer and reduces the flux decline as shown in Figure 2.10.

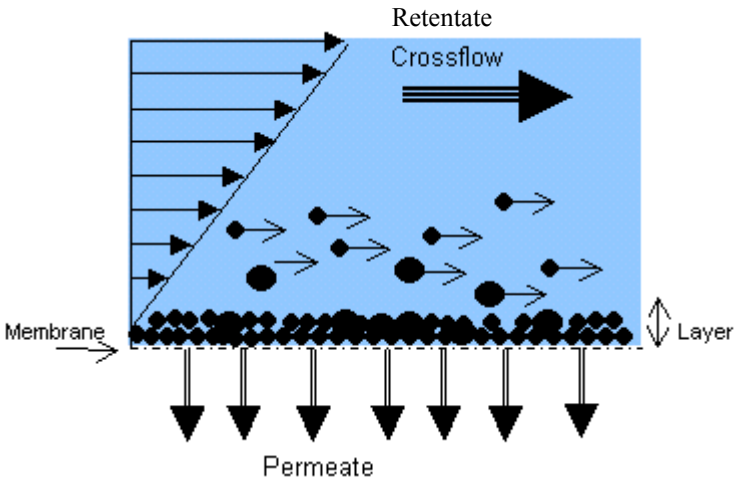

Figure 2.9: The schematic description of cross-flow mode

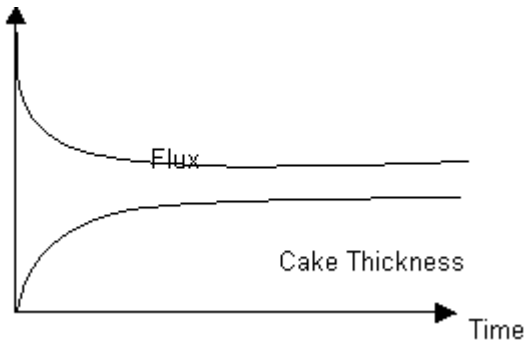

Figure 2.10: Representation of decrease in flux as cake layer thickness (resistance) is increased in cross-flow mode.

The four most common modules used for cross flow UF are flat sheet, spiral wound, hollow fibre and tubular and described in the next sections below.

2.3.6 Plate and frame module

Flat sheet modules are superficially similar to the conventional filter press. The permeate is pumped through annular discs supported by plates as shown in Figure 2.11 below. The sandwiches of membrane and support plate are separated from one and other by spacer plates, which have central and peripheral holes, through which the feed is directed over the whole membrane area. The flow through the module is laminar. The advantage of the flat sheet configuration is that damaged membranes can easily be detected because of separate permeate streams from each membrane pair. The volumetric hold-up is small, but cleaning can be difficult because these membranes cannot be back flushed. The stack requires dismantling for cleaning and fixing (Coulson et al. 1997).

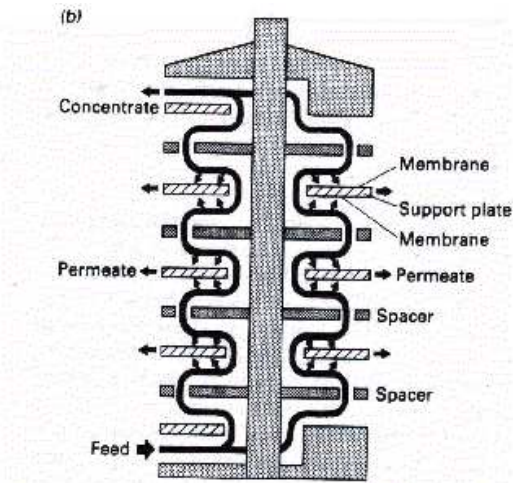

Figure 2.11: Schematic to represent a classic flat sheet module used in membrane filtration (After Coulson et al. 1997).

2.3.7 Spiral Wound module

Spiral wound modules consist of several flat sheet membranes separated by turbulence promoting mesh separators formed into a role similar to a 'Swiss roll', see

Figure 2.12 below. The feed required separating is fed at one end and encounters a number of narrow parallel feed channels formed between adjacent sheets of membrane. The permeate spirals towards the centre of the tube where it is removed through an axial pipe. Modules usually have a diameter of around 0.1m and a length of about 0.9m. The modules are very compact having a membrane surface area of about $5m^2$. Up to 6 modules may be installed in series. The advantages of these modules are that they make better use of space because they have the largest surface area per unit volume. However, they are very susceptible to fouling because of the low retentate velocities encountered and the inability to back flush for cleaning (Coulson et al. 1997).

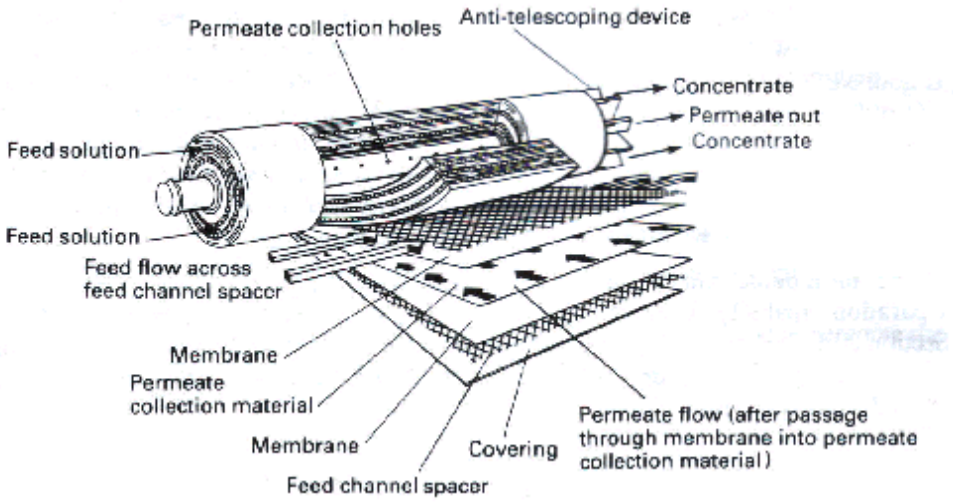

Figure 2.12: Diagram to represent a spiral wound module used in membrane separation (After Coulson et al. 1997).

2.3.8 Hollow Fibre module

The hollow fibre module consists of bundles of fine tubes of filter material bundled together inside a tubular housing (Figure 2.13). The fibre diameter is between 0.1 – 2.0 mm. Hollow fibre modules can handle high throughputs of feed, but they are not very good for processing high solids content fluids. They do have a very high surface area per unit volume, second just behind spiral wound modules. An advantage of hollow fibre modules is that they can be back flushed, which can lessen some kinds of fouling (Coulson et al. 1997).

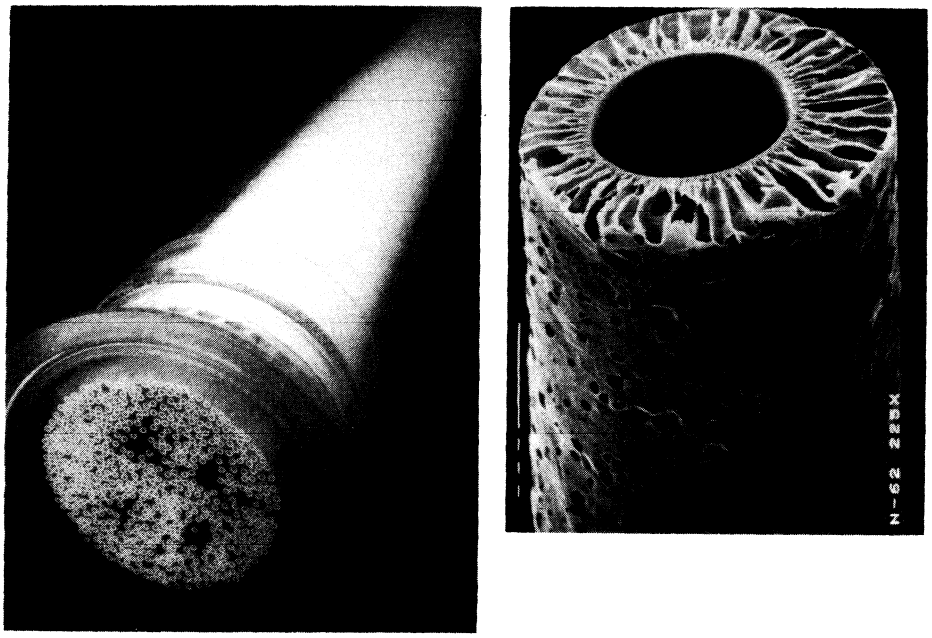

Figure 2.13: Individual Hollow fibre (right), hollow fibre module containing thousands of fibres (left) used in membrane separation (After Coulson et al. 1997).

2.3.9 Tubular module

Tubular membranes are used where a turbulent flow regime is required, for example when a high solids concentration exists in the feed. The membrane is cast on the inside of a porous support tube, which is housed within a perforated stainless steel pipe as shown in Figure 2.14 below. Individual modules contain a cluster of tubes in series held within a stainless steel permeate shroud. These tubes are generally 10 – 25 mm in diameter and 1 – 6 m long and the feed can be pumped through them at a Reynolds number greater than 10,000. Tubular modules are very easy to clean by methods such as back flushing and depending the membrane material can handle aggressive chemicals and elevated temperatures. The problems associated with tubular modules include a relatively low membrane surface area per unit volume and a high volumetric hold-up.

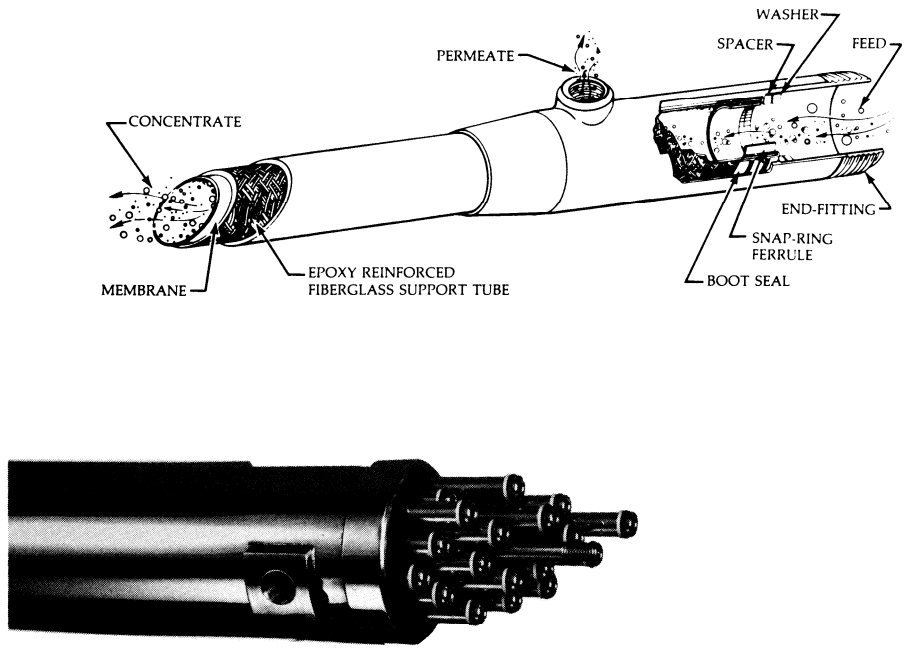

Figure 2.14: Schematic of single membrane tube (top) and picture of several tubular membrane elements housed together in its housing (bottom) (after Cheryan 1986).

	Spiral Wound	Tubular		Plate and frame system	Hollow fibre system	
		High Price	Low Price		Wide fibre	Fine fibre
Membrane Density (m^2/m^3)	high	low	low	average	average	average
Plant investment	low	high	low	high	very high	medium
Variable costs	low	high	low	average	average	low
Change of membrane only	no	yes	no	yes	no	no
Fouling tendency	average	low	low	average	low	very high
Cleanability	good	good	good	good	low	none

Table 2.6 Comparison between different membrane modules (Adapted from Wagner 2001)

Table 2.6 demonstrates a general overview of the four main module designs. The hollow fibre (wide fibre) system requires the largest capital plant investment while the fouling tendency of is low, the cleanability is also low. The use of fine fibres may reduce capital investment and running costs but the fouling tendency is very high and cleanability of membranes very low. Also these hollow fibre membranes cannot be changed within most membrane modules,

The spiral wound module system is generally the cheapest to install and run. Spiral wound modules have the added advantage of having a high membrane density, although it is not possible to change the membranes with this configuration, the same as hollow fibre modules and cheaper tubular membranes (where the whole device has to be changed instead of the whole membrane). The more expensive tubular modules require a high plant investment, high running (variable) costs and takes up a large volume of space, but the membranes can be easily changed and the fouling tendencies

of these membranes are low. Plate and frame modules have a high capital cost and average running costs and the membranes can also be easily changed like tubular modules.

2.3.10 Standard Module Configuration

The cross-flow membrane modules described above can be configured in many ways to produce a plant of the required separation capability (Coulson et al. 1997) A simple batch process can be used as shown in Figure 2.15 so that control of the system should be very simple but as the permeate is taken from the system the retentate becomes more concentrated unless water or another feed to make up the lost volume is added to the system (diafiltration) although control over this can be very difficult.

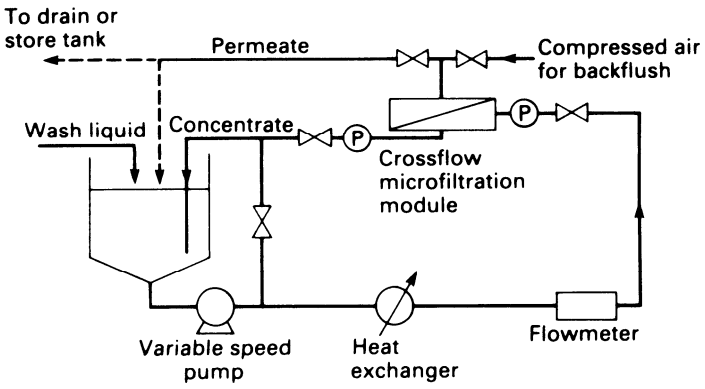

Figure 2.15: Flow diagram for a batch cross-flow system. (After Coulson et al. 1997)

Larger scale processing is also possible either by using feed and bleed or continuous single pass operations as described in Coulson et al. 1997 to overcome any issues with low flux operation or flux decline due to fouling. Hybrid processing is very useful for example when different modules and/or membranes can be used within the same process separating different materials from the feed solution.

2.4 Membrane Fouling

2.4.1 Introduction

The nature of complex feeds and membrane filtration generally causes a progressive flux decline which has a marked effect on the economic benefit of the process. This area although very well understood is still being heavily researched to understand the intricate nature of membrane fouling and inevitable flux decline.

2.4.1.1 Flux – Resistance Relationship

The flux (J_V) through the membrane can be very simply characterised by the volume of fluid V, permeating the membrane in a given time t, through a known membrane area, A_M such that the volume flux can be characterised as shown in Equation 2.1.

$$J_V = \Delta V / \Delta t A_M \qquad \textbf{Equation 2.1}$$

In membrane filtration the convective flux through the membrane can be written as shown in Equation 2.2,

$$J_V = \frac{\text{Driving Force}}{(\text{Viscosity}) \times (\text{Total Resistance})} \qquad \textbf{Equation 2.2}$$

where the driving force can be pressure, concentration, electrical or temperature as mentioned in section 2.3.1. This study will be focussed on a pressure driven process. Considering a pressure driven process where a solute is present in the feed causing additional fouling, the convective flux can then be written as shown in Equation 2.3,

$$J_V = \frac{\Delta P - \Delta \Pi}{\mu_P (R_T)} \qquad \textbf{Equation 2.3}$$

where ΔP is the hydrostatic or transmembrane pressure, $\Delta \Pi$ is the osmotic pressure, μ_P is the viscosity of the permeate solution, R_T is the total hydraulic resistance including the membrane resistance R_M and any additional resistances caused by the interaction of the solute with the membrane. The osmotic pressure of the fluid is effected by concentration and temperature and can be considered negligible in UF

(Mulder 2000) although this should be checked and does not take into account concentration polarisation. The pure water flux can then be expressed as shown in Equation 2.4 where no fouling or concentration polarisation will be observed,

$$J_W = \frac{\Delta P}{\mu_W (R_M)}$$

Equation 2.4

where μ_W is the viscosity of pure water. Equation 2.4 shows that R_M can be determined experimentally at a fixed temperature, pressure, and cross-flow velocity. Assuming the physical properties of the membrane remain unchanged throughout then R_M should be a constant. Generally there will be a change in membrane behaviour following fouling/cleaning due to permanent fouling and these changes can be determined by its pure water flux at constant conditions.

Generally a flux decline over time is noticed for separations of solutions containing solute (Figure 2.16). MF and UF process flux decline can be very severe with the process flux often being less than 5% of the pure water flux (Mulder 2000).

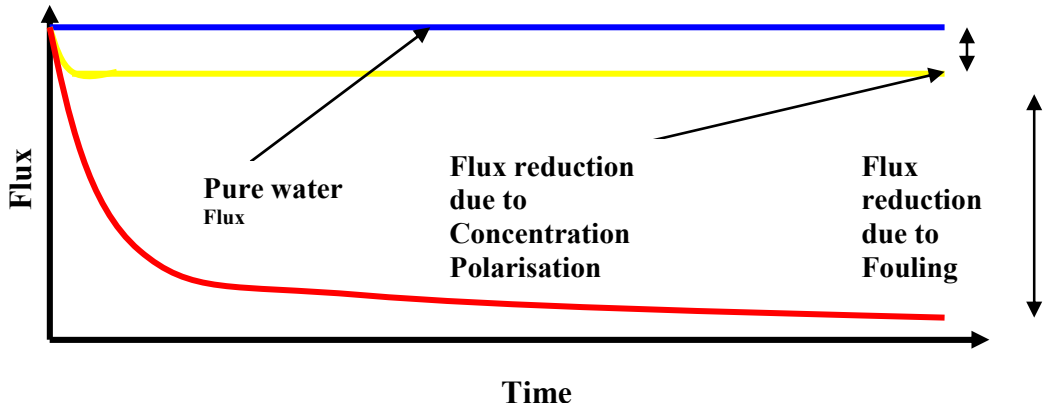

Figure 2.16: Systematic representation of flux decline in a UF process, fouling and concentration polarisation (After Bartlett 1998)

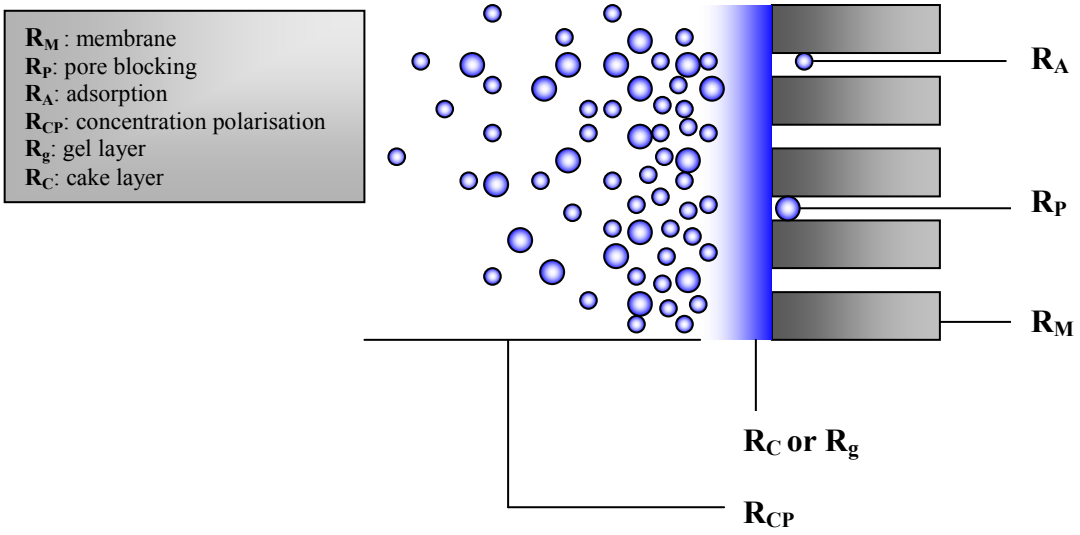

Figure 2.17: Overview of the types of resistance towards mass transport across a membrane in a pressure driven process(Adapted from Mulder 2000).

The flux decline can be cause by several increases in resistances that can be summarised as shown in Figure 2.17. During UF solutes present in the feed will initially adsorb to the membrane surface producing an adsorption resistance R_A. The solute will then attempt to travel through the porous channels of the membrane and may plug the pores producing a pore blocking resistance R_P. Solute which cannot pass through the membrane will build up at the membrane surface producing a concentration gradient. This is known as concentration polarisation and the resistance produced by trying to overcome the increase in concentration towards the membrane surface is R_{CP}. The flux decline due to concentration polarisation is shown in Figure 2.16 and discussed in more detail in section 2.4.3. This increase in concentration towards the membrane surface can cause particulates to build up forming a porous cake layer resulting in the cake layer resistance, R_C. The cake layer is usually very dense at the membrane surface and becomes less dense and more porous as the cake layer transforms to the concentration polarisation region (Tarabara et al. 2004). Instead of a cake layer sometimes a gel layer may also be formed at the membrane surface due to the high concentration and pressure associated causing a gel layer resistance, R_g. These resistances can be totalled and summarised as a resistance in series model equating to a total fouling resistance R_T as shown below:

$$R_T = R_m + R_P + R_A + R_{CP} + R_g + R_C$$

Equation 2.5

A fouling resistance R_F, can be assumed as:

$$R_F = R_P + R_A + R_g + R_C$$

Equation 2.6

so that the total hydraulic resistance can be summarised as:

$$R_T = R_m + R_F + R_{CP}$$

Equation 2.7

2.4.2 Concentration polarisation

Due to the basic principle in membrane filtration that the permeate has a lower solute concentration than the bulk feed solution an increased concentration is inevitably formed at the membrane surface due to the accumulation of the retained solute. The increased concentration at the membrane surface is now higher than the concentration in the bulk feed solution and a decreasing concentration gradient is formed from the membrane surface to the bulk feed solution. This causes a diffusive backflow of solute from the high concentration at the membrane surface to the bulk solution. After a given amount of time steady state conditions will be reached where the convective solute flow to the membrane surface will be balanced by solute flux through the membrane plus the diffusive flow back from the membrane surface (Equation 2.8). This phenomenon is termed concentration polarisation (C_P) and is summarised in Figure 2.18.

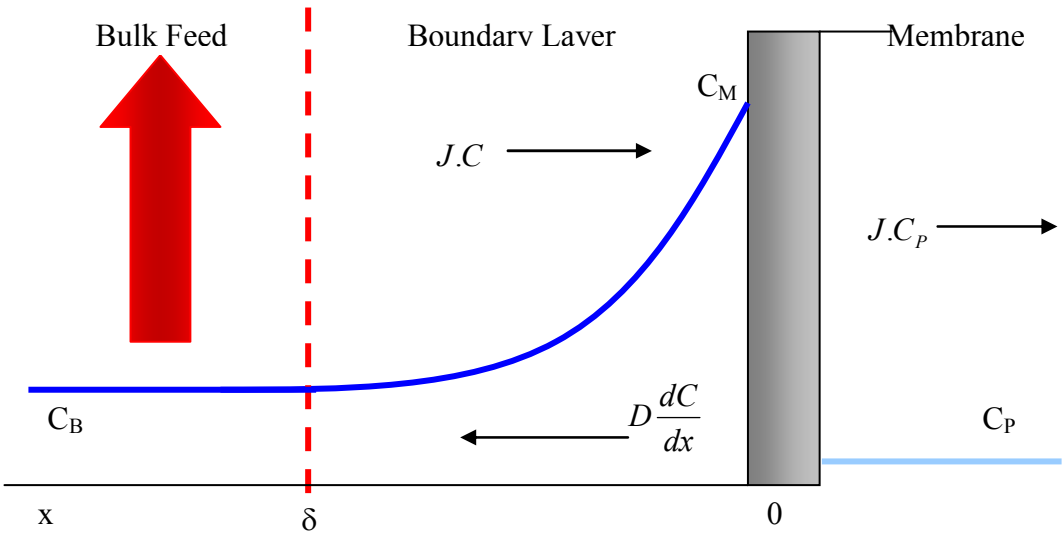

Figure 2.18: Concentration polarisation: concentration profile under steady state conditions (Adapted from Mulder 2000).

Performing a mass balance such that the convective and diffusive transports are equilibrated with the mass flux in the permeate, based on the concentration profile in Figure 2.18 leads to the following equation:

$$J.C = D\frac{dC}{dx} + J.C_P$$

Equation 2.8

where the boundary conditions are:

$x = 0 \rightarrow C = C_M$

$x = \delta \rightarrow C = C_B$

and integrating (Equation 2.8) within the stated boundary conditions results in:

$$\ln\left[\frac{C_M - C_P}{C_B - C_P}\right] = \left(\frac{J_V \delta}{D}\right)$$

Equation 2.9

The ratio of the diffusion coefficient, D and the thickness of the boundary layer, δ is termed the mass transfer coefficient:

$$k = \frac{D}{\delta}$$

Equation 2.10

Concentration polarisation, C_P, can have a variety of consequences as reported by Mulder 2000:

(i) Retention can be lower due to the build up of solutes at the membrane surface, generally true of low molecular weight solutes.

(ii) Retention can be higher especially in the case where mixtures of macromolecules solutes are present. These macromolecules form a second dynamic membrane increasing the selectivity of the membrane.

(iii) Flux will be lower due to the presence of this additional concentration polarisation resistance although concentration polarisation is not necessarily responsible for flux decline as demonstrated in Figure 2.16.

2.4.3 Gel Layer Model (Limiting Flux)

Instead of a cake layer sometimes a gel layer may be formed at the membrane surface due to the high concentration and pressure associated causing a gel layer resistance, R_g. The gel layer resistance is mostly associated with a limiting flux with an independence of TMP (Song 1998).

This model assumes that solute is totally retained and as solute builds up on the membrane surface the increased concentration causes a back diffusion, so that the convective force of solute towards the membrane surface is balanced by the diffusivity of solute back to the bulk solution. The model assumes that a limiting maximum flux has been reached independent of increased pressure. A maximum concentration gel layer is produced at the membrane surface where the thickness or compaction of the membrane increases as the TMP is increased further. Equation 2.11 has been derived from Equation 2.9 where the boundary conditions are modified such that

$$x = 0 \rightarrow C = C_g$$

$$x = \delta \rightarrow C = C_B$$

and the solute is totally retained so that $C_P = 0$.

$$J_{Lim} = k_g \ln(\frac{C_g}{C_B}) = k_g \ln(C_g) - k_g \ln(C_B)$$

Equation 2.11
(Mulder 2000)

Where,

J_{Lim} – Limiting Flux (Pressure independent region)

k_g – mass transfer coefficient (limiting flux region)

C_g – Gel concentration at membrane surface

C_B – Bulk feed Concentration

Figure 2.19 shows the difference between the pressure independent region and the pressure dependant region. For region 1 Equation 2.3 holds and for region 2 Equation 2.11 holds. The problems associated with the gel layer model are that a limiting flux

may have been reached independent of pressure but varying reports suggest very different gel concentrations. The main disadvantage of this model is the assumption that no solute passes through the membrane.

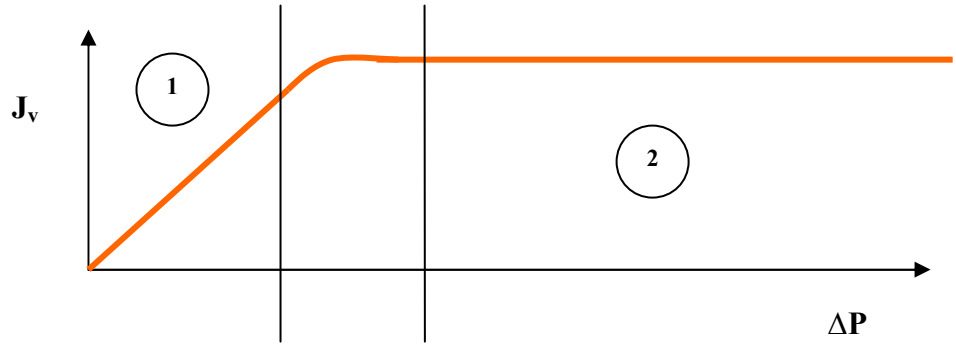

Figure 2.19: Diagram to illustrate transition for pressure dependant to pressure independent region.

2.4.4 Osmotic Pressure Model

Larger macromolecules are retained by UF membranes and smaller low molecular mass components pass through the membrane. Low molecular weight components are usually responsible for the majority of the osmotic pressure in a system, because the low molecular mass concentrations are usually similar in the feed and the permeate. In UF osmotic pressure is usually neglected.

However when operating at high flux, high rejection levels and low mass transfer coefficients, the concentration at the membrane surface can become quite high and osmotic pressure cannot be neglected (Mulder 2000). The osmotic pressure in Equation 2.3 becomes significant and the driving force is reduced due to ($\Delta P - \Delta \Pi$) causing the observed flux decline.

Aimar and Sanchez 1986 applied the limiting flux condition to this osmotic model with good results obtained in good agreement with experimental data where total solute rejection was assumed.

Meien and Nobrega 1994 suggest a mathematically intense model which includes the osmotic pressure where partial rejection of solute exists in the limiting flux region, and found that the osmotic pressure had a negligible effect on rejection and that viscosity was the major contributing factor. This model is worth considering if high

concentrations and high osmotic pressures are found, which may be affecting the flux decline in the system.

2.4.5 Boundary Layer Model

During concentration polarization, the formation of a boundary layer with higher concentration at the membrane surface exerts a hydrodynamic resistance on the permeating solvent. If it assumed that the membrane retains all the solute then the convective flow of solute to the membrane surface will be balanced by the back diffusion of solute to the bulk solution. The solvent flux can then be described by the membrane resistance (R_M) and the boundary layer resistance R_{bl}:

$$J_V = \frac{\Delta P}{\mu_P (R_M + R_{bl})}$$

Equation 2.12

Note also no gelation and limiting flux can occur with this model. Various methods have been attempted to calculate R_{bl} including using a sedimentation approach although permeate flux and rejection could not be calculated or the results were not general enough (Meien and Nobrega 1994).

2.4.6 Fouling Potential Model

The fouling potential of a membrane can be calculated based on the initial colloidal deposition onto the membrane. The fouling potential (k_f) is defined as the increment in membrane resistance per unit volume of permeate collected per unit membrane surface area as shown in Equation 2.13 below where R_T is the total membrane resistance at a given time, t, R_M is the virgin membrane resistance and V_t is the volume of permeate collected at time, t.

$$k_f = \frac{R_T - R_M}{V} = \frac{\Delta R_T}{V}$$

Equation 2.13

Song et al. 2004 demonstrate a general trend obtained from experimental work of ΔR_T vs V_t reproduced in Figure 2.20 below. The line can be separated into 3 distinct regions; the first region is the linear portion of the graph representing initial deposition of particles on the membrane surface and initial build up of cake layer. Region 2 indicates the transition to steady state conditions in region 3 where the rate of change of resistance is zero. Equilibrating mechanisms are beginning to dominate in region 3 due to tangential flow, e.g. particle rearrangement within the cake layer and the continual removal of excess particles deposited on the membrane surface. The fouling potential, k_f can thus be calculated from the gradient of the linear (Region 1) of the graph and gives a measure of how the membrane is fouled by the specific fouling material. (Song et al. 2004).

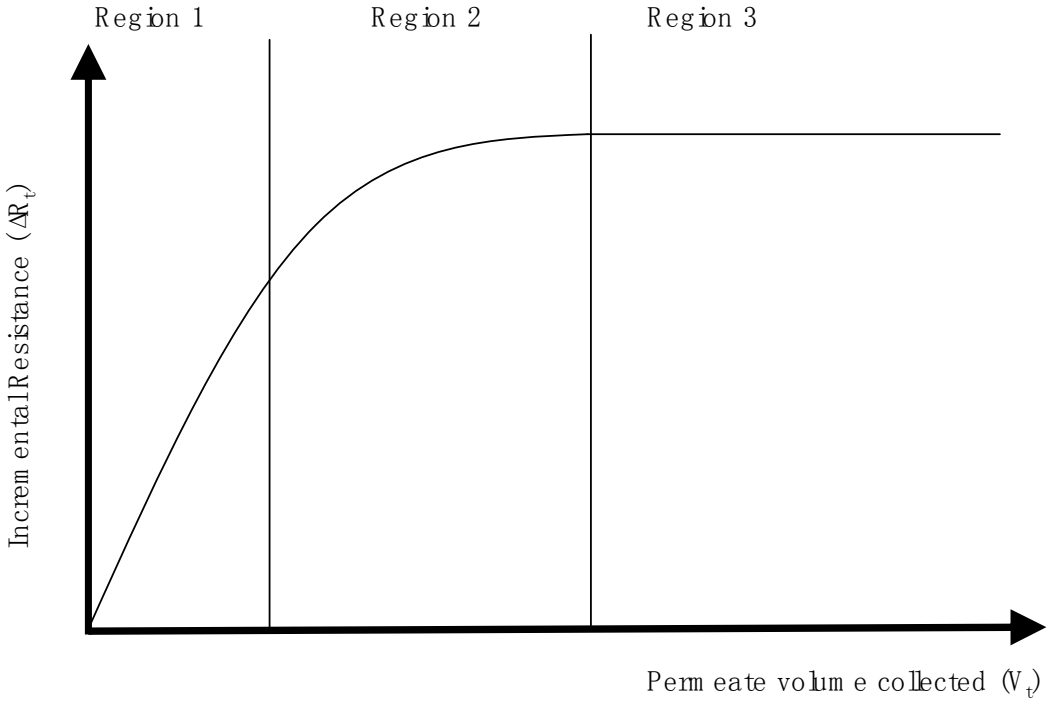

Figure 2.20: The general trend of incremental resistance vs permeate volume collected over all experiments in Song et al, 2004.

The accuracy of the fouling potential can then be tested by substituting the fouling potential in the well known cake filtration model for time dependent flux (Equation 2.14) (Singh and Song 2005).

$$J_v = \frac{J_0}{\left(1 + 2k_f \Delta P t / R_M^{\,2}\right)^{1/2}}$$

Equation 2.14

Where ΔP is the applied pressure, J_v is the permeate flux at a given time, t and J_0 is the initial virgin membrane flux. Singh and Song 2005 demonstrated that simulated (Equation 2.14) and experimental flux decline data were found to fit extremely well in all experiments performed in their study.

2.4.7 Deposit Formation

Fouling is a term that encompasses all the physiochemical causes of flux decline and change of rejection in membrane filtration processes

Depending on the type of feed and the environmental conditions of the process a number of mechanisms can occur, which lead to the formation of a deposit on the membrane surface as discussed below:

2.4.7.1 Particulate fouling

Accumulation of particulate material originally suspended in the feed. The nature in which accumulation of suspended feed occurs is of importance.

2.4.7.2 Chemical precipitation

When the feed stream becomes more concentrated, this can be due to general concentration of the retentate or due to concentration polarisation effects where increased concentrations are noticed towards the membrane surface. Solubility of the particular feed is important here and temperature effects may play a crucial role as well as concentration.

2.4.7.3 Reaction fouling

Foulants are formed by either chemical reaction within the feed fluid or on/with the membrane surface (Adsorption).

Churaev et al. 2005 studied the ultrafiltration of aqueous polyethylene glycol with different molecular masses using polysulfone membranes. The authors suggested a possible mechanism for flux reduction through adsorption of polyethylene glycol

within the pore walls which reduced the pore volume and therefore reduced the filtration velocity.

2.4.7.4 Colloidal fouling

Materials may be deposited due to their size or charge relative to membrane surface characteristics and pore size distribution. Czekaj et al. 2000 showed that beer samples with the highest initial macromolecular content cause more severe membrane fouling with cellulose acetate membranes. When polycarbonate membranes were used there was no obvious difference noticed between varied macromolecular sizes. This demonstrates the importance of membrane surface characteristics and macromolecules.

2.4.7.5 Proteinaceous fouling (proteins)

Turker and Hubble 1987 have discussed protein fouling with emphasis on adsorption to the membrane surface. A conceptual model of adsorption was constructed:

(i) Langmuir (monlayer) adsorption occurs and modifies the membrane surface properties

(ii) Kinetic deposition related to the chemical and physical environment above the membrane and the nature of the modified membrane surface.

(iii) Pressure-driven compaction of the membrane – associated protein leading to changes in flow resistance and porosity

(iv) Possibility of chemical interactions and protein denaturation leading to ageing and time-dependant changes affecting the properties of the polarised layer (Turker and Hubble 1987).

Nikolova and Islam 1998 suggest that dextran adsorbed layer resistance in UF is a linear function of the membrane surface concentration suggesting the importance of concentration polarisation and accumulation of material at the membrane surface.
Blanpain et al. 1993 notes that although protein-membrane interactions exist there is also a build up of a second dynamic membrane due to the adsorption of further layers suggesting that protein-protein interactions are also important to consider.

2.4.7.6 Summary

It is apparent that although there are different mechanisms assumed above for deposit formation that the complex situation can exist where any number of these proposed mechanisms may be occurring in simultaneously or even synergistically. For example one simple possibility is that the accumulation of solute at the membrane surface will increase the concentration at the membrane surface being enhanced by further chemical precipitation which will increase the amount of membrane adsorption occurring.

2.4.8 Fouling Mechanisms

The deposition of material from complex, multicomponent fluids has been considered to follow many different mechanisms which may be occurring in synchronisation.
Tracey and Davis 1994 suggested a potential qualitative analysis method of total resistance vs time graph could illustrate the type of fouling occurring. As illustrated in Figure 2.21, external fouling (Cake Fouling) yields a total resistance versus time curve increasing with a decreasing gradient while internal fouling is characterised by total resistance which increases with increasing gradient suggesting adsorption within pores and pore plugging. If there is a transition from internal fouling to external fouling then you would expect two distinct stages of an increasing gradient initially followed by a decreasing gradient.

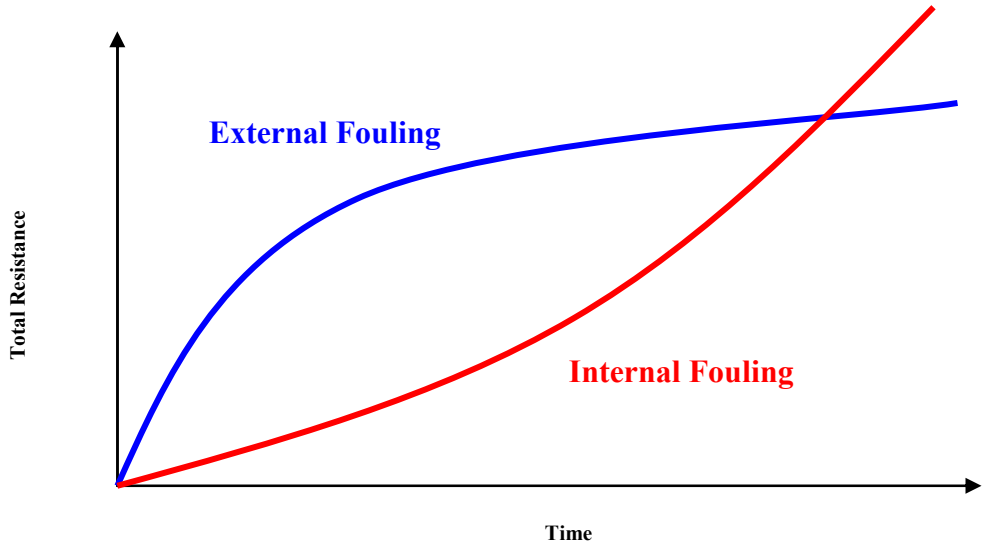

Figure 2.21: Graphs to illustrate internal/external fouling mechanisms as demonstrated by Tracey and Davis 1994.

Macromolecular transmission rates can also give an indication of membrane fouling since macromolecule transmission can be higher when internal fouling dominates, while a significant drop in macromolecule transmission accompanies external fouling (Mueller and Davis 1996).

Bowen et al. 1995 has suggested a method that MF membranes are fouled by successive or simultaneous stages:

(i) The smallest pores are blocked by all particles arriving at the membrane surface,

(ii) The inner surfaces of bigger pores are covered,

(iii) Some particles arriving to the membrane cover other already arrived particles while others directly block some of the other pores,

(iv) Finally a cake starts to be built.

Bowen et al. 1995 also describes the following classical dynamic fouling models:

2.4.8.2 Complete Blocking

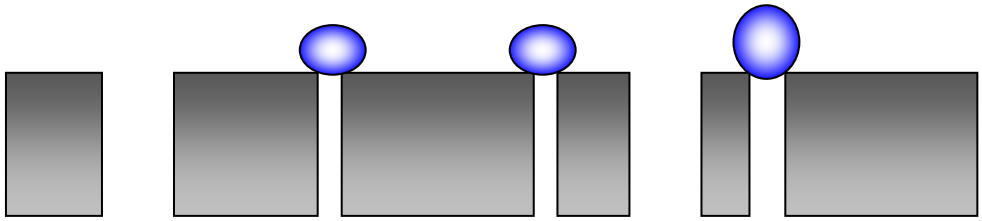

Figure 2.22: "Complete Blocking" mechanism

Complete blocking mechanism is assumed when each particle arriving to the membrane participates in blocking some pores or pores with no superposition of particles as shown in Figure 2.22.

2.4.8.3 Standard Blocking

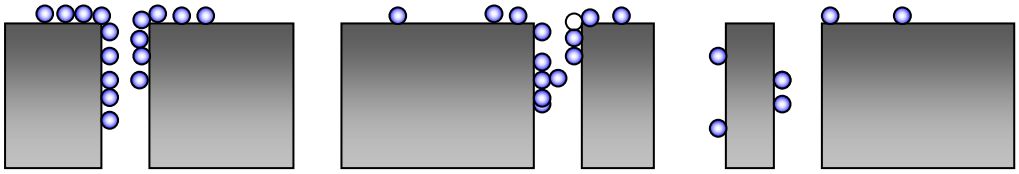

Figure 2.23: "Standard Blocking" mechanism

It is possible that each particle arriving to the membrane was deposited onto the internal pore walls leading to a decrease of in pore volume and potentially the eventual blocking of pores (Figure 2.23).

2.4.8.4 Intermediate blocking

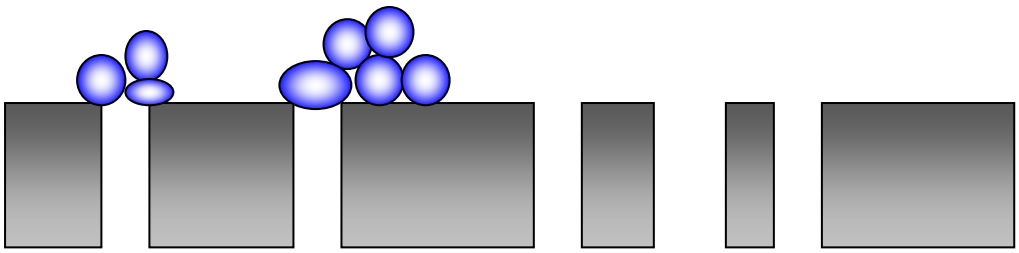

Figure 2.24: "Intermediate Blocking" mechanism

The presumption that each particle can settle on other previously arrived particles that are already blocking pores or it can directly block some membrane area is referred to as intermediate blocking (Figure 2.24).

2.4.8.5 Cake Filtration

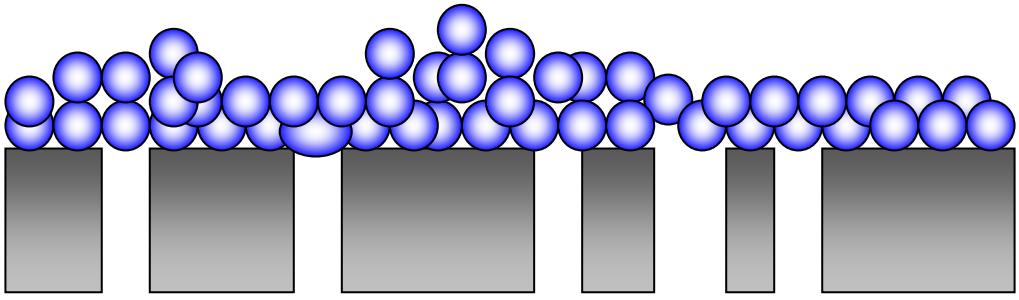

Figure 2.25: "Cake filtration" mechanism

The cake filtration mechanism occurs when each particle locates on another already arrived and already blocking some pores and membrane area. This mechanism assumes a constant increase in cake layer thickness with time (Figure 2.25).

2.4.8.6 Modelling filtration fouling mechanism

Hermia 1982 derived the intermediate blocking law and revised all four blocking laws into a common frame of a power law for non-Newtonian fluids in dead end filtration. He presented the results in the form:

$$\frac{d^2t}{dV^2} = k_H\left(\frac{dt}{dV}\right)^n$$

Equation 2.15

where V is the volume of the permeate collected in time t, where k and n are constants depending upon the mechanisms involved. The constants are summarised in Table 2.7 based on the fouling mechanisms shown in figures 2.21 – 2.25 above

Fouling Mechanism	k_H	n
Complete	K_AU_0	2
Standard	$(2K_B/A_o^{1/2})u_0^{1/2}$	1.5
Intermediate	K_A/A_0	1
Cake	$(R_rK_C/A_0^2)u_0^{-1}$	0

Table 2.7: Parameters of the blocking filtration laws for constant applied pressure

Where

K_A – blocked surface area of the membrane per unit area (m^{-1})

K_B – decrease in the cross-sectional area of the pores per unit of permeate volume (m^{-1})

K_C – area of the cake per unit of permeate volume (m^{-1})

A_0 – area of clean membrane and the cake when formed (m^2)

U_o – initial mean velocity of fluid through the membrane (ms^{-1})

R_r – ratio of the cake resistance over the clean membrane resistance

Field et al. 1995 extended Hermia's blocking laws to describe cross-flow filtration by inclusion of a back diffusion term as shown in (Equation 2.16) where the flux, J is related to the rate of flux decline/recovery (dJ/dt), the dominant mechanism can be established such that values of n are the same as with the Hermia laws as shown in Table 2.7.

$$-\frac{dJ}{dt} = k_J\left(J - J^*\right)J^{(2-n)}$$

Equation 2.16

where J^* is the flux at steady state and k_J is the fouling constant whose units depend on fouling mechanism.

Equations 2.15 and 2.16 can be fitted to curves such that an indication of the fouling mechanism can be established, a method to reduce fouling can then be implemented and cleaning procedures can be advised upon. Equation 2.15 has been fitted to many flux decline experiments in dead end mode including beer filtration (Blanpain et al. 1993). The modified cross-flow model is gaining recognition being used recently by Barros et al. 2003 to determine fouling mechanism of pineapple juice clarification in cross-flow UF.

Koltuniewicz et al. 1995 initially demonstrated the importance of the rate of change of membrane fouling resistance (R) with time and how dR(t)/dt curves can give some initial information on the mechanism of fouling occurring. Arnot et al. 2000 then extended this approach such that Equation 2.16 can be rearranged in terms of resistance such that:

$$\frac{dR}{dt} = -\frac{\Delta P}{\mu_P J^2}.\frac{dJ}{dt} = \frac{\Delta P}{\mu_P}k_J(J - J^*)J^{-n} = k_J\Delta P^{(2-n)}(\frac{1}{R} - \frac{J^*}{\Delta P})R^n$$

Equation 2.17

dR/dt is always positive or zero, but the rate of change of dR/dt with respect to time can be positive as well as negative, hence further differentiation yields:

$$\frac{d^2R}{dt^2} = \frac{k_J \Delta P}{\mu_P J^{(n+1)}} \left[(1-n)J + nJ^*\right] \frac{dJ}{dt}$$

Equation 2.18

For n = 0 (cake filtration) or n = 1 (incomplete pore blocking) the right side of Equation 2.18 will be a positive term multiplied by dJ/dt which is a negative term, due to flux decline, hence the whole of the right hand side will be negative. If n = 1.5 (standard blocking) or n = 2 (complete pore blocking) then an initial maximum will be evident in a dR/dt vs t curve. This is a good way to gain an initial analysis of the fouling mechanism occurring.

2.4.9 Fouling Conditions

Membrane fouling conditions are important to the overall process, reducing fouling and potentially increasing permeability may have a negative effect on the quality of the final product. There are many factors that can be influenced to improve the specific requirements of each system.

2.4.9.1 Temperature

The feed solution temperature can be varied consequently increasing the diffusivity of the solution and decreasing the viscosity. The decreased viscosity effects has often demonstrated increased membrane permeability and reduced total resistances (Barros et al. 2003; Vladisavljevic' et al. 2003). The positive effect of reducing viscosity can clearly be seen from Equation 2.3 where permeate flux, J_V is inversely proportional to the permeate viscosity, μ_P. The quality of permeate must be taken into consideration, Tajchakavit et al. 2001 found reduced haze in permeate of apple juice when using UF with lower feed temperatures with an obvious loss of flux. Depending on the whole process it may be desirable to perform filtration at lower temperatures saving on energy consumption to pre heat feeds. There has been little investigation into the long term fouling of membranes at varied temperatures and the mechanisms involved.

2.4.9.2 Transmembrane Pressure (TMP)

The influence of TMP on fouling conditions has been studied by many researchers with many diverse feed solutions. Generally as discussed earlier as the TMP is increased the permeate flux increases linearly eventually reaching a limiting value as represented in Figure 2.19 previously. Yeh et al. 2003 reported experimental work for the UF of Dextran T500 aqueous solutions. As the TMP was increased so was the permente flux showing that operations were within the pressure dependant region. This was also shown in Bowen et al. 1995 with the filtration of BSA. The limiting flux region has been analysed with many theories being proposed including the gel layer model and modified osmotic pressure models as discussed earlier in section 2.4.4 and 2.4.5. Barros et al. 2003 showed that flux variations in UF of pineapple juice were independent of TMP variation suggesting that they were operating within the limiting flux region. Although Vladisavljevic' et al. 2003 found that increasing TMP in UF of depectinized apple juice generally resulted in an increase in permeate flux to an optimum value, followed by a decrease in permeate flux at further increased TMP. Brujin et al. 2002 performed cross-flow UF of apple juice and showed that increasing TMP decreased permeate flux demonstrating that following this optimum region of limiting flux there can be a detrimental flux loss caused by further TMP increase.

Consideration for the quality of permeate should also be noted, Pradanos et al. 1995 found that membrane rejection decreased as TMP was increased in UF of polyethylene glycol in the pressure dependant region.

Although Barros et al. 2003 showed that little change was noticed with an increase in TMP within the limiting flux range. Blanpain et al. 1993 found that retention increased significantly as TMP was increased with MF of beer and then as the TMP was relaxed again the rejection decreased significantly. This suggests that the rejection was due to a reversible compression-relaxation mechanism that determines the porosity and hence the selectivity of a second cake layer membrane. Todisco et al. 2002 also found that increasing TMP increased rejection of the membrane when clarifying black tea using UF. Meien and Nobrega 1994 analysed the change in retention before/after the limiting flux region was reached during UF of dextran solutions. The rejection of the membrane decreased in the pressure dependant region and increased again in the pressure independent region.

2.4.9.3 Cross-flow Velocity

Generally in industry UF is performed at high cross-flow velocity causing a turbulent flow regime that reduces the formation of concentration polarisation. This has been demonstrated by many authors including Vladisavljevic' et al. 2003 and Brujin et al. 2002 who observed with the UF of apple juice that optimum flux and minimum fouling was noticed for high tangential flow across the membrane surface. Todisco et al. 2002 also found that minimum fouling resistance was noticed with a significant decrease in the rejection of polyphenols by the ceramic membranes as the CFV was increased, this observation was amplified at higher TMP. The opposite was noticed by Pradanos et al. 1995 where although the flux increased with CFV, the rejection also increased. This observation was amplified at higher pressures. Although it appears that increased CFV increases total permeability of the membrane, the increased energy consumption must be considered in the efficiency of the whole process.

2.4.9.4 Foulant Concentration

The concentration of the feed solution can affect the dynamics of the whole system. Osmotic pressure is a function of concentration and viscosity and can significantly change at higher concentrations, usually increasing. Bowen et al. 1995; Iritani et al. 1995; Yeh et al. 2003 have all demonstrated that as the foulant concentration is increased the permeability of the membrane is reduced suggesting the amount of membrane fouling or concentration polarisation is more significant at these higher concentrations. It has been reported by Marshall et al. 1993 that with regard to surface fouling, an increase of foulant concentration increases reversible fouling more significantly than irreversible fouling, although in-pore fouling is the more dominant mechanism of membrane fouling.

2.4.9.5 Feed Pre-treatment (pH)

Pre treatment of the feed solution can cause great differences in flux and transmission. pH has been shown to effect protein containing solutions where the lack of any net charge at the iso electric point (IEP) causes some interesting changes. Many authors including Iritani et al. 1995; Persson et al. 2003 have reported flux reduction at the

IEP. Reasons for this are that the protein carries no net charge at the IEP and can therefore get closer together and more concentrated in the concentration polarisation boundary layer, and therefore deposit themselves easily on the membrane surface and within the pore walls. Turker and Hubble 1987 have confirmed through protein adsorption methods that increased adsorption is noticed at the IEP. It is advantageous to pre treat the feed so that the solution is above or below the IEP providing the solution is not degraded or denatured. Persson et al. 2003 discussed membrane rejection of BSA at different pH values and found that increasing pH above the IEP increased rejection significantly compared with at the IEP as the run progressed and flux was reduced but not as much as at the IEP. When the pH was reduced below the IEP rejection was increased towards the end of the run, but the flux increased initially but then decreased with time. This demonstrates that there was increased aggregation at higher pH than lower pH due to greater ionisation of the free thiol groups responsible for aggregation. The initial increased flux at pH 3 is hypothesised to be due to swelling of the membrane at low pH values although no work was reported to demonstrate this. pH variation has also been performed with natural organic matter during reverse osmosis separation by Lee and Elimelech 2006. They discovered that pH had a significant effect on filtration with increased flux decline and increased foulant – membrane adhesion (Interfacial force measurements using AFM, section 3.5.5.5) at lower pH. At higher pH's of 6.0 and 9.0 the carboxylic groups of the natural organic matter were almost completely deprotonated and thus negatively charged. This meant that the foulant – foulant interactions were reduced due to electrostatic repulsion. Whereas at pH 3.0 the foulant was uncharged and could consequently bind with each other easily increasing the fouling layer on the membrane surface, causing increased flux decline (Lee and Elimelech 2006).

2.4.9.6 Feed Pre-treatment (Ionic Strength)

Variations in the ionic strength of the feed can significantly affect colloidal fouling. Singh and Song 2005 demonstrated that increasing the ionic strength of feed water using NaCl, increased the fouling potential of silica colloids in solution during ultrafiltration significantly. A 10-fold increase in ionic strength from 0.001 – 0.01 M for a given feed concentration had the same membrane fouling effect as doubling the

feed concentration. Persson et al. 2003 investigated cross-flow microfiltration of BSA demonstrating increased ionic strength (modified using NaCl) significantly reduced fouling flux and increased transmission of BSA. The protein molecules were shielded from each other and the filter cake by the extra ions in solution, this caused the protein molecules to act as if they were uncharged increasing BSA transmission. Although, Li and Elimelech 2004 found that ionic strength had no effect on natural organic matter filtration through a nanofiltration membrane. They investigated permeate flux decline at 10 and 100 mM feed solutions modified using NaCl. A study filtering the same natural organic matter was performed with an RO membrane by Lee and Elimelech 2006. They performed a more substantial study investigating varied ionic strengths using; 10, 30, 50 and 100 mM fouling solutions modified with NaCl also. Measurements of flux decline demonstrated that increased ionic strength reduced flux ($19\,\mu ms^{-1}$ at 10mM to $17\,\mu ms^{-1}$ at 100mM) and increased foulant adhesion (Interfacial force measurements using AFM, section 3.5.5.5). Increased ionic strength is thought to compress the electronic double layer around the charged organic matter, which would reduce electrostatic repulsion between the organic matter and the membrane surface. However changes in pH were found in this study to have a more substantial effect on adhesion measurements than ionic strength. Reducing the pH to 3.0, (where the foulant was neutrally charged) more than doubled the adhesion of natural organic matter compared with the maximum ionic strength studied. This suggests that attempted charge neutralisation of natural organic matter has a more significant influence on foulant – foulant and foulant membrane adhesion than ionic strength.

2.4.9.7 Feed Pre-treatment (Divalent Cations)

Li and Elimelech 2004 investigated the effect of adding the divalent ions; Mg^{2+} and Ca^{2+} to a natural organic matter solution to be separated by a nanofiltration membrane. The flux decline was least with no diavalent ion addition. Flux decline increased slightly with Mg^{2+} addition (1mM) and increased significantly with Ca^{2+} addition (1mM). The adhesion of model carboxyl functional groups (COO-) to the membrane was relatively small. The solution with no divalent ions had the lowest adhesion followed by Mg^{2+} then Ca^{2+} (Interfacial force measurements using AFM, section 3.5.5.5). Foulant- foulant interactions demonstrated the same trend as foulant

– membrane interactions, except that adhesion was significantly larger in the presence of Ca^{2+}. Lee and Elimelech 2006 continued to investigate calcium addition to feed solutions of natural organic matter and its effect on reverse osmosis membrane separation. They varied the Ca^{2+} concentration (0.05, 0.1, 0.3, 0.5 and 1.0mM) finding similar trends in flux decline and foulant-foulant force adhesion measurements to the previous study. Increased flux decline and increased foulant – foulant adhesion was found with increasing Ca^{2+} ion concentration. Li and Elimelech 2004 proposed a mechanism for the role of calcium, which may be attributed to intermolecular bridging / complexation of the divalent ion, which associates COO^- functional groups with COO^- groups on the clean membrane surface. When the membrane becomes fouled, the membrane surface is covered with a layer of natural organic matter, which have a greater number of COO^- functional groups causing increased adhesion and fouling.

2.4.9.8 Membrane Surface Properties

Hydrophobicity, charge, morphology and roughness of the membrane are all important factors determining transmission (Weis et al. 2003; Weis et al. 2005). Capannelli et al. 1990 have shown a good correlation between contact angle measurements and anti-fouling properties where a series of modified membranes showed that higher hydrophilicity was associated with better antifouling properties in terms of flux recovery. Vernhet and Moutounet 2002 have shown that generally hydrophobic membranes are fouled more than hydrophilic membranes when fouled with wine or its constituents. There was significantly more adsorption of polyphenols and polysaccharides under non-dynamic conditions to the more hydrophobic membranes although this deposition could not account for all the flux losses noticed. Cartalade and Vernhet 2006 followed up this work by investigating the adsorption of flavan-3-ol monomers and grape seed procyanidin fractions to differing polar polymeric microfiltration membranes. Maximum adsorbed amounts were always much higher on the more polar material. Generally monomer adsorption was partially reversible, and lower molecular weight tannis (plant polyphenols) involved an irreversible process suggesting multiple bonds with the membrane surfaces. Increasing the number of phenolic rings above two, i.e. galloylated monomers and procyanidins increased flavan-3-ol affinity for membrane surfaces whatever their

polarity (Cartalade and Vernhet 2006). Tang et al. 2003 found that the functional group for polyphenolic interaction with cellulose was the galloyl group and stronger interactions were noticed with increasing molecular weight, number of galloyl groups and the hydrophobicity of polyphenols. These hydrophobic interactions with the surface were significant and strongly depended on the flexibility of the galloyl groups. Most synthetic polymeric UF membranes with MWCO values in the range 30 kD have Ra roughness values less than 20 nm, (Weis et al. 2003) suggesting entrapment of larger macromolecules or suspended particulate may be more difficult.

2.4.9.9 Membrane Pore Size Distribution

Characterization of a UF membrane is usually based on material and molecular weight cut off (MWCO). The MWCO is calculated based on retention of a know solute where 95% of the solute is rejected. The problem with this is that no real data regarding the membrane surface is known. Gekas et al. 1990 demonstrated that porosimetric measurements of various modified polysulfone (PS) based membranes correlate more accurately to membrane performance than MWCO. The pore size and its distributions were also calculated through combined bubble pressure and solvent permeability measurements, mean radius of 5nm for 20 kDa MWCO and bimodal distribution for 50 kDa MWCO with two means of 4.3 and 15.5 nm.

Masselin et al. 2001 demonstrated that the mean pore size distribution of polyethersulfone (PES) UF membranes with a nominal MWCO of 100 kDa were around 4.5 nm by field emission electron scanning microscopy (FESEM).

Aimar et al. 1990 demonstrated that the pore radius' of 40 kDa PES UF membranes reduces following fouling with BSA whereas no change was noticed with the 10 kDa membrane. This suggests that BSA could fit to the inside of the 40 kDa membranes and not the 10 kDa membranes.

Munson-McGee 2002 show that the pore size distribution and particle size distribution is important where narrow distributions leads to a much higher membrane rejection. Results demonstrate that a 6 order of magnitude reduction in permeate concentration can be achieved with these narrow distributions.

Generally both average pore size and their distribution is important to membrane performance as well as the density of pores (porosity) contained within the membrane surface.

2.4.9.10 Particulate Size

Particle size has a profound effect on the mechanism involved in fouling, Pradanos et al. 1995 has demonstrated that different molecular weight PEG's filtered with a 2000 Da MWCO UF membrane resulted in a decrease in retention as the particle size decreases. The solute was totally retained above a MW of 4000 Da.

Pradanos et al. 1996 has analysed the fouling of inorganic UF membranes with varied proteins with different MWCO values (36, 67, 80, 150 and 270 kDa). Generally for partially retained proteins, as protein size increases the rate of flux decline decreases, although if a protein is totally retained this trend is changed somewhat. Flux decline is always divided into two successive steps separated by a narrow transition zone and when retention is appreciable a first step of pore blocking appears accounting for the major part of permeate flux decline. The nature of the second slower fouling step depends on the ratio of protein size to the mean pore size. When this ratio is far over 1.0, the retained proteins form a cake on the active side of the membrane and when below 1.0, proteins are adsorbed on the inner surface of unblocked pores leading to standard blocking (see section 2.4.8) (Pradanos et al. 1996).

Czekaj et al. 2000 found that MF of beer samples with highest initial macromolecular content caused more severe fouling when using cellulose acetate membranes. When polycarbonate membrane was used, fouling was similar for varied initial macromolecular content. Czekaj et al. 2000 also concluded that removal of all macromolecular aggregates with a MW>100 kDa almost completely eliminated the particles responsible for external fouling.

2.4.9.11 Critical Flux

The transition from only concentration polarisation to fouling has demonstrated some limiting features and is referred to as the critical flux (Goosen et al. 2004) generating a great deal of interest in the last decade. Field et al. 1995 proposed an hypothesis for MF:

"The critical flux hypothesis for MF is that on start-up there exists a flux below which a decline of flux with time does not occur; above it fouling is observed. This flux is the critical flux and its value depends on the hydrodynamics and probably other variables" (Field et al. 1995).

Experimentally, two observations have been noticed, firstly as discussed by Field et al. 1995, Benkahla et al found that as TMP was increased the flux increased linearly provided a critical flux had not been exceeded, the behaviour is totally reversible. However, if the critical flux is exceeded then reducing TMP does not restore the original flux producing hysteresis at a lower flux. It was also found that increasing CFV increased the critical flux value. Field et al. 1995 also discussed work by Hodgson et al. 1993, who found that non-intrusive observation of a 0.02 and 0.2 μm average pore size membrane surface whilst filtering a 0.1 wt% yeast suspension at low flux resulted in no cells approaching the surface.

The correct selection of initial TMP can reduce the rate of fouling providing a critical flux is not exceeded, ideally a constant-flux, rather than constant-pressure operating mode is to be preferred (Field et al. 1995).

Metsamuurronen et al. 2002 investigated critical flux using a constant flux ultrafiltration system with hydrophobic and hydrophilic membranes and dilute myoglobin solutions and baker's yeast suspensions as model colloids. The authors found two different types of critical flux. The strong form of critical flux is the point where the TMP corresponding to a set of fluxes starts to deviate from that of pure water (Figure 2.26). This type of critical flux was noticed when almost full retention occurred or when using non-retentive hydrophilic membranes at low concentrations. The weak form of critical flux is defined if the TMP of the solution deviates from the pure water TMP at the same flux, although maintaining a linear relationship as shown in Figure 2.26. This type of critical flux was observed where myoglobin molecules that were small enough to adsorb inside pore walls favouring attractive electrostatic forces and high concentrations. Critical fluxes of hydrophobic non-retentive membranes could not be found, but hydrophilic regenerated cellulose membranes were less prone to fouling and had higher critical fluxes. Generally Metsamuurronen et al. 2002 observed that critical flux increased with increasing CFV and decreasing concentration of solute. The highest critical flux was found at pH 8 in the presence of repulsive electrostatic forces between molecules and the surface of the membrane and the lowest critical fluxes at the IEP of the molecules and particles (Metsamuurronen et al. 2002).

Wu et al, 1999 also noticed that critical fluxes were increased with decreasing membrane pore size also suggesting that possible adsorption within pore walls had an adverse affect on critical flux (Wu et al. 1999).

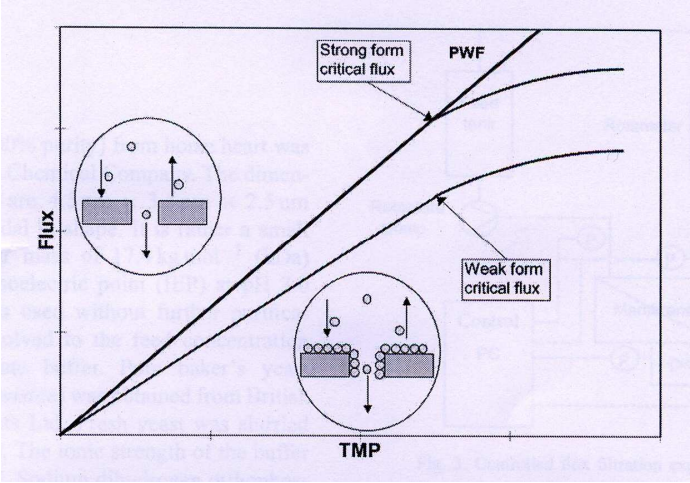

Figure 2.26: Graph to represent strong and weak forms of critical flux (from Metsamuurronen et al. 2002).

The critical flux can also be thought of as the permeate flux above which an irreversible deposit appears. Above the critical flux, fouling is self regulated where an increase in pressure leads to a higher flux than the critical flux generating a growth in deposit reducing flux accordingly to a critical value. The limiting flux (as briefly discussed in section 2.4.4) can then be thought of as the value of flux for which the critical flux is reached at all points of the membrane surface (Espinasse et al. 2002). This statement by Espinasse et al. 2002 requires significant work to understand further, Bacchin 2004 has initiated this by modelling the critical flux by the critical deposit formation at the outlet of the membrane based on mass transfer coefficients along the membrane surface. Once the critical flux has been reached along the whole membrane surface, the limiting flux is reached. The model predicts quite simplistically that the critical flux is 2/3 of the limiting flux, although further improvements are still required to fully understand critical deposit formation (Bacchin 2004).

2.5 Membrane Cleaning

2.5.1 Introduction

Even though methods to reduce fouling have been discussed in section 2.4 and should be analysed first as a method to increase the efficiency of the process, cleaning of membranes is inevitable when filtering real solutions at industrially useful fluxes.

2.5.2 Cleaning Methods

Mulder 2000 has summarised cleaning into four distinct methods: i) Hydraulic ii) Mechanical iii) Chemical and iv) Electrical. These methods are discussed below.

2.5.2.1 Hydraulic (Back flushing)

Hydraulic cleaning includes methods such as removing deposits using turbulence or reversal of TMP (only possible on tubular or hollow fibre membranes). Successful examples include: back flushing (Figure 2.27), back pulsing (or backshocking), rotating disks and secondary vortex flows although hydraulic cleaning rarely restores maximum membrane flux (Shorrock and Bird 1998). Backflushing (Figure 2.27) is a generalisation of the technique where the flow through the membrane is reversed. This is usually performed periodically to clean the membrane. More recent advances such as backpulsing (or backshocking) is a technique that entails reversing the flow through the membrane for a fraction of a second every few seconds and these times must be optimised otherwise the backflushing can be ineffectual (Mores and Davis 2002). Mores and Davis 2002 demonstrated by direct visual observations (DVO's) that fouled MF membranes with a yeast suspension were more effectively cleaned by longer and stronger backpulses although higher net fluxes were found with shorter and stronger backpulses.

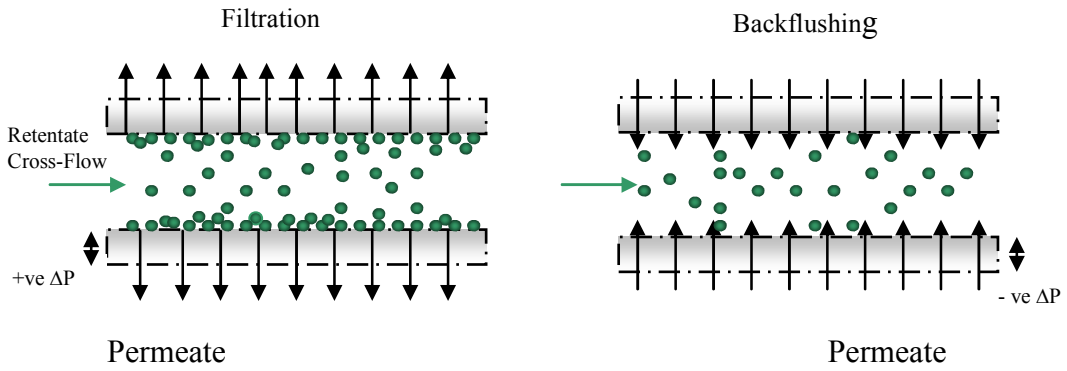

Figure 2.27: Schematic representation of membrane fouling then cleaning due to backflushing.

2.5.2.2 Mechanical

Mechanical cleaning involves scouring fouled surfaces with an abrasive material. Mulder 2000 states that mechanical cleaning is limited to tubular systems due to the accessibility and high mechanical strength of membrane surface where cleaning can be applied using oversized sponge balls (Mulder 2000). Tzeng and Zall 1990 used the scrubbing effects of carboxymethyl cellulose polymers in NaOH solution to enhance flux recovery slightly and is thought to be due to the random motion of the polymer molecules in the cleaning solution.

2.5.2.3 Electrical

Electric cleaning is performed by applying an electric field across the membrane so that charged particles or molecules will migrate in the direction of the electric field. This method can be applied without disrupting the process, although special membranes and modules are required so an electrical charge can be introduced and conducted through the membrane (Mulder 2000). The use of pulsed electric fields showed a ten-fold increase in flux when applied periodically through a process, using dispersions of both organic baker's yeast and inorganic titanium dioxide separation with sintered stainless steel MF membranes (Bowen et al. 1989). Robinson et al. 1993 also confirmed the use of pulsed electric fields as a cleaning process by demonstrating a 25 – 40% decrease in solute related resistance using UF and a bovine serum albumin feed solution (Robinson et al. 1993).

2.5.2.4 Chemical

Chemical cleaning is the most commonly used cleaning procedure in industry and usually performed as cleaning-in-place (CIP) by filling the retentate channel with a cleaning solution from a separate tank. A number of chemical cleaning agents are used (see section 2.5.3) where the nature of the deposit is significant to the choice of individual chemical or mixture of chemicals. These chemical agents can work by a number of mechanisms including chemical modification or solubilisation potentially causing displacement of the foulants from the membrane surface. Trägårdh 1989 thought that chemicals should loosen and dissolve foulants while keeping them dispersed in the solution without providing a new fouling source. The chemical resistance of the membrane is also paramount to the choice of chemical agents. In some instances use of a more chemically resistive membrane material may be advised, although care must be taken not to affect the separation process by doing this. Degradation of the membrane may occur over its lifetime due to the action of chemical agents (see section 2.5.6).

2.5.3 Chemical Cleaning Agents

2.5.3.1 Acids

Commonly mineral or organic acids such as nitric (Bartlett et al. 1995) and Hydrochloric acid (Zhang and Liu 2003) are used to chemically clean membranes. Shorrock and Bird 1998 discuss that acids are good at solubilising monovalent and polyvalent inorganic mineral salts or metal oxide films. Care must be taken with the potential corrosiveness (low pH) of acids used in membrane cleaning.

2.5.3.2 Alkali

Alkalis are very commonly used to clean fouled membranes especially when fouled with fat and/or protein containing substances. Alkalis generally saponificate fats and solubilise proteins (Shorrock and Bird 1998). Sodium hydroxide, NaOH, is probably

the most commonly used alkali because it is widely available and relatively cheap. NaOH has been used in many studies with great success to clean membranes with a variety of feed solutions including milk (Mohammadi et al. 2002) , apple juice (Brujin et al. 2002) and spent sulphite liquor (Weis et al. 2005). Optimization of alkali cleaning conditions is discussed in section 2.5.4. Li and Elimelech 2004 found that NaOH cleaning of fouled nanofiltration membranes by natural organic matter (NOM) was not significantly effective at restoring fluxes. The poor efficiency of caustic cleaning is thought to be due to the presence of Ca^{2+} cations which were shown to enhance fouling flux decline and foulant – membrane and foulant - foulant adhesion. Cleaning operating conditions such as TMP were not optimised in this study and were the same as the preceding fouling runs, optimisation of these conditions may have had an influential affect as discussed in section 2.5.4 (Li and Elimelech 2004). Similar results were found by Ang et al. 2006 investigating the same foulant on reverse osmosis membranes. Increasing NaOH cleaning time from 15 to 60 minutes also had negligible effect on cleaning efficiency suggesting limited chemical reaction between the NaOH and the foulant or that the form of deposit generated was not easily removed even at longer cleaning times.

2.5.3.3 Surface active agents (Surfactants)

Surfactants increase wettability promoting increased contact of foulant with the detergent increasing deposit removal (Shorrock and Bird 1998). Surface-active agents could be anionic, cationic, non-ionic or amphoteric. The addition of surfactants to a cleaning solution should be considered carefully as they are likely to interact with and modify the membrane surface rather that cleaning it. This was found by Weis et al. 2005 and Weis et al. 2003 when comparisons between surfactant containing *Ultrasil 11* and NaOH were made. Vaisanen et al. 2002 found that using a 0.1 wt% Libranone 960 alcohol ethoxylate non-ionic surfactant cleaning solution to recover membranes fouled with ground wood mill water resulted in an initial increase in permeability which then reduced slightly. This suggests that surfactant was initially adsorbing to the surface and then being desorbed after an amount of time.

The efficiency of a non-ionic surfactant (Tween 20) was examined to desorb lysozyme from PES membranes and was found to be efficient at cleaning over one

cycle where contact angles were recovered although removal of a hydrated lysozyme decreased in subsequent cycles (Kaplan et al. 2002). Use of the anionic surfactant, sodium dodecyl sulphate (SDS) was found by Li and Elimelech 2004 and Ang et al. 2006 to effectively clean NOM fouling of nanofiltration and reverse osmosis membranes respectively. Increasing concentration up to a critical micellular concentration (10mM) increases cleaning efficiency by solubilisation of the humic acids present in the natural organic foulant. Adsorption of the hydrophobic portion of the amphilphilic surfactant tail to the humic acid is thought to reduce the overall hydrophobicity of the foulant aiding solubilisation in solution. Due to effective cleaning at 10mM increasing the cleaning time also increased cleaning efficiency demonstrating favourable chemical reaction between SDS and the foulant layer (Li and Elimelech 2004; Ang et al. 2006). The use of surfactants on membranes used to filter food fluids is questionable, as their subsequent desorption may contaminate the food product if not adequately rinsed. Little has been published on this subject, the contamination concentrations may be very small, but surfactant toxicity must be considered.

2.5.3.4 Chelating Agents (Sequestrants)

Chelating agents are found in many detergents to prevent inorganic scale and re deposition (Shorrock and Bird 1998). Examples of chelating agents include citrate, sodium tripolyphosphate and ethylene diamine tetracetic acid (EDTA). Chelating agents are used to remove metal ions from deposits as is demonstrated by Zhang et al. 2004 with Calcium removal. EDTA did not work well on its own when used by Mohammadi et al. 2002 to clean polysulphone membranes fouled with milk. Although Na_2EDTA (a similar chelating agent) was shown to increase flux recovery of UF membranes used to treat banknote printing works wastewater where NaOH and emulsifiers were present in the cleaning solution also. EDTA was also used by Li and Elimelech 2004; Ang et al. 2006 and found to effectively clean NOM fouled nanofiltration and reverse osmosis membranes respectively. Alkali conditions (pH 11.0) were required to give maximum EDTA cleaning as well as increased concentration, cross-flow velocity and temperature. At pH 11.0, all the carboxylic functional groups of EDTA are deprotonated, thus increasing its chelating ability

enabling more effective ligand-exchange reaction between the EDTA and the alginate – calcium complexes. (Calcium intermolecular bridging discussed in section 2.4.10.7) (Li and Elimelech 2004; Ang et al. 2006).

2.5.3.5 Enzyme detergents

The use of enzymes to clean has been successful in clothes washing due to the ability of washing at lower temperatures and avoidance of extreme pH. The same advantage is possible where enzymes are usually used with sensitive membranes (Shorrock and Bird 1998).

2.5.3.6 Sanitizers

Disinfectants are used to destroy pathogenic micro-organisms (Shorrock and Bird 1998) and are usually crucial in the final step of membrane cleaning so that no biological contamination of further feed solutions can occur.

2.5.3.7 Water

Water is the solvent in which all chemicals are usually dissolved and water can produce some limited foulant removal on its own, depending upon the deposit strength, location and composition. 8% flux recovery using water was achieved by Bird and Bartlett 1995 when cleaning whey protein fouled microfiltration membranes. Minh et al. 1998 investigated water quality on cleaning with a cationic surfactant cetyl-trimethyl-ammonium bromide (CTAB), of polysulphone UF membranes fouled with reconstituted whey protein. The presence of particulates was found to contribute to severe fouling of the membrane and the presence of chloride ions dramatically decreased cleaning efficiency. Calcium and sodium ions affected cleaning mildly while nitrate and sulphate significantly enhanced cleaning efficiency. It is thought the reason for this increased efficiency is associated with the increased ionic strength, which would increase the repulsion between proteins (foulant) in solution and the membrane surface. The smaller size of chloride ions allowed closer

membrane/foulant interactions thus shielding the foulant charges causing contraction and inability of cleaning agent to penetrate the fouling layer.
Generally, increasing ionic strength was found beneficial to membrane cleaning using all ionic salts (Minh *et al.* 1998).

2.5.4 Cleaning Conditions

2.5.4.1 Concentration

The concentration of chemical cleaning agent is important for the removal of foulant deposits from membrane surface but the membrane itself must be resistant to these chemicals (discussed further in 2.5.6).
Bird and Fryer 1991 suggested a mechanism for the removal of whey protein from stainless steel heat exchanger tube using sodium hydroxide (NaOH) where initially the foulants swelled leading to a higher voidage in the fouling cake due to the inelasticity of the particles. The largest voidage can be associated with an optimum concentration of NaOH, increasing above this optimum (0 – 0.75 wt% in this case) causes a deposit which is difficult to remove by shear flow. A similar mechanism was discussed for MF in Bird and Bartlett 1995, where an optimum NaOH concentration of 0.2 wt% was found when cleaning at 0.5 bar TMP. An optimal concentration of 0.5 wt% was found for cleaning at zero bar TMP during the removal of whey proteins and whole milk deposits from sintered stainless steel membranes. The membrane type can be important to the optimisation of cleaning concentration. Bartlett et al. 1995 found NaOH optima of 0.2 wt% and 0.4 wt% for the removal of whey proteins from sintered stainless steel and ceramic MF membranes respectively. The type of feed deposited on the membrane clearly is decisive in determining the concentrations of cleaning fluid needed. Sodium hydroxide cleaning of yeast deposits formed on polyethersulphone MF membranes showed a lower optimum cleaning concentration of 0.01 wt% and cleaning of fouled UF membranes with lignosulphates showed an optimum of 0.075 wt% NaOH (Shorrock and Bird 1998). Zhang et al. 2004 demonstrated the cleaning optimisation of a mixture of cleaning agents to recover fouled UF membranes with banknote printing works wastewater. The study shows that optimum concentrations of NaOH (0.7wt%) and chelating agent, NA_2EDTA (0.8 wt%) along with an emulsifying agent, Turkey red oil (0.3 wt%) gave the optimum

cleaning conditions for this particular cleaning process. This procedure demonstrates the importance of research in membrane cleaning especially where mixtures of foulants are deposited on the membrane and a single cleaning agent may not clean the membrane adequately.

2.5.4.2 Temperature

Increasing the temperature is generally thought to increase the rate of a reaction unless degradation of chemicals occurs such as with enzymes. The viscosity of a cleaning fluid will decrease as the temperature is increased accounting for an increase in the Reynolds number. Bird and Fryer 1991 found that increasing temperature increased both initial and maximum cleaning rates, thus reducing the cleaning times for whey protein soils of stainless steel surfaces. Increasing temperature increased diffusion and reaction rates and aided dissolution of any fats present in the deposit, in their study a sudden increase in rate of cleaning was observed above 50°C. Shorrock and Bird 1998 found that when using pure water at varied temperature to clean yeast deposits on MF membranes, there was an increase in resistance recovery of the membrane with a significant increase between 40 and 50°C. This suggested that although the Reynolds Number does increase with temperature that increased thermal energy is responsible for deposit removal. Bartlett et al. 1995 studied the NaOH cleaning of MF membranes and found an optimum temperature for removal of whey proteins of 50°C for both ceramic and stainless steel membranes. This suggests that simply increasing the temperature further will not always increase flux recoveries and decrease cleaning times. Ang et al. 2006 found that doubling the temperature (°C) when cleaning with EDTA chelating agent for the removal of NOM foulant from reverse osmosis membranes, doubled the cleaning efficiency.

Overall, increasing the temperature may increase the deposit removal and rate of deposit removal from the membrane surface. This must be optimised and costs incurred by any additional heating must be balanced by additional membrane flux, reduced cleaning time and compatibility of the process at higher temperatures.

2.5.4.3 Transmembrane pressure (TMP)

A TMP is required to cause convective flow of solution through the membrane pores and during cleaning allows us to collect kinetic data. Bartlett et al. 1995 demonstrated that cleaning with a positive TMP caused a reduction in flux recovery as the pressure was increased and a maximum flux recovery was noticed at zero bar TMP. This suggests that compaction of the deposit may be reducing potential flux recovery possibly due to constituents being pushed further into pores causing increased pore blocking. Shorrock and Bird 1998 found that cleaning was enhanced with the permeate side closed suggesting that potential flow through membrane pores decreased flux recovery, this could be due to increased pore plugging potentially due to swelling. An optimum cleaning strategy is therefore likely to start with a short clean with the permeate line closed to flush away surface bound deposits, followed by a main clean at a lower TMP than was used during fouling.

2.5.4.4 Cross-flow velocity

The influence of CFV on cleaning rate has been thought to increase cleaning due to it scouring effect along the membrane surface. The change from laminar to turbulent region was investigated by Bartlett et al. 1995 and the results show a little increase in flux recovery with CFV, although negligible. This observation has also been shown by Kim et al. 1993. Potentially the reason for this is that chemical reaction with deposits on the membrane surface is critical to cleanability rather than hydrodynamic cross flow conditions. Ang et al. 2006 confirmed this by demonstrating that increasing the CFV from 0.107 – 0.428 ms^{-1} increased the EDTA cleaning efficiency of NOM reverse osmosis membrane filtration from 70 – 98%, provided the concentration was 2.0 mM. When EDTA concentration was 0.5mM no significant variation in cleaning efficiency was noticed.

2.5.4.5 Ultrasonic cleaning

In recent years, ultrasonic techniques have been used within membrane technology to prevent formation of filter cake as well as cleaning fouled membrane surfaces (Masselin et al. 2001). Ultrasound was used by Chai et al. 1999 where polymeric UF

and MF membranes fouled with peptone and were effectively cleaned by sonication, producing increased fluxes. The fouling concentration had no effect on cleanability whereas when fouling temperature was increased cleaning efficiency was also increased.

Duriyabunleng et al. 2001 showed that using ultrasonic waves on nylon 66 MF membranes whilst fouling with baker's yeast increased steady state fluxes by reducing cake resistances at the membrane surface. Optimisation of TMP and ultrasonic power was required and generally demonstrates a reduced requirement for cleaning of the membrane.

Masselin et al. 2001 subjected PES, PVDF and PAN membranes to 47kHz ultrasonic waves for two hours to determine the effect this would have on them. PVDF and PAN membranes were not significantly affected. The PES membranes were significantly affected over the whole surface increasing pore size for large pores and an overall increase in pore density and porosity. Cracks were also formed at the edges of the membrane surface. These observations must account for increased permeability noticed through the membrane after sonication. This paper shows us that care must be taken when using ultrasound on membranes where frequency and intensity must be taken into account.

Juang and Lin 2004 showed that fouling of a regenerated cellulose UF membrane with both Cu^{2+}-polyethylenimine solution and water/oil emulsions could be effectively recovered (up to 70 –80%) with low-frequency horn ultrasound (20 kHz). Under the conditions studies, careful control of ultrasonic power maintained a durable membrane and prevented any feed solution degradation.

Ultrasonic techniques have been shown to reduce the effect of fouling and enable successful cleaning, although careful consideration must be allowed for any potential degradation of membrane material and feed/cleaning solutions being used.

2.5.5 Cleaning performance analysis

2.5.5.1 Flux Recovery

The difference between the membrane permeability before fouling, after fouling, and after cleaning, can give important information in the changes that have occurred during the cycle. The flux recovery can defined as in Equation 2.19 where J_{FC} is the pure water flux of membrane subject to fouling and cleaning protocols and J_U is the pure water flux of the virgin membrane. Many variations on the same principle have been adopted such as resistance recovery (Mohammadi et al. 2002) or comparison between flux during cleaning and pure water after (Bartlett et al. 1995).

$$\%J_r = 100x\left(\frac{J_{FC}}{J_U}\right)$$

Equation 2.19
(Vaisanen et al. 2002**)**

Although useful, flux recovery does not tell the whole story. Weis et al. 2005 stated that permeate flux is a poor indicator of surface condition when more data was found by other methods. These methods are discussed in the following sections.

2.5.5.2 Membrane hydrophobicity

The hydrophobicity of a membrane surface and foulant material are of importance to the mechanism and the nature that any deposits form on the membrane surface. Many authors such as Capannelli et al. 1990; Jonsson and Jonsson 1995; Vernhet and Moutounet 2002, have demonstrated that the more hydrophobic membranes foul to a greater extent than the more hydrophilic membranes, stating that more adsorption of foulant to the membrane surface being critical to these observations.
Contact angle measurement at the membrane surface can be used to identify its hydrophobicity. The contact angle can be measured in different ways from the basic method of placing a drop on the membrane surface and measuring the angle that a tangent of the drop makes with the surface known as the sessile drop method. Also of

interest is the captive bubble method where a small air bubble is placed in contact with the membrane immersed into a liquid and the profile of this bubble measured. The main advantage of this method is that the membrane remains wet so no issues with changes in properties of the dried membranes can exist. Wilhelmy plate methods have also been used very successfully where studies of penetration velocity, contact angle hysteresis and adequate data acquisition have been studied. The method involves the immersing and withdrawing of the sample into and out of a liquid measuring the advancing and receding contact angles as shown in Figure 2.28 below (Palacio et al. 1999).

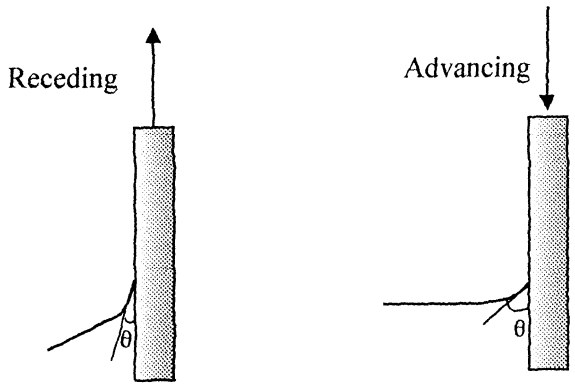

Figure 2.28: Schematic representation of the contact angle measurement with Wilhemly method (From Palacio et al. 1999).

Weis et al. 2005 examined the change in contact angle through multiple fouling and cleaning cycles of PES membranes fouled with spent sulphite liquor and cleaned with NaOH or *Ultrasil 11*. The PES membranes became slightly more hydrophobic after fouling. Cleaning with NaOH increased the hydrophobicity of the membrane from cycle to cycle. When cleaning was carried out using *Ultrasil 11,* (containing a cocktail of surfactants) a different picture appeared where the surface was initially returned to the same condition after being fouled, cleaned and then fouled again. This suggested that *Ultrasil 11* was protecting the membrane from further hydrophobic-based deposition. This protection appears to decrease with multiple fouling / cleaning cycles, where the membrane becomes more and more hydrophobic.

The contact angle measurement can also be considered in terms of the thermodynamics of the materials involved. This analysis involves the interfacial free energies between the three phases and is given by the Young equation:

$$\gamma_{lv} \cos\theta = \gamma_{sv} - \gamma_{sl}$$

Equation 2.20

Where θ is the measured contact angle, γ_{lv}, γ_{sv} and γ_{sl} refer to the interfacial energies of the liquid / vapour (surface tension), solid / vapour and solid / liquid interfaces respectively. The chemical potential in the three phases should be equal as demonstrated by Equation 2.20. The contact angle can then be used to calculate the work of adhesion, W_a, which is defined as the work required to separate the liquid and solid phases, or the negative free energy associated with the adhesion of the solid and liquid phases. This is used to express the adhesion per unit area between the two phases. It is given by the Young-Dupre equation below:

$$W_a = \gamma(1 + \cos\theta)$$

Equation 2.21

Therefore hydrophilicity is indicated by smaller contact angles and higher surface energies and hydrophobicity by larger surface energies and lower surface energies.

2.5.5.3 Surface Charge

The surface charge on membranes has a significant influence on its filtration and fouling tendencies. The surface charge of a porous membrane is related to the zeta potential of the membrane (Weis et al. 2003). The zeta potential of porous materials are usually evaluated from electrokinetic experiments, such as electroosmosis and streaming potential involving saline solutions (Martin et al. 2003). A theoretical explanation of surface effects due to zeta-potential can be found in section 3.6.5. The most widely used technique measures the streaming potential through the pores, although measurement of streaming potential along the membrane surface is possible enabling the calculation of the zeta potential of the membrane surface (Huisman et al. 2000). Nyström et al. 1994 demonstrated the effect of flux decline through UF membranes fouled with BSA using a combined streaming potential – flux method. The authors found that adsorption of BSA onto polysulfone membranes modified the zeta potential close to the zeta potential of BSA at the equivalent pH. When the

solution was modified to pH 3 the membrane became positively charged and the zeta potential was not changed by BSA. This was probably because of an electrostaic repulsion caused between BSA and the membrane surface. This paper demonstrated the importance of pore surface charge on foulant – membrane interactions. Weis et al. 2005 investigated UF of spent sulphite liquor analysing the streaming potential on pore walls of polyethersulfone membranes. The authors investigated the effect of single/multiple fouling and cleaning cycles, using NaOH and *Ultrasill 11* (containing NaOH and chelating and surfactants) cleaning solutions. The membranes became more negatively charged after fouling and using NaOH the zeta potentials were restored more closely to the virgin surface after cleaning. Over multiple fouling/cleaning cycles the zeta potentials became increasingly more negative. When cleaning with *Ultrasil 11* the results were very different, the zeta potential values progressively became more negative with subsequent fouling and cleaning treatments. The surfactants were thought to be adsorbing on the fouling layer causing these affects. The same process was repeated with regenerated cellulose (RC) membranes where little difference was noticed between the affect of NaOH and Ultrasil 11 over the first 7 cycles. After this the *Ultrasil 11* cleaning agent started to restore product fouling fluxes almost to that of the virgin membrane. It is theorised that adsorption of foulants on the membrane surface enabled surfactants from *Ultrasil 11* cleaning solution to adhere and modify the surface (Weis et al. 2005).

2.5.5.4 Membrane Surface morphology

Scanning electron microscopy (SEM) has been widely used to determine qualitative information about membrane surface morphology before and after fouling.

SEM analysis consists of an electron beam being fired upon the membrane sample that is usually coated in a conductive element if required (usually carbon or gold). A detector is used to determine a visual image of the membrane surface which can be magnified up to 80,000 times so visualisation of 100nm is possible. X rays being reflected from the membrane surface can also be determined at the same time by an x-ray detector (XRD) providing information on any elements larger than carbon. The combination of SEM and XRD can provide invaluable information on difference

between virgin membranes and fouled / cleaned membranes where characterization of deposits found are demonstrated by Rabiller-Baudry et al. 2002.

The more technically complicated transmission electron microscopy (TEM) with varied sample preparation can be used to gain insight into the asymmetric nature of the membrane (Chan and Chen 2004).

Atomic force microscopy (AFM) is primarily used to probe the membrane surface topography and interactions on the atomic-molecular scale (Chan and Chen 2004). A laser beam is reflected from the cantilever to an optical sensor, while analysis is performed, the tip is translated over the sample and the deflections are detected by this optical sensor as shown in Figure 2.29 (Chan and Chen 2004).

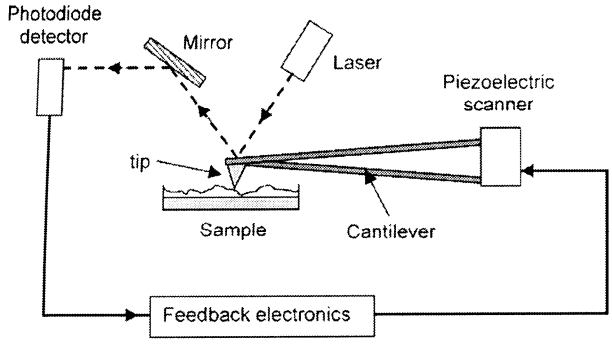

Figure 2.29: Schematic of AFM characterisation (From Chan and Chen 2004).

There are two different modes of operation; in contact mode the tip touches the surface while the cantilever moves across. In non-contact mode the tip does not physically touch the surface, although forces between the tip and the surface are still present. AFM can give a lateral resolution of 0.1nm and a vertical resolution of 0.01 nm enabling very accurate descriptions of the membrane surface. Surface morphology affects the accuracy of this method, where flatter harder surfaces result in a higher resolution than rougher surfaces (Chan and Chen 2004). AFM has been successfully used to characterize the structure and morphology of various types of UF membranes, focusing on pore size, pore size distribution, porosity and surface roughness in contact mode (Chan and Chen 2004).

2.5.5.5 Atomic Force Microscopy (AFM) with Chemical Specificity

The use of AFM has been advanced such that the silica spheres can be attached to tipless cantilevers using micromanipulation techniques. The silica probes can then be coated with gold followed by chemical modification with the desired agent. Vegte and Hadziioannou 1997 used this technique to measure intermolecular forces between different functionalities (CH_3, OH, NH_2, COOH and $CONH_2$).

There have been novel studies to examine membrane filtration mechanisms using AFM where silica probes have been modified with proteinaceous species. For example, Bowen et al. 2002 found that hydrophilicity, pH as well as fouled surface roughness were important in the separation of BSA using UF membranes.

Li and Elimelech 2004 have used interfacial force measurements to understand the nature of fouling with a model organic foulant, and effect of cleaning with different agents with nanofiltration membranes. Interfacial force measurements were performed in a wet cell using a carboxylate modified latex sphere attached to a tipless cantilever as a surrogate for the organic foulant. Attractive and adhesive (retraction) measurements were performed on a clean membrane surface to investigate the intricate nature of initial foulant deposition, (foulant – membrane interaction) and on a fouled membrane to understand the nature of foulant – foulant interaction. Fouling conditions, ionic strength and divalent ion concentration were investigated in this paper and are discussed in 2.4.10. Adhesive force measurements were performed with the modified colloid probe on a fouled membrane, in the cleaning environments similar to process conditions, where lower adhesive forces demonstrated better cleaning. NaOH, ethylenediaminetetraacetate (EDTA) and sodium dodecyl sulphate (SDS) were tested separately as cleaning agents at a constant pH of 11 and are referred to in section 2.5.3 and 2.5.4 (Li and Elimelech 2004). This work was followed up with a comprehensive study of the effect of chemical cleaning on foulant interfacial force measurements (using AFM) with varied cleaning solution type, pH and dose (Discussed in more detail in section 2.5.3 and 2.5.4) (Ang et al. 2006). Lee and Elimelech 2006 performed another comprehensive study investigating the influence of fouling conditions. Variations in foulant interfacial force measurements were conducted at varied fouling solution pH, ionic concentration, divalent concentration and organic foulant concentration. (Discussed in section 2.4.10) (Lee and Elimelech 2006).

2.5.5.6 Chemical Nature (ATR-FTIR)

Attenuated total reflection-Fourier transform infrared spectroscopy (ATR-FTIR) is generally used to understand the types of chemical bonds or functional groups present on a membrane surface. A sample is pressed against an internal reflection element (IRE), usually a block of zinc selenide or germanium under vacuum conditions. Infrared (IR) radiation (4000 – 400 cm^{-1}) is focused onto the end of the IRE where the beam undergoes total internal reflection before exiting and arriving at a detector. At each internal reflection the IR beam penetrates the surface slightly forming an evanescent wave at the interface (Figure 2.30). ATR-FTIR therefore shows the absorbance intensity vs wavenumber for the materials at the membrane surface corresponding to certain functional groups (Chan and Chen 2004). Rabiller-Baudry et al. 2002 used ATR-FTIR to determine the cleanliness of the UF membranes after fouling and cleaning with skimmed milk by comparing virgin membrane surface with that of a fouled/cleaned surface. It was shown that initial membrane surface profile could not be obtained, even though hydraulic fluxes were recovered. Weis et al. 2005 also demonstrated that even though high flux recoveries were determined following cleaning procedures over multiple cycles, FTIR identified the inability of the cleaning agent to return membrane surfaces to pristine state.

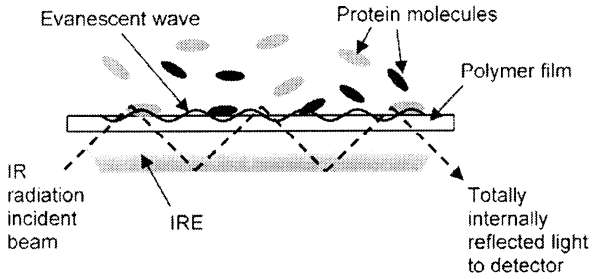

Figure 2.30: Schematic representation of ATR-FTIR (From Chan and Chen 2004).

2.5.5.7 Summary

Vaisanen et al. 2002 demonstrated that a combination of various characterization techniques; flux recovery, SEM, FTIR and AFM can provide an all round description of fouling and cleaning mechanisms. A single method does not always give sufficient information and can even result in misleading conclusions being drawn as demonstrated by a sole reliance upon flux recoveries.

2.5.6 Membrane Durability

The resistive properties of a membrane can be a limiting factor in the fouling/cleaning process over its lifetime. The chemical resistance of a membrane is an important characteristic especially where extreme pH is used either within feed solution or more commonly with the cleaning solution. The use of high pressures and temperatures during production may cause some polymeric membranes to undergo irreversible compaction, membrane 'creepage' or even the separation of the membrane from its backing material (Cheryan 1986). Persson et al. 1995 performed mechanical and hydrodynamic precompression of polymeric UF membranes. Even modest precompression (0 – 0.4 MPa) caused compaction decreasing membrane thickness and reducing water permeability, although hydrodynamic compaction gave less permeability loss than static mechanical compaction. Due to performance loss, precompression should be avoided with polymeric UF membranes.

As shown later in this study with organic membranes (section 3.1.2), the pH, pressure and temperature are given strict limits for production and cleaning by the manufacturer. Regenerated cellulose has stricter limits due to its easily degraded nature when compared with the Fluoropolymer membranes. Ceramic inorganic membranes such as oxides of zirconium and aluminium have demonstrated promise of enhanced use in industry due to their highly chemical and thermal resistance properties able to resist extreme pH and elevated temperatures (>200°C) and pressures (>30bar) (Daufin et al. 1991). However, these membranes are significantly more expensive to produce compared with organic membrane materials.

2.6 Conclusions of Literature Review

Based on the information represented in the literature review the following conclusions can be made:

Tea is largely characterised by its high polyphenol content providing antioxidant properties which have been linked by numerous studies to reduction in risk to health.
Black tea is produced via a fermentation method changing the properties of the tea leaves producing many more complicated polyphenols which are still being researched with slow progress.
Black tea is made up of many large polyphenols, proteins, methylxanthines etc and during production of RTD tea is faced with a phenomenon known as tea creaming.
Tea Creaming is a precipitation phenomenon producing haze in solution enhanced upon cooling of infused black tea, which is required to produce RTD tea. Concentration, pH and time / temperature history are the main factors determining tea cream formation.
Currently, a combination of alkali treatment with centrifugation is used to produce RTD drinks. A membrane separation process has been shown to remove the larger tea cream aggregates and larger polyphenols responsible for tea creaming. Ultrafiltration membranes with MWCO of 1000 or greater might achieve this separation.
Cross-flow UF has been successfully used in industry to separate higher concentrations of solute where fouling is significant. Flat sheet or tubular ultrafiltration modules are advantageous where high concentration severe fouling takes place. In flat sheet modules detection of damaged membranes is possible.
The biggest issue with membrane separation processes is flux decline cause by fouling. Fouling has been extensively studied based on increases in overall resistances which can be broken down into several components; membrane, pore blocking, adsorption, concentration polarisation, gel layer and cake layer resistances. Many models have been derived to describe fouling, and numerous mechanisms proposed to understand deposit formation such as the gel layer model where a limiting maximum flux is observed with a maximum membrane wall concentration. The osmotic and boundary layer model also predicts flux data, although no model exists to

predict fouling conditions in all circumstances due to the large number of variables involved.

Deposit formation on the membrane surface and within pore walls can be thought to be due to one or more of the following mechanisms; particulate fouling, chemical precipitation, reaction fouling, colloidal fouling and proteinaceous fouling.

The simplistic mechanism of this deposit formation has been analysed in terms of external and internal fouling based on resistance time data and transmission data. Although the classical dynamic fouling models describe the mechanisms in more detail; complete blocking, standard blocking, intermediate blocking and cake filtration mechanisms are possible. Some of these mechanisms can occur sequentially or simultaneously depending on filtration conditions.

The power law model for non-Newtonian fluids has been successfully used for dead end filtration and modified for cross – flow filtration such that flux vs time data can be analysed and information regarding fouling mechanism deduced.

Fouling conditions such as temperature, TMP, CFV, concentration of feed require optimising for each requirement. Feed pre treatment may be advantageous, especially where protein containing solutions are used and the pH can be varied. Ideally conditions away from the IEP of the protein are advantageous to the filtration process.

The flux at which no decline is observed with time and no fouling occurs is loosely defined as the critical flux. TMP, CFV, feed concentration, membrane surface conditions and pore size are all factors in determining the critical flux value.

In most cases where real liquors are filtered, fouling is inevitable. After filtration has been optimised to reduce fouling, cleaning is required. Cleaning can be performed hydraulically (backflushing), mechanically, electronically or most commonly, chemically. Various chemical cleaning agents can be used including; acids to remove mineral salts, alkalis to remove fat and/or protein and surfactants, chelating agents, enzymes and sanitizers. A mixture of chemicals in solution has been shown to increase cleanliness of the membrane, or a cycle of cleaning agents, for example alkali followed by acid.

Water is predominantly the solvent used for all these chemicals. The quality of this water is important to the cleaning efficiency of the cleaning solution. Particulate, chloride ions, calcium and sodium ions have been shown to affect cleaning while nitrate and sulphate ions increased cleaning efficiency. It is thought that the associated increase in ionic strength caused by the nitrate and sulphate ions increased

protein (foulant) repulsion which reduced interactions with each other and the membrane surface.

Cleaning conditions such as temperature, TMP, CFV and concentration of cleaning solution must also be optimised.

Ultrasonication of membranes can be used during filtration to reduce fouling or after fouling to clean the membrane.

Care must be taken when cleaning not to damage the membrane. Extreme pH, high pressure and temperature during filtration may cause some polymeric membranes to be irreversibly changed. Inorganic membranes are generally more resistant to damage than organic membranes.

Cleaning performance can be analysed via flux recovery of the membrane, i.e. the difference in pure water fluxes before filtration and pure water fluxes after cleaning. However, flux recovery alone does not give sufficient information regarding the cleanliness of the membrane.

There are a number of other techniques that can be used to analyse cleaning performance. Contact angle measurement and zeta potential measurements give details of membrane polarity and surface charge. SEM, XRD, TEM, AFM and ATR-FTIR together give information regarding the membrane surface morphology, pore size and distribution and detailed information regarding deposit formation on the membrane surface.

Chapter 3 Materials and Methods

3.1 Raw Materials

3.1.1 Foulant (Tea Reconstitute)

Soluble spray dried black tea powder was supplied by Unilever R&D, Colworth. Reconstituted tea was made up to the desired temperature by initially dissolving in reverse osmosis (RO) water at 80°C, then mixed with RO water at ambient temperature to obtain the desired final mixture temperature of 50°C. A feed volume of 8 litres was used.

3.1.2 Chemical Cleaning Agent

Sodium Hydroxide (NaOH) of technical grade from *Fisher Scientific* was used to clean the membranes due to its ability to break down (hydrolyze) protein/polysaccharide containing substances. The concentration and hence pH of the NaOH solution could easily be determined and was important depending on the nature of the membranes used, the pH vs wt% of NaOH follows an exponential relationship as can be seen in appendix 7.1.6 . Concentrations ranging from 0.01 – 0.5wt% (pH 10 – 13.5) were used in this experimentation, the solutions made by adding the desired mass of powder to the required mass of RO water at a desired temperature. The feed mass of cleaning agent varied from 4 – 8 kg (about 4-8 litres).

3.1.3 RO water

The water used in all experimentation was reverse osmosis (RO) treated water. The local towns water contains a significant amount of dissolved metal carbonate solids. Using a water hardness test (Gesamtharte-test) initially the composition of local tap water was in excess of 370mg/litre $CaCO_3$ (over 26°e), after filtration the permeate as used in all experiments showed a min detect value of below 50mg/litre $CaCO_3$ (below 4°e).

3.1.4 Synthetic Membranes

Seven different polymeric membranes were evaluated.
Three comprised of fluoropolymer;

(i) FP10 (FS80PP) – 10 kDa NMWCO

(ii) FP30 (FS50PP) – 30 kDa NMWCO

(iii) FP100 (FS40PP) – 100 kDa NMWCO

and one of polysulfone;

(iv) PS100 (GR40PP) – 100,000 Da NMWCO all ultrafiltration flat sheet membranes from Alfa Laval Nakskov (previously DSS / Danish Separation Systems).

In addition, three regenerated cellulose polymeric membranes were used

(v) RC10 - 10 kDa NMWCO

(vi) RC30 - 30 kDa NMWCO

(vii) RC100 - 100 kDa NMWCO from Microdyn-Nadir (previously Hoechst).
.The choice of membranes was made due to their characteristic differing properties where the FP and PS membrane are regarded as having a more hydrophobic active layer whereas the RC membrane is regarded as having a very hydrophilic active layer. The recommended operational limits of the three membranes are summarised in table 3.1 below.

		Product Filtration	Cleaning
Fluoropolymer membranes	pH range	1 - 11	1 - 12
	Pressure, bar	1 - 10	1 - 5
	Temperature, °C	0 - 60	0 - 65
Regenerated Cellulose membranes	pH range	1 - 10	1 - 10.5
	Pressure, bar	1 - 10	1 - 5
	Temperature, °C	0 - 55	0 - 60
Polysufone membranes	pH range	1 - 13	1 - 13
	Pressure, bar	1 - 10	1 - 5
	Temperature, °C	0 - 75	0 - 75

Table 3.1: Recommended operating conditions (After DSS plant No. 517551 operation manual).

3.2 Membrane module

Experiments on each of the membranes were carried out using a DSS LabUnit M10 model containing 4 polysulfone flat sheet membrane module plates in series held together by stainless steel supports, figure 3.1. The module internal volume was 57ml providing a membrane filtration area of 336cm^2. The flow paths of a single plate are shown in figure 3.2, the four plates are placed in series such that the outlet from one plate becomes the inlet to the next. The plates are in bundles of two such that there was a single permeate outlet from each bundle resulting in two permeate lines as can be seen in figure 3.1. The retentate is passed out of the other side of the module.

Figure 3.1: Picture of DSS Labunit M10 module with 4 polysulfone plastic plates in series held together by stainless steel supports.

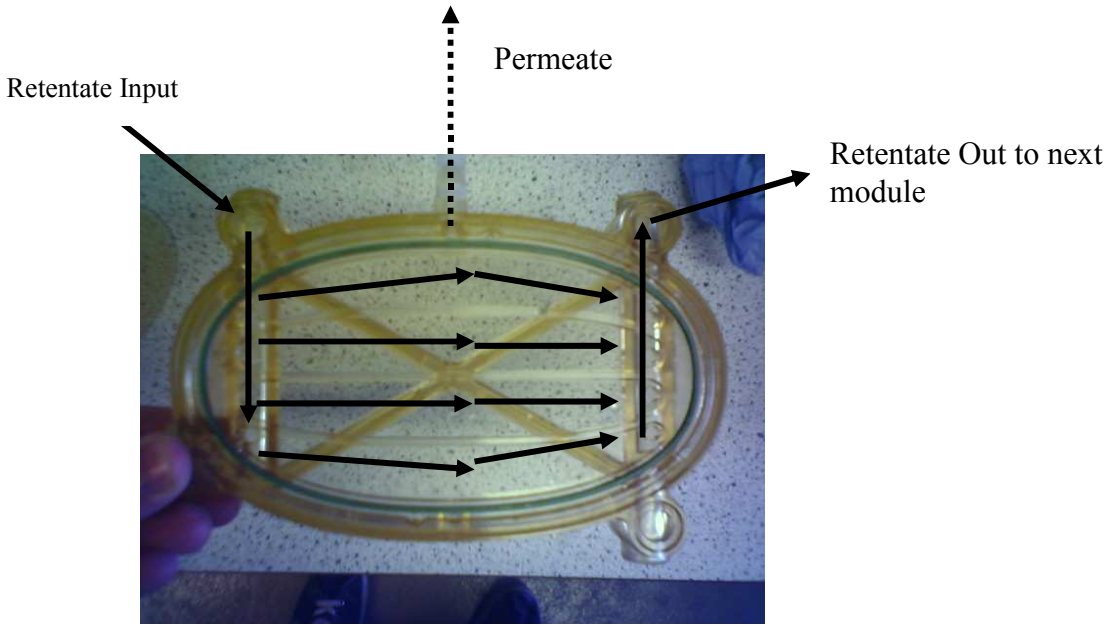

Figure 3.2: Picture of one polysulfone plastic plate showing flow paths.

3.3 Experimental Rig

3.3.1 Initial Setup

A picture of the LabUnit M10 rig can be seen in Figure 3.3and a schematic of the whole batch mode rig can be seen in Figure 3.4. A variable speed positive displacement pump was used capable of pressures up 6 bar and a heat exchanger which was used to maintain temperatures in the system using controlled temperature water from a water bath. The flow within the system was measured using a cone rotameter (calibrations shown in 7.1.4) and the transmembrane pressure (TMP) was measured by the average of pressure gauges before and after the module assuming the permeate was exiting at 0.0 bar gauge (Pressure gauge calibrations shown in 7.1.3). The flux of permeate through the membrane was calculated from the mass recorded by the College B3001-S mass balance measured to the nearest 0.1g in accordance with example calculation 7.3.1 . Two 10 litre Perspex tanks were used with this rig, one to store the feed (RO water/tea solution/NaOH solution) and the other was used as drainage when the rig was flushed. There was a sampling point for both of these tanks.

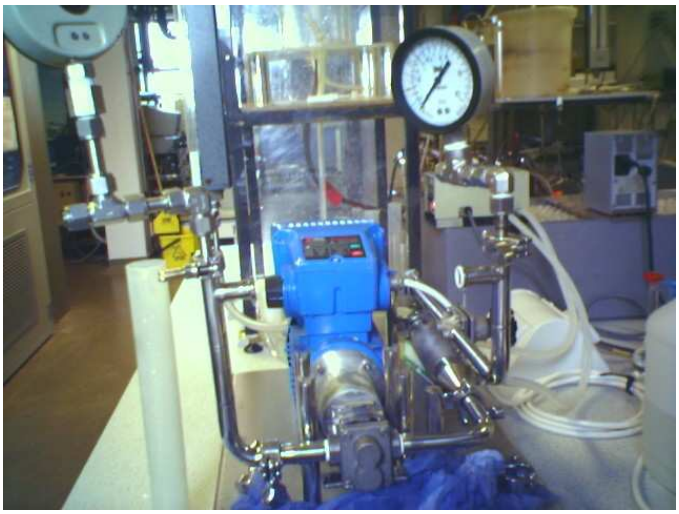

Figure 3.3: Picture of the whole DSS Labunit M10 rig without the flat-sheet module

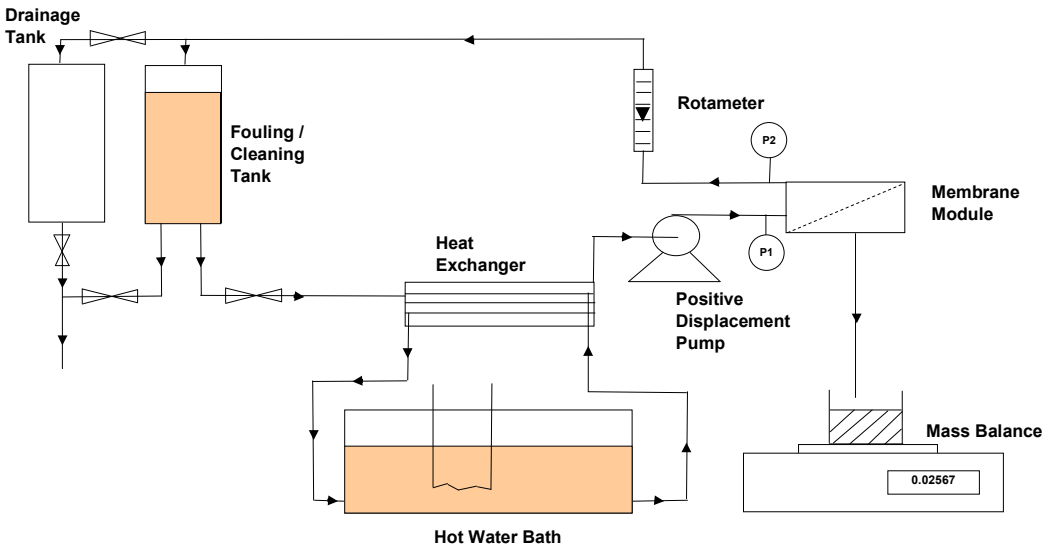

Figure 3.4: Schematic diagram of DSS Labunit M10 model, showing periphery requirements

3.3.2 Rig Modifications

The rig shown in Figure 3.4 was then modified with automatic temperature, pressure and mass balance measurements as shown in Figure 3.5 below. Two temperature thermocouples (TT) were added; one to the bottom of the feed tank (TT2) and the other at the inlet to the membrane module (TT1). The two original pressure gauges initially used to measure inlet pressure (P1) and outlet pressure (P2) from the module (Figure 3.4) were replaced by pressure transducers (DRUCK ® 0 – 7 Volts), PT1 and PT2 respectively. Calibrations for the new equipment can be found in 7.1.3 . The mass of permeate was still measured by the College B3001-S mass balance measured to the nearest 0.1g with the added capability of being automatically logged by connection to the computer system. All temperature, pressure and mass balance data were automatically logged using Advanteck VisiDAQ Version 1.1 acquisition software. The logged data was then transferred to Microsoft ® Excel, 2003 for analysis.

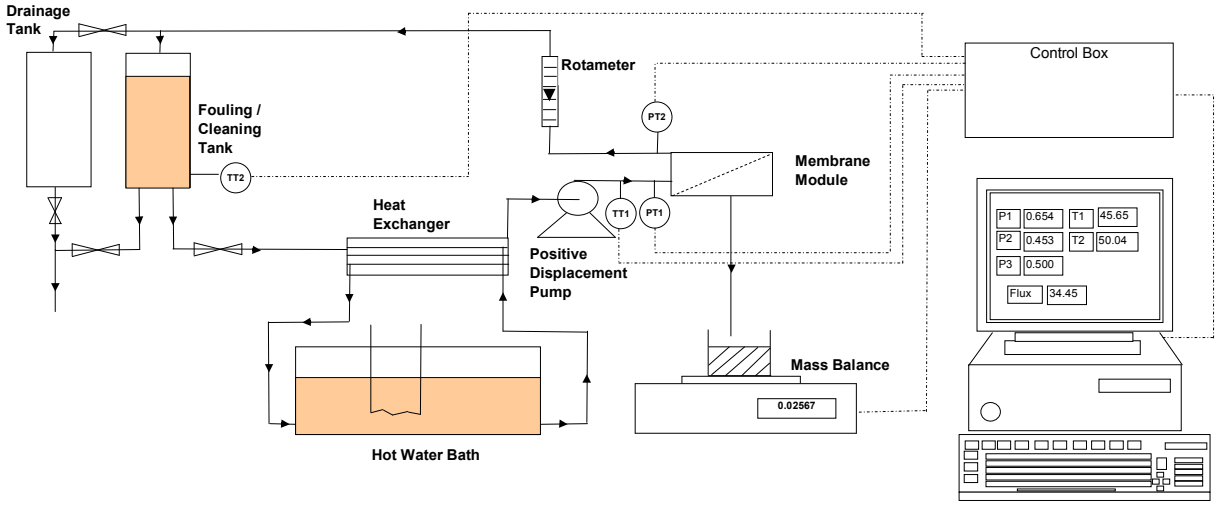

Figure 3.5: Schematic of DSS Labunit M10 showing modified model periphery requirements.

3.4 Experimental Procedure

3.4.1 Membrane conditioning

The membranes were initially conditioned using the hot wash protocol previously described by Weis et al, 2005 to remove glycerine preservative (which has been shown to affect membrane performance). The membranes were washed using RO water at 60°C for 90 min with a TMP of 1.0 bar at a cross flow velocity of 1.87 ms^{-1}.

3.4.2 Pure water flux measurements

Pure water flux measurements were determined for each membrane prior to initial fouling. Following fouling and cleaning cycles, pure water flux was again measured. The conditions used for pure water characterisation were: a feed temperature of 50°C, a TMP 0.5 bar, a cross flow velocity (CFV) 0.44 ms^{-1}, a feed volume of 6 litres, a flush time of 3 minutes and a recycle time of 7 minutes.

3.4.3 Chemical cleaning using sodium hydroxide

Under optimal thermohydraulic conditions, sodium hydroxide can be an effective cleaning agent for protein based deposition on synthetic membranes, causing peptide bond hydrolysis, swelling and dissolution (Bartlett et al. 1995; Shorrock and Bird 1998). Sodium hydroxide was therefore used as cleaning agent in cleaning and fouling investigations. The cleaning operating conditions were optimised for each membrane prior to experimentation (See results 4.5).

3.4.4 Fouling conditions with tea reconstitute

The effect of the operating conditions on permeation, ultrafiltration flux and membrane resistance were investigated by varying fouling TMP, concentration and temperature ensuring a constant laminar CFV of 0.45ms^{-1} (Re = 1184)

Flux measurements were recorded and permeate samples were taken throughout the duration of the experiment. Both retentate and permeate were recycled to the feed tank, with the exception of the small samples taken for analysis. Thus a constant feed

concentration was maintained, thereby minimising any retentate concentration effects during filtration.

The length of the filtration process (fouling) was 30 minutes unless otherwise stated. This was deemed long enough for steady state to be reached under the conditions shown in Equation 3.1, i.e. that the flux difference between J_F at time t and Δt (1 minute in this study) were less than 5% of $J_F(t)$.

$$\frac{J_F(t-\Delta t) - J_F(t)}{J_F(t)} < 0.05$$

Equation 3.1
(Bowen et al. 1995)

Table 3.2 shows a summary of the fouling/cleaning cycles used in the experiments reported in this work.

	Description	Feed Solution		Time (mins)		Temperature (°C)	TMP (bar)	CFV (ms^{-1})	Re
		Solution	Concentration (wt%)	Flush	Recycle				
RO Water 1	Determination of membrane condition before fouling	RO water		3	7	50	0.5	0.44	1171
Fouling	Foulant prepared and separated using membrane	Reconstituted Tea Solution	1.0 - 2.0	0	30, 60	Varied	Varied	0.44	1184
RO Water 2	To determine effect of fouling	RO water		3	7	50	0.5	0.44	1171
Cleaning	To remove fouled material	Sodium Hydroxide	0.01 - 0.5	1	29	Varied	Varied	Varied	3094
RO Water 3	To determine effect of cleaning	RO water		3	7	50	0.5	0.44	1171

Table 3.2: Procedure for sequential fouling/cleaning cycle

3.5 Tea Measurements

3.5.1 Solids concentration

The permeate samples were analysed for solids concentration by drying 10 ml samples in an oven at 85°C for 48 hours.

3.5.2 Colour / haze determination

Most colours can be described in terms of L* a* b*, but there is no perfect system for describing colours in terms of numbers. Section 7.4 describes the derivation of CIELAB colour system used within this study. The CIE colour tristimulus values consist of L* (lightness), a* (redness) and b* (yellowness) as shown in Figure 7.10. The haze of the permeate samples were analysed using a UV-VIS spectrophotometer (Shimadzu, Japan) powered by UV Probe software, version 2.1. Colour was characterised by transmittance measurements in the visible spectrum range between 380 and 770 nm and this transmittance data was converted by UVPC Color Analysis software, version 3.0 to L*, a* and b* values accordingly. Haze was characterised by the absorbance at the wavelength of 900 nm, corresponding to an absorbance minimum in the spectral scan of a centrifuged (haze removed) tea sample as demonstrated in section 7.1.5 . All Colour / haze measurements were performed at 35°C.

3.5.3 Tea viscosity measurement

The viscosity of the feed, μ_F was determined experimentally using a Bohlin CS50 spinning disc Rheometer set up with a 40 mm / 1° cone with a constant shear stress of 0.2145 Pa. The viscosity of a 1 wt% tea solution (equivalent to the feed) at 50°C was found to be 5.224×10^{-4} Pa s. The viscosity of RO water, μ_w was calculated using the same procedure to be 5.150×10^{-4} Pa s, a value within 5% of that quoted elsewhere in the literature (Coulson and Richardson, 1998) for pure water. The concentration of the permeate in this study ranges from 0.5 - 0.7 wt%, consequently the viscosity should lie between that of RO water and that measured for a 1 wt% solution. Rather than include multiple values of viscosity for different concentrations, in this study the

value of μ_P was assumed to be that of RO water, 5.150 x 10^{-4} PaS. This assumption leads to an error of less than 2%.

3.5.4 Total Polyphenols Assay

The polyphenols in extracts are determined colorimetrically using Folin-Ciocalteu reagent, 2N from *Sigma Aldrich* (Singleton and Rossi(Jr). 1965). The reagent comprises of phosphor-tungstic acids as oxidants, which upon reduction by readily oxidised phenolic hydroxyl groups yield a blue colour with a broad maximum absorption at a wavelength of 765nm due to formation of tungsten and molybdenum blues. Folin-Ciocalteu reagent works with a wide range of polyphenolic compounds, although the response can vary with individual components. Quantification of total polyphenols is achieved by comparison with a gallic acid standard solution.

3.5.4.1 Standard Gallic Acid solutions

An initial 1000 μg/ml standard gallic acid stock solution was made up from gallic acid monohydrate (General purpose grade form *Fisher Scientific*) dissolved in distilled water. Five separate dilutions were made up from the stock solution by dissolving in water corresponding to 10, 20, 30, 40 and 50μg/ml of gallic acid respectively.

3.5.4.2 Black tea samples

The black tea samples were diluted 9 parts tea : 1 part acetonitrile (ACN), HPLC grade form *Fisher Scientific* which helped stabilise any precipitation within the solution, then the stabilised solution is diluted 0.2 parts tea/ACN solution : 9.8 parts water. Tea concentrations analysed were between 0.4 – 1.0wt%, which when diluted accordingly provided total polyphenol measurements equivalent to the gallic acid calibration range.

3.5.4.3 Colorimetric Assay

1ml of all the gallic acid standards (for calibration), water (as reagent blank) and samples (to determine total polyphenol content) were transferred in duplicate to separate tubes. Following this 5ml of 1:10 dilution of Folin-Ciocalteu was added to

each tube. Within 3 – 8 minutes after the addition of the Foin-Ciocalteu reagent a 7.5% solution of sodium carbonate was added to the tubes and mixed well to prevent any further reagent reaction. The absorbance of the standards and samples were then measured at 765nm in a 1cm cell using a UV-VIS spectrophotometer (Shimadzu, Japan). Note the optical densities of the reagent blank were always less than 0.010 and the optical density of the samples were always within the calibration range. An example of calibration and sample calculation is shown in section 7.3.5 .

3.5.5 Theaflavins Measurement (HPLC) *(Carried out in Unilever, Colworth)*

The quantification of Theaflavin, Theafalvin-3-Gallate (TF-3-G), Theaflavin-3'-Gallate (TF-3'-G) and Theaflavin -3,3'-Gallate (TF-3,3'-G) was determined using a Hypersil C18, 3µ, 100 x 4.6mm inner diameter column. The mobile phase was split into 20% mobile phase "A" (2% acetic acid in acetonitrile) and 80% mobile phase "B" (2% acetic acid in water) carried out at 30 °C and a flow rate of 1.8ml/min. The eluents were monitored by a UV/VIS detector at 280nm. The tea samples 0.5 – 1.0wt% tea solids were diluted 9 parts tea solution: 1 part acetonitrile to stabilise the solutions before analysis. All samples were centrifuged at 14,500 rpm for 10 mins prior to injection. (Unilever, Colworth in-house standard, SAM945/002, Version 2, October 2002))

3.5.6 Caffeine Measurement (HPLC)

The quantification of caffeine was determined using a Nucleosil C18, 3µ, 120 Angston 150 x 4.6mm inner diameter column. The mobile phase was split into 14% mobile phase "A" (acetonitrile) and 86% mobile phase "B" (ultra pure water) carried out at 30 °C and a flow rate of 1.0 ml/min. A wash step was performed after every 6 samples with 50% solvent A and 50% solvent B. The eluents were monitored by a UV/VIS detector at 280 nm. The tea samples 0.5 – 1.0wt% tea solids were diluted 9 parts tea solution: 1 part acetonitrile to stabilise the solutions before analysis. All samples were centrifuged at 14,500 rpm for 10 mins prior to injection. (Unilever, Colworth in-house standard, BEV/SAM, Version 1, October 2002)

3.5.7 Particle Sizing *(Carried out in Unilever, Colworth)*

3.5.7.1 Mastersizer

The black tea feed and retentate solutions, 1.0 wt% total tea solids were measured using a light scattering Malvern Mastersizer 2000 (Malvern Instuments Ltd, Malvern, Worcestershire, UK). The black tea solution was diluted 50:50 in deionized water dispersant and injected into the presentation cell of the mastersizer, determining conditions were as follows:

Pump speed: 45% of full speed

Stir speed: 45% of full speed

Focal length: 45mm

Mean length: 2.7mm

Calculation of particle size distribution was based on the Fraunhofer method due to the opaque nature of the feed.

3.5.7.2 Zeta sizer

The permeate particle size was measured with the `Malvern` Instruments, Zetasizer nanoseries (Nano ZS) (Malvern Instuments Ltd, Malvern, Worcestershire, UK). Measurements were performed in a 1 ml plastic cuvette at 25°C.

3.6 Membrane analysis

3.6.1 Contact angle measurement

The membranes were characterized based on their wettability, which therefore gave information about the hydrophobicity of the membrane based on contact angle data. The contact angle measurements were made using the sessile drop method using a KSV CAM 101 instrument goniometer (KSV Instruments Ltd) as shown in Figure 3.6. A drop of pure water was placed with a syringe on the porous membrane surface and the contact angle θ is measured as shown in figure 3.10. This procedure is repeated 8 times at different points on the membrane with measurements taken from both sides of the drop producing a total of 16 measurements, which can then be averaged. The measurements were taken as quickly as possible so as to reduce drop volume changes due to permeation through the membrane or evaporation. For hydrophobic membranes the contact angle will be larger than 90° and for hydrophilic membranes the contact angle will be less than 90° tending toward 0° as shown in Figure 3.7.

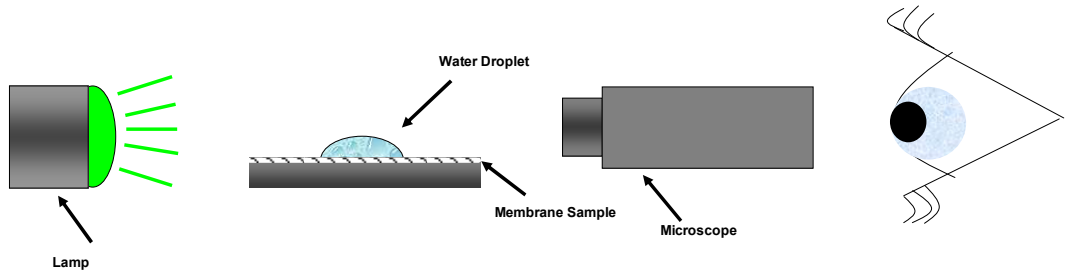

Figure 3.6: Schematic diagram of contact angle measuring device

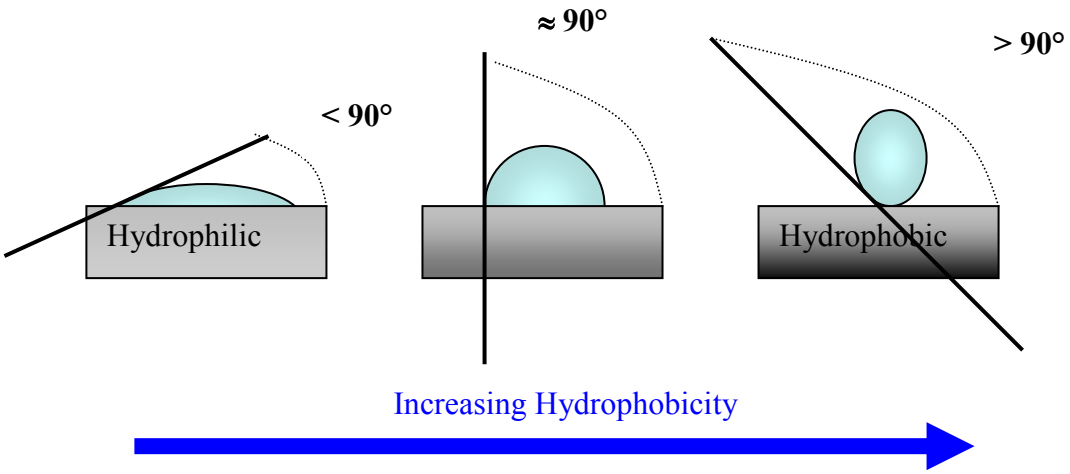

Figure 3.7: Diagram of drop of water on hydrophobic – hydrophilic surface.

3.6.2 FTIR *(Carried out in Unilever, Colworth)*

The FTIR spectra were recorded from the membrane surface using a Bio-Rad FTS-6000 spectrometer (Bio-Rad Laboratories, Cambridge MA, USA) and a golden-Gate single reflection diamond ATR unit (Specac Inc., Smyrna GA, USA). A spectral resolution of 4 cm^{-1} (aperture open) was used in this study and 256 interferograms were co-added before Fourier transformation. Acquisition software used was Bio-radWin-IR Pro Version 2.97 (Bio-Rad) and the analysis and publication was performed using GRAMS AI Version 7.2.

3.6.3 Zeta Potential through Pores *(Carried out in Lappeenranta University of technology)*

The surface charge on polymeric membranes has a significant influence upon separation properties and the nature of fouling. The surface charge density of a porous membrane is related to the zeta-potential of the membrane.

Simultaneous measurements of flux and streaming potential through the pores were obtained using an ultrafiltration module (Figure 3.9) equipped with two sets of Ag / AgCl electrodes. One electrode on the feed side of the membrane and one on permeate side enabling the measurement of the streaming potential across the membrane (Zeta potential in pores). A membrane with an area of 10.4 cm^2 was inserted into the module and stabilised at a constant pressure of 1.0 bar and flowrate of 0.5ms^{-1}(Figure 3.8). The streaming potential measurements were performed with 0.001 (10^{-3} M) KCl solution. The pH range covered was 3.7 – 7, for each pH the

pressure was varied in order to calculate the zeta potential based on the Helmholtz - Smoluchowski equation, (Equation 3.2) without corrections as shown below.

$$\varsigma = \frac{\Delta E}{\Delta P}\frac{\mu_E k_e}{\varepsilon_0 \varepsilon_r}$$

Equation 3.2

Where ΔE is the streaming potential, ΔP the transmembrane pressure drop, μ_E, the viscosity of the solution, k_e the conductivity of electrolyte in the pores (approximated as bulk conductivity), ε_0 the permittivity of a vacuum, and ε_r the relative dielectric constant of the electrolyte. The required data was collected using acquisition software programmed with MS ® quickBasic version 4.5 and using ADDA 14 interface card. The results were then analysed using MS® Excel.

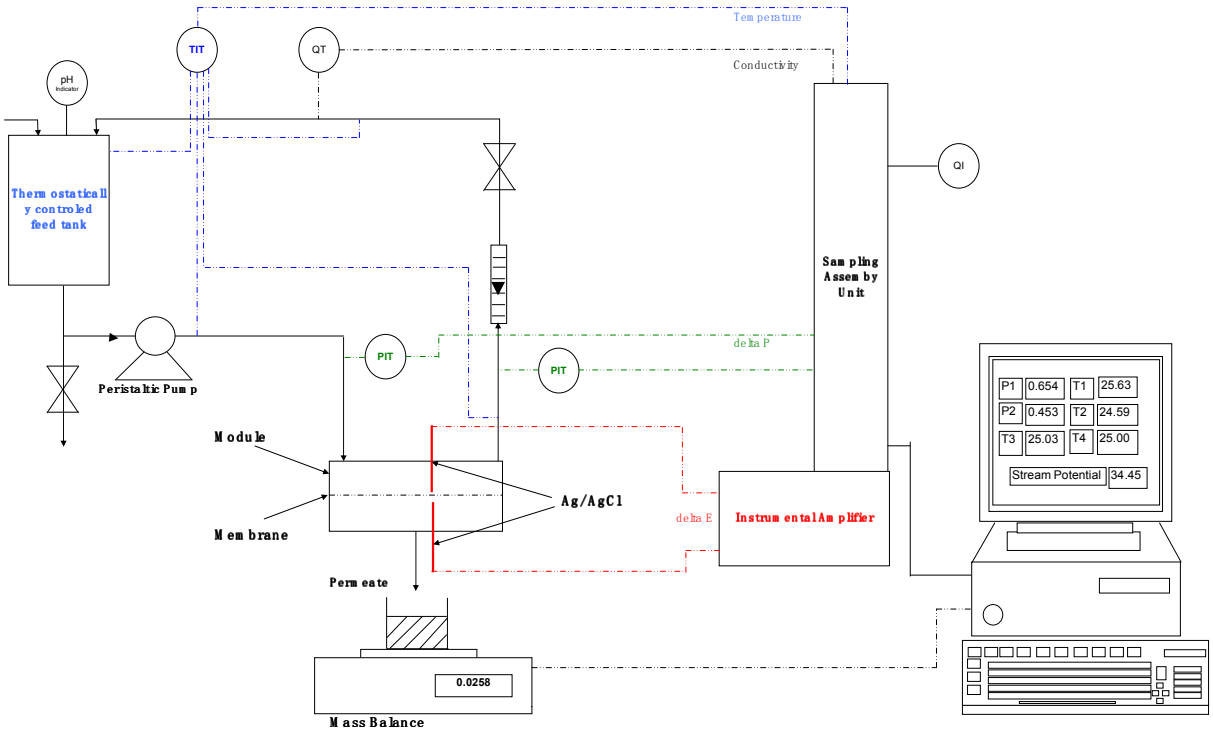

Figure 3.8: Apparatus for streaming potential measurement through pores. (After Nyström et al. 1994)

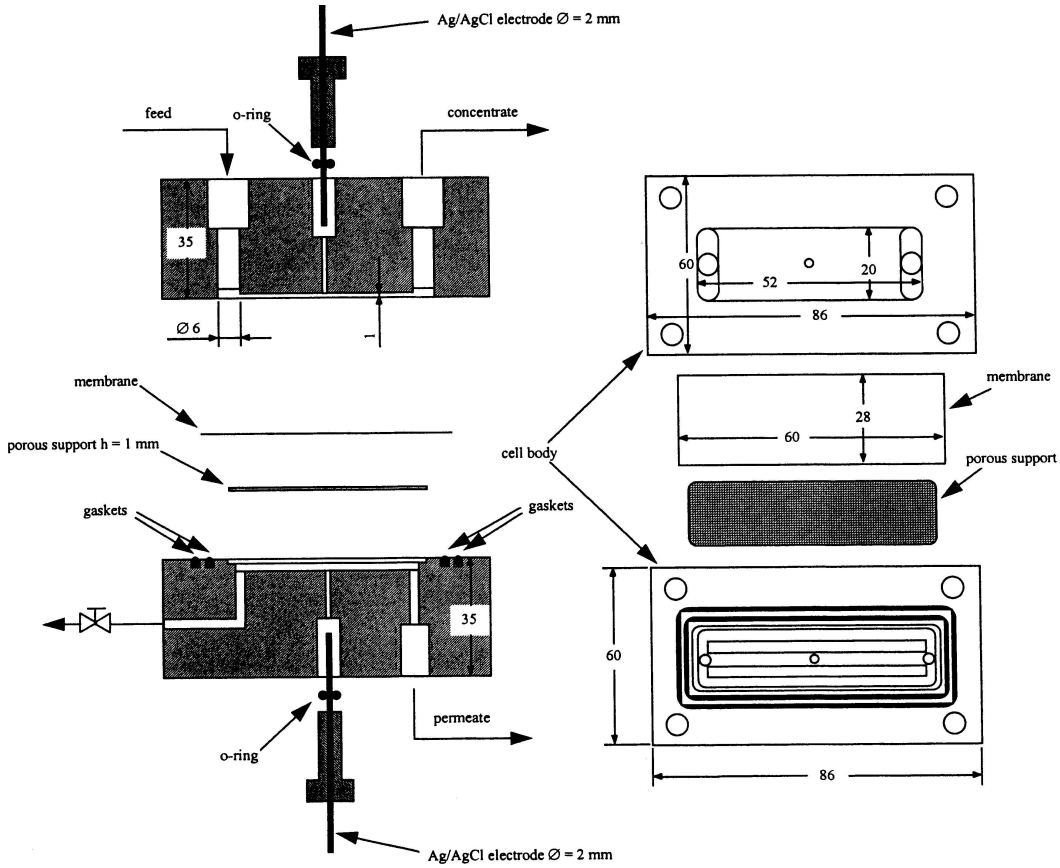

Figure 3.9: Module for streaming potential measurements through pores (After Pihlajamäki 1998)

3.6.4 AFM

3.6.4.1 Topographical Images *(Carried out in Bath, Electron Optical Suite)*

The surface roughness values of the membranes were determined by atomic force microscopy studies using a Digital Instruments / Veeco Nanoscope 3A using an E scanner in tapping mode with a silicon nitrate NP-20 tip. The membranes were attached to steel metal discs using Tempfix ® glue and all measurements were made in a fluid cell filled with RO water using Veeco Nanoscope software, version 6. Sample areas of 5 x 5 μm were used to calculate surface roughness parameters.

3.6.4.2 Force Measurements *(Carried out in Swansea university, Nanotechnology)*

Model Foulant

The purified model polyphenol, theaflavin – 3 – gallate (TF3G) of molecular mass 716 Da was supplied by *Unilever R&D, Colworth*. This particular polyphenol was decided upon based on work performed by Wu and Bird 2007 regarding ultrafiltration

of model black tea components. In this work the TF3G polyphenol was found to be one of the most significant fouling constituents studied.

Atomic Force Measurements

Force attraction / adhesion measurements of theaflavins – 3 gallate (TF3G) to / from the membranes were determined using atomic force microscopy (Digital Instruments / Veeco Nanoscope 3A) using an E scanner in tapping mode. The cantilever of known spring constant (0.4 Nm^{-2}) was modified by attachment of an approximately 10 μm diameter silica sphere using an in house micromanipulation technique. The attached sphere (Figure 3.10) was then cured using ultraviolet light for 30mins and then immersed in a 1 g/litre solution of TF3G for 30 minutes allowing adsorption of the chemical species to the silica sphere.

To test whether TF3G would adhere to the silica probes, a 1g / litre solution was placed on a flat silica (mica) surface for 30mins followed by rinsing in 0.1M NaCl buffer solution. The difference in surface roughness (R_a) was measured such that R_a increased from 0.5nm on the virgin cleaned surface to 3.2nm on the surface soaked with TF3G followed by buffer rinse, this confirming the attachment of the polyphenol to the surface.

Differently treated membranes from throughout the fouling / cleaning cycle were investigated (Virgin conditioned, fouled, fouled and cleaned and also cleaned only). The membranes were attached to steel metal discs using adhesive tape and all measurements were made in a fluid cell filled with 0.1M NaCl modified to pH 4.5 (a pH equal to that of commercial tea solution). Force measurements (repeated 200 times) were performed over 100 points on a 10 x 10 μ m membrane surface producing multiple force curves. The cantilever deflection, δ_C, can be converted to the force, F, acting on the membrane surface using Equation 3.3.

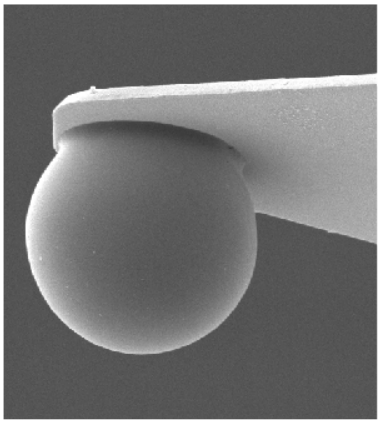

Figure 3.10: Silica sphere attached to cantilever via micromanipulation technique

$$F = -k_C \delta_C$$

Equation 3.3
(Leite and Herrmann 2005)

Where k_c is the spring constant of the cantilever. Figure 3.11 represents the effect that a sample has upon the deflection of a tip as plotted against the distance the tip is from the sample surface. At the start of the cycle, a large distance separates the tip from the membrane sample such that no interaction and thus deflection occurs (point (a)). As the tip is brought towards the surface of the membrane at a constant velocity the separation distance, D, decreases until a point close to the membrane surface. As the tip moves towards the sample various attractive forces (including electrostatic) pull on the tip, once these forces overcome the stiffness of the cantilever, the tip jumps into contact with the sample surface (points (b) – (c)). At point (d) the tip is fully pressed on the membrane surface hence the positive deflection. (a) to (d) is the approach curve towards the membrane, (d) to (h) is the withdraw curve from the membrane surface. Initially (d) to (e) represents the opposite to segment (c) to (d), if both segments are not parallel and straight to each other then this gives us information on plastic deformation of the sample. Any adhesion or bonding formed during contact with the membrane surface cause the tip to remain in contact ((e) to (f)). The tip remains in contact until the retraction force overcomes the adhesion forces and the cantilever pulls off sharply to an un-deflected or non-contact position ((f) to (g)). Finally, the tip is retracted form the membrane surface so that no forces act upon it back at the equilibrium starting position ((g) to (h)) (Leite and Herrmann 2005). Converting the deflections measured into forces using Equation 3.3 for attractive forces ((b) to (c)) and adhesion forces ((f) to (g)) we can understand the nature of TF3MG attachment to the membrane surface.

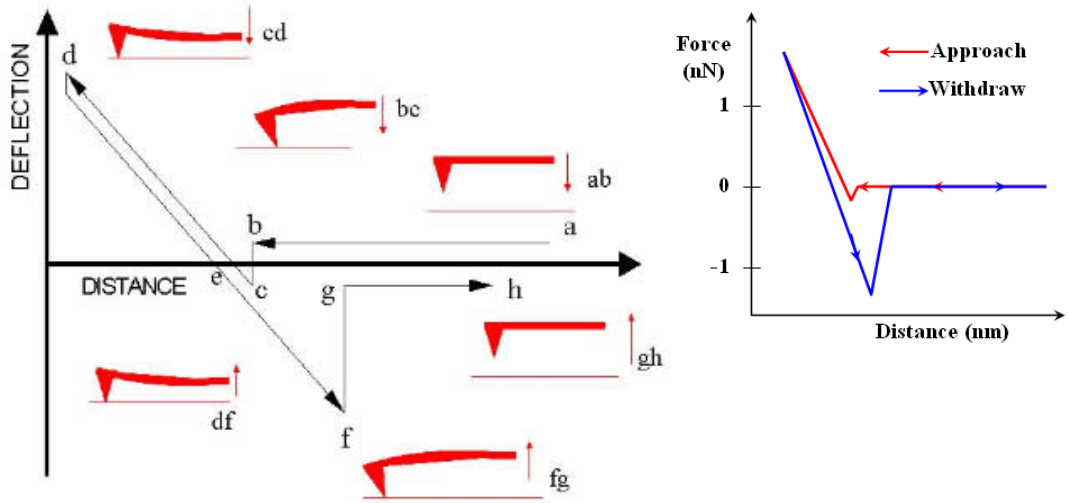

Figure 3.11: (a) Representation of the effect that a sample has upon the deflection of a tip as plotted against the distance the tip is from the sample surface. (b) Representation of the force acting upon the tip as plotted against the distance the tip is from the sample surface.

Chapter 4 Results and Discussion

4.1 Virgin membrane conditioning / characterisation

Before any membranes can be used they must be initially conditioned, a procedure used to remove any preserving solutions present on the membrane surface. Conditioning was performed with RO water at 60°C, 1.0bar TMP and 1.15ms^{-1} CFV for 90 minutes for all membranes in this study. The conditioning process was performed based on work by Weis *et al.* 2005 where these conditions were found sufficient to remove glycerine coatings used to preserve the membranes during storage.

4.1.1 Virgin Fluoropolymer Membrane

4.1.1.1 Conditioning

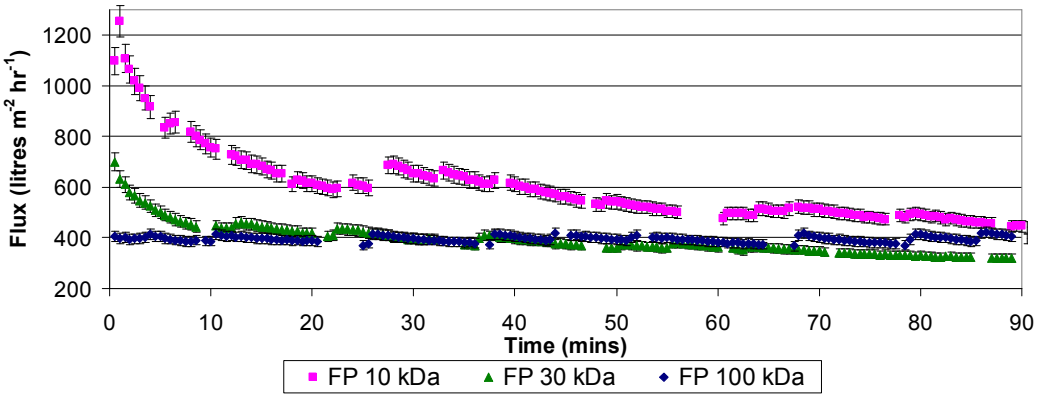

Figure 4.1: Graph to show permeate flux vs time when conditioning different MWCO Fluoropolymer membranes using RO water feed at 60°C, 1.0 bar TMP and 1.15m/s CFV.

Figure 4.1 shows the conditioning fluxes for fluoropolymer (FP) membranes of 10, 30 and 100 kDa MWCO varied for 90 mins. The FP 10 kDa membrane initially had a very high flux of 1254 litres m^{-2} hr^{-1} which reduced significantly to 477 litres m^{-2} hr^{-1} after 60 mins and display a slight further decline to 446 litres m^{-2} hr^{-1} after 90 mins. The retentate water was regularly changed for fresh water due to the concern of removed glycerine from the membrane surface re-fouling the surface. These membranes were heavily coated in glycerine preservative compared to the other membranes, because of this a longer conditioning process was performed for 215 mins, the flux had reduced to a steady state of 400 litres m^{-2} hr^{-1} (data not shown). The FP 30 kDa membrane also showed a significant reduction in flux during the

conditioning process from 700 to 363 litres m^{-2} hr^{-1} after 60 mins and 320 litres m^{-2} hr^{-1} after 90 mins. The FP 100 kDa membrane flux did not vary significantly throughout the conditioning process initially reducing from 405 to 385 litres m^{-2} hr^{-1} after 60 mins and rising again to 407 litres m^{-2} hr^{-1} after 90 mins. The initial presence of glycerine preservative on the FP10 and FP30 membrane surface allowed a higher permeability of RO water and when removed increased the membrane resistance.

4.1.1.2 Pure water flux characterisation

Immediately after conditioning the virgin FP membranes were characterised using pure RO water (Figure 4.2) where TMP was varied from 0.5 – 1.5 bar. Figure 4.2 represents the linear relationship of permeate flux and TMP, based on Equation 2.4 in 2.4.1 the membrane resistance can be calculated. The resulting membrane resistance, R_M, for the FP 10, FP30 and FP100 kDa membrane was $1.92x10^{12}$, $2.89x10^{12}$ and $2.35x10^{12}$ m^{-1} respectively (sample calculations found in 7.4.2). FP10 had the smallest nominal MWCO although it had the least membrane resistance, R_M, further discussion on this result and the effect upon fouling can be found in 4.3 .

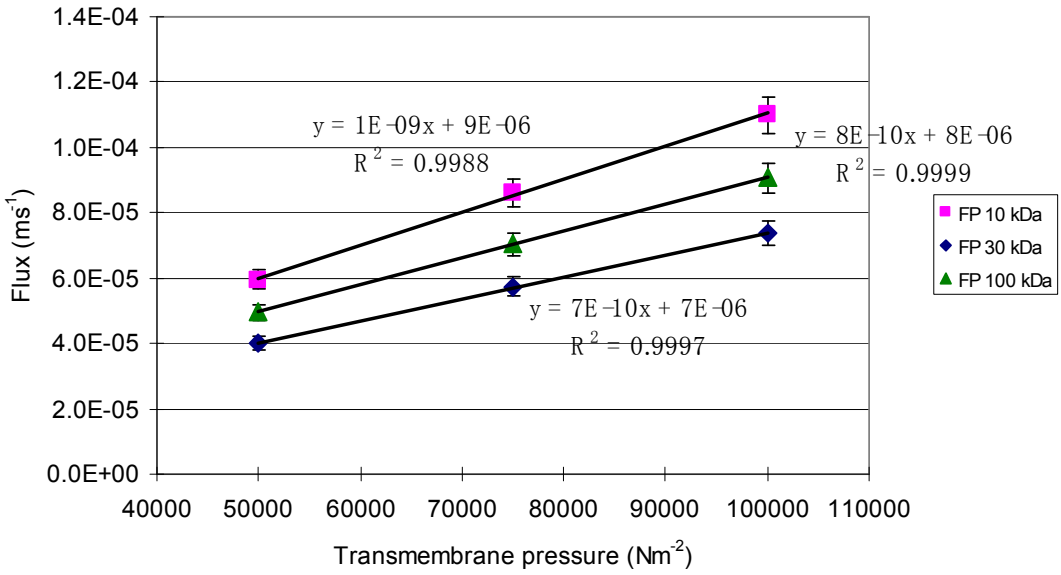

Figure 4.2: Graph to show variation in RO water flux with transmembrane pressure at a temperature of 50°C and a CFV of 0.44m/s different MWCO fluoropolymer membranes

4.1.2 Virgin Regenerated Cellulose Membrane

4.1.2.1 Conditioning

Figure 4.3 shows the conditioning fluxes for regenerated cellulose (RC) membranes of 10, 30 and 100 kDa MWCO varied for 90 mins. All the membranes demonstrated an initial increase in flux within the first 2 - 3 mins which reached a plateau for the remainder of the conditioning process. RC30 and RC100 maintained a flux of around 601 and 632 litres m^{-2} hr^{-1} respectively while RC10 a much lower flux of 67 litres m^{-2} hr^{-1}. The RC membranes did not vary significantly through the conditioning process which suggests that any preservative was easily removed. Further experimentation could potentially be performed to reduce the amount of time required for the conditioning of these membranes.

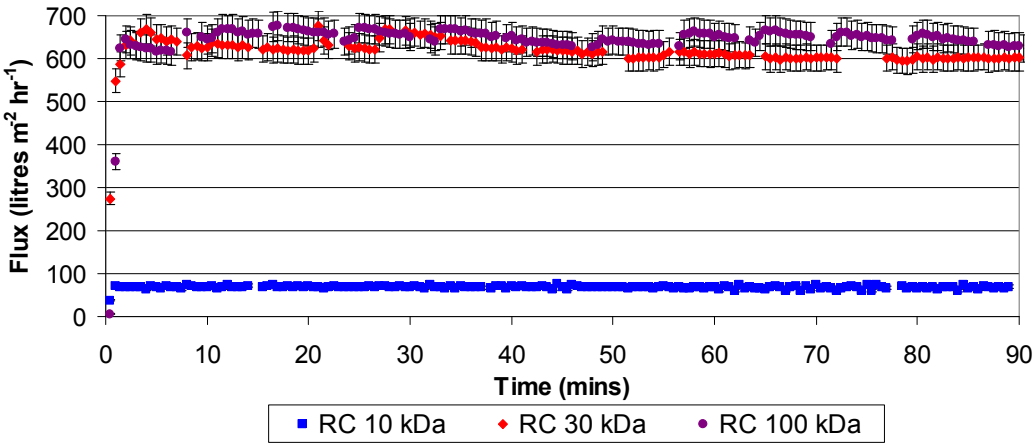

Figure 4.3: Graph to show permeate flux vs time when conditioning different MWCO regenerated cellulose membrane using RO water feed at 60°C, 1.0 bar TMP and 1.15m/s CFV.

4.1.2.2 Pure water flux characterisation

Immediately after conditioning the virgin RC membranes were characterised based on pure RO water as shown in Figure 4.4 and where TMP was varied from 0.5 – 1.5 bar. Figure 4.4 represents the relationship of permeate flux and TMP was linear and based on Equation 2.4 in 2.4.1 the membrane resistance can be calculated. The resulting membrane resistance, R_M, for RC10, RC30 and RC100 kDa was $1.18Ex10^{13}$, $1.35x10^{12}$ and $1.32x10^{12}$ m^{-1} respectively where model calculations for this can be found in 7.3.2 .

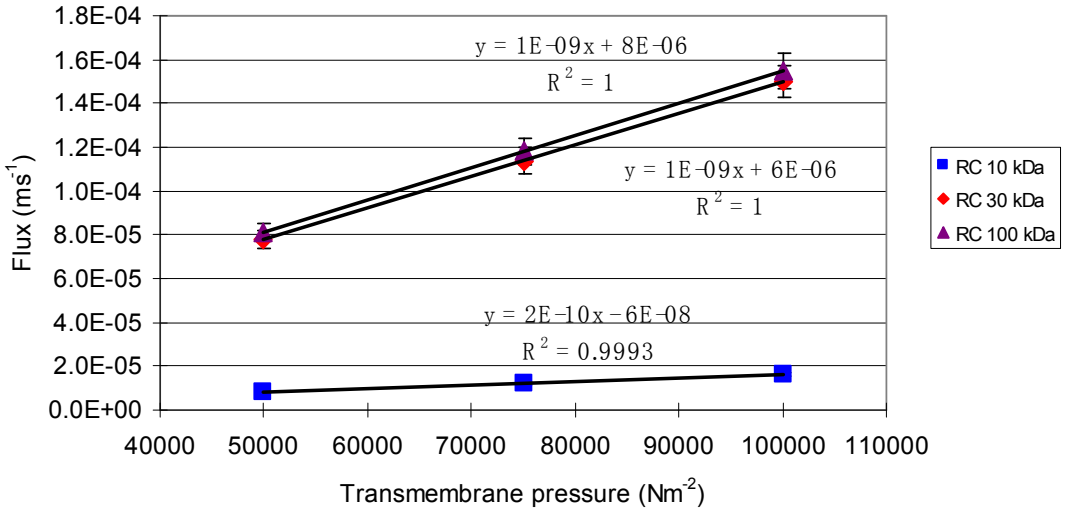

Figure 4.4: Graph to show variation in RO water flux with transmembrane pressure at a temperature of 50°C and a CFV of 0.44 ms^{-1} through different regenerated cellulose 30,000 Da MWCO membrane.

4.2 Measurement of flux decline

4.2.1 Membrane fouling resistance measurement and analysis

The resistance was measured and broken down into membrane resistance, R_M, irreversible resistance, R_I, reversible resistance, R_R and the resistance due to concentration polarisation R_{CP}.

The general membrane equation (Equation 4.1) was used to calculate the total resistance after 30 mins of fouling where steady state has been defined in accordance with Equation 3.1. This is referred to as the total resistance, R_T.

$$J_F = \frac{\Delta P}{\mu_P(R_T)}$$

Equation 4.1

Where J_F is the volumetric flux, ΔP is the TMP and μ_P is the viscosity of the permeate solution. The viscosity of the feed, μ_F was determined experimentally using a *Bohlin* CS50 spinning disc Rheometer set up with a 40mm / 1° cone with a constant shear stress of 0.2145 Pa. The viscosity of a 1wt% tea solution (equivalent to the feed) at 50°C was found to be 5.224 x 10^{-4} Pa s. The viscosity of RO water, μ_w was calculated using the same procedure to be 5.150 x 10^{-4} Pa s, a value within 5% of that quoted elsewhere in the literature (Coulson and Richardson 1998) for pure water. The concentration of the permeate in this study ranges from 0.5 - 0.7 wt%, consequently the viscosity should lie between that of RO water and that measured for a 1 wt% solution. Rather than include multiple values of viscosity for different concentrations, in this study the value of μ_P was assumed to be that of RO water, 5.150 x 10^{-4} PaS. This assumption leads to an error of less than 2%.

A membrane displays a number of potential resistive parameters properties when fouled. These can be characterised by the resistance in series model as shown in Equation 4.2.

$$R_T = R_m + R_P + R_A + R_{CP} + R_g + R_C$$

Equation 4.2

where R_m is the intrinsic membrane resistance, R_P is the resistance due to pore plugging, R_A is the resistance due to adsorption of solute to the membrane surface. R_{CP} results from an increase in concentration near the membrane surface (concentration polarisation) which causes a back diffusion to the bulk solution. This increase in concentration towards the membrane surface can cause particulates to build up forming a porous cake layer resulting in the cake layer resistance, R_C. The cake layer is usually very dense at the membrane surface and becomes less dense and more porous as the cake layer transforms to the concentration polarisation region (Tarabara *et al.* 2004). Instead of a cake layer sometimes a gel layer may also be formed at the membrane surface due to the high concentration and pressure associated causing a gel layer resistance, R_g. The gel layer resistance is mostly associated with a limiting flux and an independence of TMP Song 1998. A fouling resistance term, (R_F) in this case is defined as shown in Equation 4.3.

$$R_F = R_P + R_A + R_g + R_C$$

Equation 4.3

R_m is simply calculated by measuring RO water flux through a conditioned virgin or cleaned membrane. R_F is then determined from the initial flux of RO water through the membrane after fouling has finished. Following fouling, the tea solution is flushed from the system using RO water for a period of 3 minutes. This time was selected to be sufficient to completely replace the tea with water, as the dead volume of the system is filled with water in 35 s. The additional time was selected to enable concentration polarisation layers in the laminar sub layer next to the membrane surface to be displaced. There will be some error due to the initial removal of tea solution remaining in the system causing continued fouling, followed by the removal of any loosely bound cake layer. A knowledge of R_m, R_F and R_T enables an estimate of R_{CP} to be made using Equation 4.2 and Equation 4.3.

R_F can be broken down into a rinsable fouling resistance, R_R and an irreversible fouling resistance R_I as shown in (Equation 4.5) by noting the increase in flux when flushing with RO water after fouling had finished. In this study membranes were flushed for 10 minutes and the flux recorded at the end of this time was assumed as the irreversible flux from which R_I could be calculated using Equation 4.4 where R = R_I. R_R could then be determined (Equation 4.5). Rinsable fouling is defined here as

that which is removed by rinsing at 0.5 bar TMP and 0.44ms^{-1} CFV to remove any loosely bound particulates. Irreversible fouling is defined as not being removed by rinsing, i.e. material binding to pores or adhering to the membrane surface. These terms are relative and depend upon the rinsing conditions used (Shorrock and Bird 1998), but can be compared within the data set as rinsing conditions were kept constant. Note that $R_T = R_m + R_F + R_{CP}$.

$$J_W = \frac{\Delta P}{\mu_W (R)}$$

Equation 4.4

$$R_F = IrreversibleFouling, (R_I) + RinsableFouling, (R_R)$$

Equation 4.5

4.2.2 Fouling concentration variation

Both the 30 kDa fluoropolymer (FP) and regenerated cellulose (RC) membranes were subjected to variations in total tea solids concentration of 1.0 – 2.0 wt% at 3.0 bar TMP. Additional experiments were also carried out at 1.0 bar TMP for the FP membrane.

Figure 4.5 and Figure 4.6 demonstrate a break down of the different resistive layers present at steady state fouling (i.e. after 30 minutes of filtration) for FP and RC membranes respectively. The total resistance, R_T increased significantly as tea concentration was increased for both FP and RC membranes at 3.0 bar TMP. For the FP membrane, the total resistance increased significantly as the concentration was increased. R_{CP} contributes significantly to this, increasing from 44% at 1.0wt% to 52% at 2.0wt% of the total fouling resistance at 3.0 TMP. The irreversible fouling remains approximately constant for varied feed concentration changes at 1.0 and 3.0 bar TMP with the FP membrane. The rinsable fouling resistance does increase for the FP membrane, from 0.564 to 1.07 x10^{13} m^{-1} when feed concentration was increased from 1 to 2 wt% (at a TMP of 1 bar).

The rinsable fouling resistance increases from 1.65 to 2.86 x10^{13} m^{-1} when concentration was increased from 1.0 – 2.0wt% at a pressure of 3 bar. Thus both R_{CP} and rinsable fouling contribute to the increase in total resistance of the FP membrane.

This result agrees with the findings of Marshall et al. 1993 who report that an increase in foulant concentration increased reversible fouling more significantly than it did irreversible fouling during the filtration of protein based feeds.

Increasing the TMP from 1.0 bar to 3.0 bar for the FP membrane also increased the total resistance (see Figure 1). R_{CP} and rinsable fouling resistance were mostly responsible for the increase in total fouling resistance. This trend was also found in section 4.2.6 during the ultrafiltration of black tea for the same FP membrane.

Figure 4.6 shows that R_{CP} was the dominant resistance RC membrane resistance. R_{CP} increased from 61% of the total resistance at a feed concentration of 1.0wt%, to 72.5% of the resistance at a feed concentration of 2.0wt%. Rinsable and irreversible resistances remained approximately constant for the RC membrane as the feed concentration was increased. This demonstrates that increasing feed concentration has no additional effect upon deposit formation for the RC membrane, and that increases in overall resistance are due to increases in CP. Increases in feed concentration were found to increase rinsable fouling on the FP membrane, suggesting that fouling species interact more strongly with the FP than the RC membrane.

4.2.2.1 Membrane cleanability

There was no significant trend in cleaning fluxes following ultrafiltration of different feed concentrations, within the range tested. Fluxes of 90 – 100 and 160 – 170 litres m^{-2} hr^{-1} were recorded for the FP and RC membranes respectively. The membrane resistance after cleaning (Figure 4.7 and Figure 4.8) demonstrated no significant variation from cycle to cycle with values of *ca* 2.5 x 10^{12} m^{-1} and 1.6 x 10^{12} m^{-1} for the FP and RC membranes respectively. Note that the fouling / cleaning experiments reported were all performed on the same FP and RC membranes. For the feed filtration conditions used, the cleaning protocols applied to these membranes appear to be sufficient to regenerate fluxes.

4.2.2.2 Total tea solids rejection

The FP membrane total tea solids rejection data can be found in Figure 4.9 calculated using Equation 4.6. Within experimental error, tea solids rejection ratios were constant at the three feed solids concentrations tested (1, 1.5 and 2.0 wt %). The rejection coefficients were 0.22 +/- 0.01 and 0.36 +/- 0.02 at 1 and 3 bar respectively for a 1.0 wt% feed solution.

Figure 4.10 shows that for the RC membrane the total tea solids rejection increased from 0.40 +/- 0.02 to 0.48 +/- 0.024 when the feed concentration was increased from 1.0 – 2.0 wt% (at a pressure of 3.0 bar). The RC membrane rejected more total tea solids than the FP membrane with a 1.0wt% feed, and increasing the feed concentration caused a more significant increase in the membrane rejection. This may be due to the increased concentration polarisation occurring, which provides an increased resistance, and therefore a reduced transmission of tea solids.

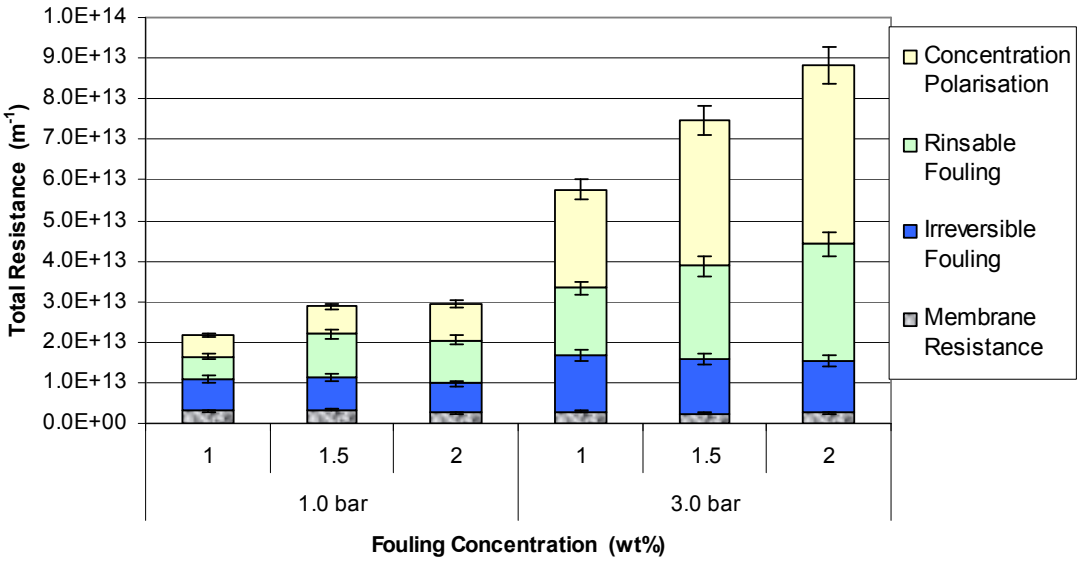

Figure 4.5: Graph to show sequential fouling resistance data for various tea concentrations on the same fluoropolymer membrane when fouled with tea (1.0 and 3.0 bar TMP, 50°C, 0.44 m/s) for 30 mins.

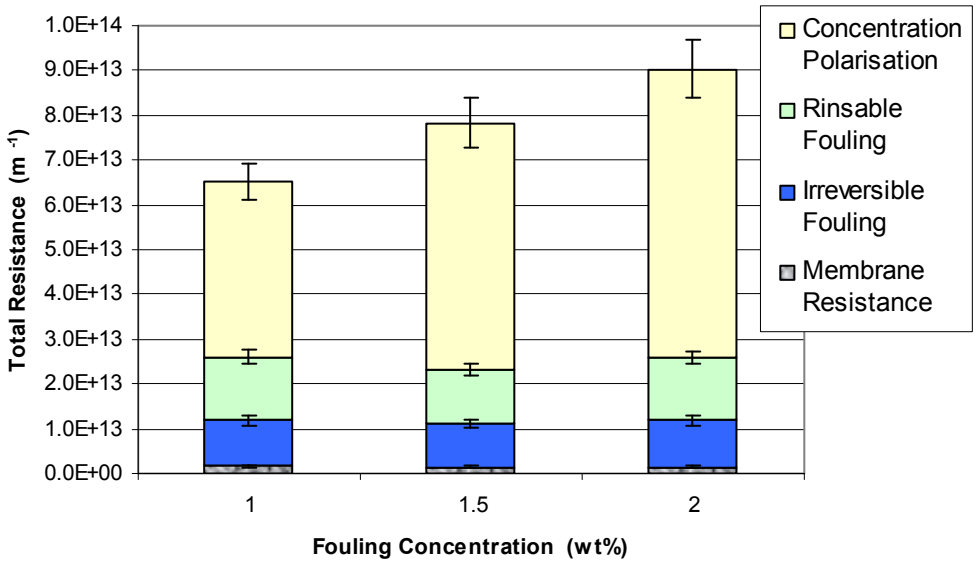

Figure 4.6: Graph to show sequential fouling resistance data for various tea concentrations on the same regenerated cellulose membrane when fouled with tea (3.0 bar TMP, 50°C, 0.44 m/s) for 30 mins.

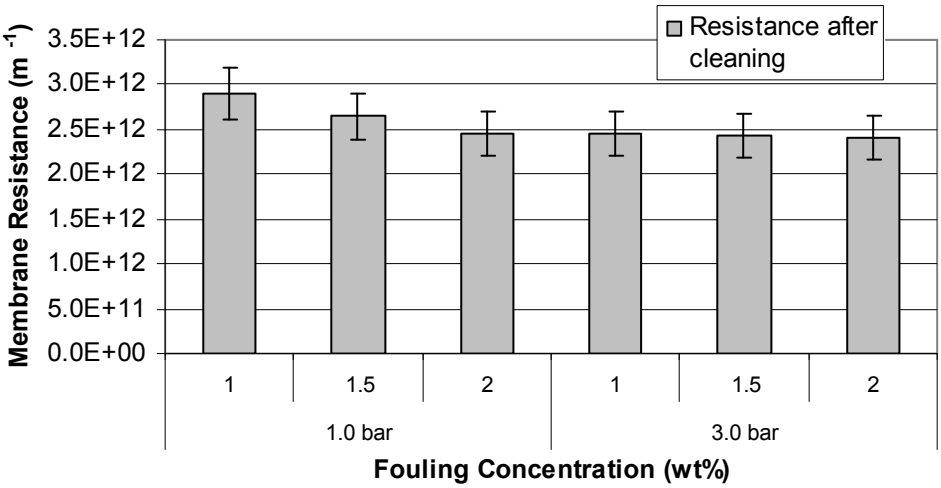

Figure 4.7: Graph to show sequential membrane resistance after cleaning for various fouling concentrations on the same fluoropolymer membrane when fouled with tea (1.0 and 3.0 bar TMP, 50°C, 0.44 m/s) for 30 mins

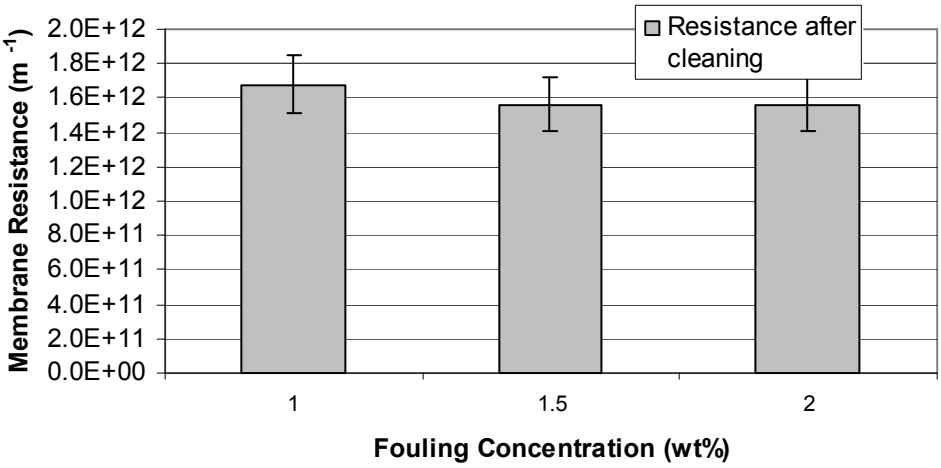

Figure 4.8: Graph to show membrane resistance after cleaning for various fouling concentration on the same regenerated cellulose membrane when fouled with tea (3.0 bar TMP, 50°C, 0.44 m/s) for 30 mins.

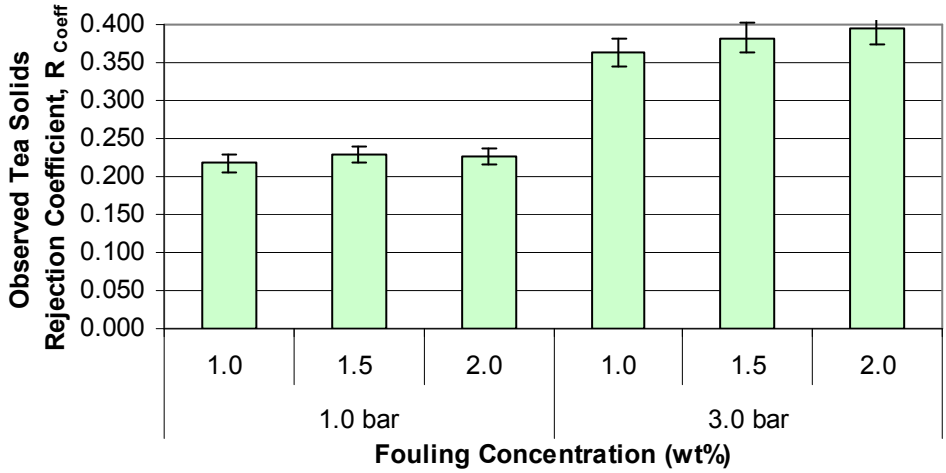

Figure 4.9: Graph to show sequential Rejection coefficients for various fouling concentrations for the same fluoropolymer membrane when fouled with tea (1.0 and 3.0 bar TMP, 50°C, 0.44 m/s) for 30 mins.

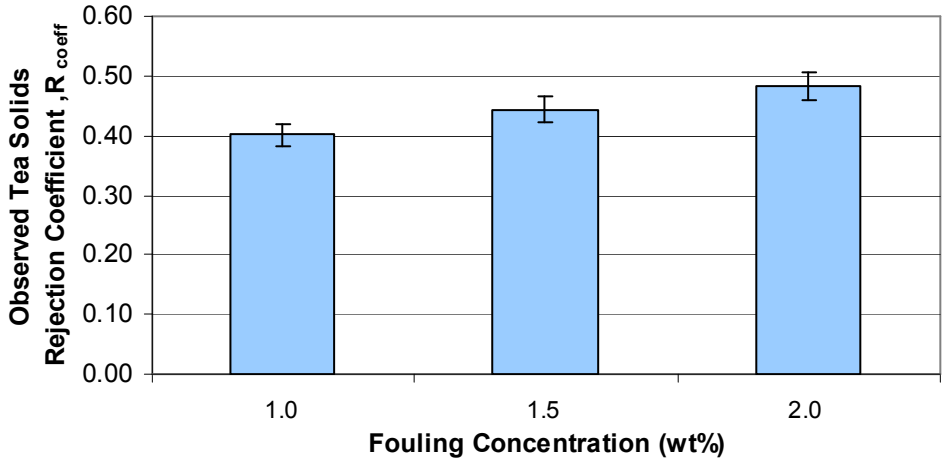

Figure 4.10: Graph to show sequential rejection coefficients for various fouling concentrations for the same regenerated cellulose membrane when fouled with tea (3.0 bar TMP, 50°C, 0.44 m/s) for 30 mins.

4.2.2.3 Simple Mass Transfer Modelling

Solutes building up at the membrane surface lead to an increase in concentration that causes a diffusive flux back to the bulk feed. After a given amount of time steady state conditions will be reached where the convective solute flux to the membrane surface will be balanced by solute flux through the membrane plus the diffusive flow back from the membrane surface. This is concentration polarisation and in the simple model described in Equation 4.7, no other fouling mechanisms are considered.

According to the traditional film-layer theory, when dealing with high pressures there is a high degree of concentration polarisation increasing the concentration at the membrane surface, C_M. The increase of C_M leads to increased fluxes that are approaching maximum limiting fluxes independent of TMP. Other work (see section 4.2.6) determined that the membranes under investigation operate in the limiting flux region when pressures exceed 3.0 bar. Based on these assumptions, the solute transport through the membrane would be mainly convective, leading to a virtually constant ratio of C_P/C_M and therefore a constant maximum true rejection coefficient, R_{Max} as defined in (Equation 4.9).

If Equation 4.6, 4.8 and 4.9 are substituted into Equation 4.7, Equation 4.10 is produced and therefore a plot of $\ln[(1-R_{coeff})/R_{coeff}]$ against J_V from would yield a straight line with a slope 1/k and intercept of $\ln[(1-R_{Max})/R_{Max}]$.

$$R_{coeff} = 1 - \frac{C_P}{C_B}$$

Equation 4.6

$$\ln\left[\frac{C_M - C_P}{C_B - C_P}\right] = \left(\frac{J_V \delta}{D}\right)$$

Equation 4.7
(Mulder 2000)

$$k = \frac{D}{\delta}$$

Equation 4.8

$$R_{Max} = 1 - \frac{C_P}{C_M}$$

Equation 4.9

$$\ln\left[\frac{1 - R_{coeff}}{R_{coeff}}\right] = \ln\left[\frac{1 - R_{Max}}{R_{Max}}\right] + \frac{J_v}{k}$$

Equation 4.10

Where,

C_B – Concentration in the bulk solution outside boundary layer (wt%)

C_M – Concentration at the membrane surface (wt%)

J_V – Steady state permeate volumetric flux (litres hr^{-1} m^{-2})

δ – Boundary layer thickness (Conc. polarisation layer thickness) (m)

D – Diffusivity (m^2s^{-1})

k – Mass transfer coefficient (ms^{-1})

R_{Max} – Maximum true rejection coefficient

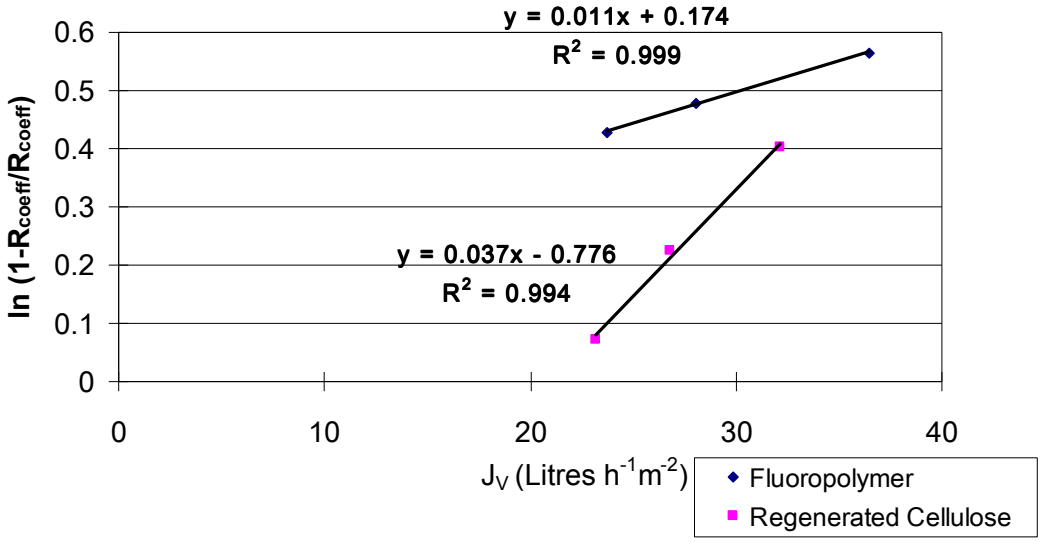

Figure 4.11: Graph to show steady state fouling flux (J_V) vs ln[(1-R_{coeff})/ R_{coeff}] to predict mass transfer data where C_B was varied for fluoropolymer and regenerated cellulose membranes maintaining a TMP of 3.0 bar, CFV of 0.44m/s and temperature of 50°C

	C_B	C_P	R_{coeff}	R_{max}	k	C_M
Membrane	**wt%**	**wt%**			**m/s**	**wt%**
Fluoropolymer	0.88	0.56	0.36	0.46	2.57E-05	1.04
	1.28	0.79	0.38	0.46	2.57E-05	1.46
	1.72	1.04	0.39	0.46	2.57E-05	1.91
Regenerated Cellulose	0.94	0.56	0.40	0.68	7.55E-06	1.78
	1.43	0.80	0.44	0.68	7.55E-06	2.53
	1.71	0.89	0.48	0.68	7.55E-06	2.81

Table 4.1: Mass Transfer Coefficient, k and membrane surface concentration C_M where the feed concentration for both fluoropolymer and regenerated cellulose membrane is varied.

Figure 4.11 shows a plot of (J_V) vs ln [(1-R_{coeff})/R_{coeff}] which, in accordance with Equation 4.10, gives a straight line enabling the calculation of mass transfer data, k and membrane surface concentrations, C_M as shown in Table 4.1 above. For the FP membrane, the concentration at the surface, C_M, was only 0.16 – 0.19 wt% higher than

that of C_B. For the RC membrane, $C_{M,}$ was 0.84 – 1.1wt% higher than that of C_B. The RC membrane showed a higher concentration at the membrane surface and consequently a mass transfer coefficient, k, ($7.55 \times 10^{-6} ms^{-1}$) of over an order of magnitude smaller than that of the FP membrane ($2.57 \times 10^{-5} ms^{-1}$). This confirms that the FP membrane is interacting with the tea foulant allowing an easier passage through the pores confirmed by increased solids transport (see Figure 4.9) through the FP membrane when compared to the RC membrane (see Figure 4.10). More foulant must be adhering to the FP membrane than the RC, based on the fact that the irreversible and rinsable fouling resistance is larger on the FP membrane, suggesting both strong and weak membrane – foulant interactions are both increased on this membrane. Streaming potential measurements have confirmed that an easier passage of tea solids and polyphenols was possible through the FP membrane. At a pH of 4.5 (the value associated with tea liquor) there is a neutral charge within the pores of the FP membrane (ie.filtration takes place at the iso-electric point). This can be compared to the more negatively charged RC membrane at the same pH (see section 4.3.5). Section 4.3.6 details FTIR studies that confirm an increased fouling deposit on the FP membrane compared to the RC membrane. Such results confirm the findings in this study. The concentration polarisation resistance, R_{CP}, was found to have approximately 20% greater effect upon the total fouling resistance for the RC membrane than for the FP membrane (see Figure 4.5 and Figure 4.6) which also explains the higher value of C_M found at the RC membrane surface.

These results demonstrate that reduced foulant – membrane interaction can reduce overall deposit formation. However, as a consequence membrane selectivity may increase and mass transfer reduce due to increased concentration of retentate at the membrane surface.

4.2.3 Feed Temperature

4.2.3.1 Fouling Resistance Data

The 30kDa FP membrane was subjected to variations in feed temperature with a constant feed concentration of 1.0wt% and a TMP of 1.0 bar. All other conditions were maintained at standard values (Table 3.2).

Figure 4.12 shows a break down of the different resistive layers present at steady state fouling (i.e. after 30 minutes fouling) for the FP membrane at varied temperature.

The total resistance, R_T increased significantly (from 2.1 to 2.7 x $10^{13}m^{-1}$) when the temperature was reduced from 50°C to 36°C. The irreversible resistance was reduced at 36°C compared with 50°C, although the rinsable and R_{CP} resistances were both increased. As the change in viscosity due to temperature changes has already been incorporated into the fouling resistance calculation, the difference must be associated with other factors, potentially due to changes in the nature of the tea solution at this lowered temperature.

4.2.3.2 Membrane cleanability

Figure 4.13 demonstrates that the cleaning agent flux was 33% higher for membranes fouled at 36°C (120 litres m^{-2} hr^{-1}) compared to membranes fouled at 50 °C (90 litres m^{-2} hr^{-1}). Figure 4.14 shows that the membrane resistance after cleaning followed a reverse trend, as expected. Membranes fouled at 50°C showed a higher resistance after cleaning than those that were fouled at 36°C (3.1.and 2.4 x $10^{12}m^{-1}$ respectively).

4.2.3.3 Total tea solids rejection

Figure 4.15 shows total tea solids rejection data for the FP membrane. Reducing the temperature from 50 – 36°C increases the rejection from 0.21 +/- 0.011 to 0.30 +/- 0.015. Aggregation (tea creaming) at lower temperatures causes an increased particulate size which may increase membrane resistance (Figure 4.12), whilst increasing the selectivity of the membrane (Figure 4.15). The larger tea cream particulates formed at lower temperatures may not adhere to the membrane surface as easily and as strongly as those formed at higher temperatures. Hence lower temperature filtration can reduce the irreversible fouling resistance and increase both rinsable and concentration polarisation resistances.

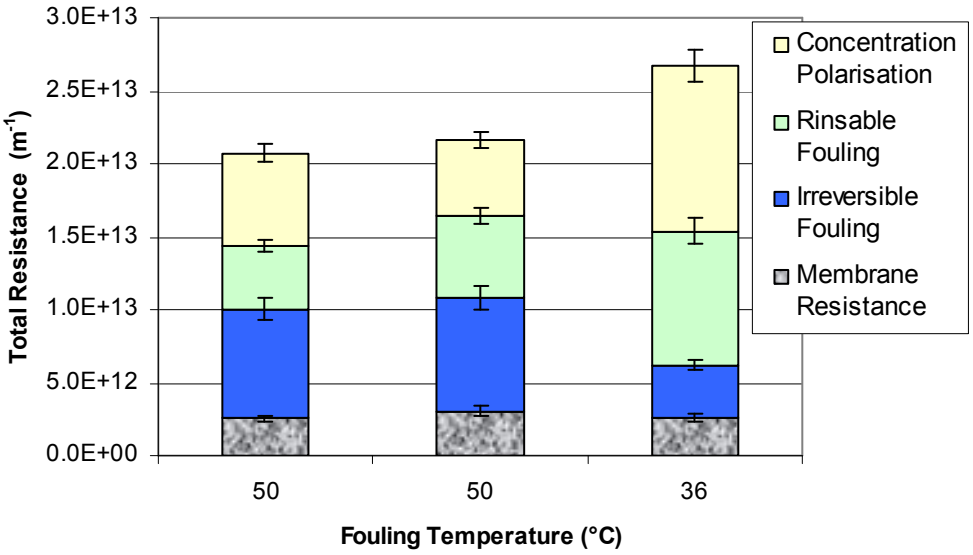

Figure 4.12: Graph to show sequential fouling resistance data vs fouling temperature on the same FP membrane when fouled with tea (1.0 bar TMP, 1.0 wt%, 0.44 m/s) for 30 mins.

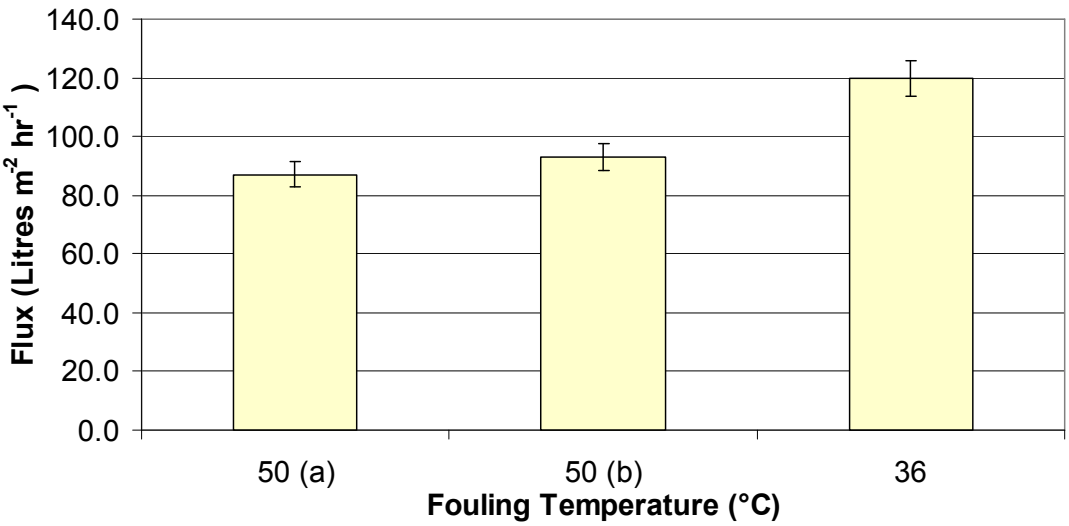

Figure 4.13: Graph to show sequential cleaning flux after fouling vs fouling temperature variation on the same FP membrane when fouled with tea (1.0 bar TMP, 1.0 wt%, 0.44 m/s) for 30 mins.

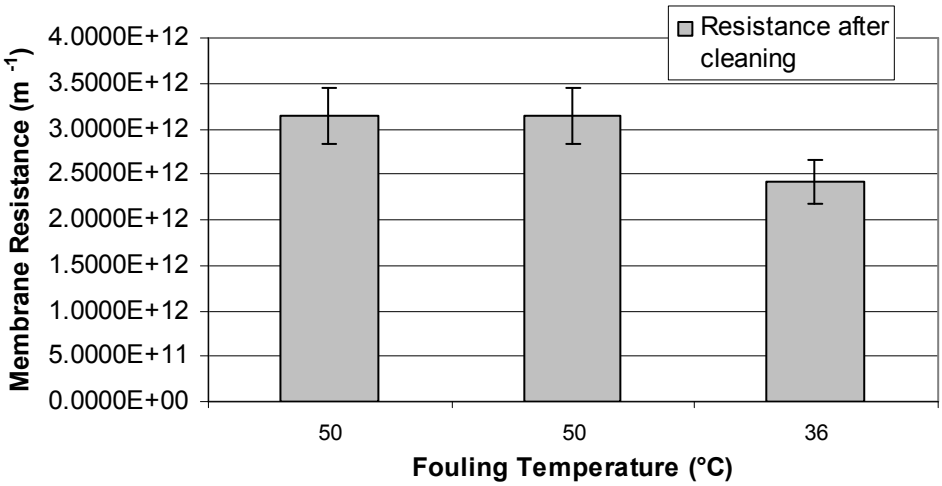

Figure 4.14: Graph to show sequential pure water membrane resistances after cleaning vs fouling temperature variation on the same FP membrane when fouled with tea (1.0 bar TMP, 1.0 wt%, 0.44 m/s) for 30 mins

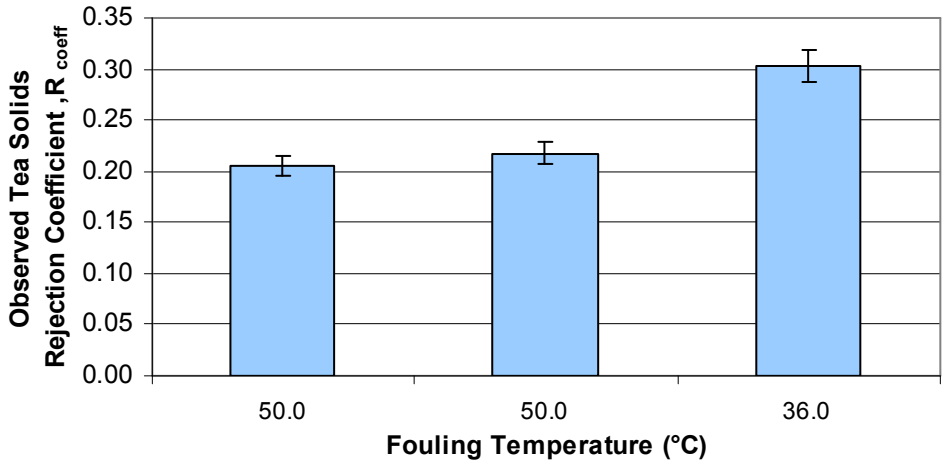

Figure 4.15: Graph to show sequential solids rejection coefficient vs fouling temperature variation through the same FP membrane when fouled with tea (1.0 bar TMP, 1.0wt%, 0.44m/s) for 30mins.

4.2.4 Feed ionic strength / Calcium content

The 100 kDa RC membrane was subjected to variations in feed ionic strength and calcium content with a constant feed concentration of 1.0 wt% total tea solids, and a TMP of 1.0 bar. All other conditions were as standard (Table 3.2). Figure 4.16 shows a break down of the different resistive layers present at steady state fouling (i.e. after 30 minutes filtration) for the conditions tested.

4.2.4.1 Effect of ionic strength

The addition of a 0.1 molar NaCl solution to the tea solution caused a 34% increase in total fouling resistance from those recorded under standard conditions (Figure 4.16).

An increased resistance or reduced flux with increased ionic strength has been demonstrated by Singh and Song 2005, for the UF of Silica colloids, by Li and Elimelech 2004 during the nanofiltration of water with natural organic matter, and by Lee and Elimelech 2006 during reverse osmosis. In this study, although the total fouling resistance increased with an increased ionic strength, the nature of fouling was also significantly changed. R_{CP} was the main contributing factor for this, increasing from 1.1 x 10^{13} m^{-1} at standard conditions to 2.5 x 10^{13} m^{-1} with an increased ionic strength. Both irreversible and rinsable fouling resistances decreased from 5.5 x 10^{13} m^{-1} and 5.53 x 10^{13} m^{-1} to 1.5 x 10^{13} m^{-1} and 3.0 x 10^{13} m^{-1} respectively. Increasing the ionic strength appears to reduce foulant – membrane interaction while allowing similar transmission of total tea solids, although a sacrifice is made in terms of a reduced flux through the membrane. Increasing the ionic strength could be reducing the electric double layer around the charged species, as is theorised by Lee and Elimelech 2006, who found that increasing ionic strength increased foulant – membrane interactions. However, in this study foulant – membrane interaction appears to be significantly reduced at an increased ionic strength, although an increased concentration polarisation effect was found. The higher R_{CP} recorded may be due to a reduced electrostatic repulsion between tea species causing an increased interaction in the solution. This would increase species concentrations towards the membrane surface. In turn this would lead to a reduced foulant – membrane interaction with an increase in concentration enhanced diffusion away from the membrane surface.

The cleanability of the standard fouled RC membrane and the 0.1M NaCl modified feed solution fouled RC membrane was similar after 15 mins of cleaning, as showed by flux measurements in Figure 4.17. However, initial cleaning rates were slightly different; standard fouled membranes displayed a slower initial flux recovery rate than the modified ionic strength feed solution. Once again, this confirms that increasing the ionic strength of the tea solution leads to a reduced degree of irreversible and rinsable fouling deposit formation.

4.2.4.2 Effect of calcium addition

The addition of 0.01M Ca^{2+} ions to the solution increased the total fouling resistance by 46% compared to the standard tea fouling conditions (Figure 4.16). R_{CP} increased

by 33% and rinsable fouling decreased by 44% on addition of calcium. The main cause of increased total fouling resistance was irreversible fouling, which increased by 157% from standard conditions. This suggests the importance of calcium in the initial intermolecular bridging of tea species (foulant) with the membrane surface, potentially followed by further foulant adhesion to previously deposited foulant. The fact that rinsable fouling reduced and irreversible fouling increased significantly demonstrates the increased adhesion of the foulant. The cleaning flux is shown in Figure 4.17. Compared to the cleaning flux following standard fouling (284 litres m^{-2} h^{-1}), there is a 31% reduction in the steady state cleaning flux of membranes fouled with the Ca^{2+} modified feed.(197 litres m^{-2} h^{-1}) , as measured after 15 mins of cleaning. Accordingly, the membrane resistance increased from 1.2 x 10^{12} m^{-1} after fouling / cleaning at standard conditions to 1.6 x 10^{12} m^{-1} after fouling / cleaning with added calcium (Figure 4.18). This also confirms that the sodium hydroxide cleaning protocol used in this study was insufficient to remove the foulant formed. Consequently, cleaning was performed with a commercial cleaning agent, *Ultrasil 11* (0.01wt%). This mixture contains sodium hydroxide, surfactants and chelating agents. Although there was a slight (11%) reduction in membrane resistance to 1.45 x 10^{12} m^{-1}, the membrane was still not returned to its initial condition. This indicates that the large irreversible fouling resistance measured in Figure 4.16 results from the adhesion of tenacious deposits.

This phenomena was also reported by Li and Elimelech 2004; Lee and Elimelech 2006 (for reverse osmosis) of natural organic matter with significantly enhanced foulant-membrane and foulant–foulant interaction in the presence of Ca^{2+} and Mg^{2+} ions. Ca^{2+} ions were found to cause stronger adhesion, with carboxyl group (COO-) complexation with Ca^{2+} ions thought to enhance interactions. This is almost certainly happening in our system, with many tea constituents (polyphenols / caffeine / proteins) containing possible functional interaction sites which could be enhanced by the presence of Ca^{2+} ions. The literature reports the influence of calcium upon tea cream formation, demonstrating the inter-reactivity of the species present in tea. Chao and Chiang 1999 demonstrated that 66% of the calcium from the original infusion participated in tea cream formation. Jobstl et al. 2005, suggested that calcium ions enhanced the self-association of polyphenols and caffeine by bridging polar groups. Tanizawa et al. 2007 investigated tea stain formation on porcelain tiles,

theorising that calcium was integral to the formation of tea stains by calcium bridging of polyphenolic constituents. This theory was then confirmed in a follow up study by Yamada et al. 2007, where the addition of extra calcium ions enhanced the calcium bridging of polar hydroxyl groups causing increased tea stain formation. Ethylendiaminetetracetic acid (EDTA) was found in this study to break up tea stains formed on the porcelain surface. However, despite containing >30% EDTA, *Ultrasil 11* was found to have a limited additional cleaning effect over NaOH under the conditions used in our study. In the current work, a maximum *Ultrasil 11* concentration of 0.01 wt% was used, meaning that a maximum EDTA concentration of 0.003 wt% EDTA was present in the cleaning solution.

The apparent membrane rejection coefficient reduced slightly from 0.27 at standard conditions to 0.25 for $CaCl_2$ modified feed (Figure 4.19). Although not experimentally significant, this does suggest that some enhanced permeation of tea solids may occur and further experiments may confirm this.

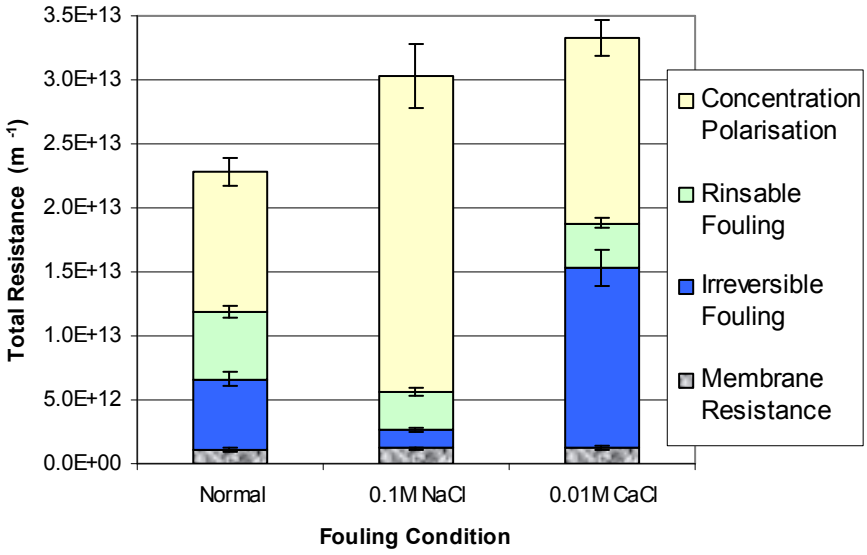

Figure 4.16: Graph to show sequential fouling resistance data vs fouling condition on the same fluoropolymer membrane when fouled with tea (1.0 bar TMP, 1.0 wt%, 0.44 m/s) for 30 mins.

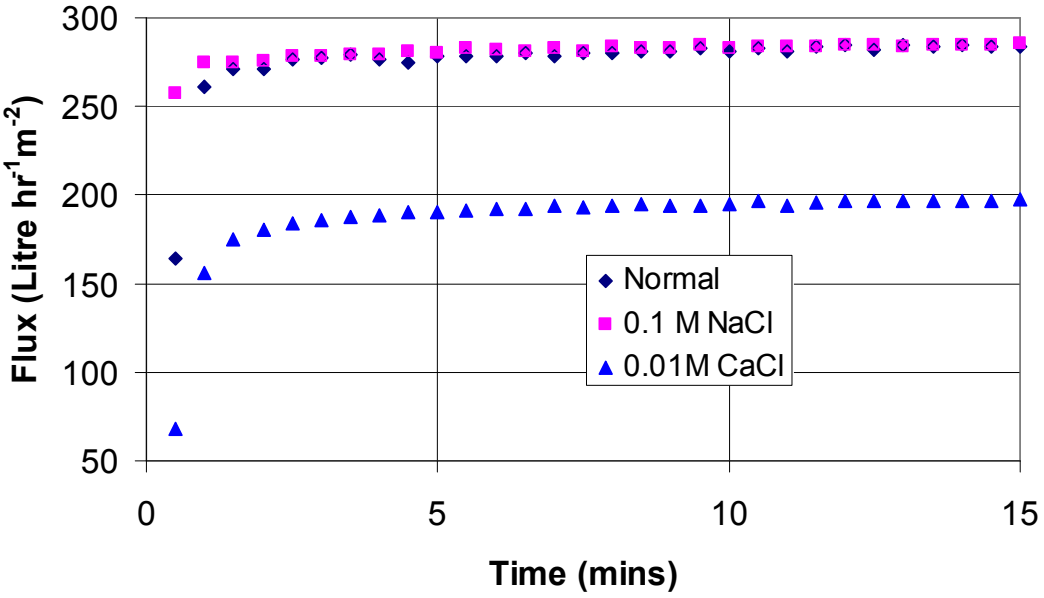

Figure 4.17: Graph to show cleaning flux after fouling vs fouling for different ionic treatment on the same regenerated cellulose membrane when fouled with tea (1.0 bar TMP, 1.0 wt%, 0.44 m/s) for 30 mins.

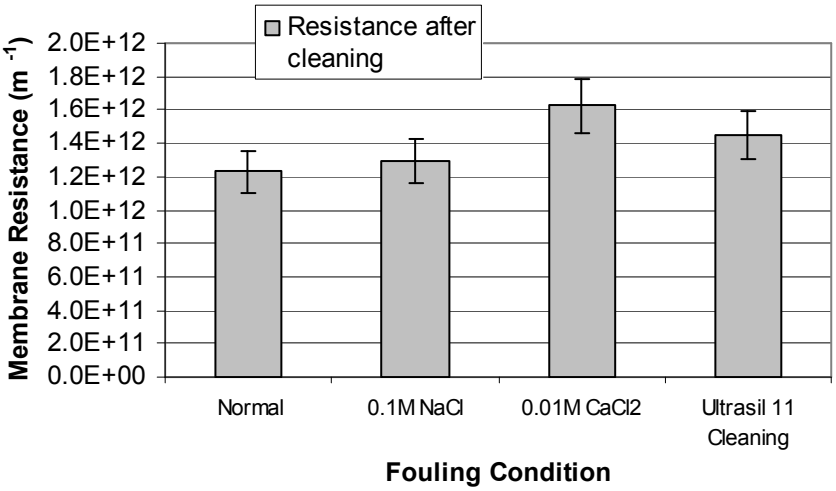

Figure 4.18: Graph to show sequential pure water membrane resistances after cleaning vs fouling temperature variation on the same fluoropolymer membrane when fouled with tea (1.0 bar TMP, 1.0 wt%, 0.44 m/s) for 30 mins

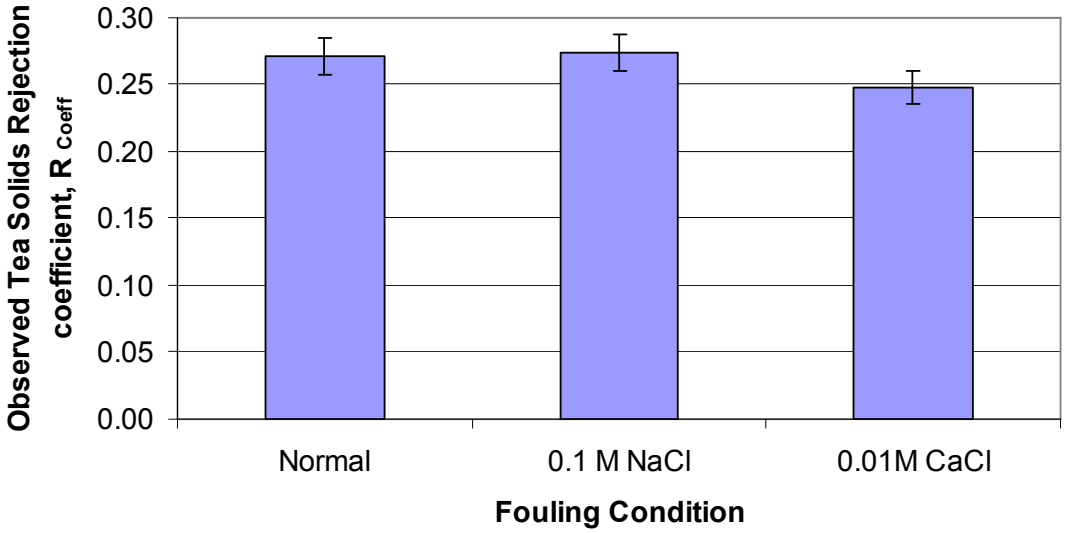

Figure 4.19: Graph to show solids rejection coefficient vs fouling ionic condition through the same RC membrane when fouled with tea (1.0 bar TMP, 1.0 wt%, 0.44 m/s) for 30 mins.

4.2.5 Summary

This section has investigated the influence of black tea feed concentration and temperature on two different material FP and RC membranes. Also initial findings regarding the influence of feed ionic strength and calcium ion content were investigated. Generally the RC membrane demonstrated a reduced foulant – membrane interaction and thus a reduced overall deposit formation when compared to the FP membrane. However, as a consequence, the membrane selectivity was increased for the RC membrane and mass transfer reduced due to an increased concentration of feed close to the membrane surface.

The importance of feed condition upon filtration performance due to variations in fouling mechanism and cleaning efficiency has been demonstrated.

Concentration polarisation contributes predominantly for the conditions examined, increasing the total resistance of both membranes as the feed concentration was increased. Feed concentration had no extra effect on deposit formation on the RC membrane, whereas rinsable fouling deposit did increase on the FP membrane surface. This suggests that there was a somewhat stronger interaction of fouling species with the FP membrane than with the RC membrane.

Total fouling resistance and membrane rejection were increased upon cooling of the black tea feed. A lower temperature feed reduced the extent of irreversible fouling

while increasing rinsable fouling and concentration polarisation, suggesting that enhanced aggregation (tea creaming) decreased foulant – membrane interactions.

Increasing the ionic strength of the tea solution increased the total fouling resistance (R_F) thus reducing performance, while decreasing the severity of deposition fouling due to an increased concentration polarisation. Addition of calcium to the feed stream (which is known to increase aggregation and creaming within the black tea system) caused a significant increase in irreversible fouling deposition. This could not be removed effectively either by the standard sodium hydroxide cleaning regime adopted, or by the use of a formulated agent in the concentration range studied.

4.2.6 TMP variation on single fluoropolymer membrane

4.2.6.1 Fouling Flux

Figure 4.20 and Figure 4.21 display fouling flux data for FP and RC membranes respectively. Standard conditions for pure water, fouling and cleaning cycles have been maintained, and only the fouling TMP has been varied. The data is represented such that the average fouling flux is shown in conjunction with the first and last fouling flux value. The last fouling point demonstrates that the flux has tended towards a steady state value. All steady state data satisfied the condition required in Equation 3.1. For the FP membrane, (Figure 4.20) increasing fouling TMP increased fouling flux at low pressures. A limiting fouling flux appears to be reached in the region of 3 – 4 bar, with steady state fluxes of 35.7 and 36.3 litres h^{-1} m^{-2} (LMH) for 3 and 4 bar TMP respectively. When returning to 1.0 bar fouling following the 4.0 bar fouling cycle, hysteresis is clearly observed in the fouling flux value. A steady state fouling flux value of 33.1 LMH is recorded compared to one of 23.0 LMH for the initial fouling cycle at 1.0 bar.

A further fouling and cleaning cycle using a fouling pressure of 1.0 bar resulted in an insignificant drop in the steady state flux (32.3 LMH) from that recorded for the previous fouling cycle (33.1 LMH).

Figure 4.21 shows that for the RC membrane, although initial fouling fluxes are increasing with TMP, steady state fluxes have approached a maximum of 32.1 LMH by 1.0 bar TMP. This suggests that a limiting flux has been reached and accordingly a maximum concentration may have been reached at the membrane surface, leading to the possible formation of a gel layer (Song 1998).

Experiments performed at 0.5 bar TMP show that the system is fractionally below the limiting flux, which is clearly established between 0.5 and 1.0 bar under the conditions examined.

The steady state flux values recorded for the FP membrane at 1.0 bar following multiple fouling and cleaning cycles, and that of RC at 1.0 bar (33.8 and 32.1 LMH respectively) suggest that the FP membrane once modified has similar fluxes to the RC membrane.

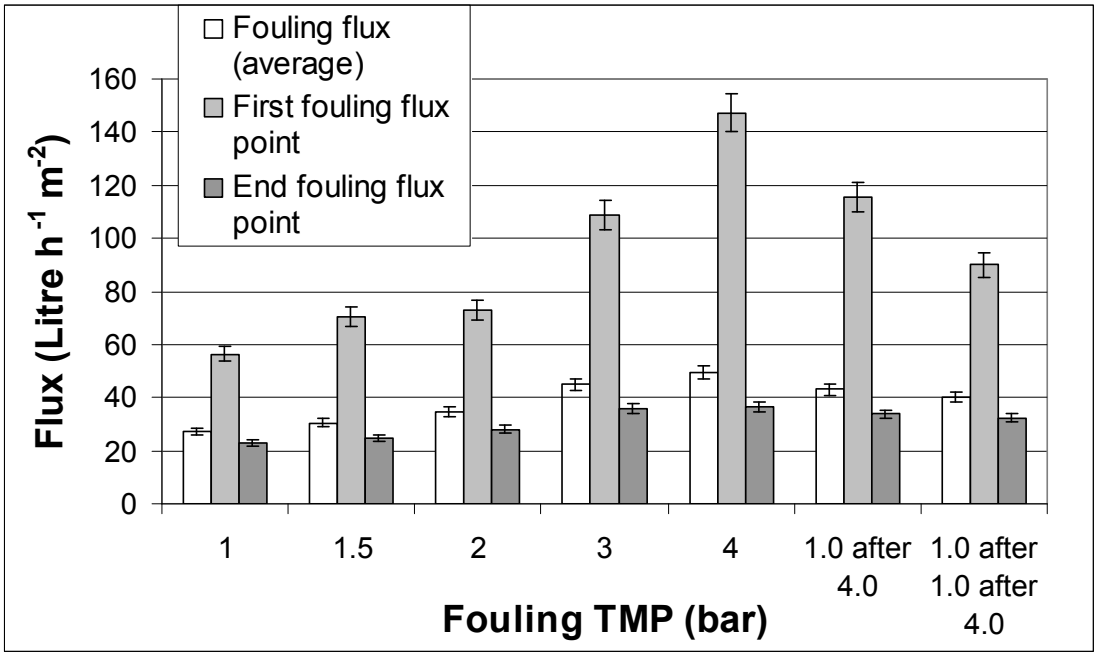

Figure 4.20: Graph to show sequential fouling flux data versus TMP variation on the same fluoropolymer (FP) membrane when fouled with tea (1.0 wt%, 50°C, 0.44 ms^{-1}) for 30 minutes starting initially at 1.0 bar increasing to 4.0 bar then returning to 1.0 bar again.

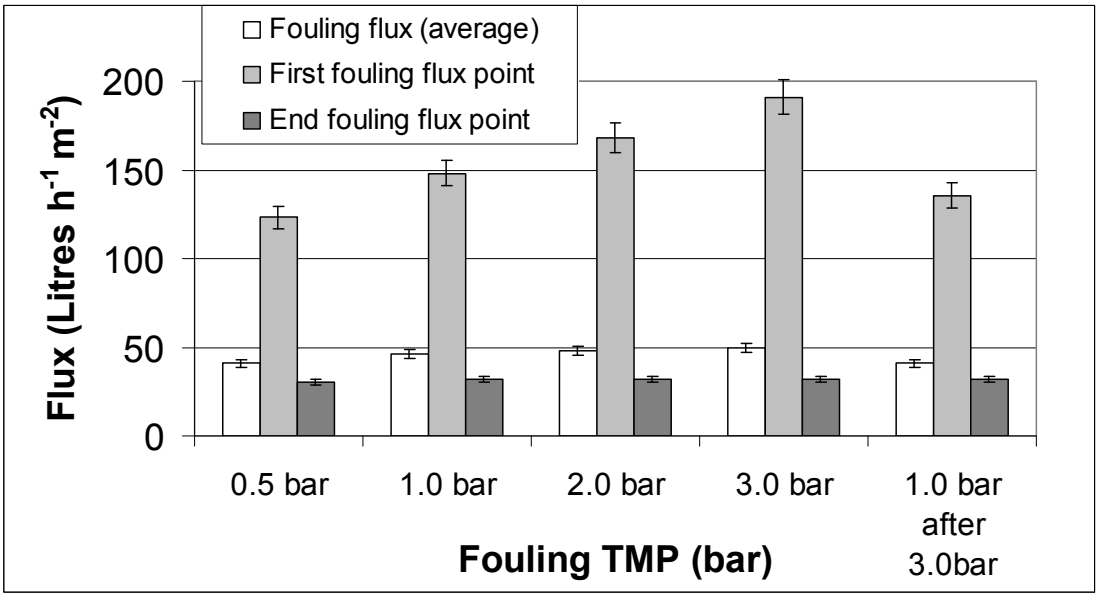

Figure 4.21: Graph to show sequential fouling flux data vs TMP variation on the same regenerated cellulose (RC) membrane when fouled with tea (1.0 wt%, 50°C, 0.44 ms^{-1}) for 30 minutes starting initially at 1.0 bar increasing to 3.0 bar, then performing cycle at 0.5 bar and returning to 1.0 bar again.

4.2.6.2 Fouling resistance data

Figure 4.22 and Figure 4.23 show a break down of the different resistive layers present at steady state fouling (i.e. after 30 minutes fouling) for FP and RC membranes respectively where the only parameter varied in the pure water/fouling/cleaning cycles was the fouling TMP (technique discussed in 4.2.1).

The total resistance, R_T increased significantly as TMP was increased for both FP and RC membranes where concentration polarisation, R_{CP}, is responsible for the significant increase in resistance, and becomes more significant with increasing TMP. For the FP membrane, R_{CP} was 17% of total resistance at 1.0 bar and 56% of total resistance at 4.0 bar, whereas for the RC membrane R_{CP} was 39% of total resistance at 1.0 bar and 60% of total resistance at 3.0 bar. This suggests that there is significantly more back diffusion from the RC membrane initially at 1.0 bar although when the TMP is increased both display similar relative amounts of back diffusion.

For the FP membrane, there was hysteresis shown when the fouling cycle TMP was reduced to 1.0 bar from 4.0 bar. The combination of initial membrane resistance and irreversible fouling were mainly responsible for this decrease in resistance, 1.89 x $10^{13}m^{-1}$ before any increase in pressure at 1.0 bar then reducing to approximately 1.00 x $10^{13}m^{-1}$ after increasing the pressure to 4.0 bar TMP. The combination of

concentration polarisation and rinsable fouling stay ≈ 1.0 x $10^{13}m^{-1}$. This suggests that the FP membrane has been altered after the fouling / cleaning cycles so that it's resistance during fouling is similar to that of the RC membrane; when fouling at 1.0 bar TMP both membranes have a resistance of ≈ 2.0 x $10^{13}m^{-1}$.

4.2.6.3 Membrane resistance after cleaning

Figure 4.24 and Figure 4.25 show the membrane resistances after the standard cleaning protocol had been carried out following fouling at different TMP values. This demonstrates how the membrane performance has permanently changed after fouling. The resistances were calculated using Equation 4.4 and the flux data from the standard procedure with RO water.

Figure 4.24 shows that the virgin FP membrane resistance has reduced by 62% from 1.46 x 10^{13} m^{-1} to 5.6 x 10^{12} m^{-1} after twelve fouling / cleaning cycles, with 1.0 bar fouling and varied cleaning conditions during optimisation. This value was reduced still further after 4.0 bar TMP fouling to 2.55 x $10^{12}m^{-1}$. This suggests there has been some significant irreversible adsorption on the membrane surface, either within the membrane pores or on the external surface, increasing RO water permeation, and suggesting that the membrane has become more hydrophilic. This was confirmed by contact angle measurement (Table 4.2). The normalised flux recovery values of the membrane after fouling at 3.0 and 4.0 bar TMP were 130% and 160% respectively of the initial value. The membrane resistance of the second 1.0 bar fouling cycle following the 4.0 bar fouling had increased slightly from 2.82 x 10^{12} to 2.90 x 10^{12} m^{-1}. This difference is within the limits of experimental error. There are two phenomena occurring here, multiple cycle effects and increased TMP effects. Further work is discussed in 4.2.7 and 4.2.8 on the relative contribution of each to the flux values recorded.

In contrast to the resistance data for the FP membrane, there is no real trend for the resistance change of the RC membrane after fouling at different TMP following cleaning (Figure 4.25). The resistance does increase slightly from the virgin membrane resistance of 1.6 x $10^{12}m^{-1}$ to around 1.7 x $10^{12}m^{-1}$ for subsequent fouling / cleaning cycles. This increase is not statistically significant. The permeate flux was easily recovered after subsequent fouling / cleaning cycles, with an average flux recovery of 100 +/-2%.

4.2.6.4 Membrane rejection and permeate colour data

Figure 4.26 and Figure 4.27 show the observed rejection coefficients (R_{coeff}) for the FP and RC membranes respectively where only the fouling TMP has been varied. As the TMP increases, both FP and RC membranes reject more tea solids. Although this contradicts the findings of Pradanos *et al.* 1995, this trend was also reported by Todisco *et al.* 2002 for polyphenol rejection when fouling TMP was increased using a ceramic tubular (ultrafiltration) membrane. Blainpain *et al*. 1993 reported that internal fouling may increase rejection slightly but external fouling forms a second composite membrane which increases rejection more significantly. In addition, higher pressures lead to an increase in concentration polarisation (as also demonstrated in this study) and hence a higher rejecting composite membrane can be obtained. Meien and Nobrega, 1994, found that rejection of dextran was increased in the limiting flux region as TMP was increased and this was thought to be due to viscosity effects. Mulder, 2000, stated that retention can be higher than expected when mixtures of macromolecular solutes are present and larger solutes are completely retained forming a second dynamic membrane which results in higher retentivity for the lower molecular weight solutes. This appears to be the case in the current investigation. Liang and Xu, 2001 and Liang *et al.*, 2002 report that the majority of the tea cream particles formed are in the size range 0.1 – 5.07 μm. Increased tea concentration has been shown to increase the amount and rate of tea cream formation (Tolstoguzov 2002). Therefore the concentration polarisation of tea cream species close to the membrane surface may lead to an increased aggregation in this region.

For the FP membrane, the solids rejection during the 1.0 bar fouling cycle that followed the 4.0 bar cycle was the same value as that recorded for the initial 1.0 bar cycle before the TMP was increased (Figure 4.26). The L*a*b* value of the permeate from both these runs also remained unchanged, indicating that no pore widening had occurred as a result of the cumulative pressure treatments. This also suggests that any irreversible adsorption to the FP membrane did not influence the solids rejection value or colour of the permeate. Figure 4.27 shows that the RC membrane showed a higher rejection of solids (0.27 at 1.0 bar) compared to the FP membrane (0.21 at 1.0 bar). The higher rejection of solids by the RC membrane may explain why a limiting flux

was reached at a lower pressure, as fewer solids were being transported through the membrane, therefore causing a greater build up of solids at the membrane surface increasing the concentration to a maximum gel concentration at a lower pressure than for the FP membrane. The membrane is effective at rejecting haze and tea cream aggregates, but transmits lower molecular mass compounds that lead to a relatively low overall rejection of solids by the membrane.

Figure 4.28 shows the difference between reconstituted powder colour and haze without treatment and colour and haze from FP and RC permeates. The concentrations are similar for all conditions to facilitate a comparison. Prior to analysis, the permeate appeared to the naked eye to be considerably clearer and lighter than the initial reconstitute. Analysis confirmed this, with a significantly increased Lightness (L *), an increased yellowness (b*), and a considerably reduced haze (by a factor of 10). A small increase in the amount of redness (a*) detected in the FP permeate suggests that thearubigins and/or theaflavins were passing through the membrane. This contrasted with the reduced a* value detected for the RC permeate. Care must be taken when considering the results for yellowness and redness as haze contributes significantly to these values and a reduction in haze in the permeate may account for some of the changes noticed. The fact that the FP permeate has a higher haze and redness than the RC membrane permeate confirms the potential transmission of some larger molecular weight compounds. These results confirm that ultrafiltration may be considered as a process for clarifying and reducing haze for ready to drink tea, allowing higher concentrations with lower haze. Further work is required to characterise the stability of these clarified solutions over time. The choice of membrane material is clearly critical to the viability of the process.

4.2.6.5 Membrane and tea foulant interaction

Species charge, solution ionic strength, and the hydrophobicity, charge, morphology and roughness of the membrane are all important factors determining transmission Persson *et al.* 2003; Weis *et al.* 2003; Weis *et al.* 2005.

The relative importance of membrane hydrophobicity in the system under investigation has been determined as shown in Table 4.2. Prior to conditioning, the virgin RC membranes were highly hydrophilic in nature (18°) and were difficult to measure after conditioning due to the very small angles recorded (<15°). The FP

membranes were considerably more hydrophobic (virgin membrane - 65°, conditioned membrane - 62°). These values are still considered to be moderately hydrophilic as the contact angles measured were less than 90^{o}.

Table 4.2 shows that the RC membrane contact angle had increased to 50° after fouling at 1.0 bar. This indicates that the membrane surface had been fouled with more hydrophobic species. After multiple fouling and cleaning cycles the membrane surface contact angle was returned to 18°, demonstrating that most of the fouled material had been removed.

By contrast, the FP membrane contact angle had reduced from 62 for the conditioned membrane to 42 and 43° after fouling at 1.0 bar and 4.0 bar respectively. After multiple fouling and cleaning cycles, the membrane surface had a contact angle between that of a virgin and a fouled surface (52°). This measurement explains the increased permeability and reduced resistance displayed by the fouled FP membrane compared to the conditioned virgin surface. There may be significant in-pore adsorption that is not represented by the contact angle measurement and this may be responsible for a further reduction in the overall membrane resistance.

The precise mechanism of surface interaction between the tea species and the membrane polymers remains uncertain. The surface roughness values of the conditioned FP and RC membranes are 24.8 nm and 6.5nm respectively (determined by atomic force microscopy studies (see section 3.6.4.1). Consequently, direct entrapment of the larger tea cream aggregates (0.1 – 5.07μm) due to surface roughness is not possible. It seems more likely that the more hydrophobic FP membrane surface is first modified by attachment of hydrophilic material; sub micelles or other protein / polyphenol complexes. Further attachment is noticed at higher fouling TMP due to increased concentration polarisation with higher concentrations at the membrane surface. The effect of cleaning with NaOH is to modify the surface hydrophobicity to a value between that of the fouled and the cleaned surface. The hydrophobicity of the once-fouled FP membrane is less than that recorded for a once-fouled RC membrane (43 and 50^{0} respectively). These contact angle differences are not accounted for by experimental error, implying that absorption of hydrophilic substances is preferentially occurring on the FP membrane surface.

There are many parameters that affect the interaction occurring between bio products and polymeric surfaces, of which hydrophilicity is only one. Nevertheless this result implies that moderately hydrophobic membranes may offer definite operational advantages over highly hydrophilic materials for the UF processing of tea solutions.

4.2.6.6 Summary

This section has examined the performance of two ultrafilters for the clarification of black tea liquor at varied TMP. At 1.0 bar TMP and 30 minutes of fouling, the FP and RC membranes have steady state fluxes of 23.0 and 32.1 LMH respectively, rejecting 21% and 27% of tea solids respectively. For both membranes examined, the permeate lightness and yellowness were increased and the haze was significantly reduced. The redness of the FP permeate was also increased.

Initially at 1.0 bar TMP, the FP membrane had a lower steady state flux and a lower rejection of tea solids when compared to the RC membrane. Concentration polarisation was responsible for significantly more of the RC membrane resistance at these initial conditions than for the FP membrane.

Membrane rejection was found to increase for both membranes as the TMP increased. The RC membrane showed higher total solids rejection ratios than the FP membrane at the same TMP.

The RC membrane had reached a limiting flux by 1.0 bar TMP and the FP membrane appeared to be approaching a limiting flux at 4.0 bar TMP.

The RC membrane resistance was very stable as TMP was increased from cycle to cycle, increasing by approximately 10% from virgin membrane conditions. Multiple operational cycles produced a clean RC membrane that had a similar hydrophilicity to that of a virgin RC membrane.

The cleaned FP membrane resistance was reduced as the membrane was fouled at higher TMP values and the membrane surface became more hydrophilic. However, the membrane's solids rejection ratio and the L*, a* and b* values of the permeate did not change over multiple cycles.

The precise mechanism of surface interaction between the tea species and the hydrophobic FP membrane remains uncertain. Modifications in the zeta potential of the surface before and after fouling and cleaning treatments are reported in section 4.2.8.4 and 4.3.5 demonstrating the importance of surface charge in the fouling process. It seems likely that the moderately hydrophobic membrane surface is first

modified by surface fouling with hydrophilic sub micelles or other protein / polyphenol based foulants, followed by a reaction with the NaOH cleaning solution to produce a further modified membrane surface that has a hydrophilicity between that of the virgin and the fouled surface.

The experimental findings reported here are industrially relevant as they indicate that moderately hydrophobic membranes, with their advantages of chemical and thermal stability, maybe modified by selective adsorption of hydrophilic tea species to give fluxes similar to those seen with more hydrophilic materials. There may therefore be a distinct processing advantage in using moderately hydrophobic polymeric membranes over highly hydrophilic materials for the filtration of tea liquors.

Membrane	Unconditioned	Conditioned	Fouled (at 1.0bar TMP)	Fouled (at 4.0bar)	After Cleaning cycles
Fluoropolymer	65 +/- 1.8	62 +/- 1.5	43 +/- 3.5	42 +/- 3.2	52 +/- 2.7 (23 cycles)
Regenerated Cellulose	18 +/- 3.4	< 15 *	50 +/- 2.3	N / A	18 +/- 3.6 (16 cycles)

*Note - very difficult to read conditioned RC membrane contact angle because the value recorded was so small.

Table 4.2: Contact angles measured using the sessile drop method for fluoropolymer (FP) and regenerated cellulose (RC) membranes.

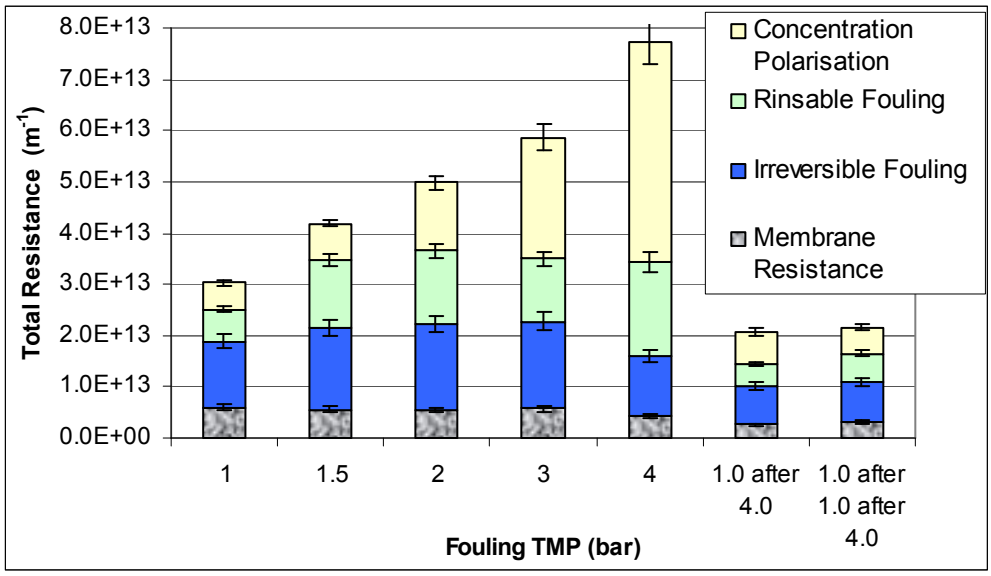

Figure 4.22: Graph to show break down of fouling resistance at steady-state (after 30mins) when TMP is varied on the same fluoropolymer membrane when fouled with tea (1.0 wt%, 50°C, 0.44 ms^{-1}) starting initially at 1.0 bar increasing to 4.0 bar.

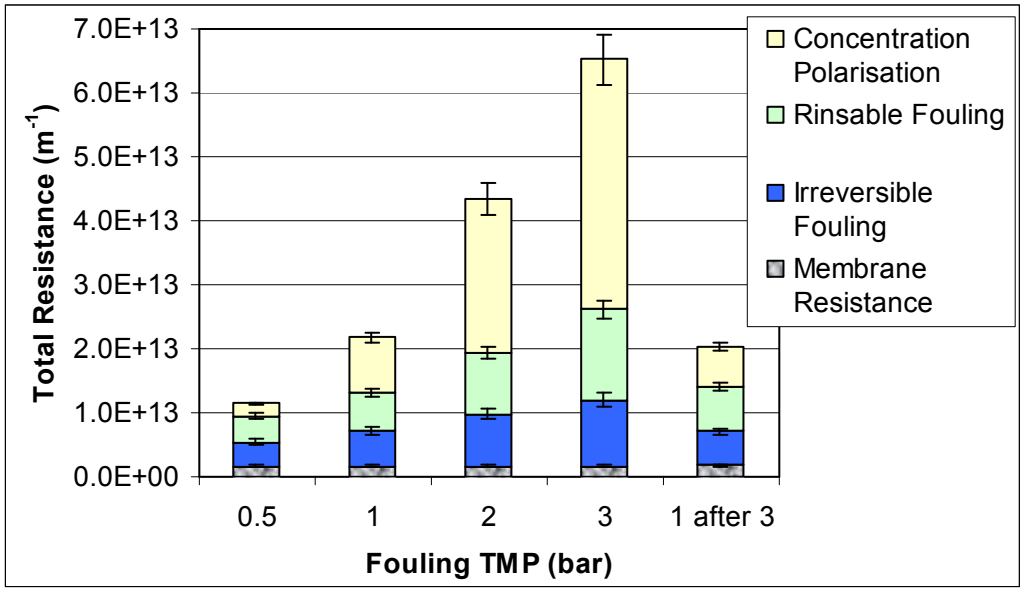

Figure 4.23: Graph to show break down of fouling resistance at steady-state (after 30 mins) when TMP is varied (0.5 – 3.0bar) on the same Regenerated Cellulose membrane when fouled with tea (1.0 wt%, 50°C, 0.44ms^{-1}).

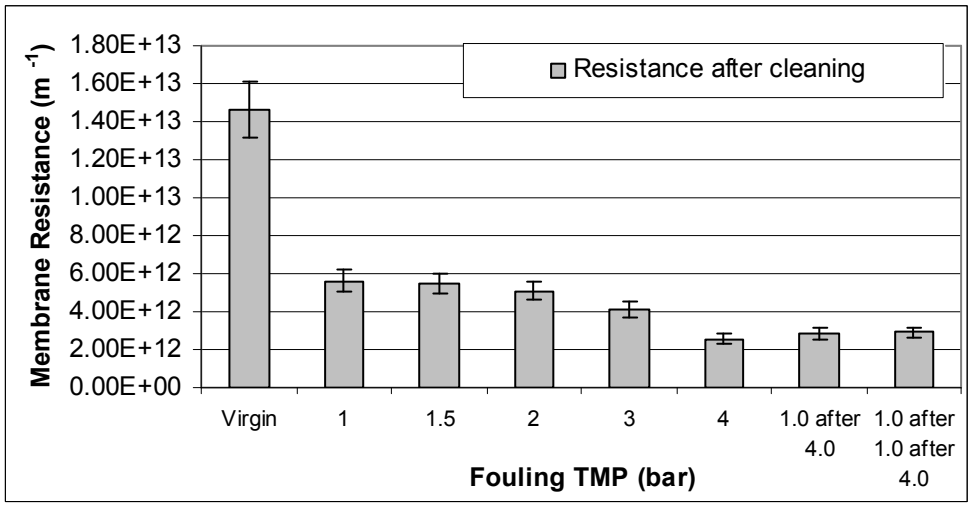

Figure 4.24: Graph to show membrane resistance after the application of a consistent cleaning protocol for fluoropolymer membranes; fouled at various TMP values.

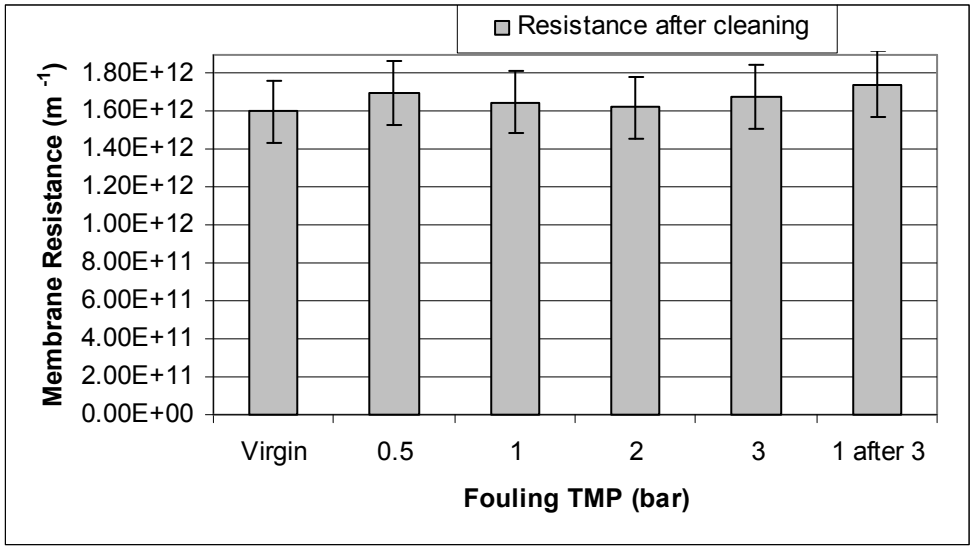

Figure 4.25: Graph to show membrane resistance after the application of a consistent cleaning protocol for regenerated cellulose membranes; fouled at various TMP values.

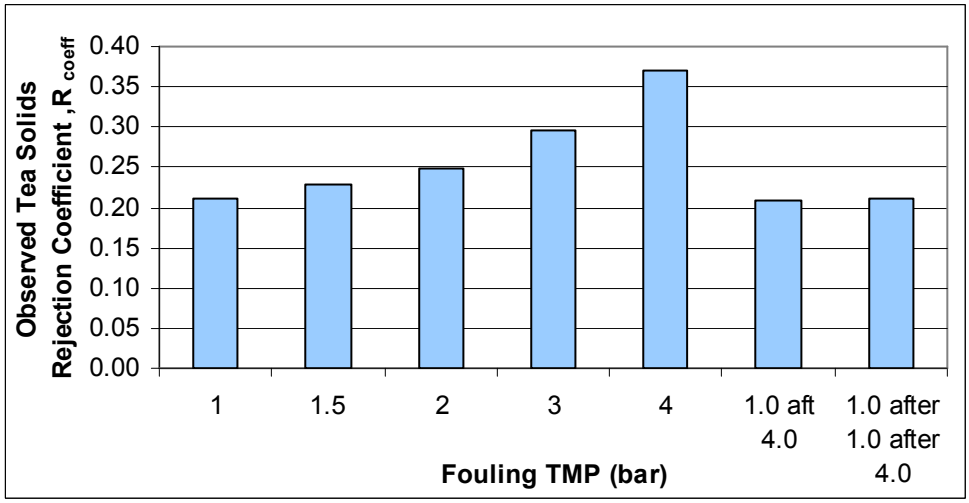

Figure 4.26: Graph to show average membrane rejection vs TMP for the same fluoropolymer (FP) membrane fouled with tea (1.0 wt%, 50°C, 0.44 ms^{-1}) for 30minutes. TMP values were initially started at 1.0 bar increased to 4.0 bar. A final cycle was performed at 1.0 bar.

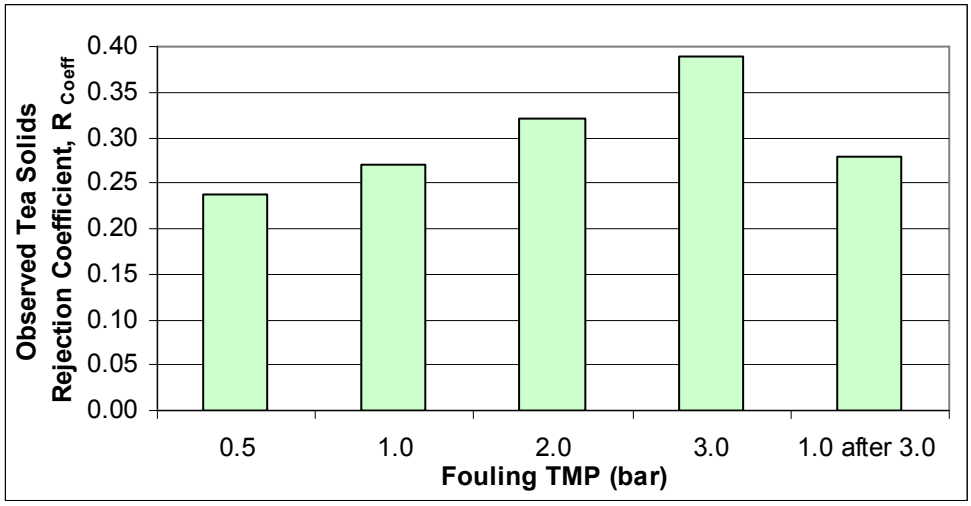

Figure 4.27: Graph to show average membrane rejection vs TMP for the same regenerated cellulose (RC) membrane fouled with tea (1.0 wt%, 50°C, 0.44ms^{-1}) for 30 minutes. TMP values were initially started at 1.0 bar and increased to 3.0 bar. Two subsequent cycles were performed at 0.5 bar and 1.0bar.

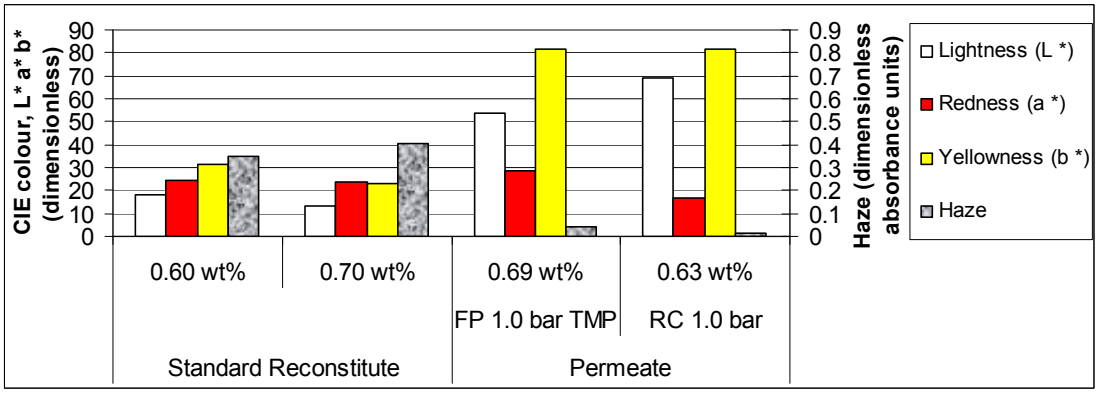

Figure 4.28: Graph to show the comparison between a standard unfiltered reconstituted powder and ultrafiltered permeate using fluoropolymer and regenerated cellulose membranes operating under the same conditions (1.0 bar TMP, 0.44ms^{-1}, 50°C).

4.2.7 Transmembrane pressure variation on individual membranes

The previous section (4.2.6) discussed the effect of varying the TMP from cycle to cycle on the same FP and RC membranes. This section will examine the effect of TMP variation using fresh virgin conditioned membranes for each cycle. Pure RO water, fouling and cleaning fluxes and the total tea solids rejection coefficient of the membranes were recorded throughout the cycle. Theaflavins and caffeine transmission are also reported and the chemical nature of the membrane surface measured using the FTIR technique at different stages throughout the fouling / cleaning cycle.

4.2.7.1 Fouling Flux

Figure 4.29 displays the steady state fouling fluxes (In accordance Equation 3.1) for virgin conditioned FP and RC membranes fouled with black tea liquor at 1 bar TMP and fresh virgin conditioned FP/RC membranes fouled at elevated TMP of 4.0 / 3.0 bar respectively. During the fouling / cleaning cycle for each membrane tested, standard conditions for pure water, fouling and cleaning cycles have been maintained (Table 3.2), and only the fouling TMP has been varied. Increasing the TMP from 1.0 to 4.0 bar for the FP membrane increases the steady state flux from 22 LMH to 25 LMH. The RC membrane demonstrated a limiting flux, (as in the section 4.2.6) such that increasing the TMP from 1 to 3 bar TMP maintained an approximate flux of 24 LMH. The RC membrane could not be operated above 3.0 bar TMP due to the possibility of breakthrough of the retentate at this pressure. However, the membrane did not appear punctured following a pressure of 4 bar. When the pressure was reduced back to 1.0 bar the membrane performed normally. No transmission measurements were taken during this phenomena and the membranes discarded.

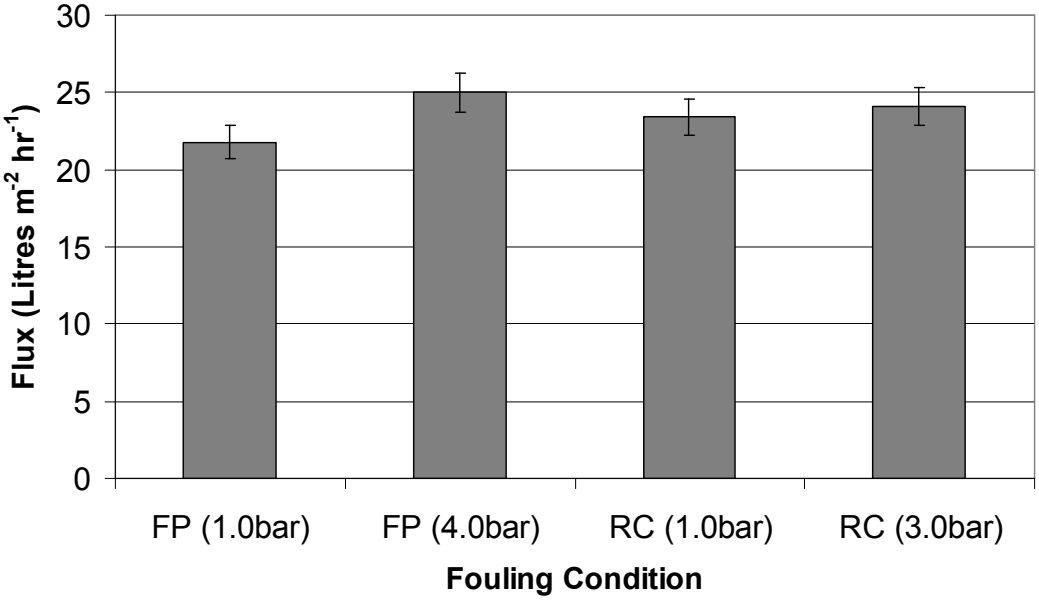

.

Figure 4.29: Steady state fouling flux data for virgin conditioned Fluoropolymer and Regenerated Cellulose membranes fouled with black tea (1.0wt%, 50°C, 0.44m/s) for 60 min at varied TMP.

4.2.7.2 Total tea solids membrane rejection coefficient

Figure 4.30 shows the total tea solids rejection coefficient (Equation 4.6) for virgin conditioned FP and RC membranes fouled with black tea liquor at 1 bar TMP and fresh virgin conditioned FP/RC membranes fouled at elevated TMP of 4.0/3.0 bar

respectively. The FP membrane rejects less tea solids (0.31) compared to the RC membrane (0.35) at 1.0 bar TMP. Increasing the TMP of the FP / RC membrane to 4.0 / 3.0 bar significantly increases the membrane rejection to 0.47 and 0.45 respectively. This data confirms the results reported in section 1.3.6 where the TMP was varied on the same FP and RC membranes where consecutive TMP variations were performed on the unchanged membrane of each material.

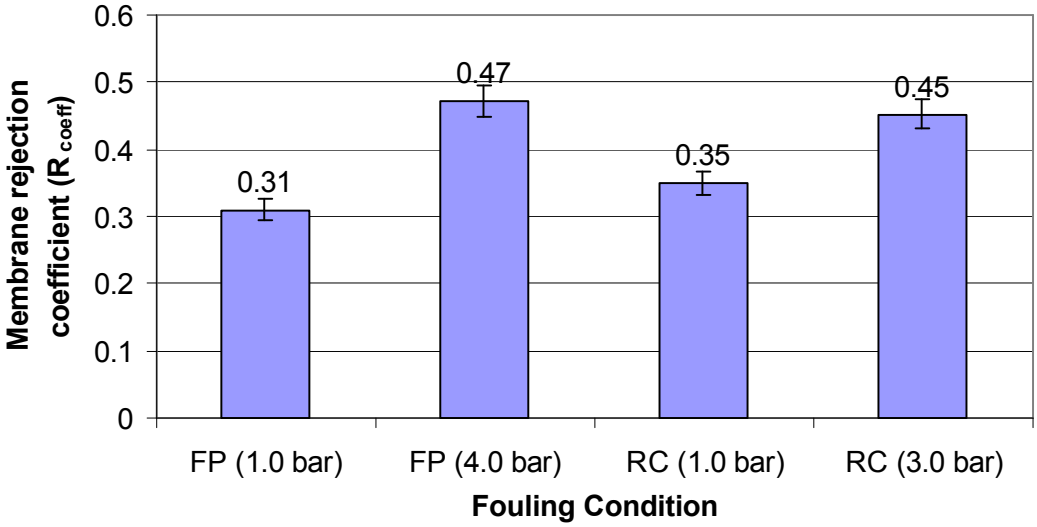

Figure 4.30: Total tea solids membrane rejection coefficient for virgin conditioned Fluoropolymer and Regenerated Cellulose membranes fouled with black tea (1.0wt%, 50°C, 0.45 m/s) for 60 min at varied TMP.

4.2.7.3 Pure water flux characterisation

Figure 4.31 displays the normalised pure water flux (Equation 4.13) for each FP and RC membrane fouling / cleaning cycle investigated for variation in fouling TMP. The RC membranes demonstrated approximately 100% flux recovery after both 1.0 and 3.0 bar TMP fouling. The FP membranes demonstrated flux recoveries significantly above 100%, after 1.0 bar fouling the flux recovery was 125% whereas after 4.0 bar the flux recovery was 158%. This data confirms the previous results obtained during TMP variation on the same FP membrane as represented in section 4.2.6 . Increasing the TMP during a black tea fouling run permanently modifies the membrane surface enhancing both pure water and black tea fouling fluxes.

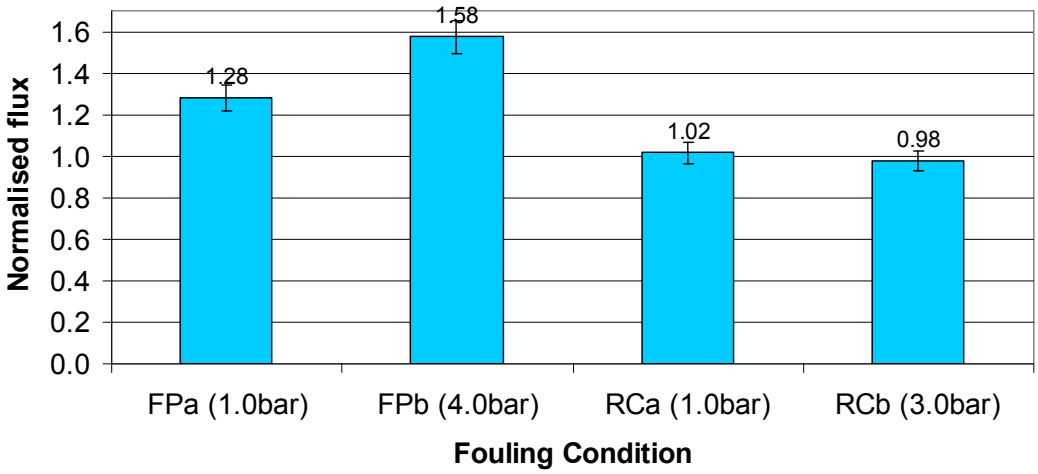

Figure 4.31: Pure water flux recoveries of Fluoropolymer and Regenerated Cellulose membranes fouled with black tea (1.0wt%, 50°C, 0.45 m/s) for 60 min at varied TMP and then regenerated with standard NaOH cleaning protocol.

4.2.7.4 HPLC Characterisation

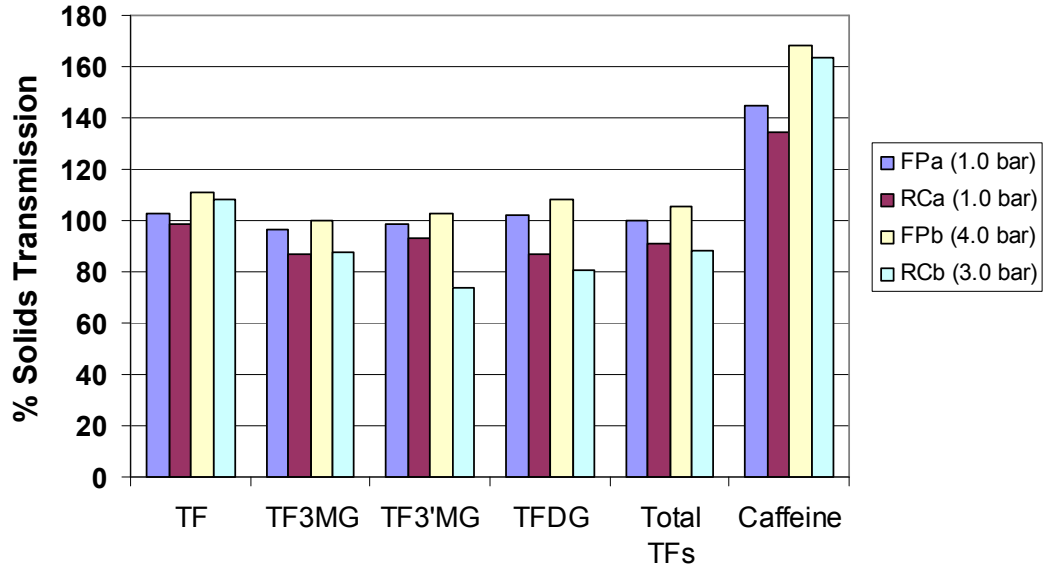

Figure 4.32: Theaflavins and Caffeine transmission through fluoropolymer and Regenerated cellulose membranes at different transmembrane pressure.

Figure 4.32 presents theaflavins and caffeine transmission through the 30kDa FP and RC membrane at different TMP values calculated using Equation 4.12. These measurements represent the concentration of each constituent in the tea solids fraction of the permeate compared to the original feed. Transmission values of greater than 100% are apparent when the constituent passes through the membrane to a greater extent than other components within the tea solids fraction. Fewer of the entire

theaflavins passed through the RC membrane (91%) than the FP membrane (100%) at 1.0 bar TMP. Increasing the operating TMP caused the relative concentration of all theaflavins to increase in the FP permeate, whereas in the RC permeate, TF and TF3MG increased, and TF3'MG and TF3DG decreased quite significantly. Caffeine, having a smaller molecular mass, transmitted through the FP and RC membranes readily with values of 145 and 134% respectively at 1.0 bar TMP. Therefore, increased concentration of caffeine was then was present in the permeate total tea solids than the original feed black tea liquor tea solids. Increasing the operating TMP significantly increased caffeine transmission to 168 and 163% for the FP and RC membrane respectively.

As also discussed in section 2.1.4 , the clarified black tea liquor will be spray dried or concentrated for transportation to the required production location. Although the total tea solids transmission decreased upon increasing the operating TMP as shown in Figure 4.30, the relative amount of the important theaflavins and caffeine in the clarified liquor increased and most importantly the stability was also increased (Figure 4.28).

4.2.7.5 FTIR Characterisation

Figure 4.33 and Figure 4.34 display the FTIR scans of the FP membrane during a fouling cleaning cycle for 1.0 and 4.0 bar TMP respectively. The fouled 1 and fouled 1 / cleaned 1 traces have had the virgin conditioned trace subtracted so the variation caused by the treatment can be observed. Comparing the fouled 1 surface for each TMP demonstrates the nature of the deposit formed. The intensity of the fouled 1 surface at 4.0 bar was typically more than twice that of the fouled 1 surface at 1.0 bar TMP, confirming an increased deposit formation as a result of enhanced fouling. Both FP membrane surfaces after fouling and cleaning demonstrated a permanent modification to the surface. These results suggest that either the membrane was not adequately cleaned of tea constituents, or was modified during the NaOH cleaning. This is clarified in section 4.3 .

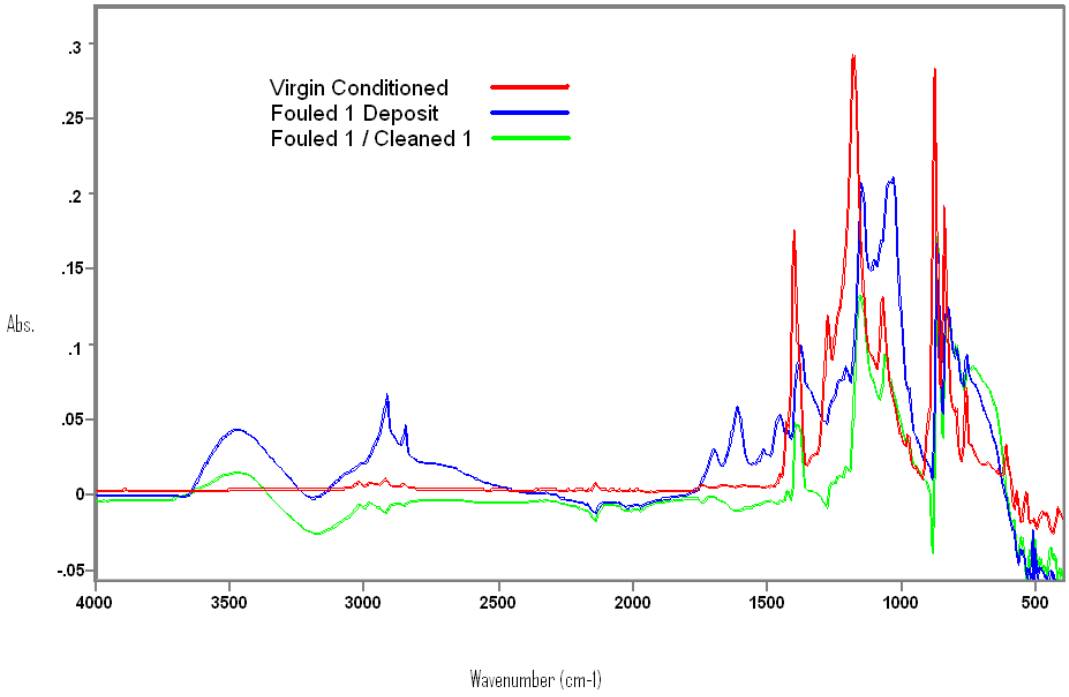

*Figure 4.33: Infrared spectra comparison of virgin conditioned fluoropolymer membrane, and differently treated **1.0 bar TMP** fouled and fouled 1 / cleaned 1 fluoropolymer membranes with virgin conditioned spectra subtracted. (All spectra shown with water subtracted)*

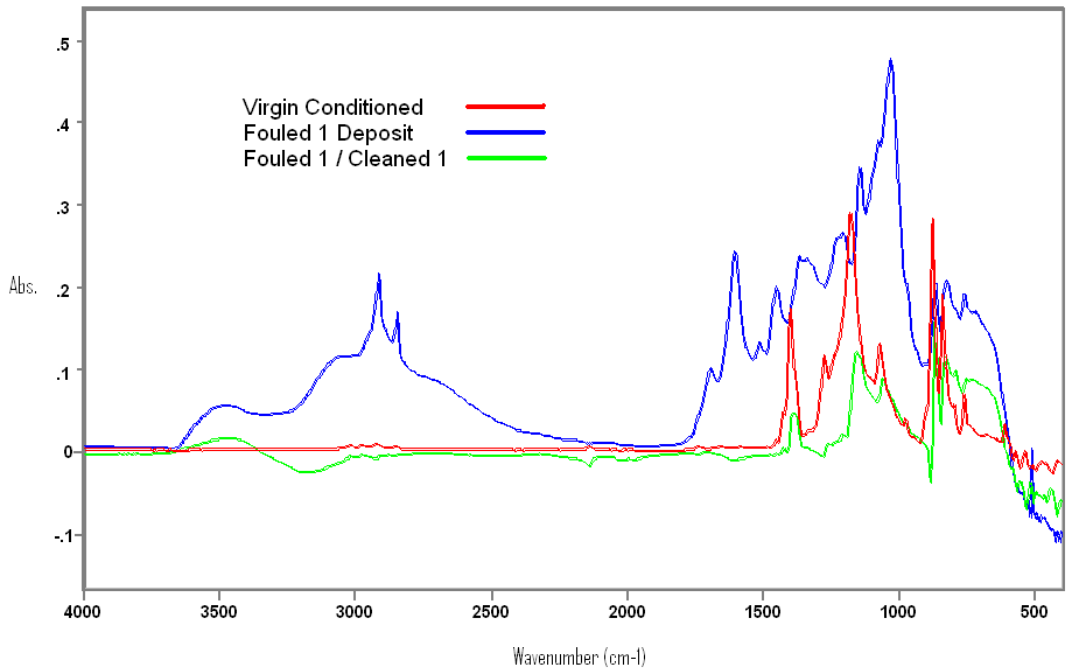

*Figure 4.34: Infrared spectra comparison of virgin conditioned fluoropolymer membrane, and differently treated **4.0 bar TMP** fouled 1 and fouled 1 / cleaned 1 fluoropolymer membranes with virgin conditioned spectra subtracted. (All spectra shown with water subtracted)*

Figure 4.35 and Figure 4.36 display the FTIR scans of the RC membrane during a fouling cleaning cycle for 1.0 and 3.0 bar TMP respectively. The fouled 1 and fouled 1 / cleaned 1 traces have had the virgin conditioned trace subtracted so the variation caused by the treatment can be observed. Comparing the fouled 1 surface for each TMP demonstrates the nature of the deposit formed. The intensity of the fouled 1 surface at 3.0 bar was not significantly different to that of the fouled 1 surface at 1.0 bar TMP suggesting no additional fouling was observed by increasing the operating TMP. Both RC membrane surfaces after fouling and cleaning demonstrated no permanent modification to the surface and thus a cleaning protocol that returned pristine membrane surface equal to the virgin conditioned surface.

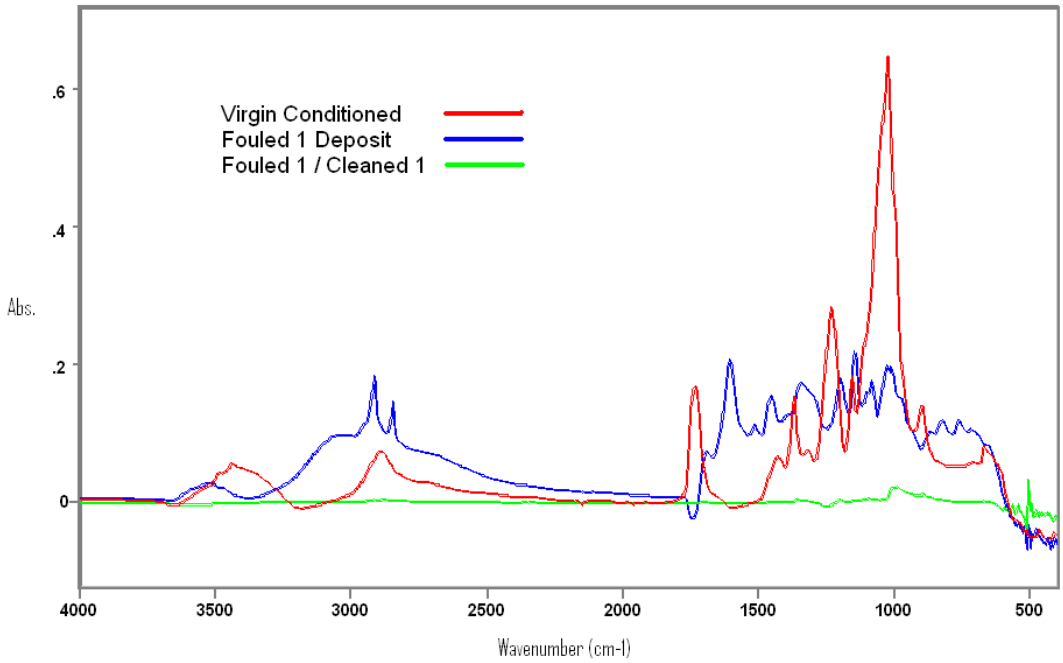

*Figure 4.35: Infrared spectra comparison of virgin conditioned regenerated cellulose membrane, and differently treated **1.0 bar TMP** fouled 1 and fouled 1 / cleaned 1 regenerated cellulose membranes with virgin conditioned spectra subtracted. (All spectra shown with water subtracted)*

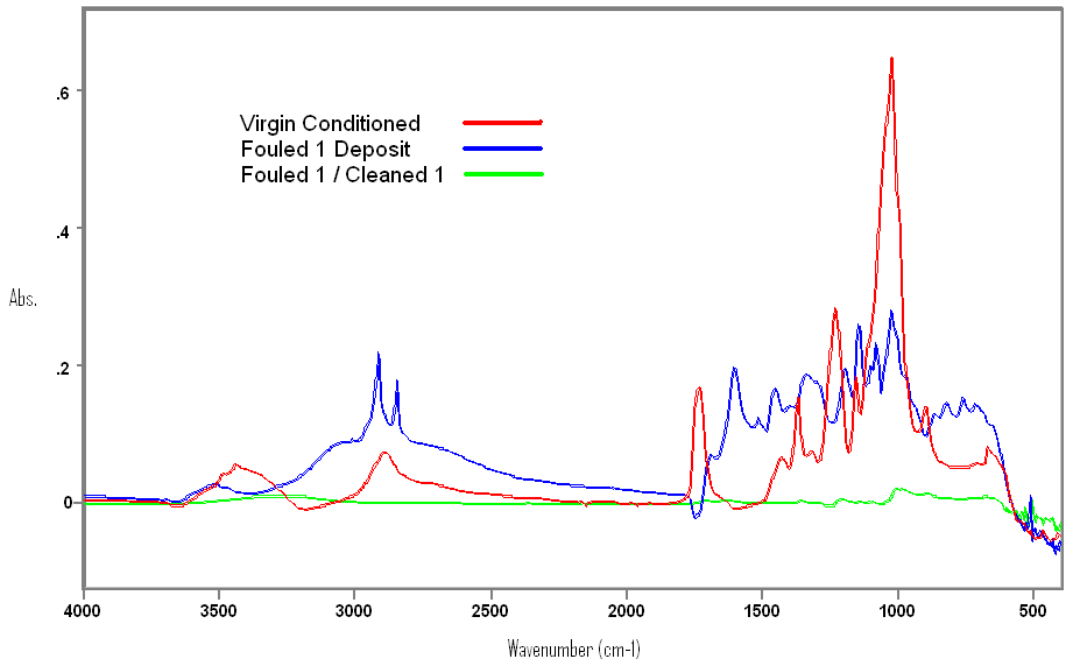

*Figure 4.36: Infrared spectra comparison of virgin conditioned regenerated cellulose membrane, and differently treated **3.0 bar TMP** fouled 1 and fouled 1 / cleaned 1 regenerated cellulose membranes with virgin conditioned spectra subtracted. (All spectra shown with water subtracted)*

4.2.7.6 Summary

Increasing the TMP from 1.0 to 4.0 bar with the FP membrane increased the steady state flux from 22 LMH to 25 LMH using fresh conditioned virgin membranes. The RC membrane demonstrated a limiting flux, such that increasing the TMP from 1 to 3 bar TMP maintained a flux of 24 LMH.

The FP membrane rejects less tea solids (0.31) compared to the RC membrane (0.35) at 1.0 bar TMP. Increasing the TMP of the FP / RC membrane to 4.0 / 3.0 bar significantly increases the membrane rejection to 0.47 and 0.45 respectively.

Although the total tea solids transmission decreased upon increasing the operating TMP, the relative amount of the important theaflavins and caffeine in the clarified liquor increased.

The RC membrane demonstrated no additional fouling by increasing the operating TMP. Both RC membrane surfaces after fouling (1.0 / 3.0 bar) and cleaning demonstrated no permanent modification to the surface and thus a cleaning protocol that returned pristine membrane surface equal to the virgin conditioned surface.

The FP membrane demonstrated over twice the fouling deposit during 4.0 bar fouling compared to 1.0 bar fouling confirming enhanced fouling at elevated TMP. Both FP

membrane surfaces after fouling and cleaning demonstrated a permanent modification to the surface. Either the membrane was not adequately cleaned of tea constituents or was modified during the NaOH cleaning process.

4.2.8 Multiple fouled and cleaned fluoropolymer membrane

Section 4.2.7 reports the effect of TMP variation on the fresh virgin conditioned FP membranes while 4.2.6 reports the effect of TMP variation on the same FP membrane. This section completes the story by investigating the effect of multiple fouling / cleaning cycles on the same FP membrane to try to determine the effect of repeated cycles on the same membrane.

4.2.8.1 Fouling Flux

Figure 4.37 represents the steady state fouling flux data (In accordance with Equation 3.1) for 17 black tea fouling / NaOH cleaning cycles using a FP 30 kDa MWCO membrane. All fouling and cleaning cycles were maintained at standard conditions of 1.0wt% black tea solids, 50°C, 0.44m/s CFV, 1.0 bar TMP and 30 mins of fouling and 0.5wt% NaOH, 60°C, 1.15m/s CFV, 0.5 bar TMP and 30 mins of cleaning. Initially on the first cycle the fouling flux was 27.9 LMH which progressively increased from cycle to cycle such that the flux was 30.9 LMH on the 17^{th} cycle. The variation in this data was not experimentally significant; the increase in black tea flux was negligible over 17 cycles.

4.2.8.2 Total tea solids rejection

The membrane total tea solids rejection also varied insignificantly throughout the 17 cycles examined, changing from 0.2 – 0.24 (Figure 4.38).

4.2.8.3 Pure water characterisation

The normalised pure water fluxes after cleaning (Equation 4.13) of the FP membrane are shown in Figure 4.39 where initially on the first cycle the pure water flux increased by 115% and then decreased throughout the subsequent cycles such that after 17 cycles the pure water flux was 91% of that recorded for the original virgin conditioned membrane. This demonstrates the importance of performing these experiments to demonstrate the significance of multiple fouling and cleaning cycles. Although pure water flux can be a poor indicator of membrane cleanliness, it does indicate whether any changes have taken place to the membrane surface.

4.2.8.4 Zeta potential

Membrane surface measurements of the zeta potential through the pores were performed to understand further the effect of fouling and cleaning upon the surface. They are displayed in Figure 4.40 and demonstrate that the virgin FP membrane had an iso-electric point around pH 4.5.accepting more negative charge at higher pH and more positive charge at lower pH. Upon fouling once, for the pH range studied the charge became significantly more negative suggesting negatively charged foulant had adhered to the pore wall surface. After cleaning of the fouled once surface, the membrane charge lay between the virgin membrane and the fouled membrane. This suggests that either the NaOH cleaning solution was not completely removing the tea foulant from the pore walls or the NaOH was completely removing the foulant and then modifying the membrane polymer. FTIR studies discussed in section 4.2.6.5 verify a chemical change to the membrane surface after fouling and then cleaning although could be attributed to either of these theories. This is discussed further in 4.3.6 .

Following 18 fouling and 17 cleaning cycles, the charge on the pore walls were less negative than when fouled once only and after cleaning the 18th time the charge was not significantly different to the membrane fouled 18 times and cleaned 17. Multiple fouling and cleaning cycles have changed the membrane differently to a single cycle such that the surface on the pore walls were less negative when fouled and has a shallower gradient of charge after fouling and cleaning.

4.2.8.5 Summary

Multiple fouling / cleaning cycles were performed using the 30kDa FP membrane, the black tea fouling flux and total tea solids rejection varied insignificantly over the 17 cycles examined. The pure water fluxes after cleaning increased initially for the first few cycles, and then decreased to 91% of the initial virgin membrane flux by cycle 17.

Negatively charged foulant adhered to the virgin conditioned membrane pore wall surface during the black tea filtration run. Subsequently, cleaning of the fouled surface reduced the negative charge such that it lay between the virgin membrane and the fouled membrane. This suggests that either the NaOH cleaning solution was not completely removing the tea foulant from the pore walls or the NaOH was completely removing the foulant and then modifying the membrane polymer. Multiple fouling

and cleaning cycles modified the pore wall charge differently to a single cycle such that the surface on the pore walls were less negative when fouled and had a shallower gradient of charge after fouling and cleaning.

.

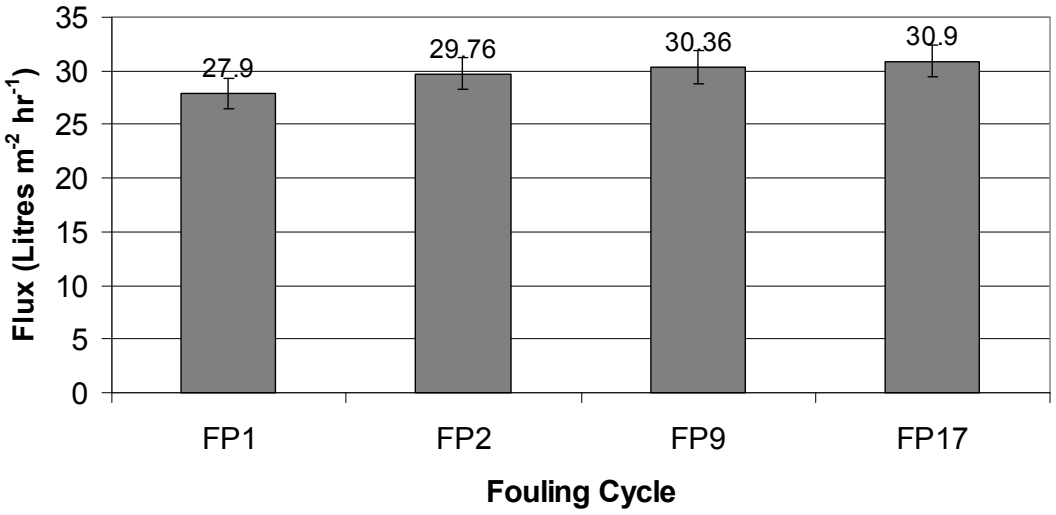

Figure 4.37: Fouling flux data for a virgin conditioned Fluoropolymer membrane fouled with black tea (1.0wt%, 50°C, 0.45m/s, 30mins) over 17 progressive fouling and standard NaOH cleaning cycles.

4.2.8.6 Total tea solids membrane rejection coefficient

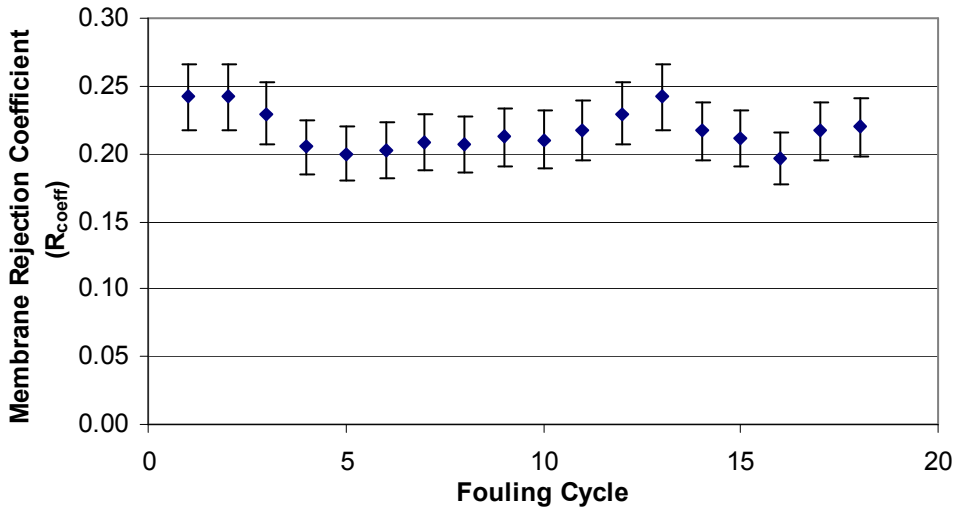

Figure 4.38: Solids transmission data for a virgin conditioned Fluoropolymer membrane fouled with black tea (1.0wt%, 50°C, 0.44m/s, 30mins) over 17 progressive fouling and standard NaOH cleaning cycles.

4.2.8.7 Pure water flux characterisation

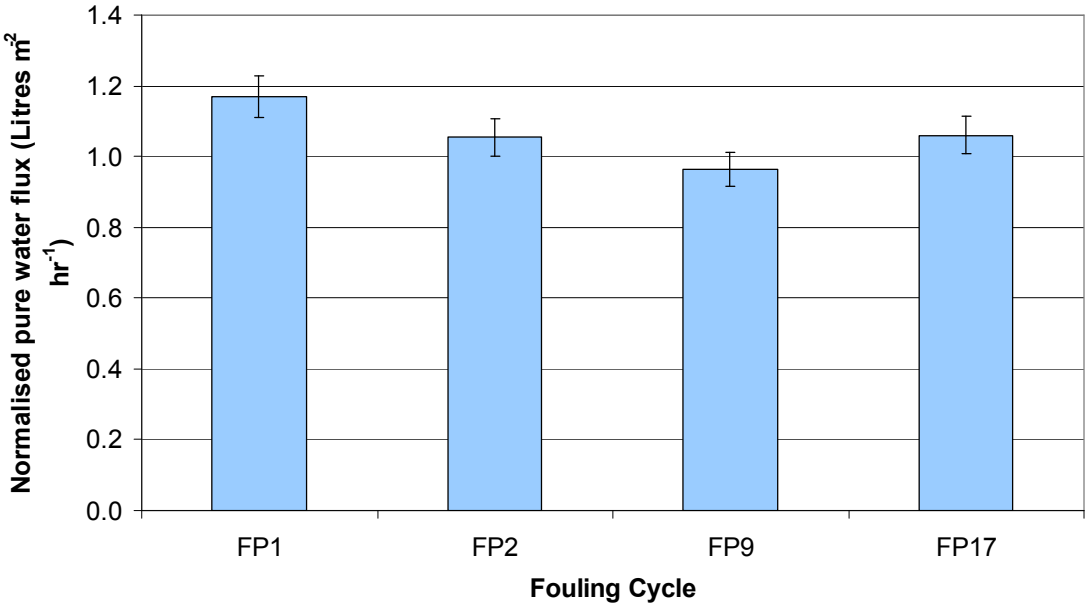

Figure 4.39: Normalised Pure water flux for a virgin conditioned Fluoropolymer membrane fouled with black tea (1.0wt%, 50°C, 0.44m/s, 30mins) over 17 progressive cycles and regenerated using the standard NaOH cleaning protocol

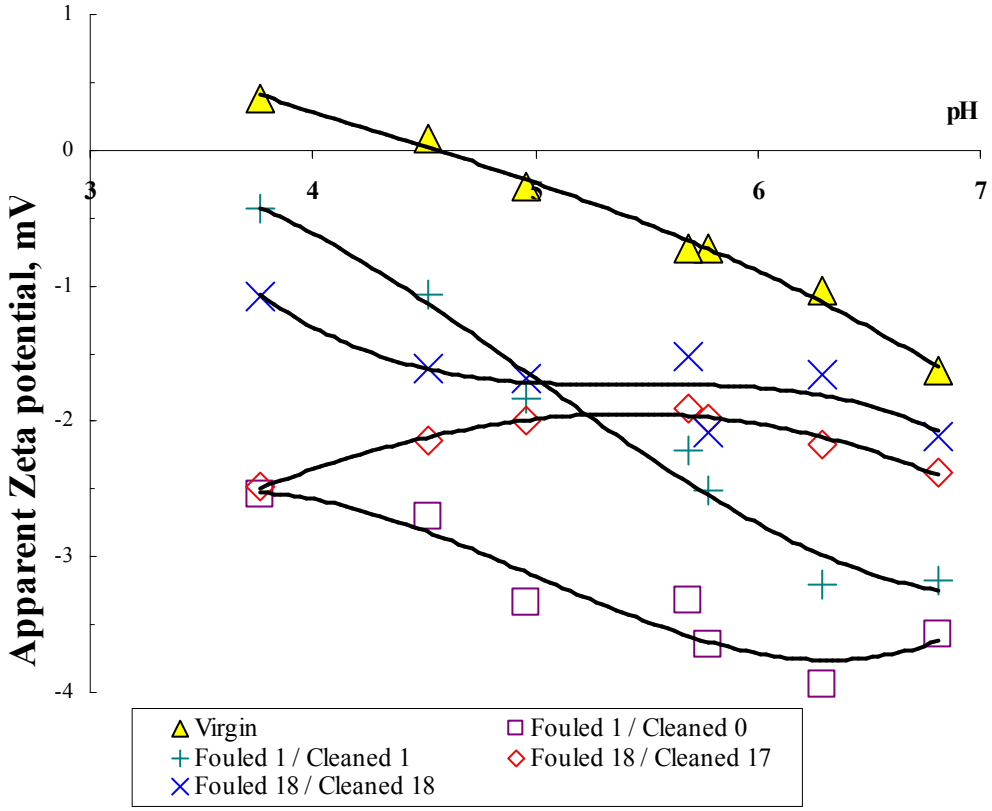

Figure 4.40: Apparent zeta potential on pore walls of a 30 kDa fluoropolymer membrane after different treatments.

4.2.9 Pressure stepping experiments

This section investigates the effect of varying the TMP during a black tea fouling run. Online TMP variation gives a large amount of information regarding the nature of the fouling occurring within the membrane and on the membrane surface.

4.2.9.1 Constant TMP

Figure 4.41 displays a typical 1.0 bar TMP, 1.0 wt% black tea fouling cycle performed for 80 mins using a 30 kDa RC membrane. The flux reduced from an initial value of 145 to a steady state value of about 20 litres m^{-2} hr^{-1}. The total tea solids transmission (Figure 4.42) remained approximately constant around 63 % and the polyphenolic transmission around 50% (Equation 4.11). Therefore around 84% of the total polyphenols present within the tea solids were transmitted through the RC membrane.

4.2.9.2 Varied TMP, 1.0 wt% feed

Figure 4.43 displays the fouling flux for the same 30 kDa RC membrane, this time the TMP was varied from an initial 0.5 bar and intermittently increased to 4 bar, subsequently decreased again to 0.5 bar TMP using a 1.0 wt% black tea feed. The flux did increase somewhat initially when the TMP was increased for most pressure increments, although would then decrease after a few mins. The solids transmission (Figure 4.44) increased initially from 0.5 bar to 0.75 bar followed by a decrease in solids transmission for further increments in TMP, the same trend was observed with polyphenolic transmission. Initially 88% of the polyphenolics in the feed tea solids were transferred into the permeate from 0.5 bar to 1.0 bar followed by a decrease to 80% at 4.0 bar. The insignificant variation in flux and reduction in solids / polyphenolic transmission following 1.0 bar TMP are characteristic of the limiting flux region as also found in 4.2.6 .

The total tea solids and polyphenol content in the permeate were lower for equal TMP during the pressure relaxing period (52 – 62% solids and 40.5 – 45% polyphenol transmission from 3 – 0.75 bar) compared to the pressure ramping period, (59.5 – 70% solids and 49.5 – 60.5% transmission between 3 – 0.75 bar) which suggests a permanent modification to the membrane surface. Fouling within the pores or/and a more impenetrable cake layer may have lowered transmission of total solids and polyphenols during the relaxing period.

4.2.9.3 Varied TMP, 0.5wt% feed

A similar experiment was performed with the same membrane and similar TMP ramping / relaxing protocol, from 0.25 bar to 3.0 bar for a 0.5wt% black tea feed. The flux variation is shown in Figure 4.45, upon increasing the TMP from 0.25 to 0.5 bar the flux increases significantly from 68 to 96 litres m^{-2} hr^{-1} although increasing again from 0.5 to 0.75 bar caused much less of an increase in flux from 72 to 76 Litres m^{-2} hr^{-1}. Also, the solids transmission increases from 66.6 to 72.6% from 0.25 to 0.75 bar respectively and upon further TMP increments to 3.0 bar the solids transmission decreases to 59.8%. The same trend is evident with the polyphenolic profile. Approaching the limiting flux at 0.75 bar could be responsible for this, similar to the 1.0wt% feed. Initially at 0.25 bar 66.6% and 63.5% of the total solids and polyphenols respectively transmit the membrane, following ramping / relaxing procedure at 0.25 bar again the total tea solids and polyphenolic transmission did not vary significantly to 71.5 and 62.2% respectively.

The total tea solids and polyphenol content in the permeate were lower for equal TMP (same as with 1.0wt% feed) during the pressure relaxing period (60 – 69% solids and 50 – 57% polyphenol transmission from 2 – 0.75 bar) compared to the pressure ramping period, (65 – 72% solids and 58 – 66.5% transmission between 0.75 – 2 bar) which suggests a permanent modification to the membrane surface. The same mechanisms as discussed previously for the 1.0wt% feed were occurring here.

4.2.9.4 Summary

A lower transmission of polyphenols occurred during TMP ramping suggesting that increased concentration polarisation (reported in 4.2.6.2) was increasing the selectivity of the membrane. Increased concentration at the membrane surface then caused an increase in adsorption and led to the formation of a cake layer. During high TMP / high concentration polarisation periods the tea constituents (polyphenols / caffeine / proteins) were in a higher concentration environment, consequently increased interactions causing increased aggregation (Tea creaming, section 2.2.1). This phenomenon would enhance tea constituent precipitation and thus adsorption and / or build up of solute at the membrane surface. During the pressure relaxing period, fouling flux, total tea solids and polyphenolic transmission were lower at equal TMP values to those seen during the pressure ramping period. This variation demonstrates

that the formation of the cake layer caused a secondary boundary to the membrane which increased the membrane selectivity.

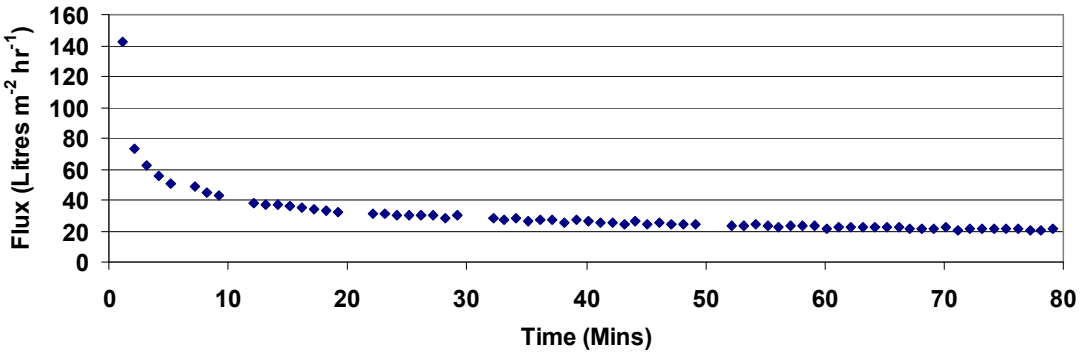

Figure 4.41: Graph to show fouling flux of a 1.0 wt%, 50°C black tea solution being filtered through a 30kDa Regenerated Cellulose membrane at 1.0bar TMP and 0.44m/s CFV.

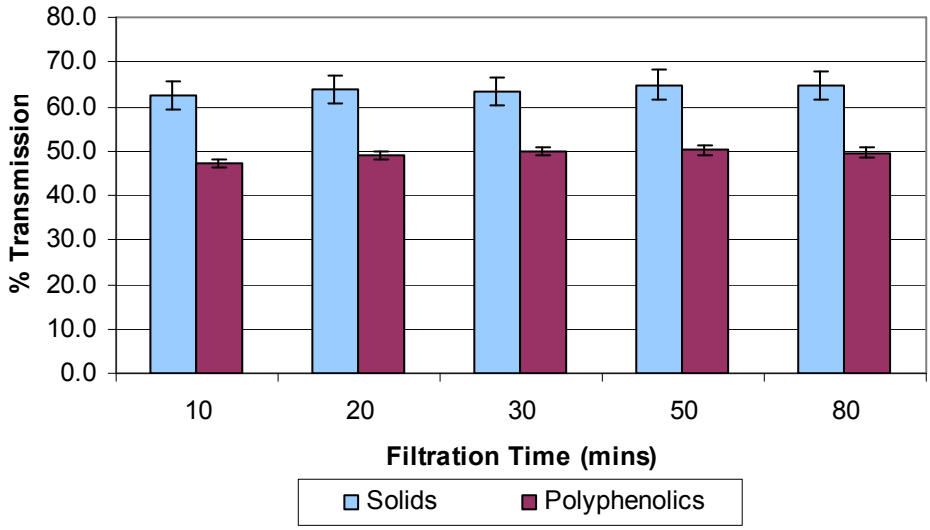

Figure 4.42: Solids and polyphenolic % transmission for a 1.0wt%, 50°C black tea solution being filtered through a 30kDa Regenerated Cellulose membrane at 1.0bar TMP and 0.44m/s CFV.

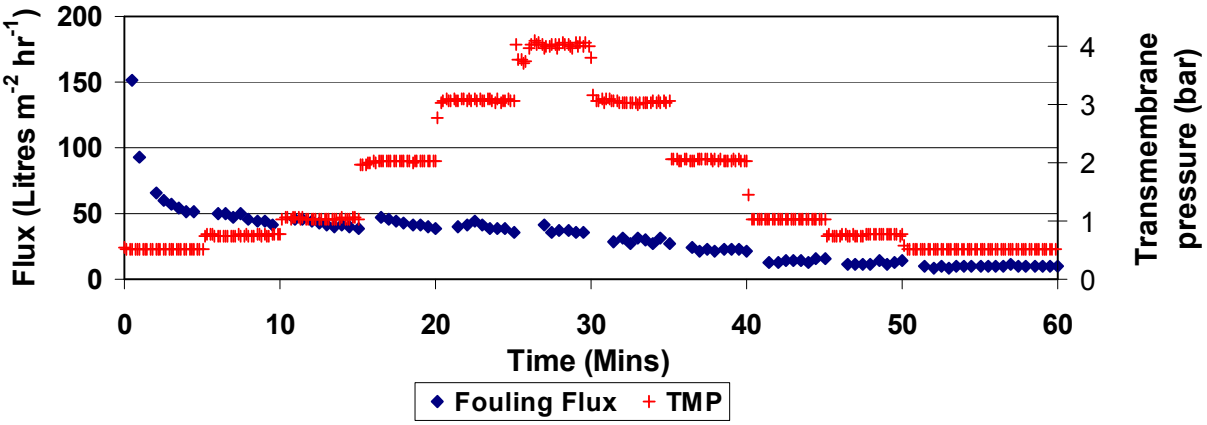

Figure 4.43: Graph to show fouling flux of a 1.0wt%, 50°C black tea solution being filtered through a 30kDa Regenerated Cellulose membrane at 0.44m/s CFV and varied TMP.

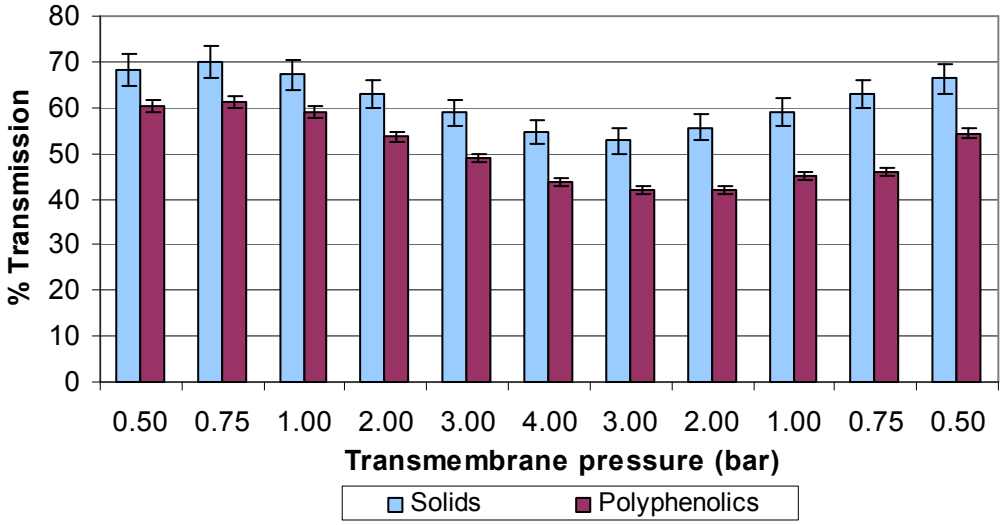

Figure 4.44: Solids and polyphenolic % transmission for a 1.0wt%, 50°C black tea solution being filtered through a 30kDa Regenerated Cellulose membrane at 0.44m/s CFV and varied TMP.

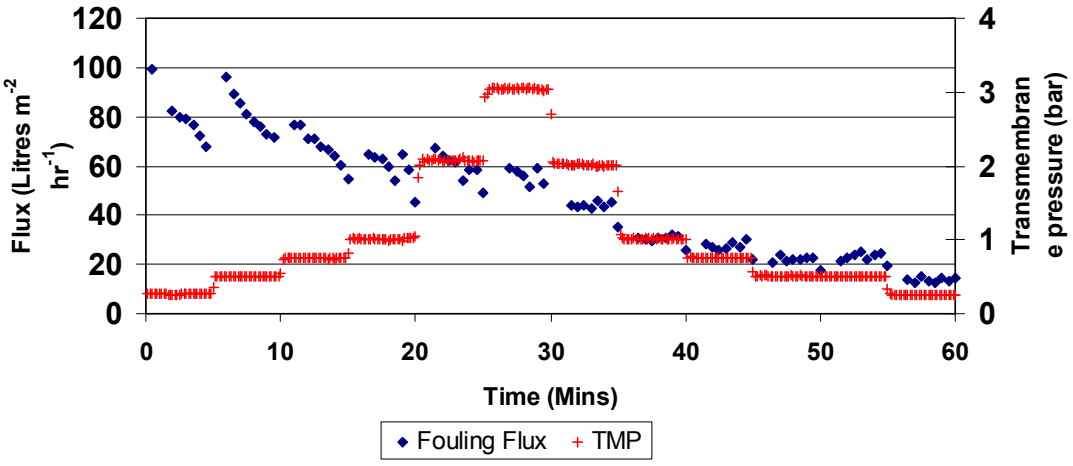

Figure 4.45: Graph to show fouling flux of a 0.5wt%, 50°C black tea solution being filtered through a 30kDa Regenerated Cellulose membrane at 0.44m/s CFV and varied TMP.

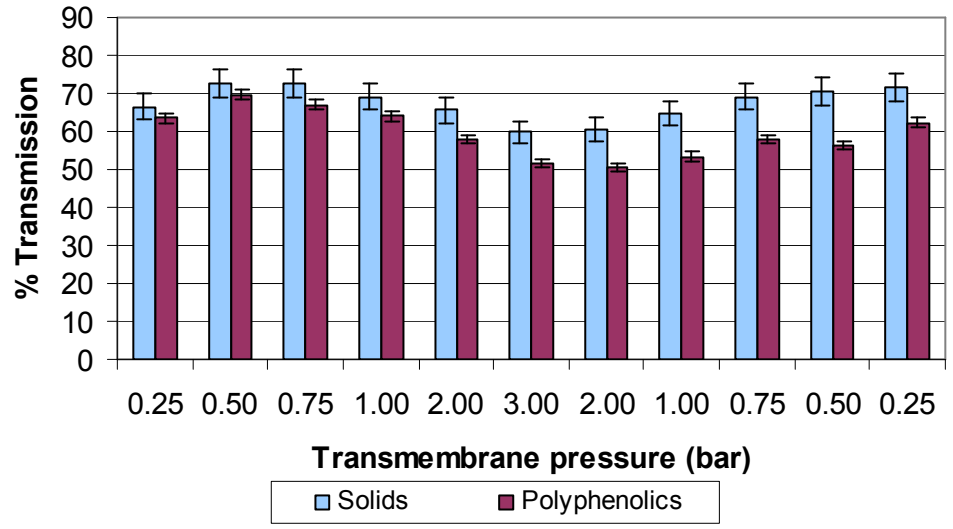

Figure 4.46: Solids and polyphenolic % transmission for a 0.5wt%, 50°C black tea solution being filtered through a 30kDa Regenerated Cellulose membrane at 0.44m/s CFV and varied TMP.

4.2.10 Black tea ultrafiltration performance

The majority of the work performed in this investigation demonstrates the effectiveness of black tea clarification using ultrafiltration. This is based on the quality of the final ready-to-drink product and an analysis of foulant – membrane – cleaning agent interactions to aid future understanding and optimisation of the process. In this section the total volume and tea solids transmission of clarified permeate were measured and are discussed for an enhanced filtration period of 5 hours.

Figure 4.47 and Figure 4.48 display the flux and total solids membrane rejection coefficients for varied volume and concentration feeds during normal operation mode such that the feed retentate was concentrated. Also runs were performed in diafiltration mode where RO water was added to the feed in equal quantities to the permeate leaving the system.

Starting with an 8 litre feed solution during concentration mode caused a flux decline after 5 hours to 15 litres m^{-2} hr^{-1} ,(filtering 43% of feed volume, concentration factor – 1.76) whereas during diafiltration the flux only declined to 20 litres m^{-2} hr^{-1} maintaining approximately equal membrane rejection coefficients of 0.4 for both operating modes. Reducing the volume from 8 to 2 litres reduced the flux from 20 to 15 litres m^{-2} hr^{-1} due to an increase in the membrane rejection coefficient from approximately 0.3 for both initial volumes to 0.40 and 0.52 respectively after 140 mins of filtration.

Reducing the feed volume to 2 litres and operating under concentration mode could only be performed for 140.5 mins as the feed tank was then empty. 65% of the feed volume had been treated, (Concentration factor – 2.86) although the flux was 15 litres m^{-2} hr^{-1} at the end of this run and could have continued if the dead volume of the system was smaller (0.7 litres). Starting with a 2 litre feed and operating in diafiltration mode maintained a flux of 25 litres m^{-2} hr^{-1} after 140.5 mins compared with 15 litres m^{-2} hr^{-1} during concentration mode. During diafiltration, operation was continued for a total of 300 mins (5 hours) where the flux was maintained at 25 litres m^{-2} hr^{-1}. The membrane rejection coefficient increased significantly for both operation modes increasing from 0.32 initially to 0.52 and 0.47 for concentration and diafiltration modes respectively after 140.5 mins. During diafiltration mode the membrane rejection continued to increase to 0.6 to the end of the run (after 5 hours). Reducing the 2 litre feed concentration to 0.5wt% operating in diafiltration mode caused an expected increased flux of 27 litres m^{-2} hr^{-1} after 5 hours operation. The membrane rejection increased significantly during the filtration run from 0.28 to 0.75. Due to the high fluxes associated with these conditions the retentate, although becoming more dilute (due to diafiltration) contains the larger tea constituents which cannot penetrate the membrane, hence increased membrane rejection coefficient.

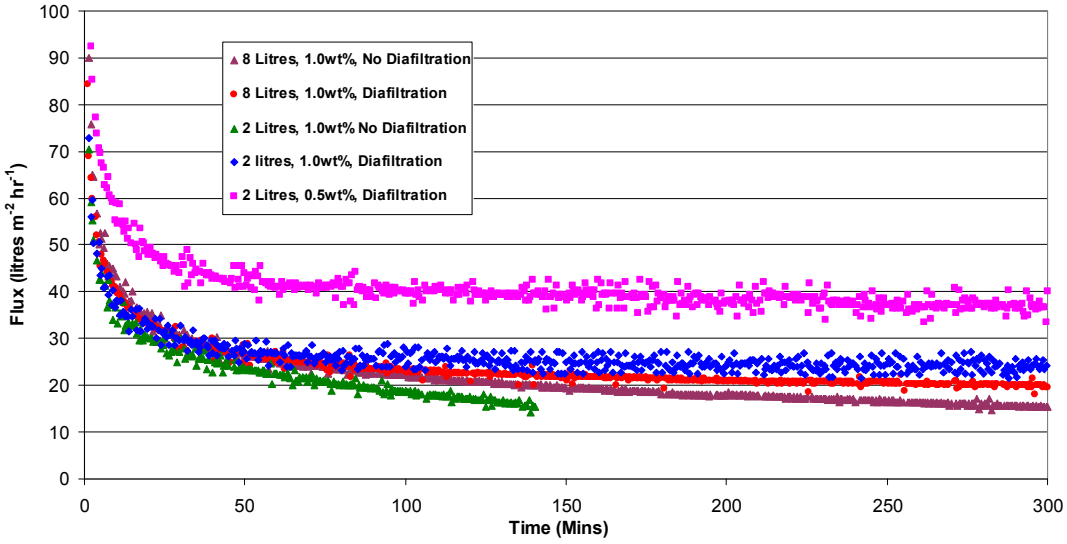

Figure 4.47: Flux through 30 kDa MWCO Regenerated cellulose membrane when fouled with 1.0 wt% and 0.5wt% black tea at 50°C, 1.0bar TMP and 0.44m/s CFV.

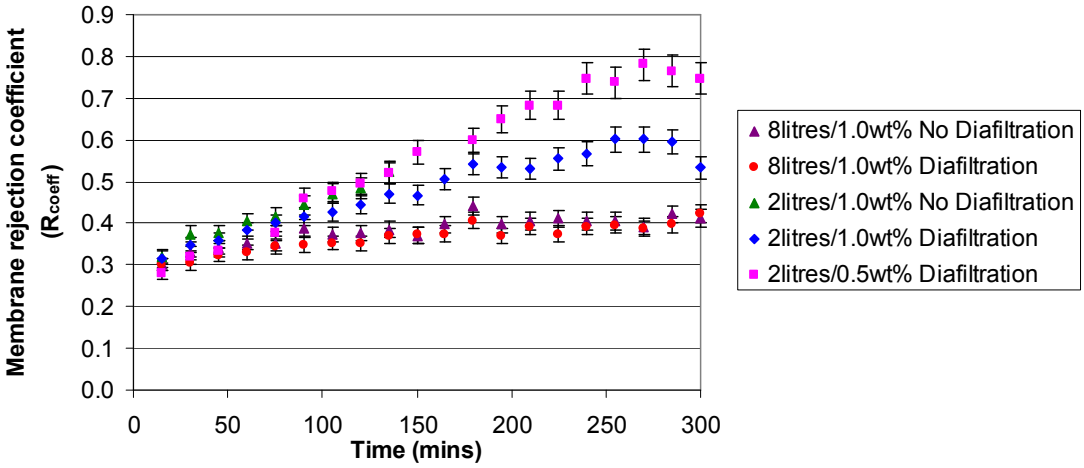

Figure 4.48: Total membrane rejection coefficient by a 30 kDa MWCO Regenerated cellulose membrane when fouled with 1.0 wt% and 0.5wt% black tea at 50°C, 1.0bar TMP and 0.44m/s CFV.

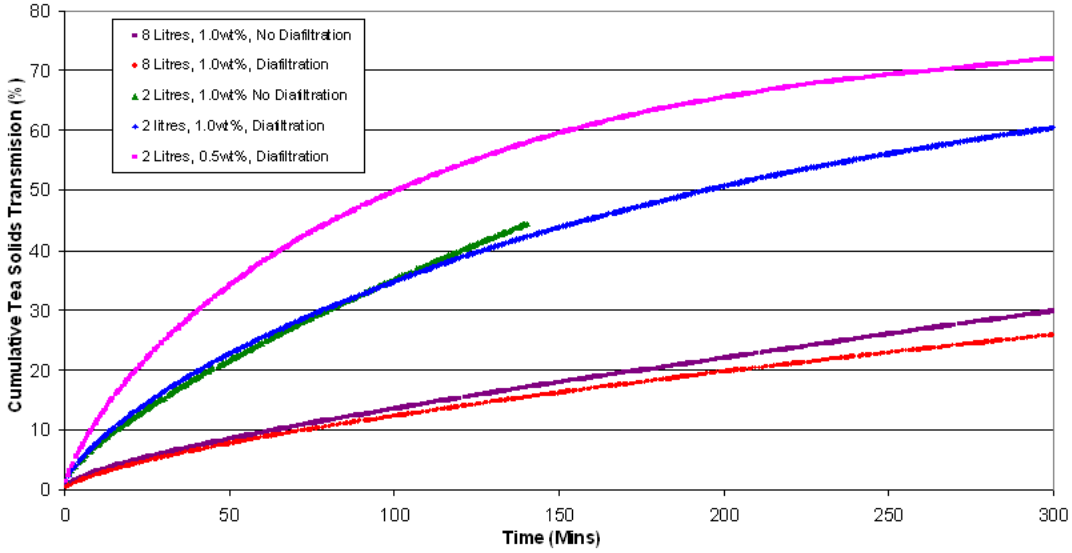

Figure 4.49: Cumulative percentage feed tea solids transmitted to permeate using a 30 kDa MWCO Regenerated cellulose membrane when fouled with 1.0 and 0.5wt% black tea at 50°C, 1.0bar TMP and 0.44m/s CFV.

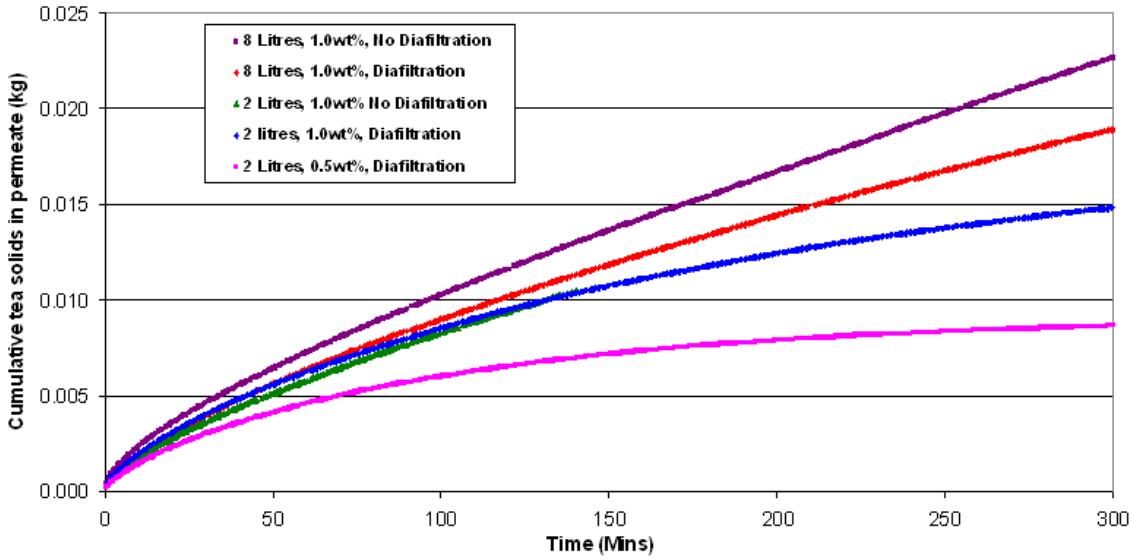

Figure 4.50: Cumulative tea solids transmitted to permeate using a 30 kDa MWCO Regenerated cellulose membrane when fouled with 1.0 and 0.5wt% black tea at 50°C, 1.0bar TMP and 0.44m/s CFV.

Figure 4.49 and Figure 4.50 represent the cumulative percentage and actual tea solids transmitted into the permeate respectively. This provides an interesting way of understanding the efficiency of the ultrafiltration process under different operating conditions. The 0.5 wt% feed demonstrated the maximum transmission (72%) of total tea solids after 5 hours filtration operated under diafiltration conditions. Whereas, during diafiltration mode, the 1.0wt% feed allowed 60.4% of total tea solids

transmission through the membrane after 5 hours. This demonstrates that the operating efficiency of the system using a 0.5wt% feed is enhanced; although based on total solids output (Figure 4.50) the 0.5wt% feed produced 8.66g of tea solids whereas the 1.0wt% feed produced 14.82g, 70% more over the same time period (5 hours).

These experiments are limited because they have not been taken to completion but will be useful when considering operation modes and process conditions. If the economics were such that the price of processing were to outweigh the cost of feed product, then operation under higher concentration and a concentration process would provide larger output of product for the ranges tested in this investigation. However, if the maximum conversion of feed product to clarified final product is required then operation at lower feed concentrations would be advantageous. Further experimentation is required to determine whether concentration or diafiltration mode should be used in this instance.

4.3 Influence of membrane surface properties

The efficiency of separation and final product quality were investigated using regenerated cellulose (RC) and fluoropolymer (FP) membranes of different nominal molecular mass cut-off values. The hydrophobicity, surface charge on the pore walls, surface roughness and chemical properties of the membrane were monitored throughout the fouling and cleaning cycle during filtration. In addition, the fouling flux decline curves were analysed and fitted using the Field *et al.* 1995, model, to gain a further understanding of the possible fouling mechanisms. This section further demonstrates the importance of understanding the surface science in the interaction between surfaces, foulants and cleaning agents.

4.3.1 Total solids / polyphenol transmission

The transmission of total tea solids were calculated using Equation 4.11 and are shown in Figure 4.51.

$$T\% = \left(\frac{C_P}{C_B} \right) \times 100$$

Equation 4.11

Where C_P is the tea solids concentration in the permeate stream and C_B is the tea solids concentration in the bulk feed solution (calculated as a wt% of the total stream). The FP30 membrane demonstrated higher total solids percentage transmission (**73** +/- 3.7) than FP10 (**65** +/- 3.3) and the FP100 (**62.5** +/- 3.1). The RC membranes demonstrated similar solids percentage transmissions, RC10 (**72** +/- 3.6), RC30 (**69** +/- 3.5) and RC100 (**73** +/- 3.7).

Total polyphenol transmission was calculated using Equation 4.12 below and shown in Figure 4.52 and Figure 4.53.

$$T_S\% = \left(\frac{C_{PS}}{C_{BS}} \right) \times 100$$

Equation 4.12

C_{PS} and C_{BS} are concentrations of polyphenols within the dehydrated solids fraction of the permeate and feed streams respectively. (wt%). All RC membranes tested allowed the transmission of approximately 90% of the total polyphenols. However, the FP membranes displayed a greater variation in transmission values (**78**% - **92**%. (+/- 1.8%)). This variation is discussed in section 4.3.5 . This data presented in Figure 4.52 and Figure 4.53 suggest that *ca* 90% transmission of important polyphenols can be achieved when ultrafiltering using FP or RC membranes. This is important, as polyphenols are responsible for colour, and also impart flavour, astringency, acidity, body and delightful aromatics of black tea. (Liang and Xu 2001; Todisco *et al.* 2002).

4.3.2 HPLC determination of Theaflavins and Caffeine

Figure 4.52 and Figure 4.53 show HPLC determined results for the transmission of theaflavins through different pore sized FP and RC membranes. Results were calculated using Equation 4.12, where C_{PS} and C_{BS} were concentrations of theaflavins within the dehydrated solids fraction of the permeate and feed streams respectively (wt%). There was not a significant variation in the total TF transmission through the RC membranes, with values of 99 – 101% recorded (TF molar masses ranged from 564 – 868 g mol^{-1}) This suggests that concentrations of theaflavins were similar in the permeate tea solids to the initial feed solution as is desired to maintain final product quality. However, the FP membranes showed a substantial variation in transmission of total TF from 64% - 108%. This will be discussed further in section 4.3.5.

Figure 4.52 and Figure 4.53 also shows HPLC determined results for caffeine transmission through all of the membranes studied. The FP membranes allowed the transmission of 117 - 141% and RC membranes transmitted 125 – 136% of caffeine. This demonstrates that the caffeine (with a small molar mass of 238 g mol^{-1}) was transmitted through the membrane easily, and was thus found in higher relative concentrations in the permeate tea solids than other tea constituents when compared with the feed tea solids. The virgin FP30 membrane displayed a caffeine transmission of 116%. This was raised to a value of 127% following multiple cleaning.

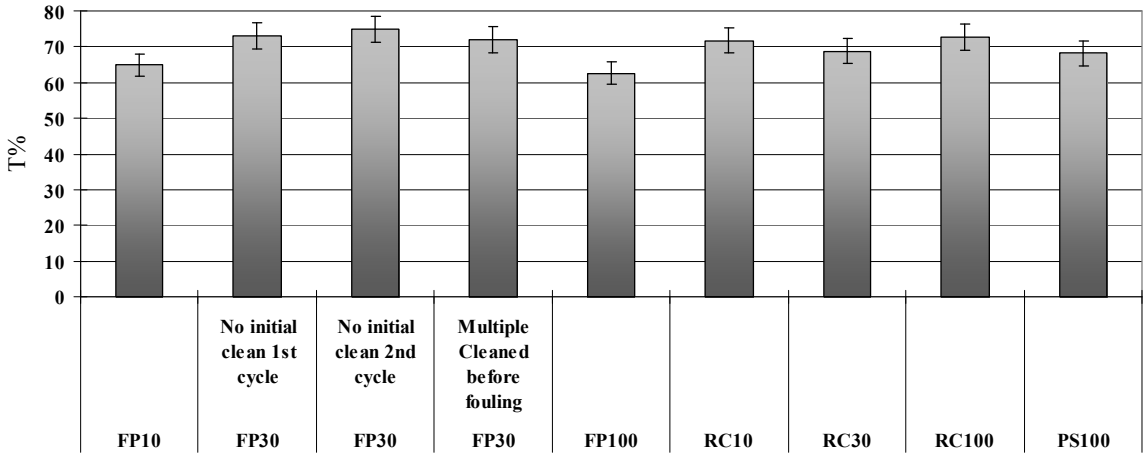

Figure 4.51: Total Solids transmission through different material, pore size and treated membranes.

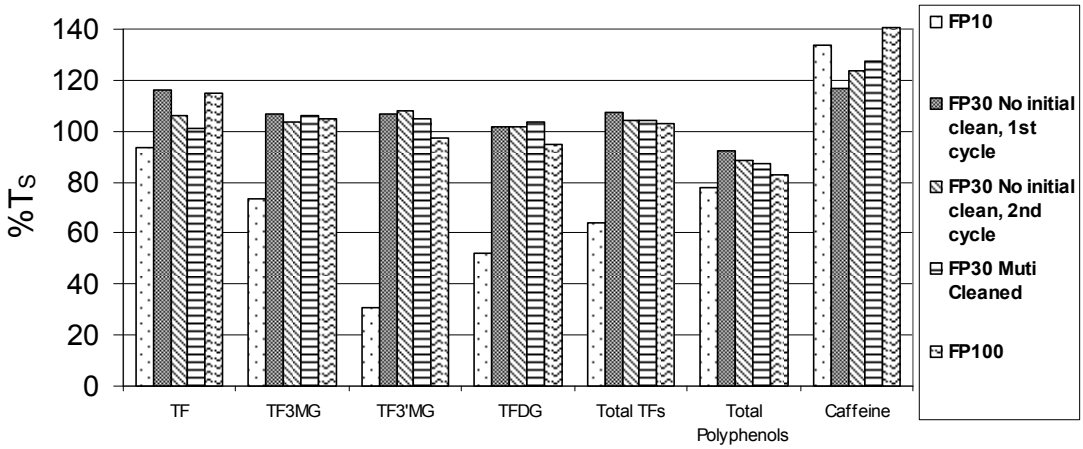

Figure 4.52: Total Polyphenolic, Theaflavins and Caffeine transmission through fluoropolymer membranes of different pore sizes.

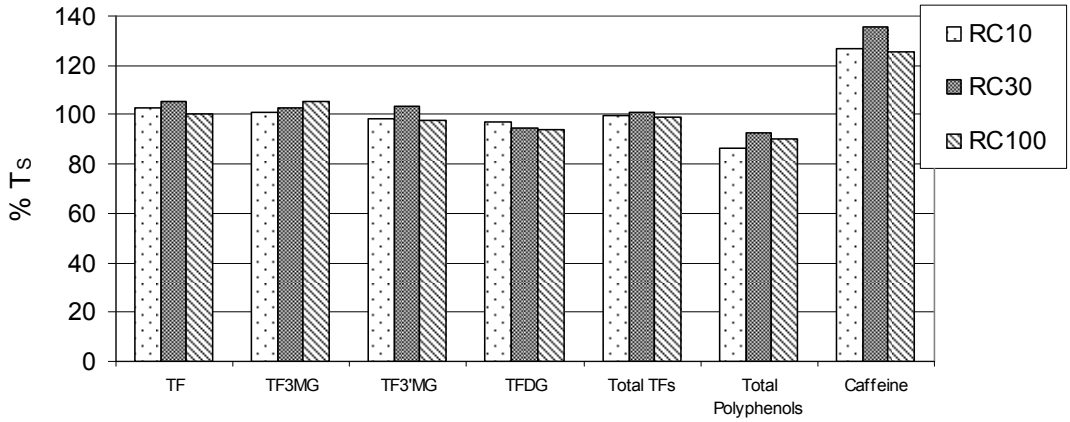

Figure 4.53: Total Polyphenolic, Theaflavins and caffeine transmission through regenerated cellulose membranes of different pore sizes.

4.3.3 Colour / Haze

Table 4.3 shows the CIE colour parameters and measured haze of all permeates produced measured at a total solids concentration of 0.2 wt%. FP30 on the first and second cycle showed the reddest (a*) and yellowiest (b*) solution of FP membranes which coincides with the largest transmission of theaflavins (Figure 4.52) which are known to be responsible for producing solutions of bright red colour (Liang and Xu 2003). RC100 gave the reddest and yellowiest solution produced from RC membranes although similar amounts of theaflavins were transmitted through each RC membrane (Figure 4.53).

When comparing all the filtered results to those for a 0.2 wt% solution that has not been treated, it is apparent that a large amount of the redness has been removed in addition to some of the yellowness. The haze has been significantly removed by filtration, and thus the lightness (L*) was significantly increased. This demonstrates that higher total solids concentrations of the filtered solutions could be used in iced tea production, especially considering the relatively low concentrations used in commercial products currently.

	Temp. °C	L*	a*	b*	Chroma	Haze (900nm)	
Experiment					C*	% Beam Transmittance	Abs.
FP10	35	92.92	-3.32	32.54	32.71	100.76	-0.003
FP30 No initial clean, 1st cycle	35	86.35	0.83	47.54	47.55	100.45	-0.002
FP30 No initial clean, 2nd cycle	35	85.89	1.19	48.19	48.20	100.49	-0.002
FP30 Muti Cleaned	35	86.99	0.34	45.86	45.86	100.37	-0.001
FP100	35	90.86	-2.14	37.65	37.71	100.68	-0.003
RC10	35	87.79	-0.06	45.89	45.89	99.83	0.001
RC30	35	88.36	-0.39	43.46	43.46	99.74	0.001
RC100	35	85.16	1.9	49.32	49.36	99.6	0.002
PS100	35	88.09	-0.29	44.51	44.51	99.73	0.001
No Treatment (0.2wt%)	35	64.16	12.03	59.83	61.03	84.36	0.074
No Treatment (0.14wt%)	35	71.97	7.85	55.48	56.03	90.44	0.043
Liptons Ice Tea (0.14wt%)	35	79.97	2.63	41.3	41.38	94.26	0.025

*Table 4.3: CIE colour parameters (L*a*b*) and haze parameters of tea solutions measured at 0.2wt% and at 35°C.*

4.3.4 Hydrophobicity - Contact Angle

The hydrophobicity of the membranes was characterised by recording contact angle measurements (Table 4.4). All the membranes studied were hydrophilic by nature, i.e. displayed contact angles of less than 90°. Measurements of the regenerated cellulose membrane could not be recorded, due to the very hydrophilic nature of the membrane.

After conditioning, FP10 and FP100 membranes displayed similar contact angles of 49° and 47° respectively, whereas FP30 showed a more hydrophobic surface, with an angle of 68° reported. Adhesion of foulants after a single cycle typically lead to a more hydrophilic surface, with contact angles for FP10 of 49° for the virgin, conditioned surface reducing to 39° following a single fouling cycle. The FP100 membrane showed values of 47° & 21° for virgin conditioned & single fouled membranes respectively. For the PSF membrane the virgin conditioned & single fouled contact angles were 64 & 37° respectively.

Cleaning of a virgin conditioned FP10 membrane resulted in a more hydrophobic surface (changing the contact angle from 49° to 60°). A subsequent fouling and cleaning cycle only slightly increased the hydrophobicity from 49° (virgin conditioned surface) to 54°. An explanation for this could be the additional removal of preservatives such as glycerine that were not removed during the normal conditioning protocol. Fouling and cleaning of FP100 reduced the hydrophobicity slightly from 47 (virgin conditioned surface) to 42°.

Interestingly, when FP30 was cleaned once only, the hydrophobicity did not change significantly (68 – 65°). However, when the surface was either fouled and cleaned twice or multiple-cleaned, then the surface became more hydrophilic (with contact angle of 60 and 50° for the two treatments respectively). This phenomenon was previously found, (see section 4.2.6), where surfaces were either modified by foulants, cleaning agents or both.

	Average	Standard Error
Sample		
FP10 Virgin conditioned	**49**	1.4
FP10 Fouled 1	**39**	1.0
FP10 Fouled 1 / cleaned 1	**54**	0.9
FP10 Cleaned 1	**60**	1.6
FP30 Virgin Conditioned	**68**	1.0
FP30 Fouled 2 / cleaned 2	**60**	1.0
FP30 Multiple cleaned and fouled	**50**	0.8
FP30 Cleaned 1	**65**	0.8
FP100 virgin conditioned	**47**	1.5
FP100 Fouled 1	**21**	1.1
FP100 Fouled 1 / cleaned 1	**42**	1.4
PSF Virgin conditioned	**64**	1.2
PSF Fouled 1	**37**	1.5
PSF Fouled 1 / cleaned 1	**49**	1.8

Table 4.4: Contact angle of water drops made with membrane surfaces after different fouling / cleaning treatments.

4.3.5 Streaming Potential through Pores

Figure 4.54 (a) – (f) show the apparent zeta potential (ZP) on the pore walls of all the membranes examined in this study. Over the pH range examined, the virgin conditioned FP membranes tended to display a fairly low charge (+0.5 mV to -3.0 mV) and the virgin conditioned RC membranes had almost no charge (-0.5 mV to -2.5 mV). Only two of the six virgin membranes tested displayed iso-electric points (IEP) within the pH range examined (4- 7). These were the FP10 and FP30 membranes, with IP values of 5.25 and 4.5 respectively.

Fouling caused both FP and RC membranes to have a greater negative charge, due to negatively charged species deposited on or within the pores. This negative charge was somewhat stronger on the FP membranes (-2.0 mV to -5.5 mV) than the RC membranes (-1.5 to -3.0 mV) suggesting that the FP membranes have undergone a greater degree of in-pore fouling than have the RC membranes. This conclusion is supported by fouling flux data (Figure 4.58) indicating that steady state fluxes were generally lower for the FP membranes (14 – 29 LMH) than for the RC membranes (29 – 32 LMH) of a similar MMCO. The ZP curves for fouled membranes tended to have a shallow negative gradient with increasing pH value. This indicates that the foulants on these surfaces weakly attract additional negative charge despite a pH increase of 3.

There was very little difference in ZP profiles recorded for the virgin conditioned RC membranes and fouled then cleaned membranes (Figure 4.54 (d) – (f)) suggesting that these membranes are easily cleaned or returned to virgin charge conditions. The FP100 membrane (Figure 4.54 (c)) was also easily cleaned to provide a similar ZP profile to the RC membranes, with the Zeta Potential within the pores recovered to a similar extent for that seen for the virgin conditioned FP 100 membranes. The other two FP membranes behaved rather differently (Figure 4.54 (a) and (b)). The FP10 membrane showed a ZP profile for the fouled then cleaned membrane that was between that seen for the virgin and the virgin /cleaned surface, and much less negative than the curve for the fouled FP10 membrane. This indicates that the cleaning process is removing negatively charged foulants in this case. This pattern was repeated for the FP30 (Figure 4.54 (b)), where the ZP profile for the fouled then cleaned membrane was almost equidistant between that seen for the virgin and once fouled samples.

Additional investigations were carried out on the FP30 membrane (Figure 4.54 (b)), the virgin membrane was cleaned once only, and another virgin membrane was initially multiple cleaned 8 times with separate cleaning solutions and then subjected to a fouling cycle. In addition, the virgin FP30 membrane was fouled twice and cleaned twice. There were modest differences between all the treatments of FP30 membrane samples that were subjected to a fouling / cleaning cycle or where the membrane was only cleaned. Again the ZP profiles for these additional investigations on fouled and/or cleaned membranes were almost equidistant between those seen for the virgin and once fouled samples.

This suggests that the action of sodium hydroxide (NaOH) cleaning was to increase the magnitude of the negative charge of the fluoropolymer within the pores primarily, although modification of the foulant cannot be discounted It seems most likely that the cleaning solution is removing the majority of the foulant thus reducing the magnitude of the negative charge, and then modifying the fluoropolymer, increasing the magnitude of the negative charge within the pores, possibly by adsorption of hydroxyl ions.

Virgin conditioned FP 10 and FP30 membranes had isoelectric points at pH 5.1 and 4.5 respectively (Figure 4.54 (a) and (b)). When FP10 was fouled once and cleaned once, the membrane's IEP reduced slightly to around 4.8 and when cleaned once only,

the IEP was reduced still further to 4.5. This indicates that fouling or cleaning treatments modified the virgin surface by adsorption of negatively charged foulants and / or hydroxyl ions.

When the FP30 membrane was (i) fouled once / cleaned once and (ii) cleaned once only, the IEP can be estimated by extrapolation to be around pH 3.0 in both cases. This substantial increase in the magnitude of the negative charge is again indicative of the adsorption of negative species to the virgin surface.
Interestingly, the pH of normal strength tea is 4.5, so that the FP30 membrane would have no net charge within the pores during the filtration of a tea solution. At pH 4.5, the FP10 membrane would have a slight positive charge whilst the FP100 membrane would have a slight negative charge. This suggests that the negatively charged molecules (based on negative charge in pores of all fouled membranes) would theoretically pass through the FP30 membrane the easiest, whilst an interaction or repulsion would be more likely with the FP10 and FP100 membranes. This is supported by the transmission data (Figure 4.51, 52 and 53) where the highest percentage transmissions were seen for the FP30 membrane (**73** +/-3.7% and **92** +/-1.9% for solids and phenolic transmission respectively). FP10 and FP100 had lower solids transmission (**65** +/-3.3% and **62** +/-3.1% for the two membranes respectively) and also lower polyphenolic transmission (**78** +/-1.6% and **83** +/-1.66% for the FP10 and FP100 membranes respectively).

Figure 4.52 shows the HPLC results for transmission of theaflavins through a range of FP membranes based on where C_{PS} and C_{BS} were concentrations of theaflavins within the permeate and feed tea solids respectively (wt%). Transmissions ranged from 30 – 118%. The FP10 membrane showed the lowest transmission of theavflavins, ranging from 31% (for TF3'MG) to 94% (for molecular theaflavin). There was a lower transmission of total TFs through the virgin conditioned FP10 (**64**%) than FP100 (**103**%) membrane, whereas FP30 (**108**%) had the highest transmission of theaflavins which again could be associated with the neutral charge in the pores of this membrane. The difference in total TFs transmission through FP10 and FP100 could be associated with difference in ZP and the charge within the pores at the pH of tea (pH = 4.5). The FP10 had a slight positive charge which might reduce transmission of negatively charged theaflavins. FP100 had a slight negative charge which could

ease passage of theaflavins through the pores (as not forming interactions with the pore surface) causing the observed increased transmission of the total theaflavins.

Although the FP30 membrane pores were modified such that they were more negatively charged on the second cycle and after multiple cleaning, the transmission of total solids and total TFs remained approximately constant, although the total polyphenols transmission was reduced slightly from 92 – 87%.

For the range of MMCO values examined, the transmission of theaflavin compounds through different pore size RC membrane all appear similar, with total TF transmission values of 99 – 101% (Figure 4.53). All membranes displayed a similar magnitude of negative charge. It is likely that charge controlled the rejection values recorded, rather than the pore size of the membrane.

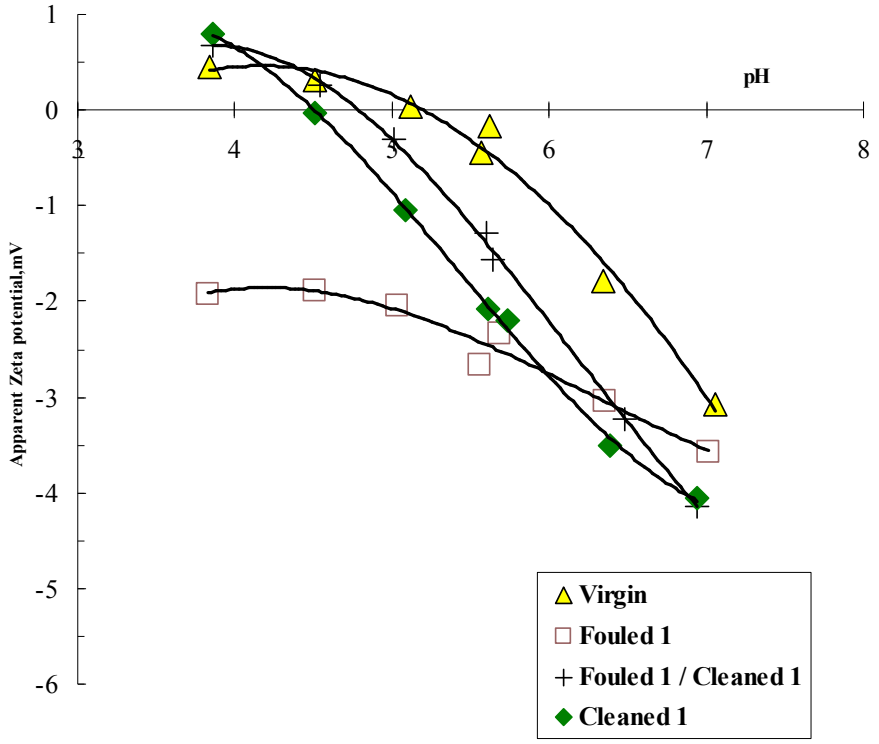

Figure 4.54: (a). Apparent zeta potential on the pore walls of FP10 membrane.

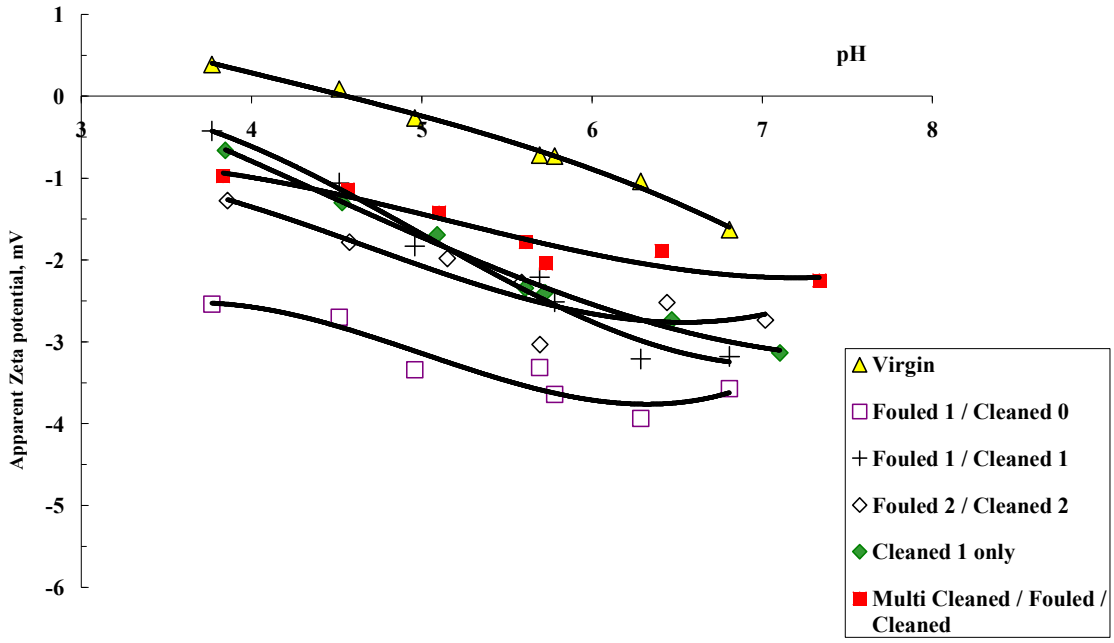

Figure 1.54 (b): Apparent zeta potential on the pore walls of FP30 membrane.

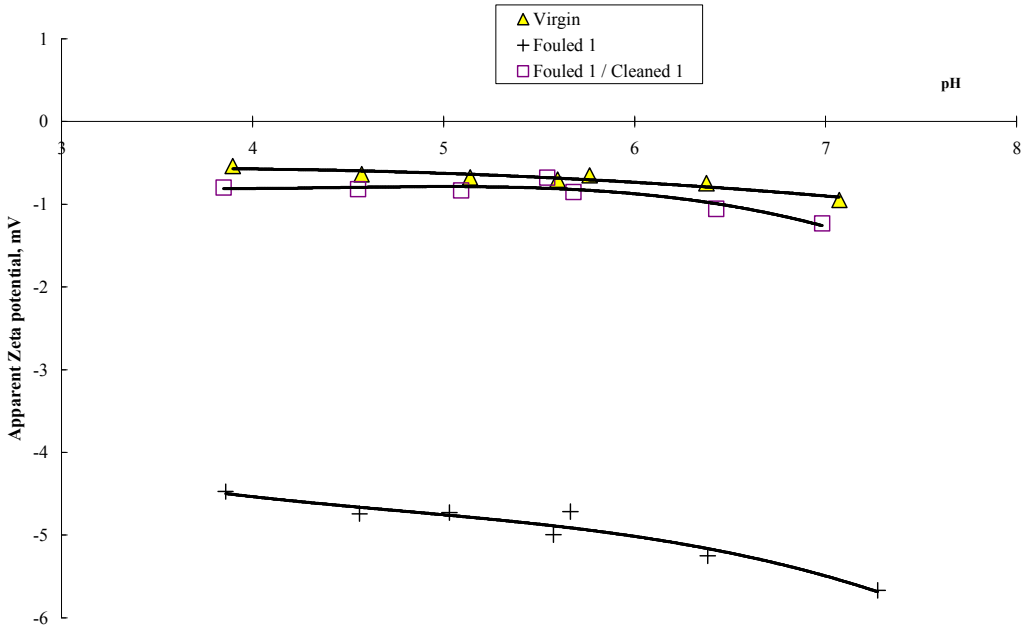

Figure 1.54 (c): Apparent zeta potential on the pore walls of FP100 membrane.

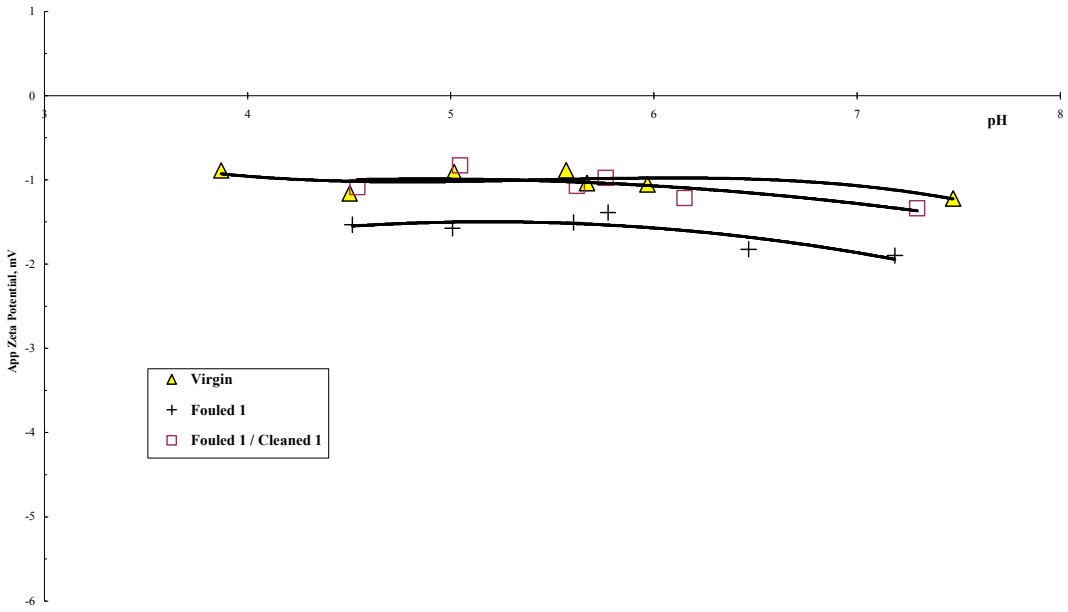

Figure 15.4 (d): Apparent zeta potential on the pore walls of the RC10 membrane.

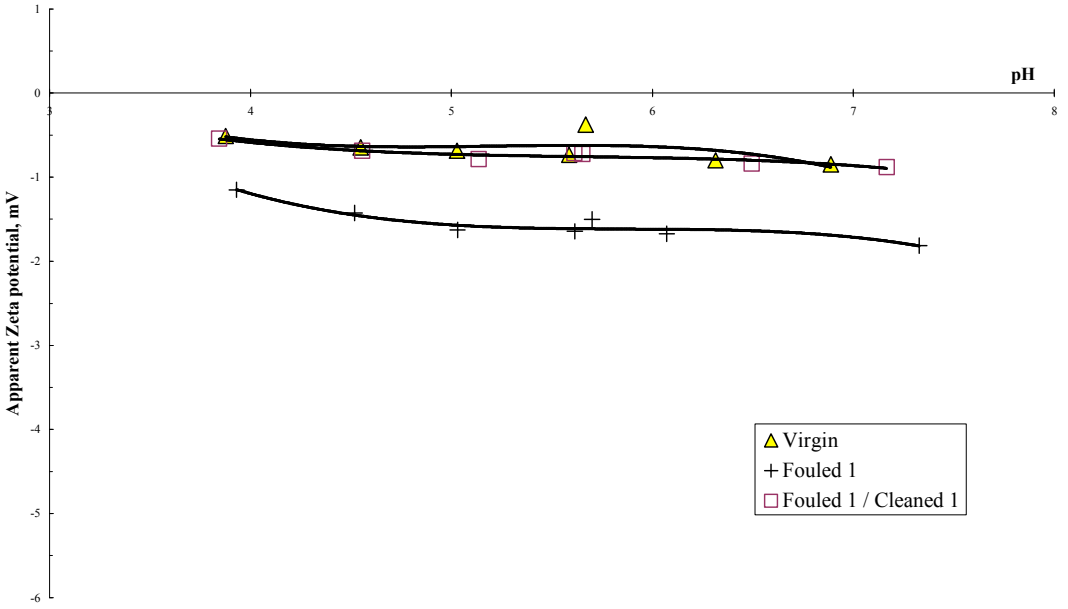

Figure 1.54 (e): Apparent zeta potential on the pore walls of RC30 membrane.

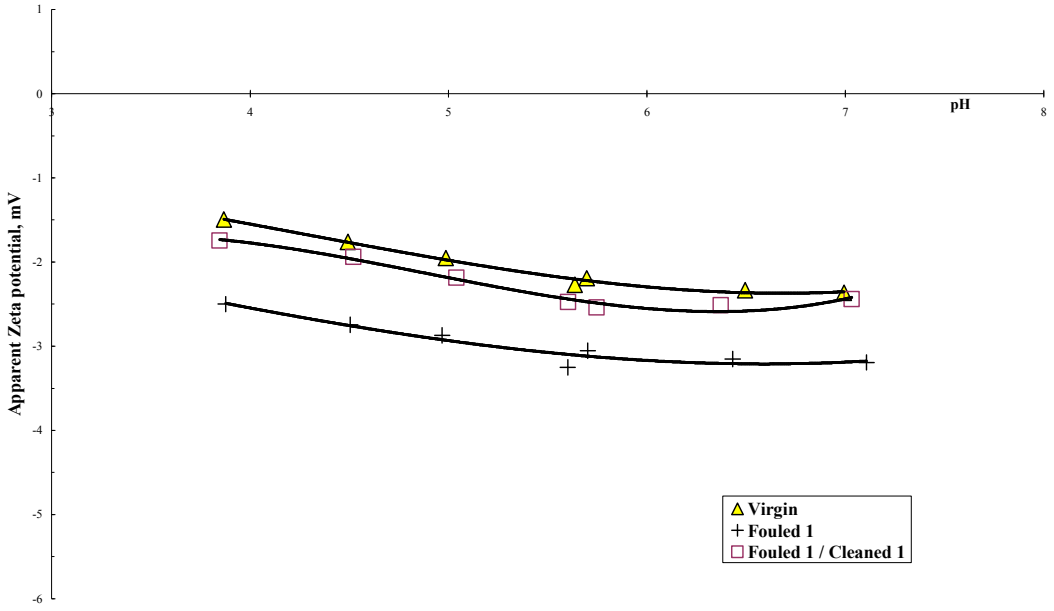

Figure 1.54 (f): Apparent zeta potential on the pore walls of RC100 membrane.

4.3.6 Surface chemistry (FTIR)

Figure 4.55 ((a) and (b)) show the FTIR spectra recorded for all FP and RC membranes that have been fouled once only. A scan for water and virgin membranes have been subtracted from the graphs, so that the scans shown in Figure 4.55 ((a) and (b)) indicate only those of the foulant deposited on the membrane surface, or within the porous structure. The spectra have all been normalised to the same y limits so that intensity of each peak can be assessed and thus a relative determination of deposit estimated. The FP membranes generally show higher intensity of foulant compared with RC membranes, although there are some discrepancies at some peaks. This demonstrates that more foulant was deposited on the FP membranes than on the RC membranes. This could either be due to the FP membranes being rougher and trapping more deposits (see Figure 4.57), and/or the fact that FP membranes are significantly more hydrophobic (see Table 4.4) attracting substances to adhere to the membrane surface.

The intensity of FP membrane deposits vary with pore size such that FP30>FP10>FP100, therefore the amount of deposit found on the FP membrane surfaces or within the pores was largest with FP30 kg mol^{-1} and least with FP100 kg mol^{-1}. This corresponds with the roughness (mean R_a values) of the virgin

conditioned membranes (Figure 4.57) such that the roughest FP surface was FP30 (R_a = 59nm) followed by FP10 (R_a = 27nm) and then FP100 (R_a =11nm) suggesting that the rougher surfaces are potentially trapping more foulant. In addition solids, phenolics and TF transmission data (Figure 4.51, 52 and 53) are highest for the FP30 membrane demonstrating that more tea species are travelling through the pores. An hypothesis for this based on charge within the pores is discussed in section 4.3.5 . The FP30 membrane had the greatest hydrophobicity of the membranes examined (with a contact angle of 68°) as shown in Table 4.4. The more hydrophobic surface would potentially attract more hydrophobic substances present in tea, explaining the increased fouling tendency of this membrane. FP10 having a lower hydrophobicity (with a contact angle of 49°) had less deposit and the FP100 membrane was the most hydrophilic (with a contact angle of 47°) and attracted the least deposit.

The intensity of RC membrane deposits vary with pore size such that RC10>RC30>RC100, therefore the amount of deposit found on the RC membrane surfaces or within the pores was largest with nominal 10 kg mol^{-1} MMCO and least with nominal 100 kg mol^{-1} MMCO. All RC membranes are quite similar in roughness (Ra = 3nm, Figure 4.57) and more deposit was found on the lower nominal MMCO membrane. This could be explained the higher surface area available for interaction in the smaller pore membranes. It would also be expected that the higher molecular mass species would be rejected by the smaller pore membrane, providing an increased fouling tendency. However the total transmission of species through all RC membranes examined was similar for solids (Figure 4.51), polyphenolic, TFs and caffeine (Figure 4.52 and Figure 4.53). This could be due to the formation of a cake layer on each surface which dominates filtration properties once established acting as a secondary active layer. This will be discussed in Section 4.3.8 .

The spectrum of catechin, found in green and black tea show typical peaks of OH in the region of *ca* 1350cm^{-1}, C=C at 1450 – 1600 cm^{-1}, CO at 1200 – 1300 cm^{-1} and CH and/ or ether (COC) at 1000 – 1150 cm^{-1}. Coinceanainn *et al.* 2003, performed FTIR work to study complexation of metals with theaflavins suggesting focussing on 1550 – 1750 cm^{-1} region, in which C=O stretching frequencies occur. The deposits in Figure 4.55 do correspond with the typical regions for polyphenolic substances mentioned above. Identification of specific compounds present is very difficult due to the complexity of the black tea liquor used in this study.

FP10 and FP100 membranes fouled once then cleaned once (Figure 4.56 (a) and (c) respectively) appear to be equal in shape and intensity to their respective virgin conditioned membranes, thus no modification or tea deposits remain on the these surfaces. FP10 cleaned once only (Figure 4.56 (a)) without any fouling appears to have been modified slightly with slightly increased intensity at 1000-1150 cm^{-1}, associated with CH and –(COC)- This could be due to removal of some preservatives (namely glycerine) which may not have been removed during conditioning, which thus masked the original virgin surface and enhanced the original surface peaks. The hydrophobicity of FP10 cleaned once was also increased (Table 4.4) suggesting potential removal of preservatives; future conditioning protocols for this membrane should involve a caustic cleaning process.

All fouled once then cleaned once RC membranes shown in Figure 4.56 (d) – (f) appear to be equal in shape and intensity to their respective virgin conditioned membranes. There does appear to be some extra intensity around 1000 – 1200 cm^{-1} as with FP10 and FP100 although this is not caused by the tea deposits. This could be caused by removal of preservatives or small errors in the subtraction of scans as some negative subtraction appears in these traces.

Figure 4.56 (b) shows the different scans performed on differently treated FP30 membrane surfaces. The fouled once then cleaned once surface is clearly different to the virgin conditioned surface suggesting that either tea deposits remain on the surface (modified or not) or the surface has become modified by cleaning agent. The multiple cleaned membrane followed by a fouling cycle also shows some remaining peaks but at a much lower intensity. The fouled twice and cleaned twice membrane showed a very similar scan to the virgin conditioned membrane. The membrane that was cleaned once only showed a low intensity additional peak not caused by tea deposits, suggesting some initial masking with preservative or small errors between the two scans. There is clearly a modification to the FP30 membrane after the first fouling / cleaning cycle on a virgin membrane or a multi cleaned membrane. There are no significant changes to the membrane fouled twice, cleaned twice and cleaned once only.

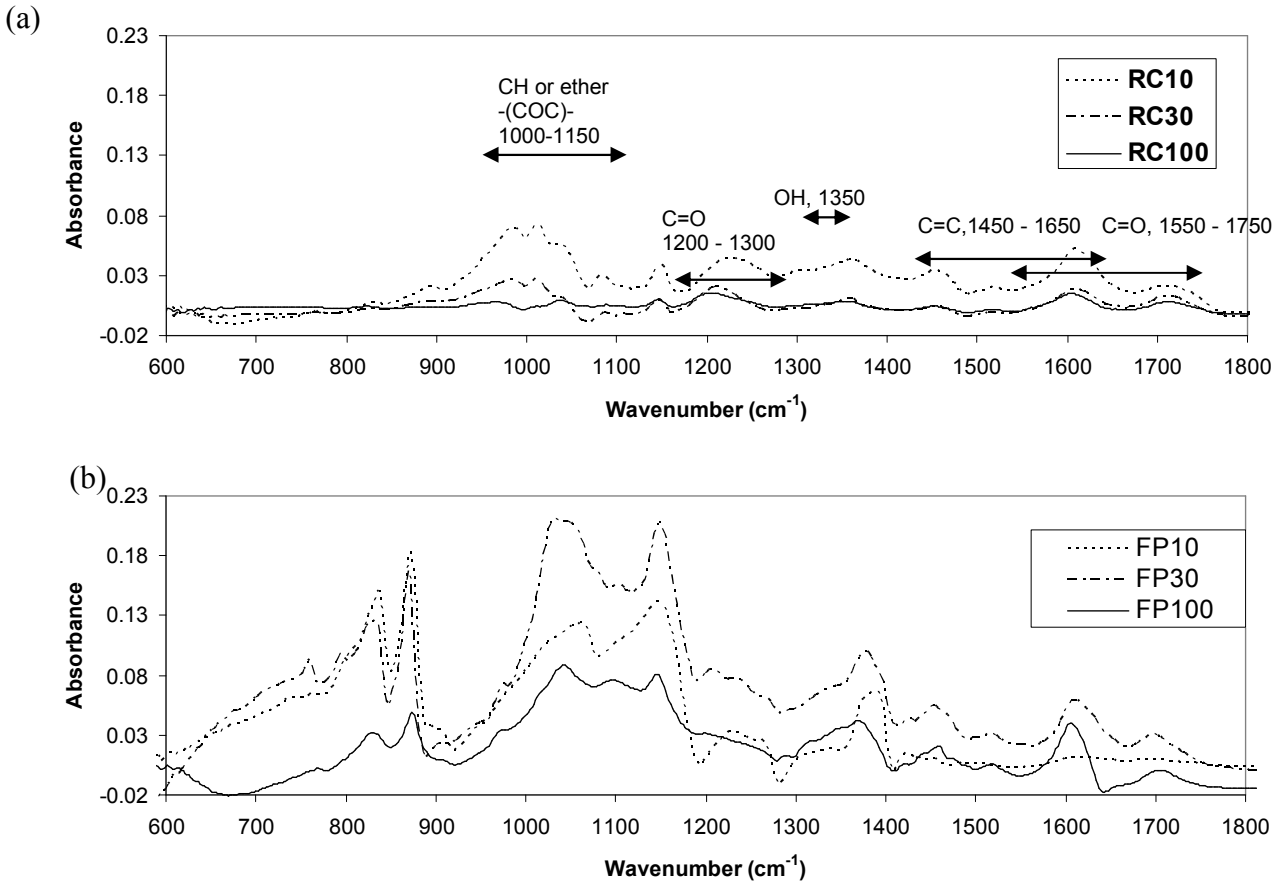

Figure 4.55: Infrared spectra of tea residues (foulant) deposited on the different membranes tested: (a) Regenerated Cellulose membranes and (b) Fluoropolymer membranes

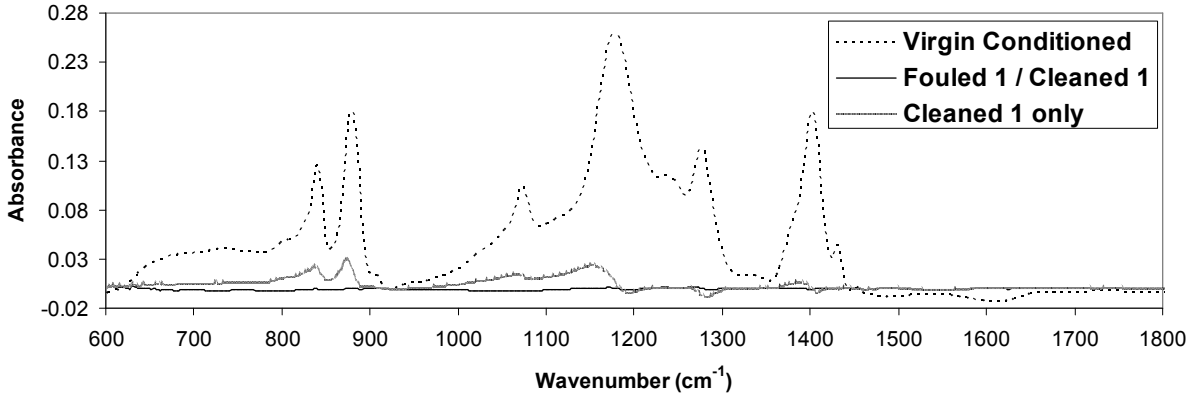

Figure 4.56: (a) Infrared spectra comparison of virgin conditioned FP10 membrane, and differently treated FP10 membranes with virgin conditioned spectra subtracted: (all spectra shown with water subtracted)

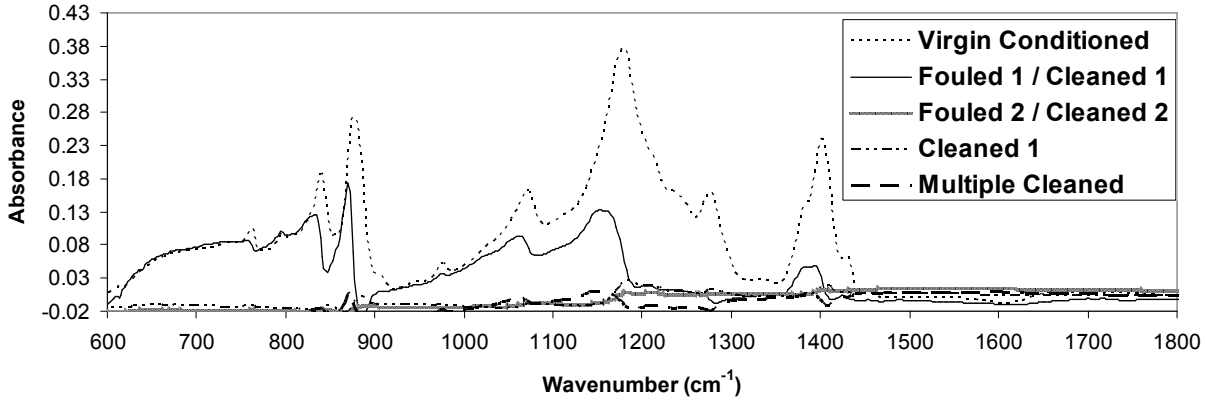

Figure 6 (b) Infrared spectra comparison of virgin conditioned FP30 membrane, and differently treated FP30 membranes with virgin conditioned spectra subtracted. (all spectra shown with water subtracted)

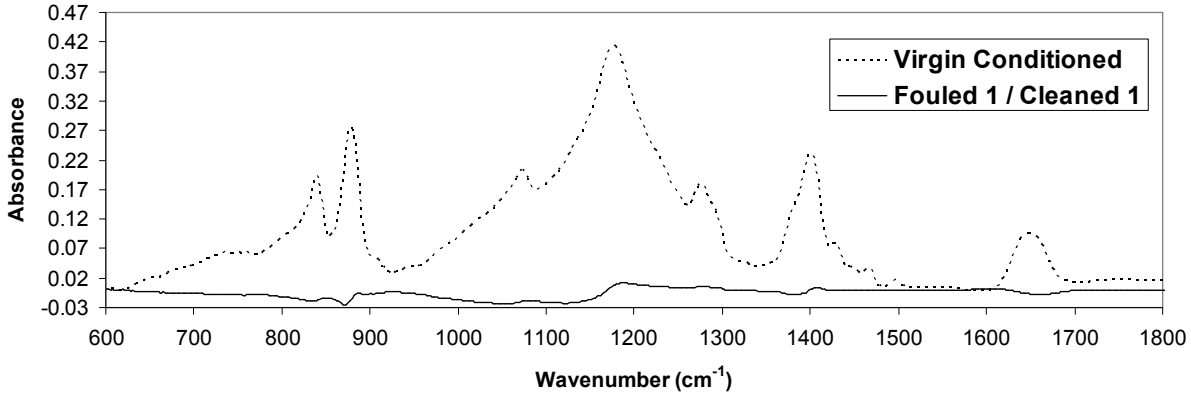

Figure 6 (c) Infrared spectra comparison of virgin conditioned FP100 membrane, and differently treated FP100 membranes with virgin conditioned spectra subtracted. (All spectra shown with water subtracted)

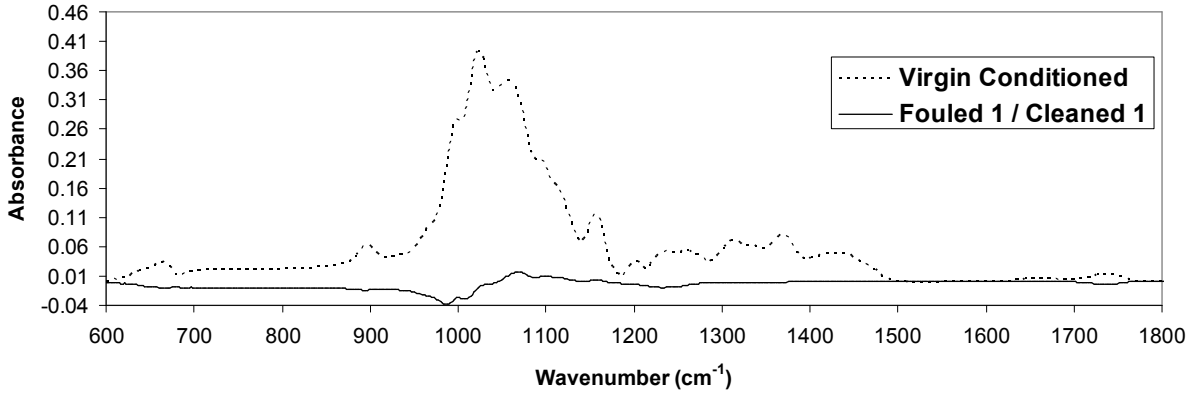

Figure 6 (d) Infrared spectra comparison of virgin conditioned RC10 membrane, and differently treated RC10 membranes with virgin conditioned spectra subtracted. (All spectra shown with water subtracted)

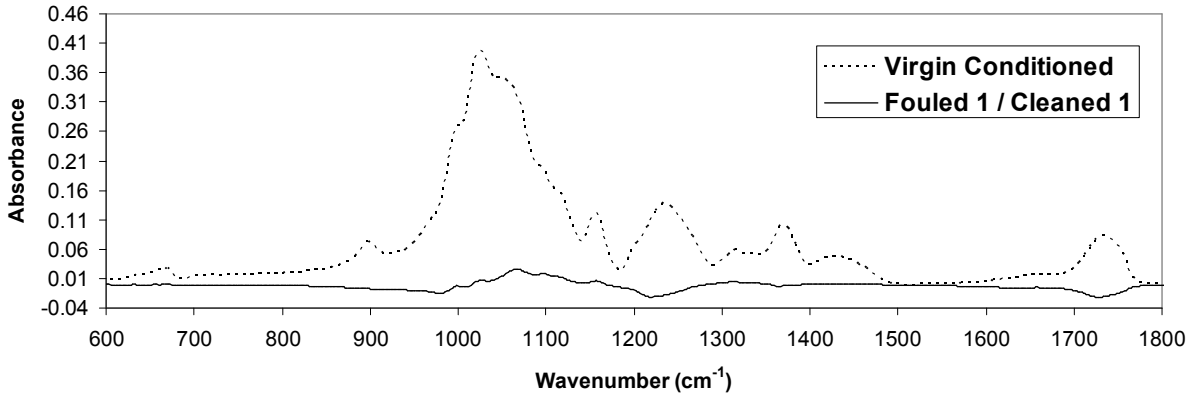

Figure 6 (e) Infrared spectra comparison of virgin conditioned RC30 membrane, and differently treated RC30 membranes with virgin conditioned spectra subtracted. (All spectra shown with water subtracted)

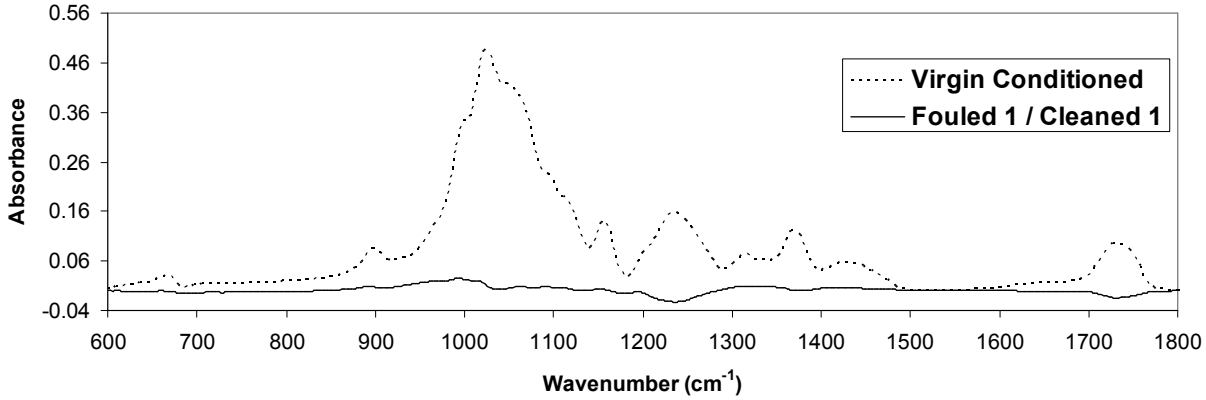

Figure 6 (f) Infrared spectra comparison of virgin conditioned RC100 membrane, and differently treated RC100 membranes with virgin conditioned spectra subtracted. (All spectra shown with water subtracted)

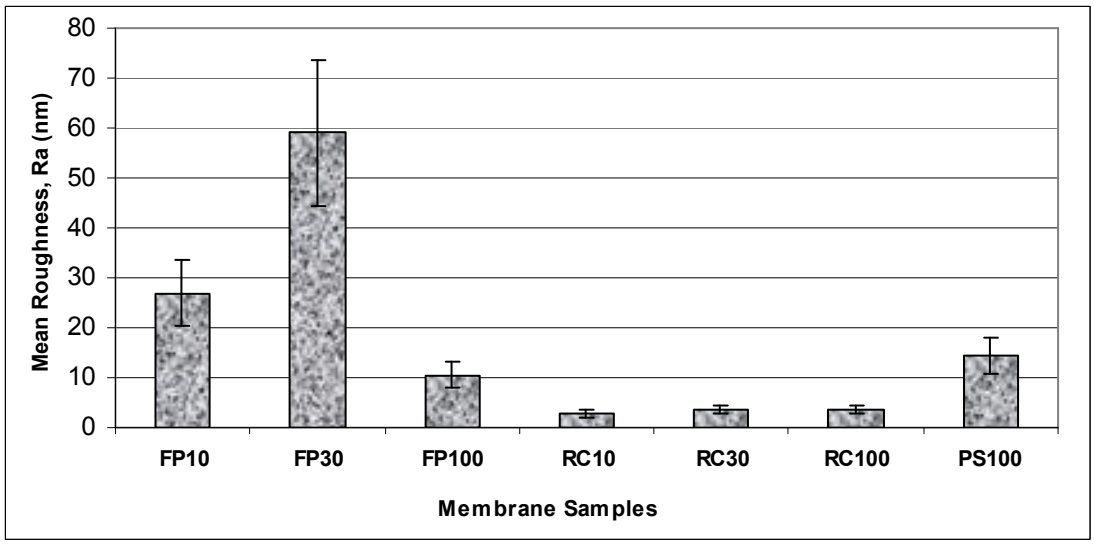

Figure 4.57: Mean roughness (R_a) of virgin conditioned membranes.

4.3.7 Flux measurements

Figure 4.58 and Figure 4.59 shows the fouling and pure water fluxes respectively of all the membranes studied. The FP membranes generally showed lower fouling fluxes than the RC membranes. FP10 displayed the lowest steady state flux of 14 LMH (litres m^{-2} h^{-1}) and RC100 the highest of 32 LMH. FP30 and FP100 gave similar fluxes; 27 and 29 LMH respectively. There were no significant changes in fouling flux through the FP30 membrane during second cycle or after initial cleaning, the steady state fouling flux did increase slightly from 27 LMH to 28 LMH on the second fouling cleaning cycle although not experimentally significant. Section 4.2.6 reports work on the FP30 membrane showing that increasing the fouling TMP from fouling / cleaning cycle to cycle, (on the same membrane) gave a permanent modification to the membrane, causing an increase in steady state fouling fluxes under standard conditions.

Section 4.2.8 indicated that multiple fouling / cleaning cycles (on the same membrane) at standard conditions used in this study do not permanently modify membranes such that there are increases in fouling (product) flux.

The changes in pure water flux (PWF) after a fouling and cleaning cycle can provide useful information regarding the membrane and its cleanliness (Vaisanen *et al.* 2002). Care must be taken to use this information alongside other indicators of cleanliness such as charge, hydrophobicity and surface roughness. Figure 4.59 demonstrates that the FP10 gave the highest PWF of all virgin conditioned membranes (214 – 288 LMH). Upon a fouling and cleaning cycle the PWF increased by 79% and upon cleaning only the PWF increased by 58%. An increase in PWF after fouling and or cleaning was also evident with the FP30 membrane with an initial increase of 30.5% from 144 LMH to 188 LMH after a fouling / cleaning cycle. No further significant change in PWF was evident on the second fouling / cleaning cycle or if multiple cleaning of the membrane was initially performed.

The PWF did not vary significantly following a fouling cleaning cycle of the FP100 membrane or any of the RC membranes. FP100 and all the RC virgin conditioned and fouled / cleaned membranes had very low negative charge (Figure 4.54 (c) – (f)) and the surface chemistry, as indicated by FTIR, was not changed following fouling

and cleaning cycles (Figure 4.56 (c) – (f)). The PWF of virgin conditioned RC10 membrane was 30 LMH, significantly lower than RC30 and RC100 with fluxes of 280 and 292 LMH respectively. Note that the initial lower fluxes during the fouling cycle of RC10 (Figure 4.58) suggesting that initially the membrane performs poorly and was then modified giving a similar performance to RC30 and RC100 membranes. This suggests that a cake layer may dominate filtration properties with this membrane which is evident with similar solids (Figure 4.51), polyphenolic, theaflavins and caffeine (Figure 4.52 and Figure 4.53) transmissions for all membranes evaluated.

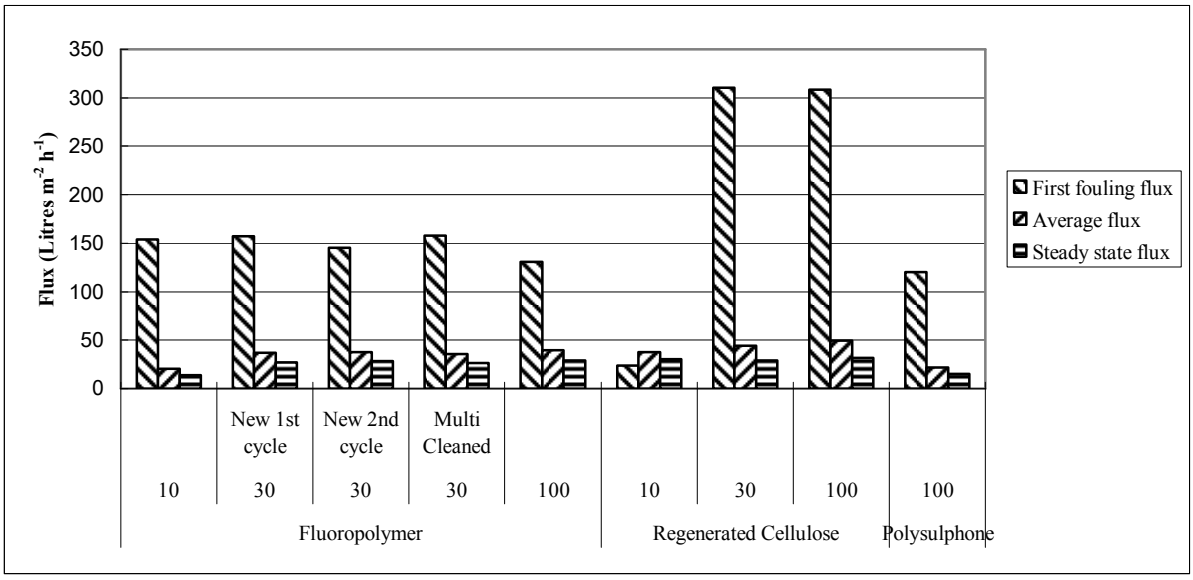

Figure 4.58: First, average and steady state fouling fluxes for different membranes fouled by a feed solution of 1.0 wt% black tea at 1.0 bar TMP, 50^{o}C and 0.44 ms^{-1} CFV

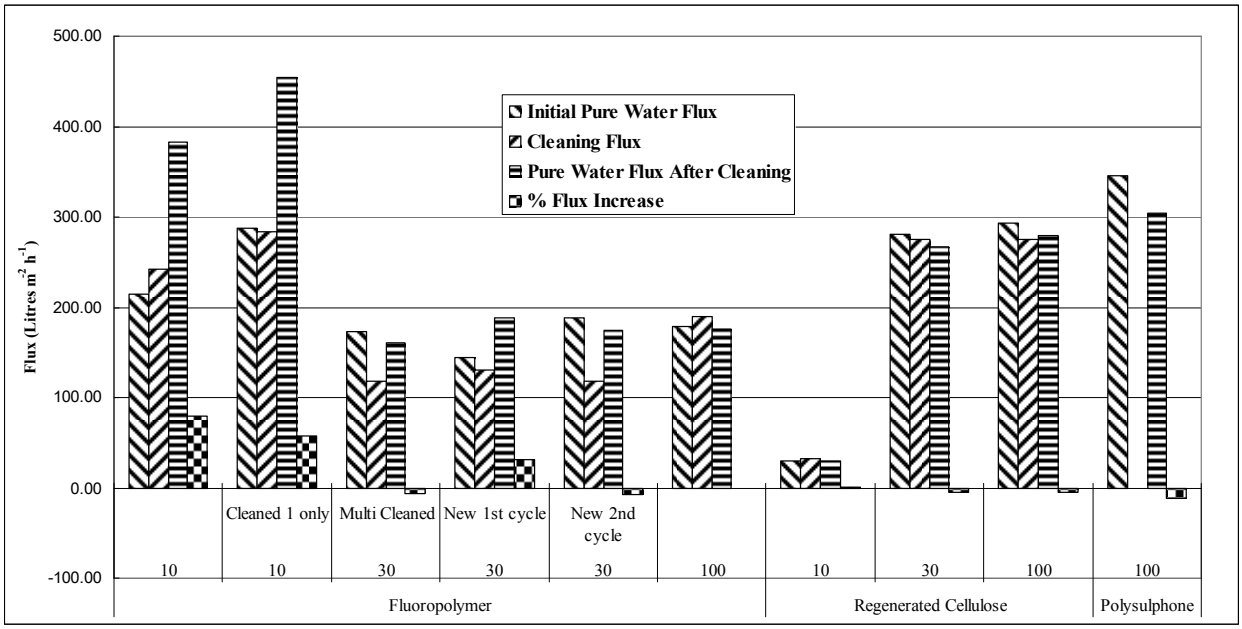

Figure 4.59: Pure water fluxes and flux recoveries of fouled and cleaned membranes measured under standard conditions.

4.3.8 Fouling flux mechanisms

The model presented in Field *et al.* 1995, for constant pressure filtration with allowance for cross flow, has been applied to the flux data recorded in this paper. The general equation is shown in section 2.4.8.6 (Equation 2.16)

Modelling was carried out using a commercial package, *Scientist*^{TM} (Version 3.0). The approach to modelling employed the use of the package's non-linear regression routine for parameter estimation, coupled with numerical integration. Equation 2.16 and Equation 2.17 were modelled simultaneously, the values of R modified by a constant such that they were of equal order of magnitude to flux values. The parameters varied were k_J, J_s and J_o, all of which were allowed to float. The initial values of n were set based on an analysis of dR/dt versus t curves to determine maximum or negative trend. For all data in this study, no maximum was found, hence n could only have values of 1 or 0. The best fit of modelled data to actual data in terms of flux and resistance was studied for the whole curves for each data set as demonstrated in Figure 4.61 and Figure 4.62 below for the RC30 membrane which also demonstrating the residuals for n=0 (Cake filtration mechanism).

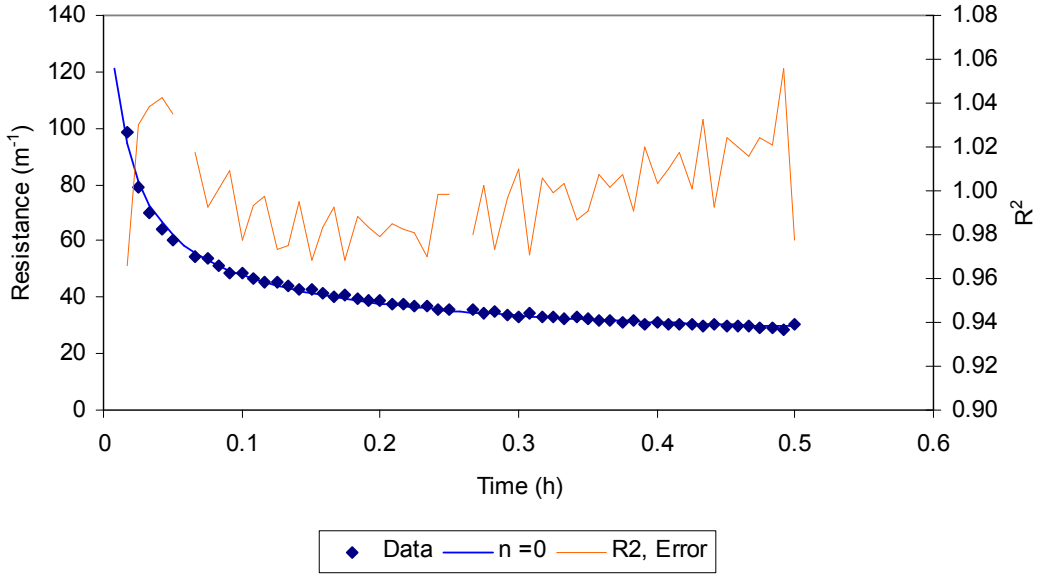

Figure 4.60: Example fit of flux data to Field et al. *1995 model and associated residuals for the 30 kg mol^{-1} regenerated cellulose membrane.*

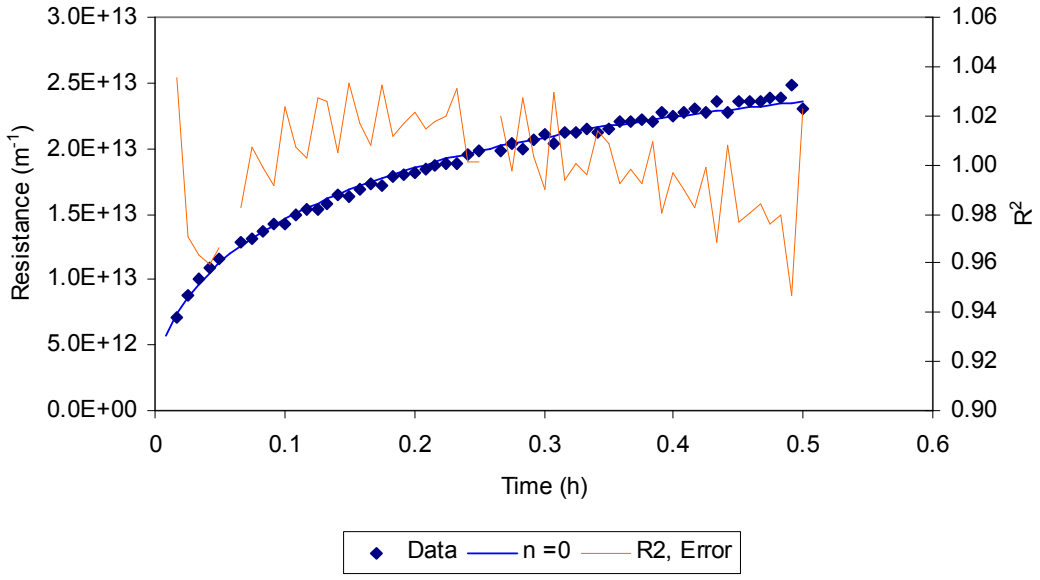

Figure 4.61: Example fit of resistance data to Field et al. *1995 model and associated residuals for the 30 kg mol^{-1} regenerated cellulose membrane.*

The parameters for each pore size are shown in Table 4.5, in all cases cake filtration (n = 0) was found to dominate as a fouling mechanism. Given the nature of the feed, 1.0 wt% tea solution and the presence of larger macromolecular tea cream this is as expected. k_J can be thought of as a "rate of fouling" term and does vary from membrane to membrane. FP membranes generally have a higher rate of fouling than RC membranes confirming previous discussions in sections 4.3.5 and 4.3.6 . FP10 has a significantly higher rate of fouling by an order of magnitude over all other

membranes. Cleaning FP30 membranes increases the fouling rate of FP30 membranes although the variation is not significant.

Membrane	Conditions	n	k_J ($m^{-2}h^1$)	J* (mh^{-1})	J_o(mh^{-1})
FP10	Virgin conditioned	0	0.0213	13.6	67.4
FP30 (1)	Virgin conditioned	0	0.0041	25.0	67.4
FP30 (2)	2nd cycle	0	0.0057	27.6	110.8
FP30 (multi)	Initially cleaned 8 times	0	0.0082	26.8	138.5
FP100	Virgin conditioned	0	0.0049	28.1	147.0
RC10	Virgin conditioned	0	0.0020	20.6	63.6
RC30	Virgin conditioned	0	0.0034	25.7	121.3
RC100	Virgin conditioned	0	0.0027	26.5	197.3

Table 4.5 Parameters used to model fouling mechanisms based on model developed by Field et al (1995).

4.3.9 Summary

Black tea clarification has been investigated using two different ultrafiltration membrane materials, namely regenerated cellulose and fluoropolymer of three different nominal molar mass cut-offs (10, 30 and 100 kg mol^{-1}). Ultrafiltration produces clarified black ready to drink tea beverage with increased stability and significantly reduced haze.

The FP membranes generally showed lower fouling fluxes than the RC membranes, FP10 the lowest steady state flux of 14 LMH (litres m^{-2} h^{-1}) and RC100 the highest of 32 LMH. FP30 provided the highest total tea solids transmission of 73% while FP10 (65%) and FP100 (62.5%) gave the lowest solids transmission of all FP membranes. The RC membranes all gave similar solids transmissions of 69 – 73%. All the RC membranes and the FP30 membrane performed such that around 90% and 100% of the important total polyphenols and more specifically, total theaflavins were transferred into the permeate respectively. FP10 gave lowest transmission of total polyphenols (78%) and theaflavins (62%). All membranes produced permeates with a higher relative concentration of caffeine than the initial feed solution, 118 – 142% transmission.

The results shown and discussed in this paper demonstrate that flux and defined molar mass cut-off are not adequate by themselves to decide upon membrane choice for

filtration. Surface science parameters are important to the filtration properties and fouling and cleaning mechanisms.

Increased deposition (FTIR) and increased negative charge (ZP) on the FP membranes caused higher fouling rates (k_J) resulting in lower fouling fluxes. The deposits and negative charge were observed such that FP30 > FP10 > FP100 which corresponds to the increased roughness (Ra) of the FP membranes, FP30 (59 nm), FP10 (27 nm) and FP100 (11 nm). The foulant appears to be more significantly entrapped by rougher surfaces.
The FP membranes were also significantly rougher (R_a) than the RC membranes (3nm) demonstrating why the RC membranes had less deposit and negative charge than the FP membranes. The amount of deposit on the FP membranes correlated to the hydrophobicity of the surfaces such that FP30 was the most hydrophobic and FP100 was the least hydrophobic. This suggests that the foulant – membrane interactions are hydrophobic in nature.

The virgin FP30 membrane displayed an isoelectric point at pH 4.5, the same as that recorded for the tea used in this study. At this pH, the FP10 membrane had a slightly positive charge and FP100 a slightly negative charge. Increased solids, polyphenolic, theaflavins and caffeine transmission were apparent through the FP30 membrane compared to to either FP10 or FP100. This suggests that the negatively charged molecules (based on negative charge in pores of all fouled membranes) would theoretically pass through FP30 easiest whilst an interaction or repulsion would be more likely with the FP10 and FP100 membranes.

Cake filtration was confirmed as a fouling mechanism for all membranes used in this study. Due to similar surface charge properties, formation of a cake layer might dominate filtration with all RC membranes which was apparent due to similar solids, polyphenolic, theaflavins and caffeine transmissions.

FP100 and RC membranes all had comparatively low negative ZP values which did not vary significantly with varying pH, i.e the membranes did not accept a lot of negative or positive charge. Subsequently all membranes recovered initial PWF values, ZP profiles and chemical nature (as detected by FTIR) after a fouling /

cleaning cycle. Generally all the RC membranes demonstrated high fouling fluxes with the least fouling. This might indicate that over longer fouling runs the performance of RC membranes might be superior to the FP membranes which demonstrated increased fouling.

FP10 and FP30 membranes had a negative charge following fouling then cleaning or cleaning of the virgin membrane. This charge was between that of the virgin surface and that of the fouled membrane. This suggests that the action of NaOH cleaning increased the negative charge of the fluoropolymer within the pores primarily, although modification due to foulant interaction cannot be disregarded. It seems most likely that the cleaning solution is removing the majority of the foulant thus reducing the negative charge, and then modifying the fluoropolymer increasing the negative charge within the pores, possibly by adsorption of hydroxyl ions.

There were no significant changes in fouling flux through the FP30 membrane during second cycle or after initial cleaning. Although FP10 and FP30 demonstrated increases in PWF values following fouling and/or cleaning, the FP100 and all the range of RC membranes tested showed no significant variation in PWF through successive fouling & cleaning cycles.

4.4 Polyphenol - membrane force measurements

4.4.1 Introduction

The use of AFM force interaction measurements has been carried out for a model polyphenol present in tea, theaflavin-3-gallate, (TF3G) with a regenerated cellulose ultrafiltration membrane. This study has investigated the influence of multiple (200x) measurements of force curves at different points on the membrane surface. Previous work reported in the literature has typically been limited to a much smaller number of different locations for characterisation of a whole surface. In addition to the adhesion force measurements that are usually reported, this section also reports approach force data to the membrane surface.

The results demonstrate the usefulness of this technique for understanding foulant – membrane – cleaning agent interactions at different stages during a fouling / cleaning cycle. This information will aid understanding of the nature of fouling and cleaning mechanisms in these systems.

4.4.2 Adhesive forces

Figure 4.62 represents the frequency diagram of TF3G adhesion (retracting) forces from the regenerated cellulose membrane surface at different stages along the fouling / cleaning cycle. The graph shows the frequency of adhesive measurements for each force range at varied locations along the membrane surface. The results demonstrate that the virgin membrane surface and the F1C1 surface behave in a similar way with average adhesive forces of 1.34+/-0.03 and 1.38+/-0.05 nN respectively and matching curves ranging between 0 and 3 nN with a single shallow peak. This confirms other results found in this study (reported in section 4.3) where the same regenerated cellulose membrane was found to be intrinsically clean following a fouling and cleaning cycle, based on surface chemistry, charge and flux recovery.

The TF3G adsorbs with nearly half the average adhesive force (0.76+/-0.04 nN) to the fouling deposit than to the virgin surface or F1C1 surface with a much narrower adhesion force distribution, demonstrating a reduced foulant – foulant interaction. Therefore during black tea ultrafiltration using this membrane there was less foulant – foulant interaction. This system has the potential for reduced fouling over longer runs and a corresponding reduction in the cleaning requirement.

In a separate experiment, the regenerated cellulose membrane was initially conditioned in the same way as all other treatments, but then followed by a NaOH clean. Interestingly average adhesion force measurements to this surface were reduced by nearly half (0.78 +/-0.02 nN) compared to the virgin conditioned surface and the F1C1 surface. The narrow spread of the adhesion data following cleaning of the virgin surface (0.25 – 1.0 nN) is indicative that exposure of the membrane to a simple liquid (NaOH) has acted on some of the charged groups on the surface rendering it more uniform in terms of components controlling adhesion. This is different to the fouling and cleaning history (which displays a wide distribution - 0 – 3 nN), where a more heterogeneous system than the virgin membrane was acted on by the NaOH. This demonstrates that TF3G would adhere less strongly to a regenerated cellulose membrane surface following a NaOH cleaning protocol than the virgin conditioned or F1C1 membrane. Clearly this result has practical implications, indicating that an initial treatment of the membrane with NaOH may reduce subsequent fouling tenacity as a result of tea filtration. Further experimentation is required for other model components present in tea to determine those constituents mostly responsible for fouling, thus building a greater understanding of the fouling and cleaning mechanisms of other fouling constituents.

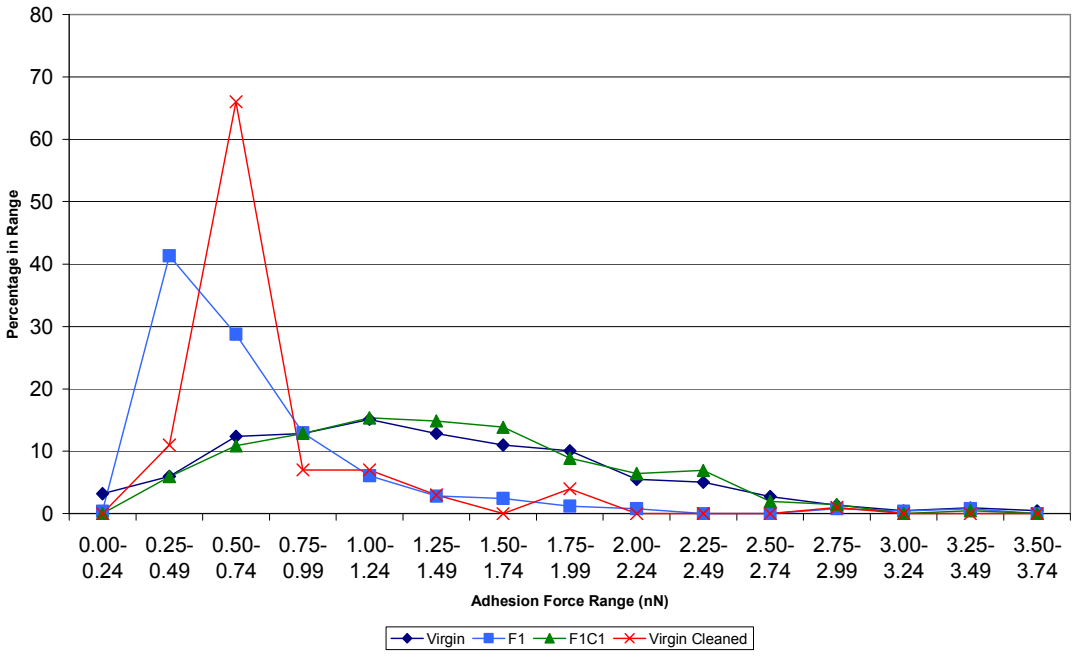

Figure 4.62: Frequency curve of multiple TF3G adhesion forces measured over a 10 x 10 μm regenerated cellulose membrane area

4.4.3 Attractive forces

Figure 4.63 represents the frequency diagram of TF3G attractive (approaching) forces to the regenerated cellulose membrane surface at different stages along the fouling / cleaning cycle. The graph shows the frequency of attractive force measurements for each force range at varied locations along the membrane surface. The virgin conditioned membrane surface had the largest average attractive force (0.85+/-0.06 nN) compared to the fouled, F1C1 and cleaned 1 membrane surfaces with average attractive forces of 0.60+/-0.02, 0.50+/-0.007 and 0.65+/-0.002 nN respectively. Section 4.3 demonstrated an intrinsically clean membrane surface following cleaning on the same regenerated cellulose membrane surface, therefore no tea foulant was present on this surface and the virgin cleaned membrane only had NaOH as a possible modifying agent. The uniform narrow distribution of attraction forces (0 – 1 nN) to the fouled and cleaned surfaces could be due to uniformly charged foulant / hydroxyl ions adhered to the membrane surface whereas the virgin membrane distribution was very wide (0 – 3 nN) demonstrating no charge modification on this surface.

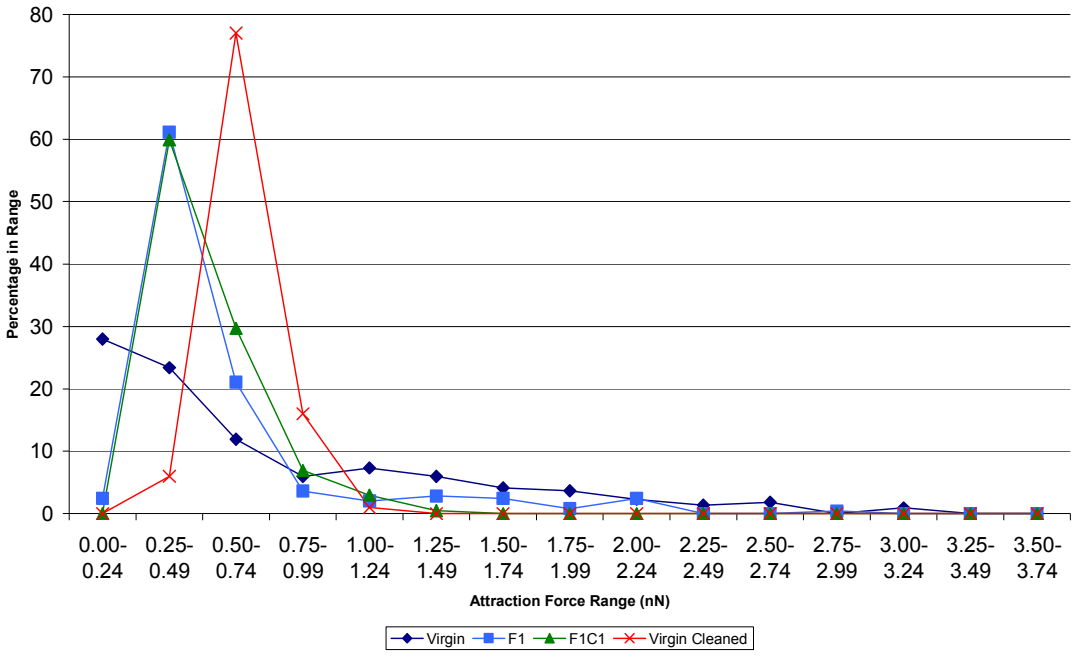

Figure 4.63: Frequency curve of multiple TF3G attraction forces measured over a 10 x 10 μm regenerated cellulose membrane area

4.4.4 Summary

AFM force interaction measurements have been used to investigate the interaction of a model polyphenol present in tea (theaflavin-3-gallate) with a regenerated cellulose ultrafiltration membrane. This study has investigated the influence of multiple (200x) measurements of force curves at different points on the membrane surface. Approach force data to the membrane surface has been analysed in addition to adhesion force measurements that are usually reported.

The results demonstrate the usefulness of this technique for understanding foulant – membrane – cleaning agent interactions at different stages during a fouling / cleaning cycle. The average adhesion forces of the foulant to the virgin and the F1C1 membrane surface were larger than those seen for the foulant – foulant interactions. Sodium hydroxide cleaning of the virgin conditioned membrane reduced foulant – membrane adhesion force compared to that seen for the virgin or F1C1 surface. The uniform narrow distribution of attraction (approach) forces to the fouled and cleaned surfaces helps explain this due to uniformly charged foulant / hydroxyl ions adhered to these membrane surfaces whereas the virgin membrane distribution was very wide demonstrating no charge modification on this surface.

AFM has helped increase the level of understanding of membrane fouling and cleaning mechanisms.

4.5 Effect of cleaning upon flux recovery

Two different membrane materials, namely fluoropolymer and regenerated cellulose were investigated based on cleaning optimisation after standard protocol black tea filtration. Cleaning, normalised pure water and filtrate fluxes were recorded and the selectivity of the membrane to total tea solids was also obtained.

The normalised pure water flux J_N was calculated using Equation 4.13 which is based on the percentage flux recovery equation in Vaisanen *et al.* 2002 where J_{FC} is the pure water flux after a fouling / cleaning cycle and J_U is the pure water flux of the virgin conditioned membrane.

$$J_N = J_{FC} / J_U$$

Equation 4.13

The apparent membrane rejection coefficient (R_{coeff}) was recorded using Equation 4.6 in all instances.

4.5.1 Fluoropolymer membrane cleaning optimisation

In this section cleaning conditions have been optimised as a function of TMP, sodium hydroxide concentration (NaOH), temperature and cross flow velocity (CFV) for a 30 kDa MWCO membrane. In each investigation only one physical parameter was varied.

4.5.1.1 Transmembrane Pressure (TMP)

The TMP was varied maintaining a constant NaOH concentration of 0.5wt%, a CFV of 0.44 ms^{-1}, a temperature of 50°C for 30 mins where constant fouling conditions with tea reconstitute were used in each cycle (1.0wt%, 50°C, 0.44 ms^{-1}) for 30 minutes. The RO water flux characterisation was maintained constant before and after fouling and after cleaning as shown in Table 3.2.

The cleaning fluxes increased with increased TMP as expected due to extra force on the membrane surface (Figure 4.64), although normalised pure water fluxes (Equation 4.13) after cleaning were highest at 0.5 bar TMP (Figure 4.65). Many authors have demonstrated (Section 2.5.4.3) that cleaning should be performed at low pressures, (ideally with zero applied TMP) to avoid compaction of the membrane. However, in this study this was not practical in terms of collecting kinetic data. An investigation into closing the permeate side of the membrane may produce some interesting results

regarding the requirement of transmission of cleaning fluid as discussed in 2.5.4.3 . Steady state product fouling fluxes (fouling flux following cleaning treatment) varied insignificantly with cleaning TMP (Figure 4.66). Initial product fouling fluxes were highest and the total solids membrane rejection coefficient was highest after cleaning at 0.5 bar (Figure 4.66 and Figure 4.67). Therefore the separation efficiency of the membrane was at a maximum after cleaning at this TMP. The transmission data suggests that less material is removed from the membrane after cleaning at higher TMP than 0.5 bar allowing higher transmission rates due to less resistive forces through the membrane.

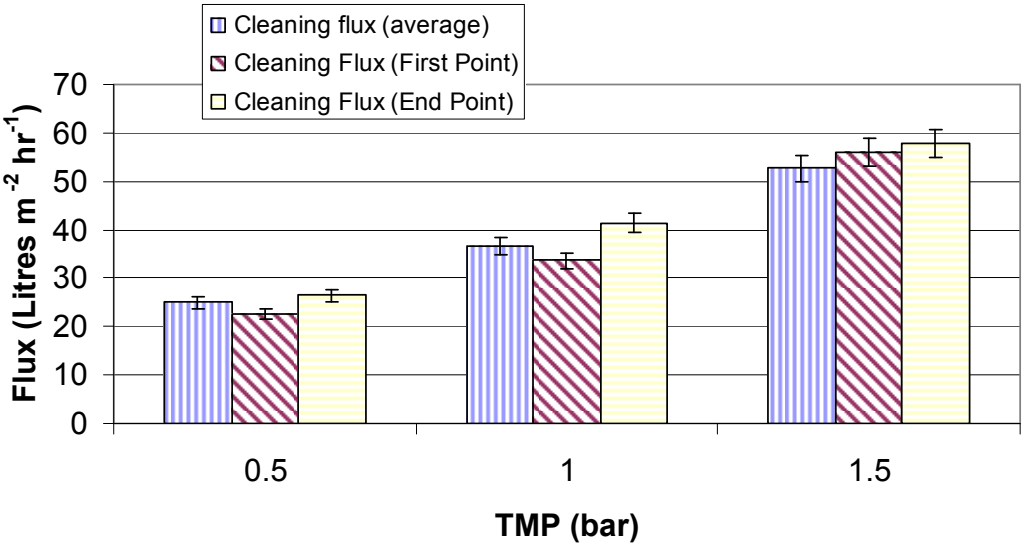

Figure 4.64: Graph to show sequential NaOH cleaning flux vs cleaning TMP variation on the same fluoropolymer membrane when fouled with tea (1.0wt%, 50°C, 0.44m/s) for 30mins.

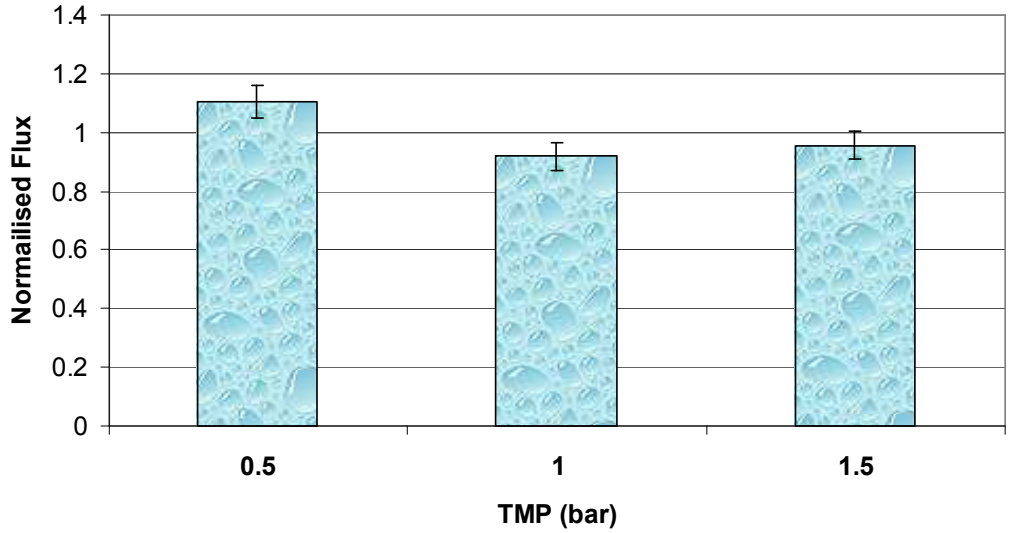

Figure 4.65: Graph to show normalised pure water flux after cleaning vs cleaning TMP variation on the same fluoropolymer membrane when fouled with tea (1.0wt%, 50°C, 0.44m/s) for 30mins.

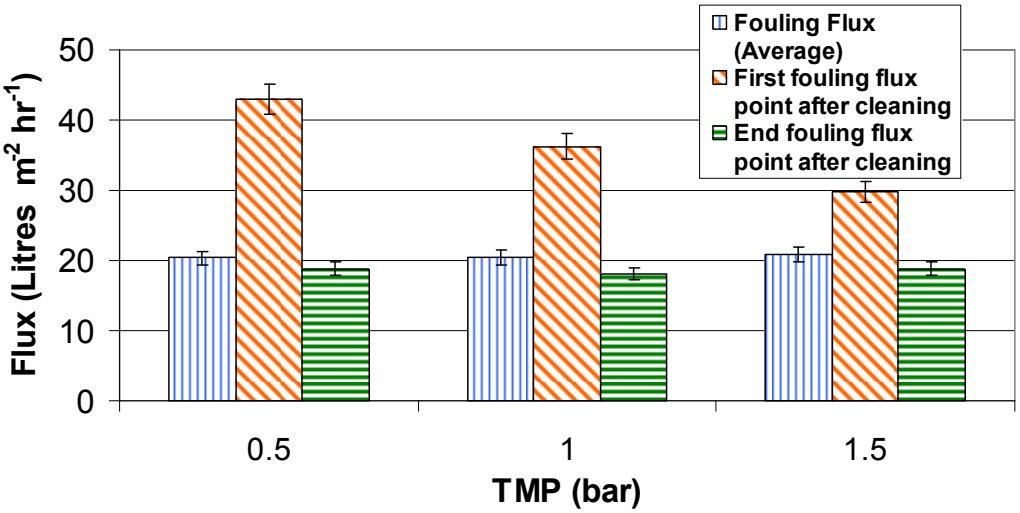

Figure 4.66: Graph to show product fouling flux vs cleaning TMP variation on the same fluoropolymer membrane when fouled with tea (1.0wt%, 50°C, 0.44m/s) for 30mins.

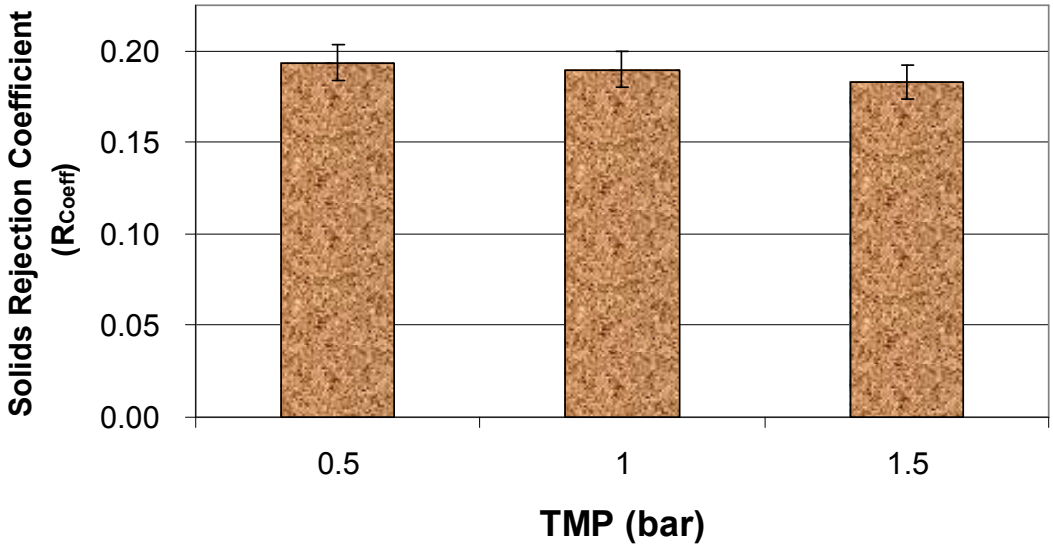

Figure 4.67: Graph to show total tea solids rejection coefficient of a fluoropolymer membrane filtering black tea (1.0wt%, 50°C, 0.44m/s) after cleaning at various TMP's.

4.5.1.2 NaOH concentration

The NaOH concentration was varied maintaining a constant TMP of 0.5bar, a CFV of 0.44 ms^{-1} and a temperature of 50°C for 30 mins where constant fouling conditions with tea reconstitute were used in each cycle (1.0wt%, 50°C, 0.44 ms^{-1} for 30 minutes). The RO water characterisation protocol was maintained before and after fouling and after cleaning as shown in Table 3.2.

The cleaning fluxes did not vary significantly with NaOH concentration as shown in Figure 4.68, although the normalised pure water fluxes after cleaning increased quite considerably as can be seen in Figure 4.69. Logically a further increase in NaOH concentration should be considered but as demonstrated by Figure 7.5, the pH of the cleaning solution becomes higher as NaOH increases and the manufacturing limits of the membrane become an issue. Therefore 0.5wt% NaOH was the maximum cleaning concentration used for these FP membranes. The product fouling fluxes also increased quite significantly following an increased cleaning concentration (0.5wt%) (Figure 4.70) and the membrane rejection coefficient decreased considerably from 0.45 after 0.1wt% cleaning to 0.18 after cleaning with 0.5wt% NaOH. (Figure 4.71). A number of theories could be advanced;

(i) Lower cleaning concentrations caused less foulant removal from the membrane surface and/or pores, thereby increasing the selectivity.

(ii) Higher NaOH cleaning concentrations widen the pore size distribution by chemical reaction of NaOH with the membrane surface material

(iii) Reaction of NaOH with adsorbed foulant within the pore walls causing them to swell and increase the size of pores before being removed.

Although the theory (ii) was a concern in particular where membrane durability was concerned, later data (figures 4.42) demonstrate that the membrane rejection coefficient remains around 0.2 when 0.5wt% NaOH was used through multiple cycles. This suggests that theory (i) and (ii) are possible explanations. A significantly reduced initial cleaning agent flux would be expected if the foulant initially expands within the pore structure which was not found at any concentration demonstrating that theory (i) is more likely correct. Although theory (iii) cannot be discounted as the swelling / removal phenomenon may have occurred at an increased rate compared to the flux measurements.

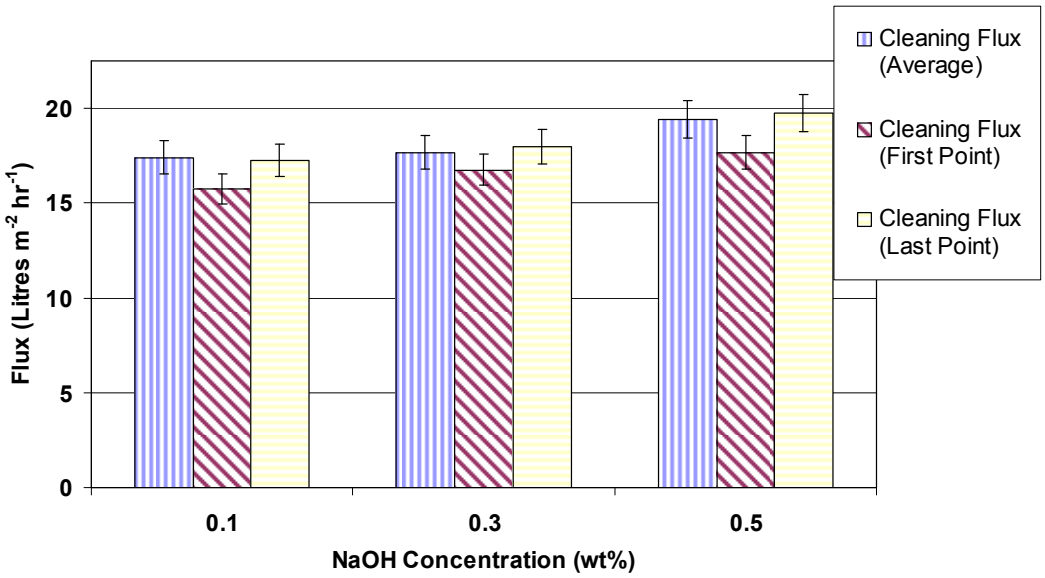

Figure 4.68: Graph to show sequential cleaning fluxes vs cleaning concentration variation on the same fluoropolymer membrane when fouled with tea (1.0wt%, 50°C, 0.44m/s) for 30mins.

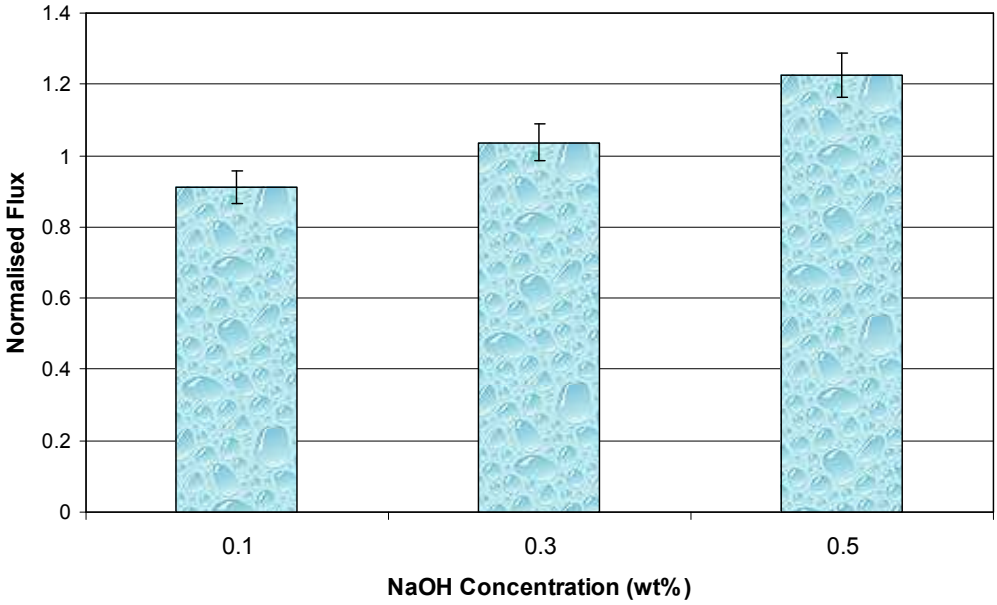

Figure 4.69: Graph to show normalised pure water flux after cleaning vs cleaning concentration variation on the same fluoropolymer membrane when fouled with tea (1.0wt%, 50°C, 0.44m/s) for 30mins

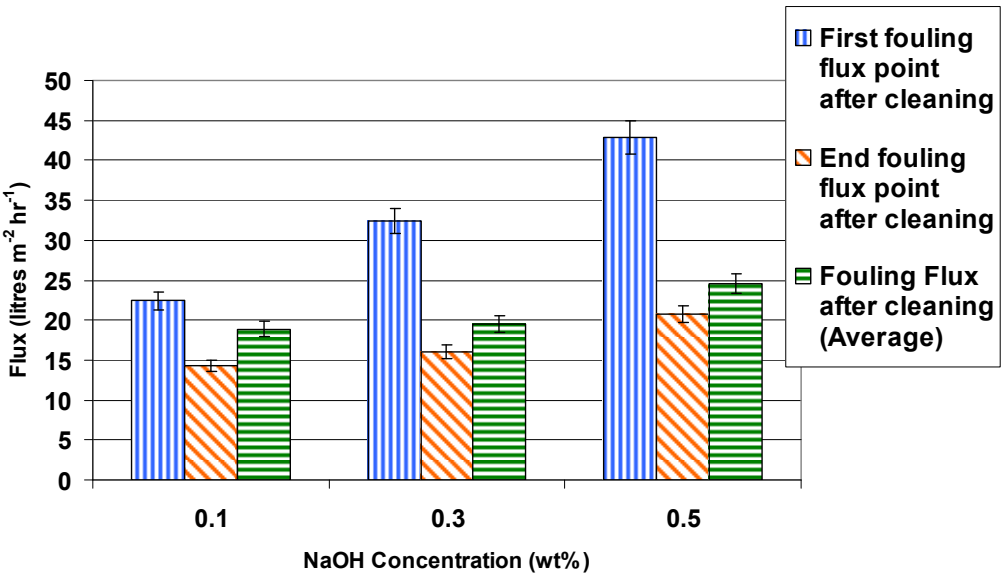

Figure 4.70: Graph to show product fouling flux vs cleaning concentration variation on the same fluoropolymer membrane when fouled with tea (1.0wt%, 50°C, 0.44m/s) for 30mins.

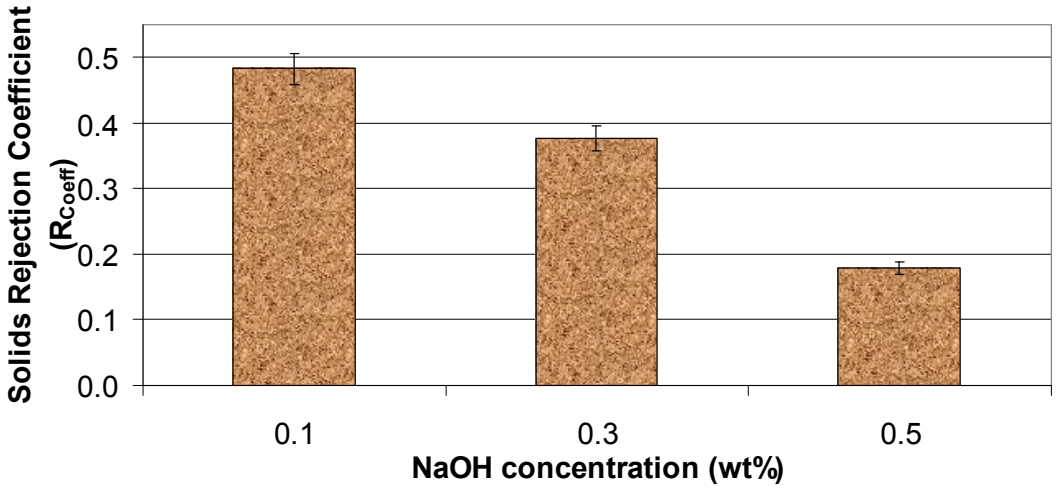

Figure 4.71: Graph to show total tea solids rejection coefficient of a fluoropolymer membrane filtering black tea (1.0wt%, 50°C, 0.44m/s) after cleaning at various NaOH concentrations.

4.5.1.3 Temperature

The cleaning temperature was varied whilst maintaining a constant NaOH concentration of 0.5wt%, a CFV of 0.44 ms^{-1} for 30mins where constant fouling conditions with tea reconstitute were used in each cycle (1.0wt%, 50°C, 0.44 ms^{-1}) for 30 minutes. The RO water flux characterisation protocol was maintained before and after fouling and after cleaning as shown in Table 3.2.

It must be noted that the experiments were performed such that 30°C cleaning cycle was performed first followed by the 65°C cycle then the 50°C cycle.

The cleaning flux increased with increased temperature most likely due to decreased viscosity of the permeate at increased temperature as shown in Figure 4.72. The normalised pure water fluxes after cleaning increased with increasing cleaning temperature (Figure 4.73). This corresponds to previous literature (as discussed in section 2.5.4.2) where decreasing viscosity and increasing reaction rates are responsible for increased cleaning rates. Product fouling fluxes varied insignificantly as the cleaning temperature was varied (Figure 4.74) although the total tea solids membrane rejection coefficient slightly higher after cleaning at 65°C (0.18), suggesting some enhanced cleaning.

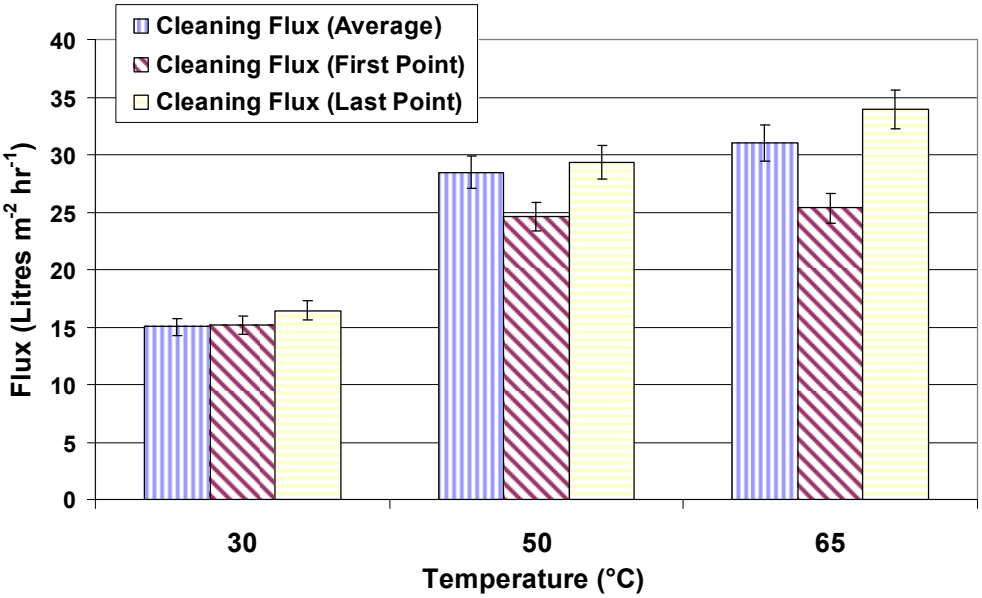

Figure 4.72: Graph to show sequential cleaning fluxes vs cleaning temperature variation on the same fluoropolymer membrane when fouled with tea (1.0wt%, 50°C, 0.44m/s) for 30mins.

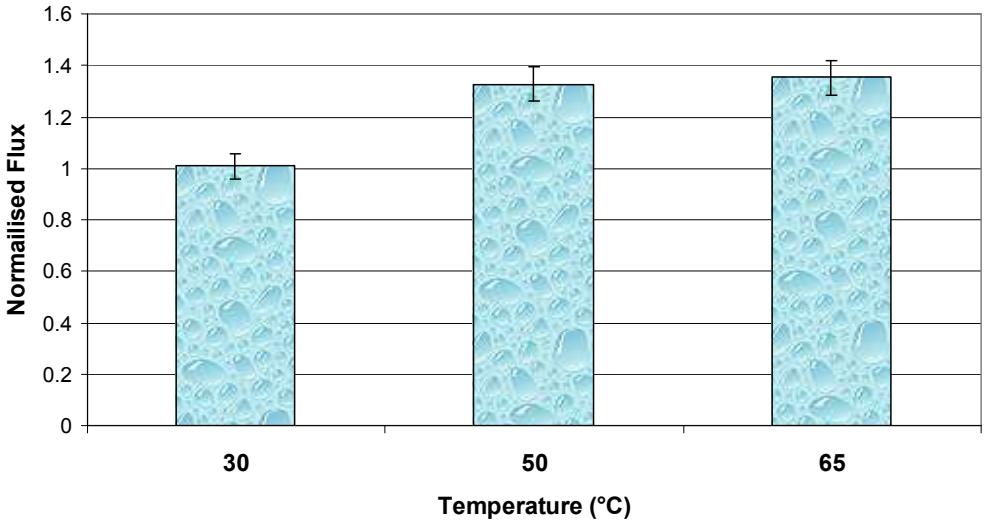

Figure 4.73: Graph to show normalised pure water flux after cleaning vs cleaning temperature variation on the same fluoropolymer membrane when fouled with tea (1.0wt%, 50°C, 0.44m/s) for 30mins

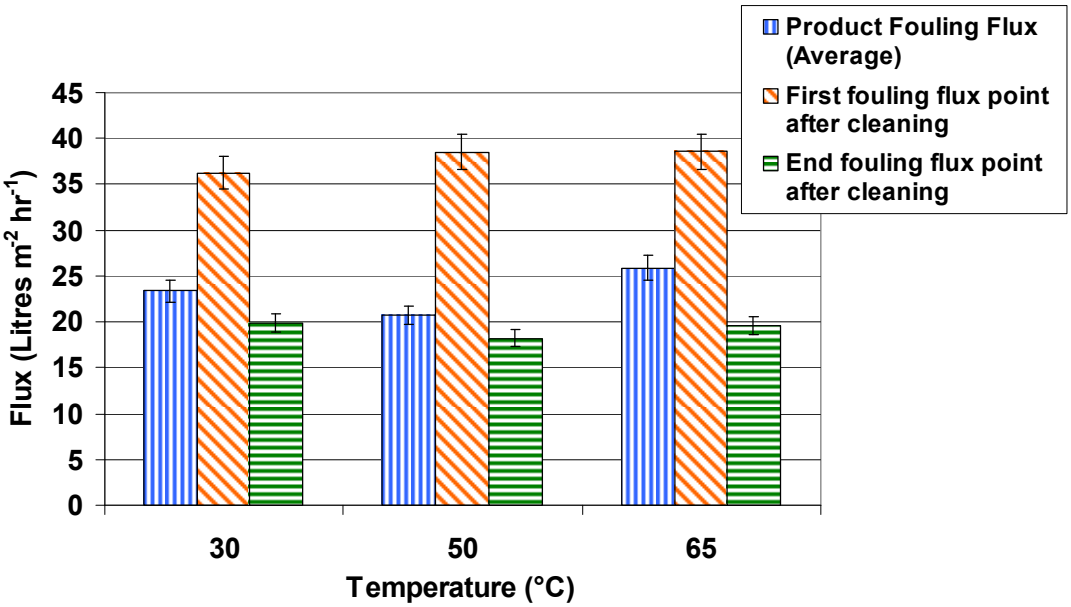

Figure 4.74: Graph to show product fouling flux vs cleaning temperature variation on the same fluoropolymer membrane when fouled with tea (1.0wt%, 50°C, 0.44m/s) for 30mins.

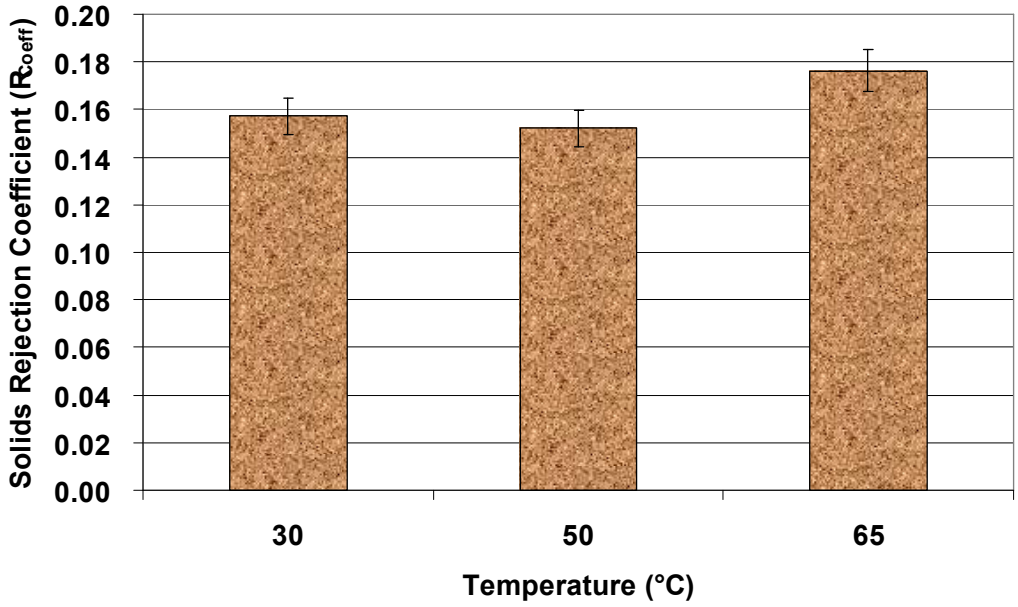

Figure 4.75: Graph to show total tea solids rejection coefficient of a fluoropolymer membrane filtering black tea (1.0wt%, 50°C, 0.44m/s) after cleaning at various temperatures.

4.5.1.4 Cross – flow velocity

The cleaning CFV was varied maintaining a constant NaOH concentration of 0.5wt%, a TMP of 0.5 bar and a temperature of 50°C for 30mins where constant fouling conditions with tea reconstitute were used in each cycle (1.0wt%, 50°C, 0.44 ms^{-1}) for 30 minutes. The RO water flux characterisation protocol was maintained before and after fouling and after cleaning as shown in Table 3.2. A repeat of the maximum cleaning CFV (1.15ms^{-1}) was repeated a second time labelled (b).

The effect of cleaning CFV on flux can be seen in Figure 4.76 where increasing the CFV from 0.44 to 0.67 ms^{-1} demonstrated an increase in cleaning flux from 34 to 41 litres m^{-2} hr^{-1} which was not enhanced upon with further increases in CFV. Figure 4.77 shows that the normalised pure water flux after cleaning increases significantly (1.0 to 1.6) as the cleaning CFV is increased from laminar (Re = 1480) to a turbulent regime (Re = 3912). This confirms that higher shear rates must be removing more foulant material providing a higher flux. No significant variation in product flux and total tea solids membrane rejection coefficient was noticed with variation in cleaning CFV (Figure 4.78 and Figure 4.79), although it is still recommended to clean with a turbulent CFV due to increased pure water fluxes after cleaning.

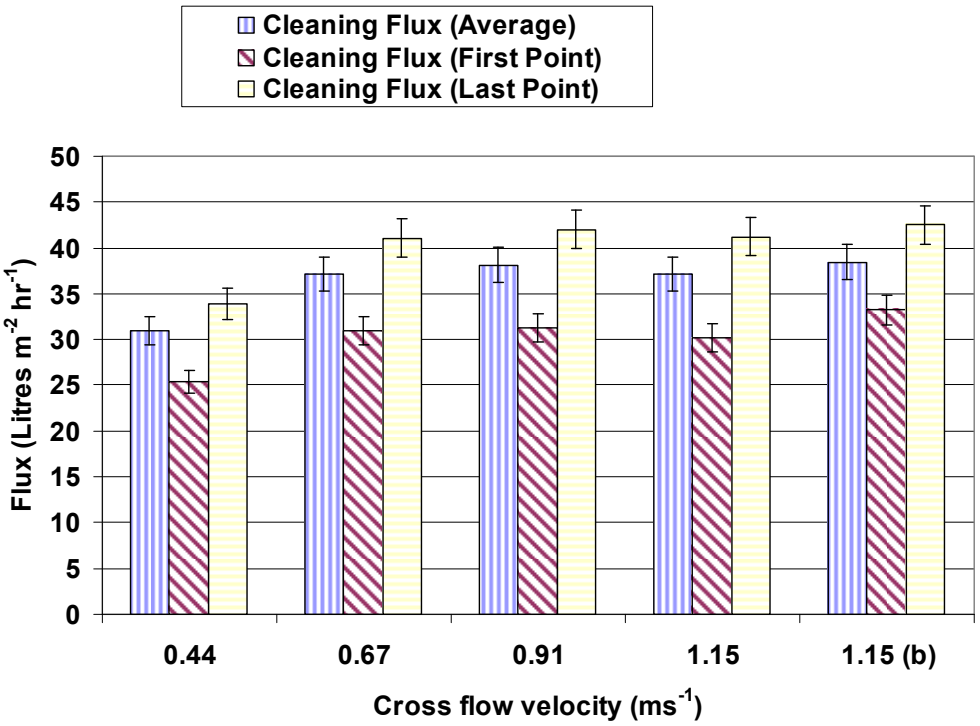

Figure 4.76: Graph to show sequential pure water flux after cleaning vs cleaning CFV (including repeat of 1.15 m/s) variation on the same fluoropolymer membrane when fouled with tea (1.0wt%, 50°C, 0.44m/s) for 30mins.

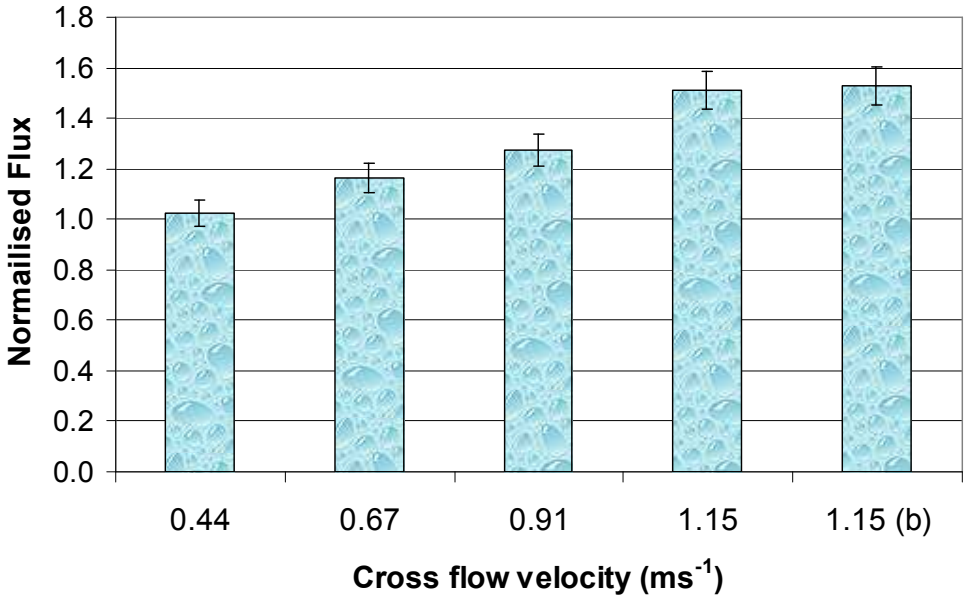

Figure 4.77: Graph to show normalised pure water flux after cleaning vs cleaning CFV variation on the same fluoropolymer membrane when fouled with tea (1.0wt%, 50°C, 0.44m/s) for 30mins.

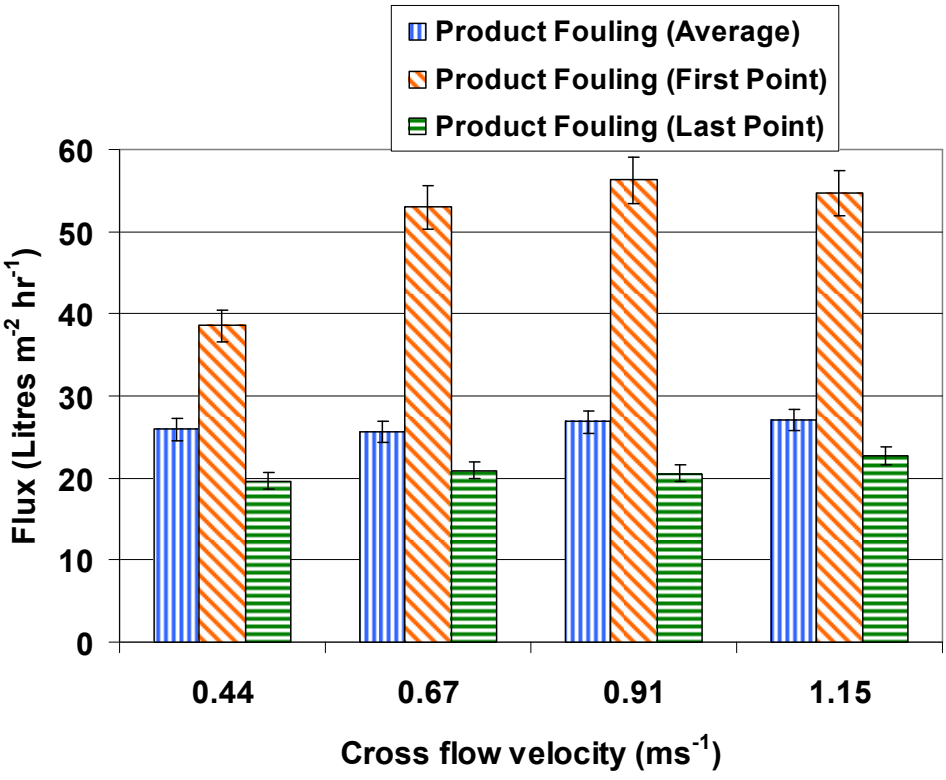

Figure 4.78: Graph to show product fouling flux vs cleaning CFV variation on the same fluoropolymer membrane when fouled with tea (1.0wt%, 50°C, 0.44m/s) for 30mins.

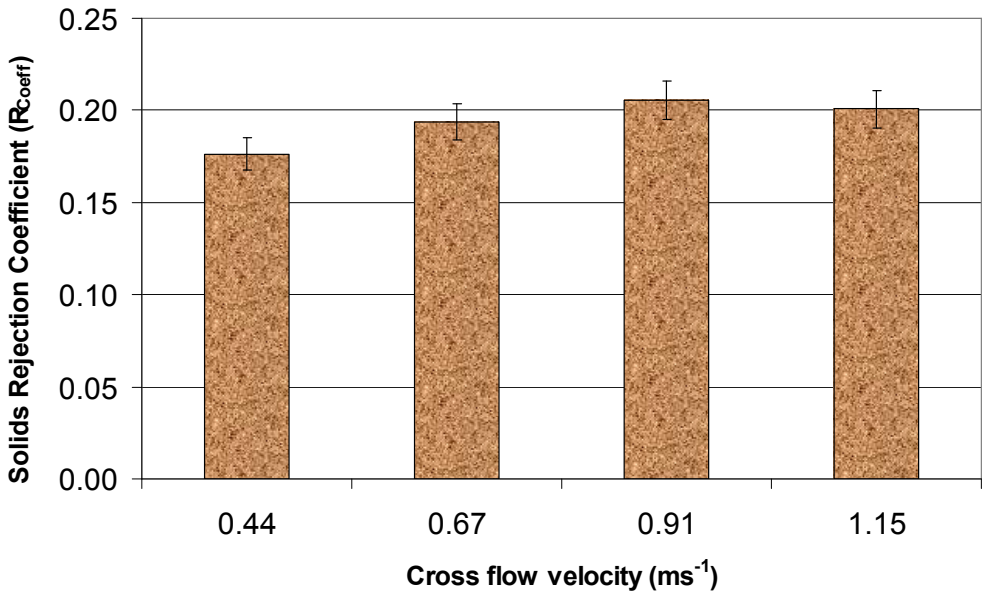

Figure 4.79: Graph to show total tea solids rejection coefficient variation as a function of cleaning CFV for a fluoropolymer membrane filtering black tea (1.0wt%, 50°C, 0.44m/s) after a standard cleaning protocol with varied CFV..

4.5.1.5 Summary

The optimum cleaning conditions were found to be: 0.5wt% NaOH, 60°C feed temperature, 0.5bar TMP and 1.15ms^{-1} CFV for the FP membrane. All conditions were found to affect membrane flux recovery after each cycle although TMP and NaOH concentration were found to be the most significant in terms of product fouling fluxes and product solids transmission of tea solutions. Note a maximum temperature of 60°C was used in further experiments due to the difficulty of operating at 65°C using the current water bath set-up.

4.5.2 Regenerated cellulose membrane cleaning optimisation

The regenerated cellulose membrane has strict operational pH and temperature limits (Table 3.1), due to the physical nature of the membrane. Within the current study, cleaning was only optimised based on CFV, all other conditions were maintained constant. The NaOH concentration of 0.01wt% was used to maintain the cleaning pH within operational limits and a slightly lower temperature (45°C) reducing any potential membrane damage.

4.5.2.1 Cross – flow velocity

The cleaning CFV was varied maintaining a constant NaOH concentration of 0.01wt%, TMP of 0.5bar and temperature of 45°C for 30mins. Constant fouling conditions were used in each cycle with tea reconstitute (1.0wt%, 50°C, 0.44 ms^{-1}) for 30 minutes. The RO characterisation protocol was maintained constant before and after fouling and after cleaning as shown in Table 3.2.

The variation of cleaning CFV on flux can be seen in Figure 4.80 where no significant change can be seen, also the normalised pure water flux after cleaning remained constant (Figure 4.81)

No significant variation in product flux or total tea solids membrane rejection were found with variation in cleaning CFV (Figure 4.82 and Figure 4.83), although a turbulent CFV is recommended to ensure maximum removal of any cake layers present.

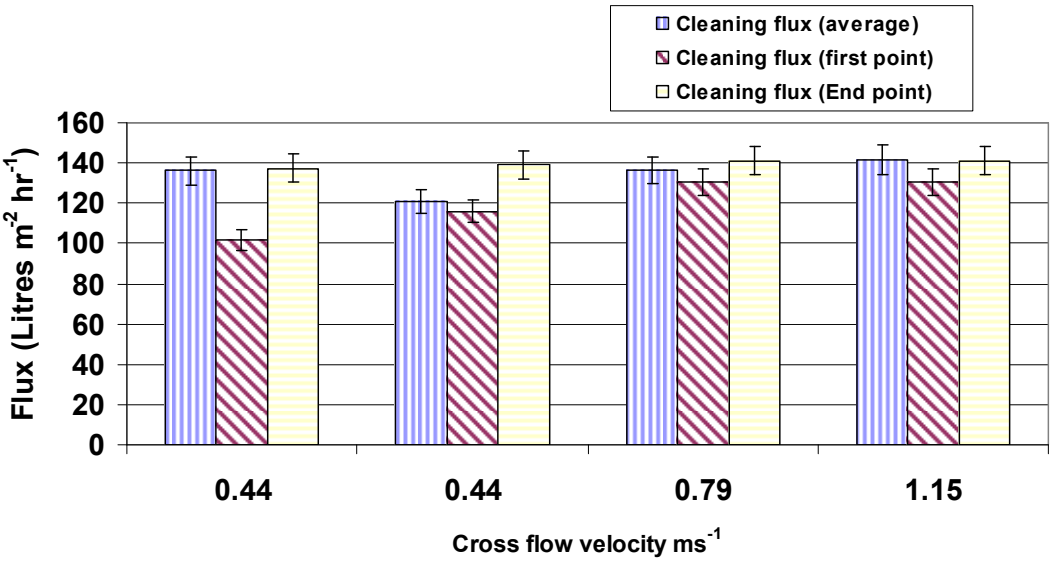

Figure 4.80: Graph to show sequential cleaning flux data vs cleaning CFV variation on the same regenerated cellulose membrane when fouled with tea (1.0wt%, 50°C, 0.44 m/s) for 30mins.

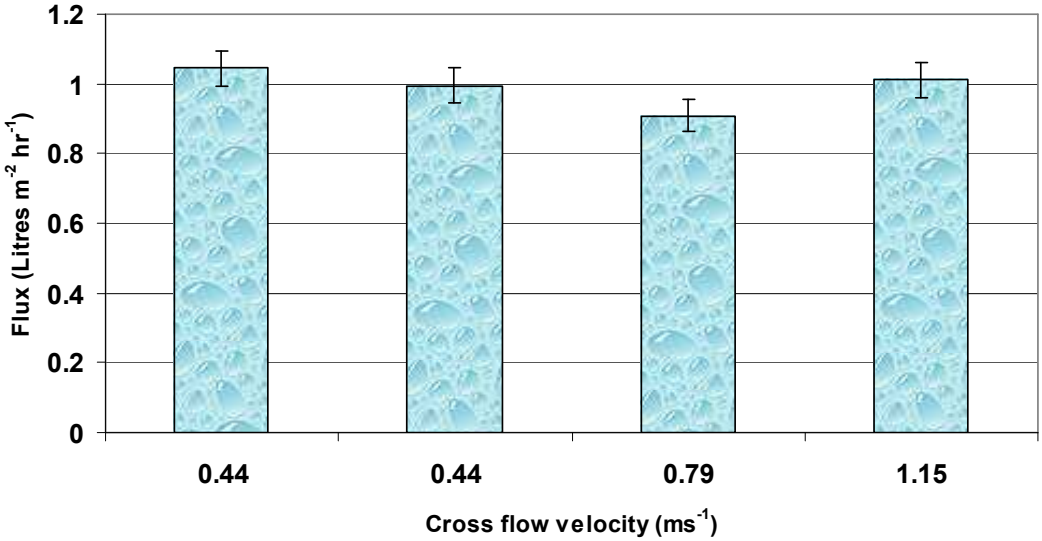

Figure 4.81: Graph to show normalised pure water flux data after cleaning vs cleaning CFV variation on the same regenerated cellulose membrane when fouled with tea (1.0wt%, 50°C, 0.44m/s) for 30mins.

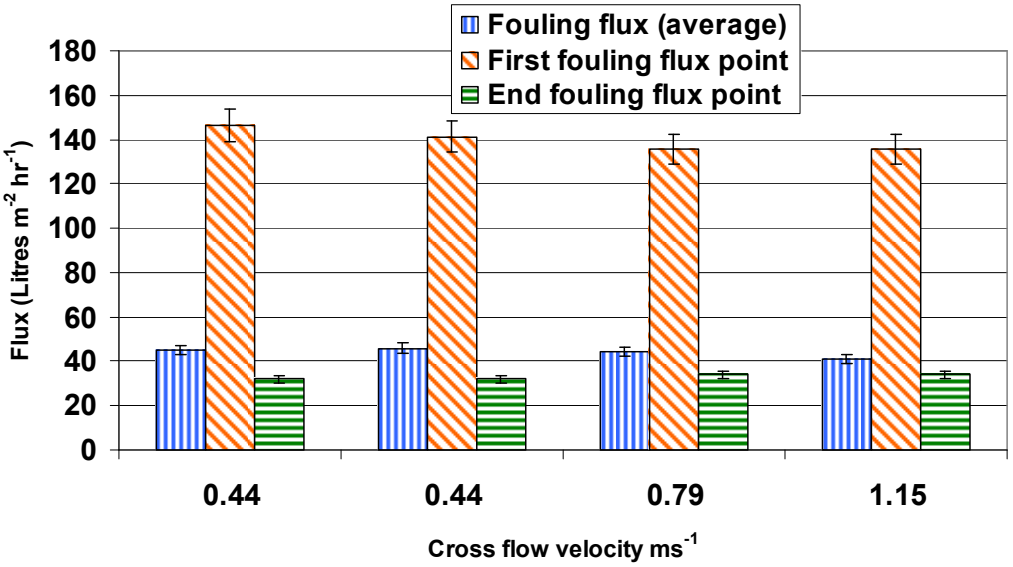

Figure 4.82: Graph to show sequential product fouling flux data after cleaning vs cleaning CFV variation on the same regenerated cellulose membrane when fouled with tea (1.0wt%, 50°C, 0.44m/s) for 30mins.

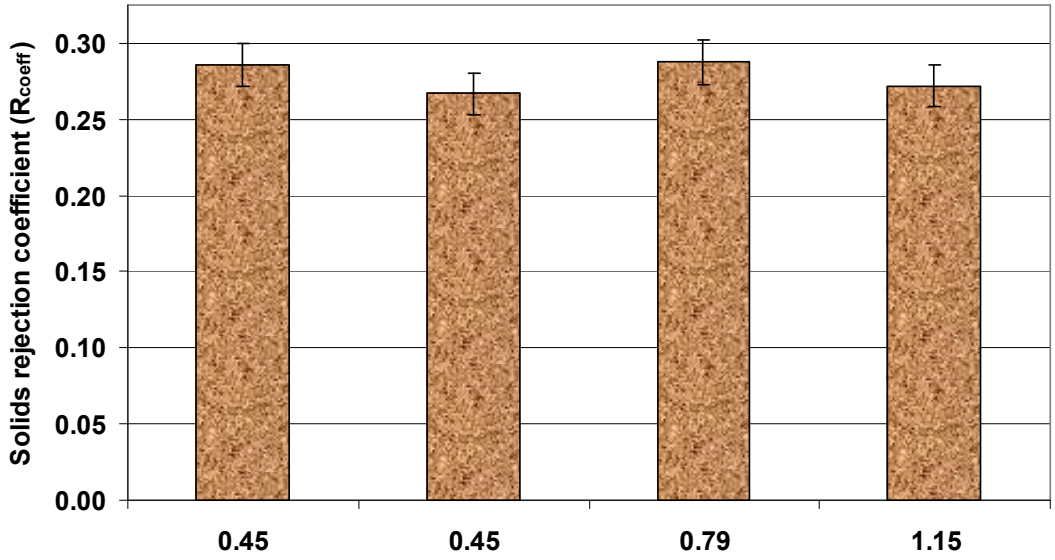

Figure 4.83: Graph to show sequential product solids rejection coefficient for the regenerated cellulose membrane after cleaning vs cleaning CFV variation on the same regenerated cellulose membrane when fouled with tea (1.0wt%, 50°C, 0.44m/s) for 30mins.

4.6 Physical properties of Black Tea

This section will investigate the physical properties of black tea solutions including the effect of total solids concentration and temperature on viscosity, colour and haze. Storage of black tea solutions has been investigated and the benefit of ultrafiltration as a clarification procedure is demonstrated. Particulate size of black tea aggregates are also discussed in this section.

4.6.1 Viscosity

The viscosity of black tea was measured for variations in solution temperature and total tea solids concentration using the method described in section 3.5.3 . The viscosity of feed solutions during membrane separation is important because they can affect mass transfer to the membrane surface and the nature of flow across the membrane surface during cross flow filtration.

Figure 4.84 shows the viscosity of various tea reconstitute concentrations at different temperatures (25 – 50°C). The viscosity measurements were increased at higher tea concentrations and lower solution temperatures. The viscosity increase with concentration was larger at lower tea temperatures, i.e. at 25°C the viscosity increased from 8.09 x 10^{-4} PaS at 0.5 wt% to 9.23 x 10^{-4} PaS at 2 wt% total tea solids, a difference of 1.14 x 10^{-4} PaS. Whereas, at 50°C the viscosity increased from 5.21 x 10^{-4} at 0.5 wt% to 5.85 x 10^{-4} PaS at 2 wt% total tea solids, a difference of 0.64 x 10^{-4} PaS. As expected, these results demonstrate that both a reduction in temperature and an increase in concentration increased the viscosity of black tea solutions.

Although there was a slight increase in viscosity from 0 wt% tea solids (i.e. pure RO water) to 0.5wt% tea concentration, the viscosity does not increase significantly for all temperatures until reaching 1.25wt%.There was less than 7% difference between pure RO water viscosity and a 1.25 wt% tea solution in all cases and only a 0.7% change at 50°C. There appears to be a more significant step change in viscosity increase from 1.25 – 1.5wt% total tea solids concentration for all temperatures. This change may be due to a critical change in the solution stability resulting in formation of a greater amount of tea cream aggregates. As expected, temperature had a significant effect on viscosity, the viscosity of a 1.0 wt% reconstituted tea solution decreased from 8.16 to 5.15 x 10^{-4} Pa s as the temperature was increased from 25 – 50°C.

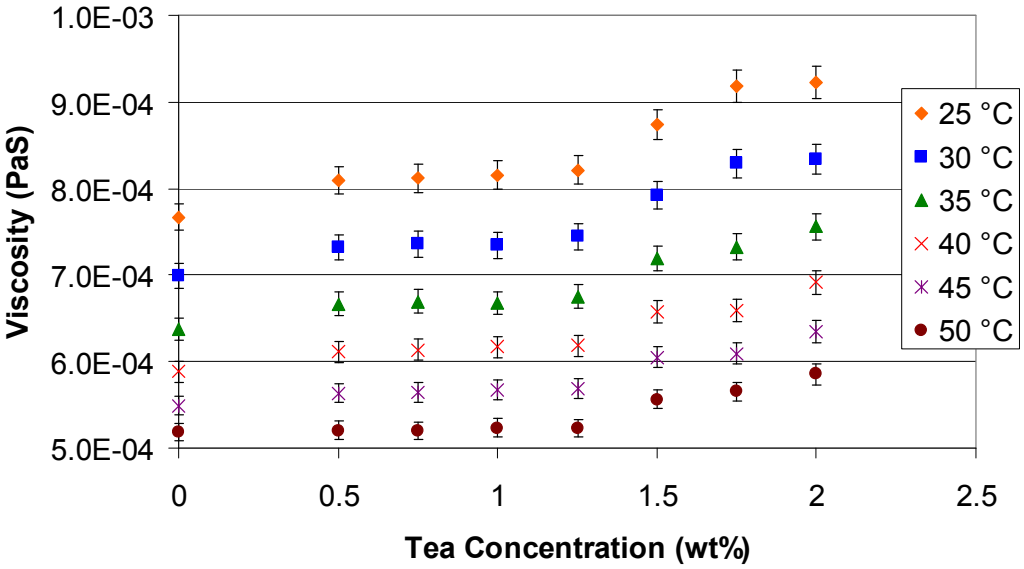

Figure 4.84: Graph to show variation in tea viscosity with concentration and temperature measured at a constant shear stress of 0.2145 Pa

4.6.2 Colour / Haze of tea solutions

4.6.2.1 Concentration

The colour / haze of the tea solutions were analysed based on the UV spectrophotometry as described in 3.5.2 . Figure 4.85 and Figure 4.86 shows how the colour / haze vary with tea reconstitute concentration. All these experiments were performed with tea reconstitute at 35°C.

Figure 4.85 shows the variation of lightness (L*) plotted against tea solution concentration where it can be seen that L* decreases linearly from 89 to 18 for an increase in total tea solids concentration from 0.125 wt% to 0.6 wt%. The tea solution is totally opaque after a total tea solids concentration of 1.5wt% such that L* approaches a minimum of 0. Figure 4.85 also shows the variation in redness (a*) as the total tea solids concentration is varied, a* increases linearly until 0.4wt% (25.0) and then approaches a maximum at 0.5wt% (26.0) before decreasing again. Figure 4.85 shows the variation in yellowness (b*) with increasing tea concentration where b* increases linearly until 0.2wt% (60.0) reaching a maximum at about 0.3wt% (63.0) before decreasing again and approaching a yellowness of 0 at 1.5wt%. Chroma is a measure of colour quality where yellowness and redness are attributed to its derivation such that Chroma = $(a^2+b^2)^{1/2}$. Chroma varies in a very similar way to the yellowness (b*) with a maximum at 0.3wt% of 67.0.

The absorbance of light at a wavelength of 900nm through the tea samples at various concentrations is shown in Figure 4.86. The absorbance increases with total tea solids concentration which demonstrates that haze formation in black tea solution increases significantly as solids concentration is increased. The absorbance of the tea solution was approximately linear as the tea solids concentration increased from 0 to 0.4 wt%. Subsequently with higher tea solids concentration (> 0.4 wt%) the absorbance continued to increase with a higher rate, demonstrating an increased rate of haze formation. Once the tea concentration was over 1.0wt%, less than 20% of light was transmitted through the solution, which suggests that significant macromolecular aggregation is occurring. This explains the observations in Figure 4.85 where redness, yellowness and the chroma parameters reach a maximum at total tea solid concentration values of 0.5, 0.3 and 0.4 wt% respectively. Thus the solution haze was enhanced more significantly after 0.4wt% total tea solids, which caused a decrease in redness, yellowness and the chroma parameters. Based on these results all tea solutions were diluted to 0.2wt% so that analysis is within the linear range of all variables tested.

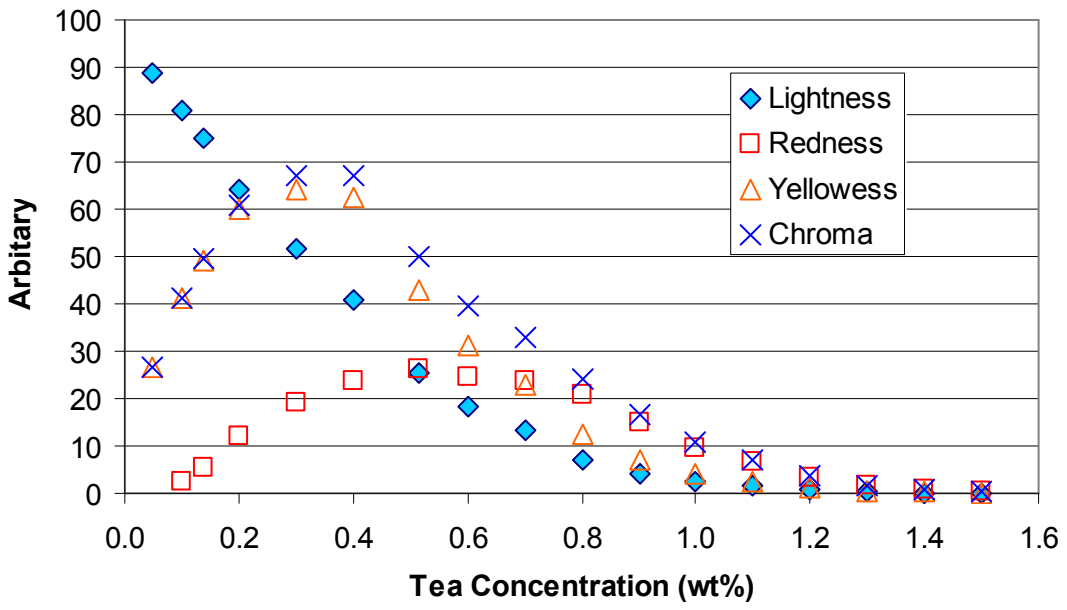

Figure 4.85: Graph to show how the Lightness, (L), redness (a*), yellowness (b*) and Chroma (C*) of a reconstituted black tea solution varies with tea solids concentration.*

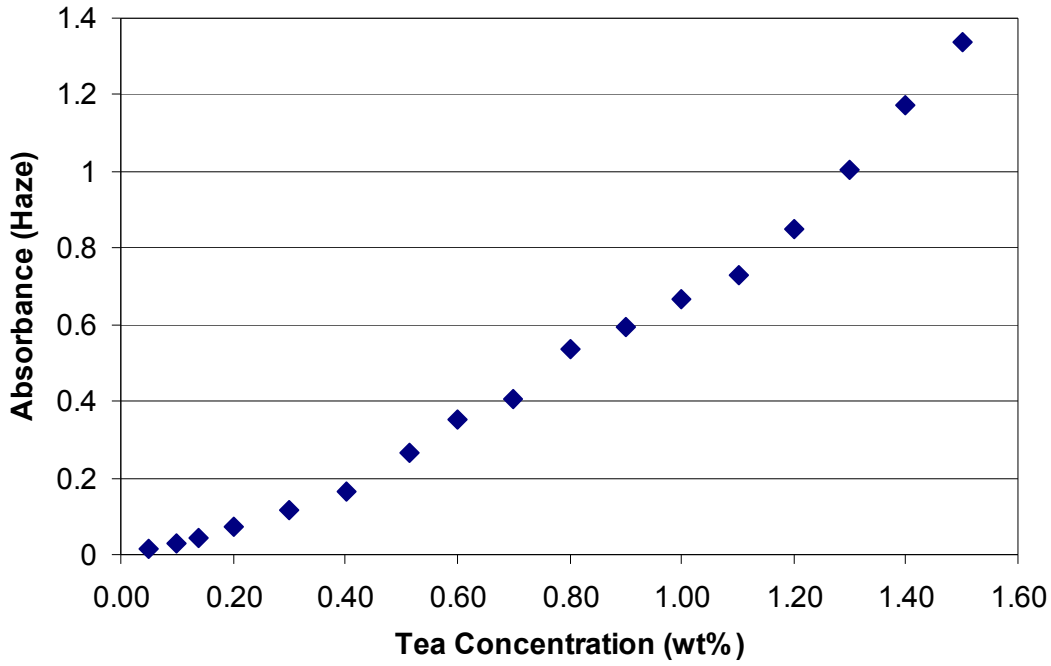

Figure 4.86: Graph to show how the absorbance varies with varied concentration of reconstituted black tea solution

4.6.2.2 Temperature

The colour-haze relationship of tea solutions was investigated based on increasing the temperature from 26°C to 35°C at three different total tea solids concentration (0.25, 0.5, 0.7wt%) as represented in Table 4.6. As can be seen all colour parameters (L* a* b*) are increased with the increase in temperature with the exception of L* for the 0.25wt% solution which decreased very slightly. The changes in these values were much higher for the larger concentration solutions suggesting the importance of concentration and temperature on colour quality of the tea samples. The absorbance decreases as the temperature was increased for all concentration samples demonstrating reduced haze and thus more stable tea solutions. The decrease in haze as temperature increases is more significant at higher concentrations again demonstrating that stability is both temperature and concentration dependent.

0.7wt% Tea Reconstitute					
Storage time	Temperature	L*	a*	b*	Abs
(mins)					900nm
34:00	26	18.96	25.99	32.26	0.314
39:00	35	23.14	28.18	39.32	0.241

0.5wt% Tea Reconstitute					
Time from sampling	Temperature	L*	a*	b*	Abs
					900nm
38:00	26	34.68	26.31	56.58	0.183
46:00	35	36.26	27.03	59.02	0.158

0.25wt% Tea Reconstitute					
Time from sampling	Temperature	L*	a*	b*	Abs
					900nm
42:00	26	59.32	15.04	63.74	0.083
48:00	35	59.22	15.29	64.29	0.078

Table 4.6: Change in colour and haze values at different tea concentrations and temperatures. Analysis performed within 1 hour.

4.6.2.3 Time (Storage)

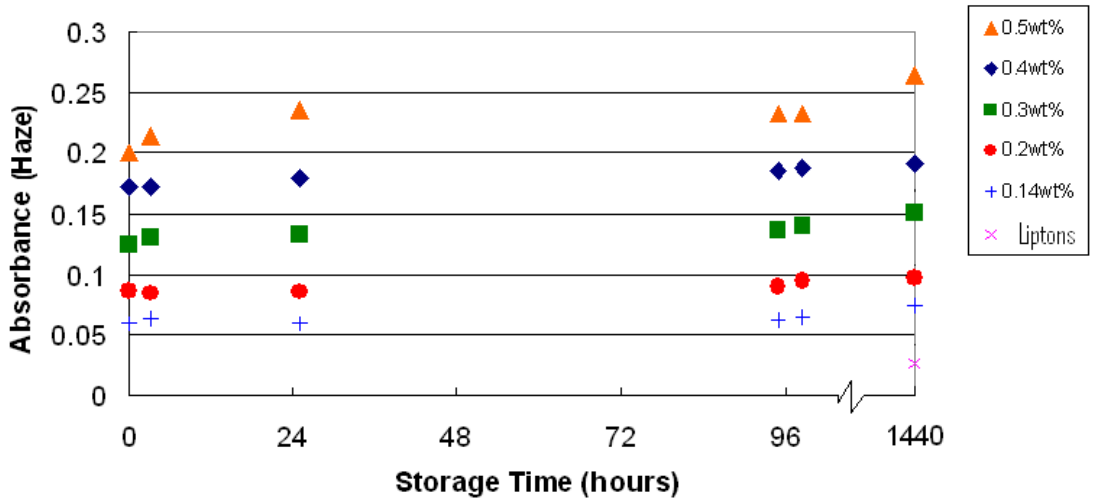

Figure 4.87: Graph to show how the absorbance changes for various concentrations of reconstituted black tea solution (solutions stored at 5°C).

Figure 4.87 shows how the stability (haze measurements) of 0.14 – 0.5 wt% total tea solid concentration black tea solutions were affected over time (60 days) when stored at 5°C which represents similar storage conditions for actual iced tea product. The absorbance and thus haze increase after 60 days were larger for increased tea solids concentration solutions, 0.200 to 0.264 for a 0.5 wt% solution and only 0.059 to 0.075 for the 0.14 wt% solution. This confirms that increased concentration reduces the stability of tea solutions which is enhanced over longer periods of time.

Figure 4.88, 4.87 and 4.88 all show the change in L*, a* and b* respectively when the tea solution was stored at 5°C for 60 days. The lightness of the black tea solutions at various concentrations all decreased over time whereas the redness of all solutions increased. The lightness decrease was due to the increased haze observed during storage (Figure 4.87). The observed increase in redness suggests changes had occurred within the tea solutions during storage. As observed previously, the redness of a black tea solution increased with total solids concentration (Figure 4.85) to a maximum value due to the increased quantities of polyphenols present in tea responsible for this colour. This suggests that during storage of black tea solutions increased polyphenol – polyphenol interactions occur producing a larger proportion of the polyphenols responsible for the red colour of tea solutions. The yellowness of both the 0.1 and 0.2 wt% solution did not change significantly during the 60 days of storage, and concentrations above this up to 0.5wt% show a reduction in yellowness values during storage with an increase in haze the most likely the reason for this.

Comparisons can be made with *Lipton iced tea* (off the shelf) for all these measurements. *Lipton iced tea* final product has been measured and represented in Figure 4.87 to 4.88. As the time of storage is not known, comparisons have been made with 60 days of storage assuming the properties of the treated *Lipton iced tea* does not vary significantly over time. The concentration of *Lipton iced tea* is 0.14 wt% and can be compared with our measurements for 0.14 wt% accordingly. The current *Lipton ice tea* treatment causes a reduction in absorbance (haze) and thus increases in lightness, although the redness and yellowness (key tea quality indicators-section 2.1.2.5) are significantly reduced as a consequence.

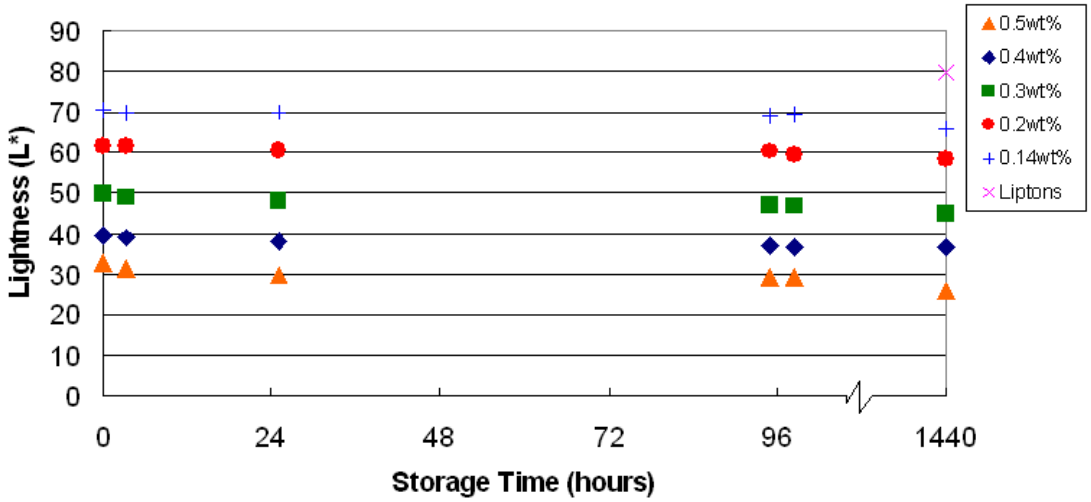

Figure 4.88: Graph to show how the Lightness (L) changes for various concentrations of reconstituted black tea solution (solutions stored at 5°C).*

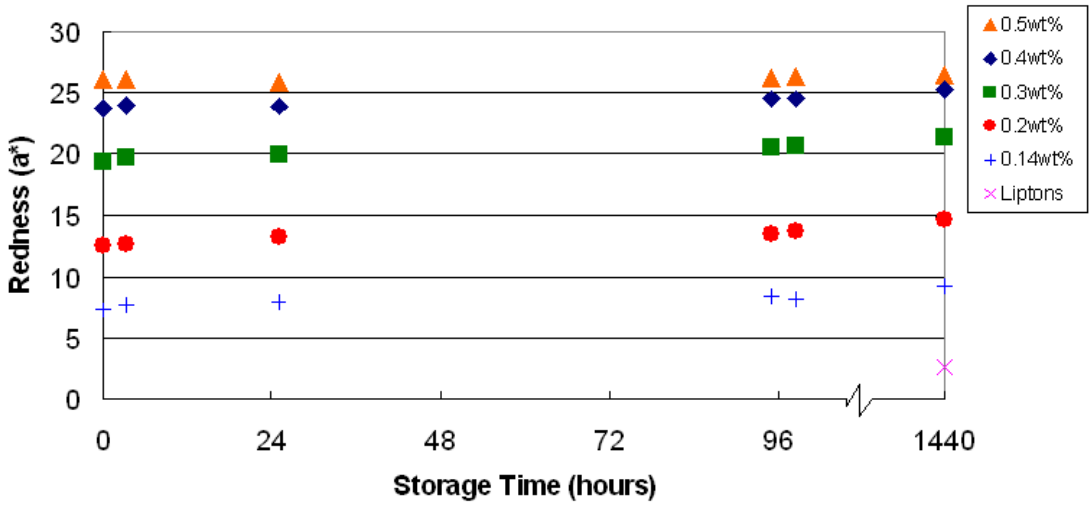

Figure 4.89: Graph to show how the Redness (a) changes for various concentrations of reconstituted black tea solution (solutions stored at 5°C).*

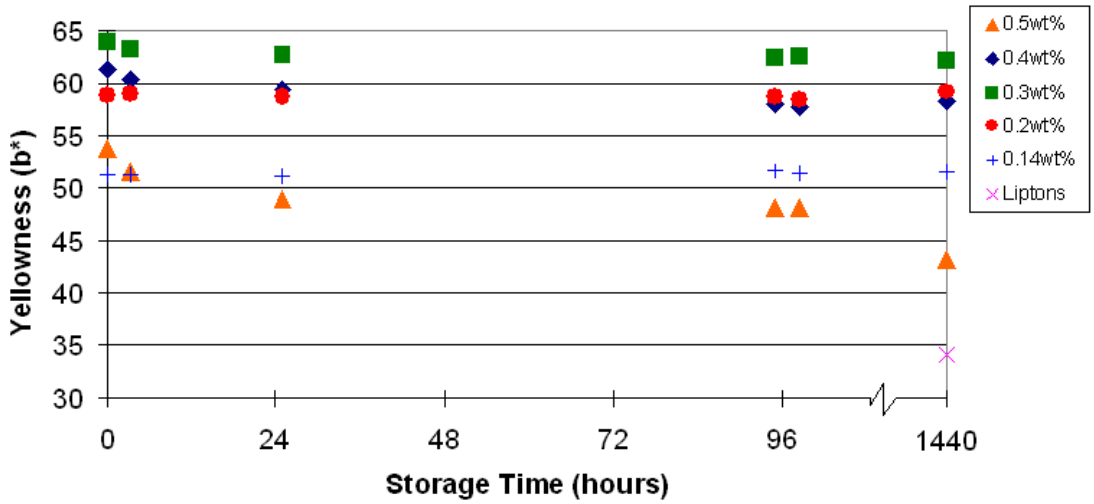

Figure 4.90: Graph to show how the Yellowness (b) changes for various concentrations of reconstituted black tea solution (solutions stored at 5°C).*

4.7 Will Ultrafiltration of black tea extract increase stability and quality of the final product?

4.7.1 Colour / Haze

Figure 4.91 shows the initial absorbance of permeate produced during black tea filtration using the 30kDa fluoropolymer membrane compared with the absorbance after 22 days of storage at 5°C. The permeate produced had a total tea solids concentration of 0.62 wt%, initially the absorbance was only 0.004 whereas a reconstituted original tea solution of the same concentration had an absorbance of 0.27. This demonstrates that the haze was significantly reduced by fluoropolymer ultrafiltration and after 22 days of storage the permeate absorbance did increase by 0.004 to 0.008 whereas the reconstituted original sample of the same concentration increased considerably by 0.032. to 0.302.

Figure 4.93 shows the initial absorbance of permeate produced during black tea filtration using 30kDa regenerated cellulose membranes compared with the absorbance after 22 days of storage at 5°C. The permeate produced had a total tea solids concentration of 0.54 wt%, initially the absorbance was only -0.001 whereas a reconstituted original tea solution of the same concentration had an absorbance of 0.222. This demonstrates that the haze was significantly reduced by regenerated cellulose ultrafiltration and after 22 days of storage the permeate absorbance did increase by 0.002 whereas the reconstituted original sample of the same concentration increased considerably by 0.050.

Diluting the FP permeate to 0.2wt% and comparing with untreated tea solution of 0.2wt% meant lightness was increased from 65 to 85, redness was reduced from 12 to 2 and the yellowness from 61.5 to 51.5 (Figure 4.92). The RC permeate diluted to 0.2wt% and comparing with untreated tea solution of 0.2wt% meant lightness was increased from 90, redness was reduced 0.1 and the yellowness to 44 (Figure 4.94). The redness and yellowness are indicative of the quality of the tea solution as discussed in section 2.1.2.5 . A reduction in redness and yellowness of the clarified permeate suggests a reduction in the polyphenols responsible for these colours.

When stored at 5°C a 0.2wt% solution had an absorbance of 0.067 compared to the treated solutions by UF using FP and RC membranes diluted to 0.2wt%, reduced to absorbance's of 0.002 (Figure 4.91) and 0.001 (Figure 4.93) respectively. These measurements were compared with *Lipton iced tea* off the shelf which has been treated using Unilever's current practice as discussed in section 2.1.4 . The concentration of Lipton's iced tea is 0.14wt% (lower than our samples) but had an absorbance of 0.025 which is higher than the clarified liquors using FP and RC membrane UF.

For both membrane processes the clarified products (diluted to 0.2wt%) showed an increase in redness and yellowness when stored for 20 days at 5°C and a slight reduction in lightness. Comparing with the measurements for *Lipton iced tea* for both membranes the lightness and yellowness of the clarified liquor was higher demonstrating a clearer yellow solution. The permeate from the FP membrane demonstrated an increase in redness compared tothat of Lipton's iced tea whereas the permeate from the RC membrane showed lower redness (Figure 4.92 and Figure 4.94). Optimising the concentration of the clarified permeate solutions would give desired visual properties based on the required colour, and a decreased haze in the final product as demonstrated in Figures 4.89 - 91 for variations in concentration. This would lead to an increased total tea solids concentration in the final iced tea (RTD) product.

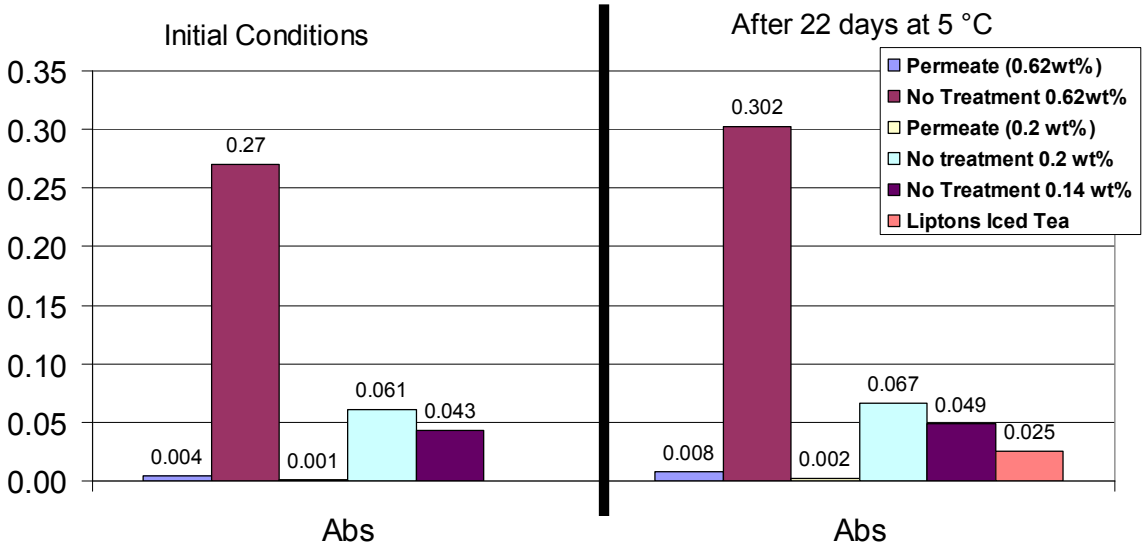

Figure 4.91: Graph to show effect of ultrafiltration using 30kDa fluoropolymer membranes on stability of final product for clarification of 1wt% total tea solids black tea solution at 50°C.

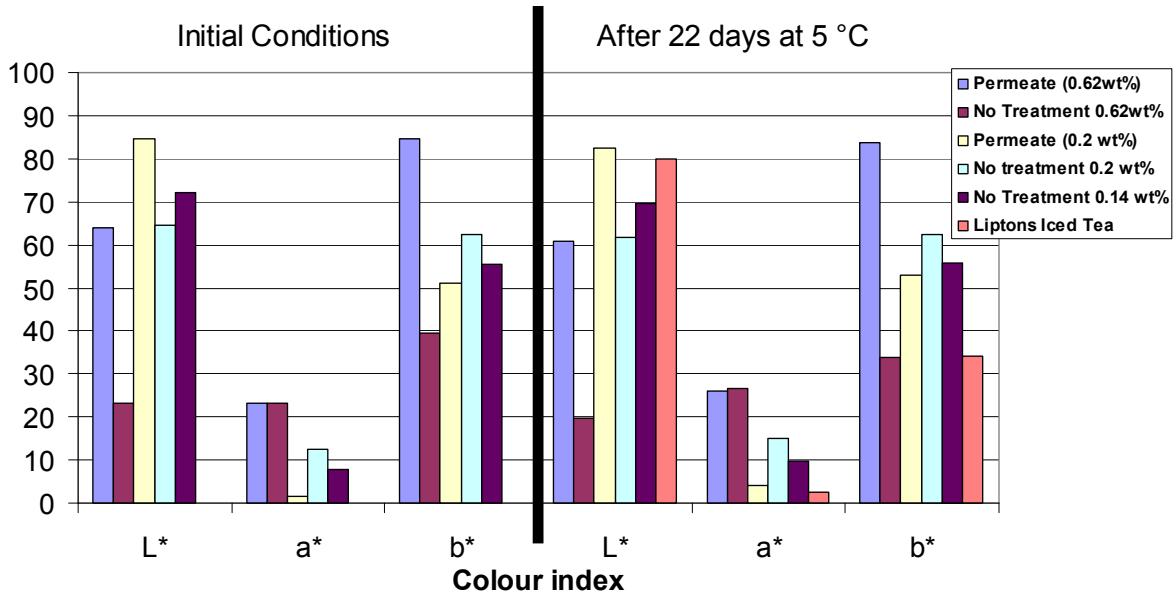

Figure 4.92: Graph to show effect of ultrafiltration using 30kDa fluoropolymer membranes on the colour of final product for clarification of 1wt% total tea solids black tea solution at 50°C.

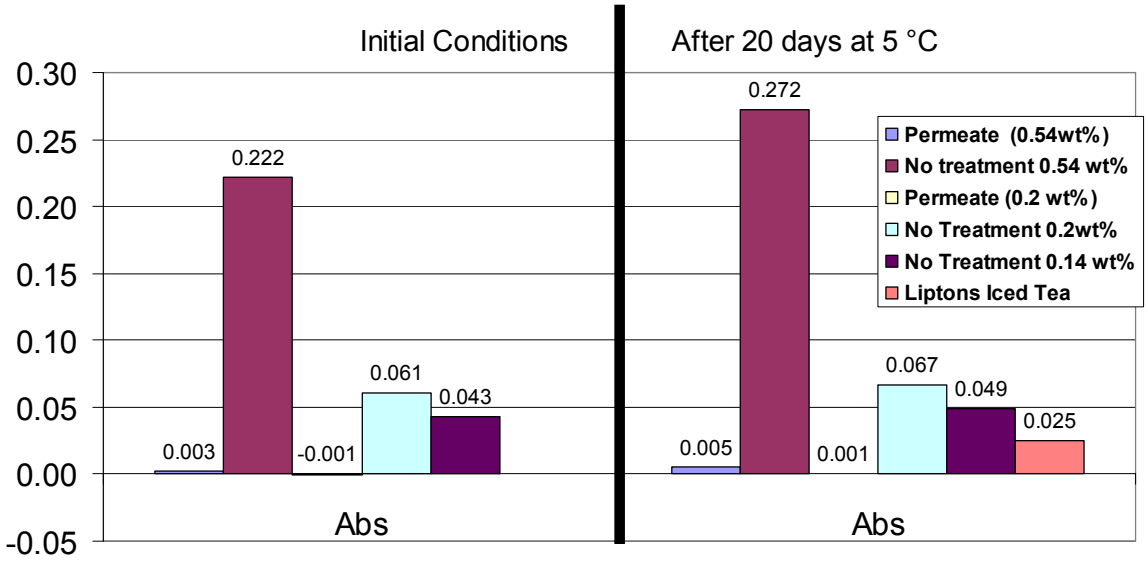

Figure 4.93:Graph to show effect of ultrafiltration using 30kDa regenerated cellulose membranes on stability of final product for clarification of 1wt% total tea solids black tea solution at 50°C.

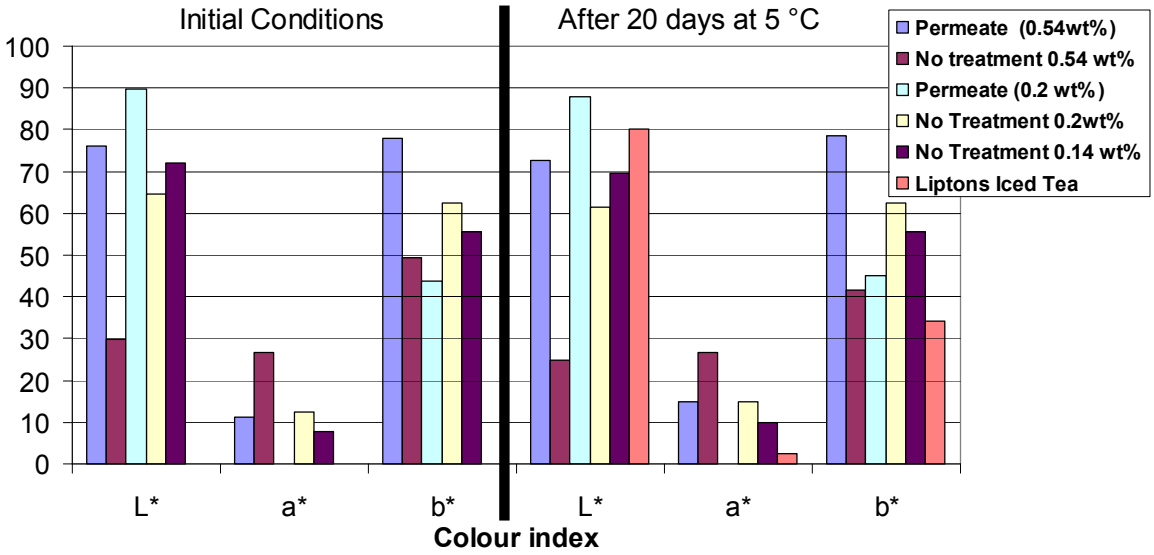

Figure 4.94: Graph to show effect of ultrafiltration using 30kDa regenerated cellulose membranes on the colour of final product for clarification of 1wt% total tea solids black tea solution at 50°C

4.7.2 Particle Sizing

Figure 4.95 and Figure 4.96 show the particle size of the feed and retentate for the fluoropolymer and regenerated cellulose membrane UF respectively for the clarification of a 1wt% black tea liquor. The particle size distribution measurements were performed using a Malvern mastersizer as described in section 3.5.7.1 . The initial black tea solution feed had a very broad particle size distribution of 0.5 - 120 µm. Following 1 min of filtration the FP and RC membrane had little effect on the retentate and the RC membrane showed a very slight narrowing of particle size distribution. The particle size of the retentate after 60mins of UF for both membranes narrowed significantly (0.5 - 60µm) such that the larger particles were removed. The reasons for this could be two-fold:

(i) The larger aggregates could have adsorbed to the membrane surface

(ii) Mixing caused by the gear pump lead to the break up of the larger aggregates.

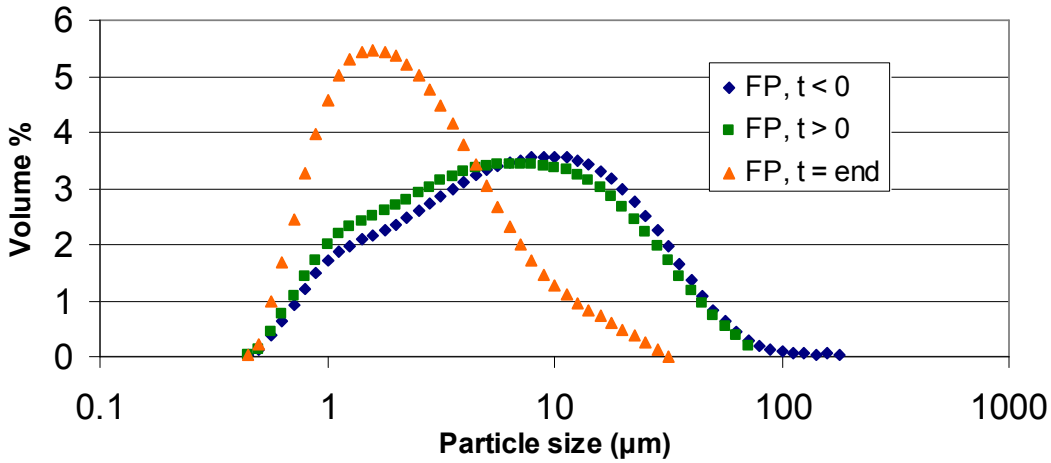

Figure 4.95: Particle size distribution of the feed / retentate 1.0wt% black tea solution ultrafiltered using 30 kDa fluoropolymer membrane.

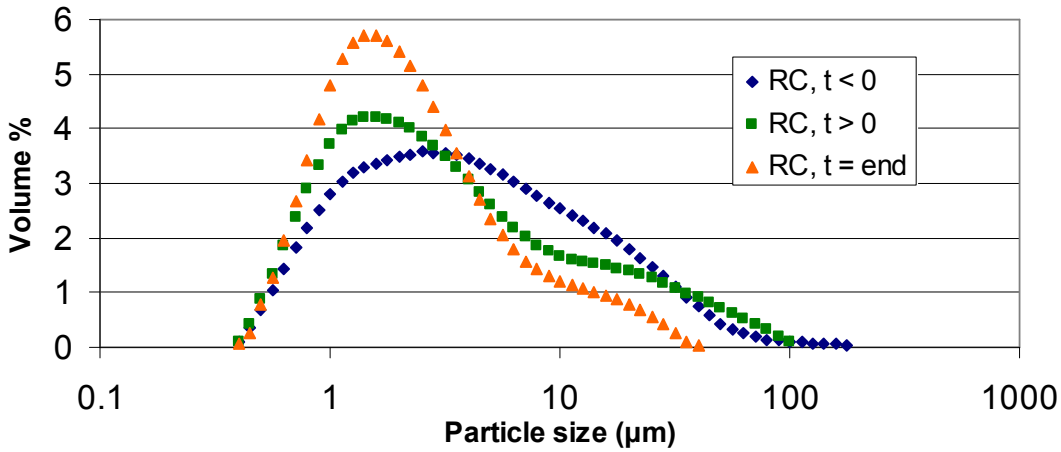

Figure 4.96: Particle size distribution of the feed / retentate 1.0wt% black tea solution ultrafiltered using 30 kDa regenerated cellulose membrane.

No particles were detected in the permeate using the mastersizer. Subsequently the zeta sizer was used where (method described in section 3.5.7.2). Initially no particles were detected 2 hours after both FP and RC membrane clarification. However after 20 hours of storage at 5°C formation of some particles and thus haze had occurred. Figure 4.100 shows the permeate produced using the RC membrane. Figure 4.97, 4.96 and 4.97 show the particle size distribution of the permeate from the FP membrane after 8, 20 and 30 hours of storage respectively. Initially no particles were detected up to 2 hours after clarification, however, after 8 hours of storage particles were formed in the range 100 – 500nm. After further storage of up to 20 hours the particle size distribution increased from 100 – 600nm and after 30 hours of storage the particle size distribution significantly increased from 150nm – 1500nm. These particulates are most likely formed from polyphenol – polyphenol interactions potentially also involving caffeine and must account for the small amount of haze observed as discussed in section 2.2 .

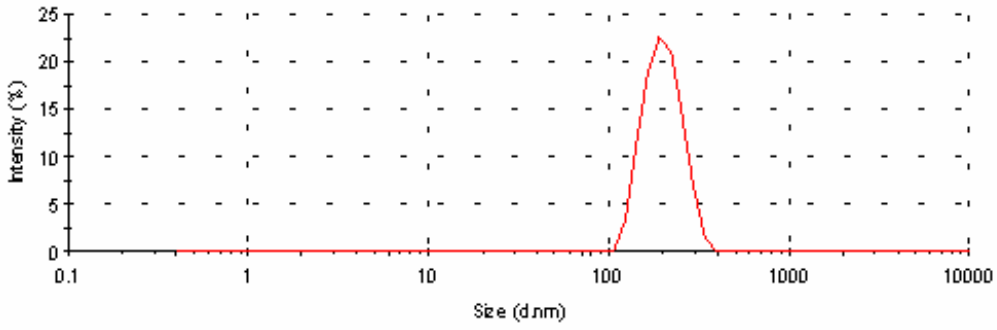

Figure 4.97: Particle size distribution of the fluoropolymer permeate after 8 hours storage for a 1.0wt% black tea solution ultrafiltered using 30 kDa fluoropolymer membrane at 1.0 bar transmembrane pressure .

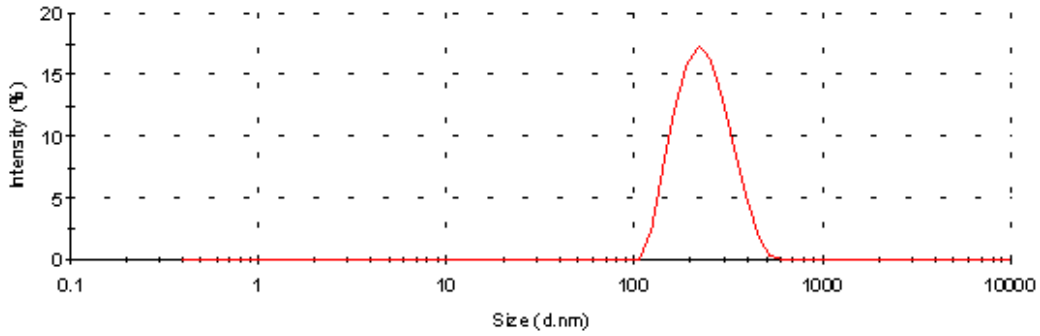

Figure 4.98: Particle size distribution of the fluoropolymer permeate after 20 hours storage for a 1.0wt% black tea solution ultrafiltered using 30 kDa fluoropolymer membrane at 1.0 bar transmembrane pressure.

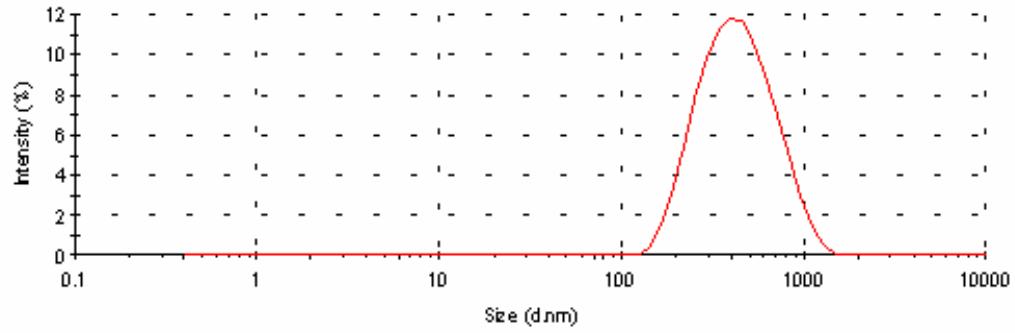

Figure 4.99: Particle size distribution of the fluoropolymer permeate after 30 hours storage for a 1.0wt% black tea solution ultrafiltered using 30 kDa fluoropolymer membrane at 1.0 bar transmembrane pressure .

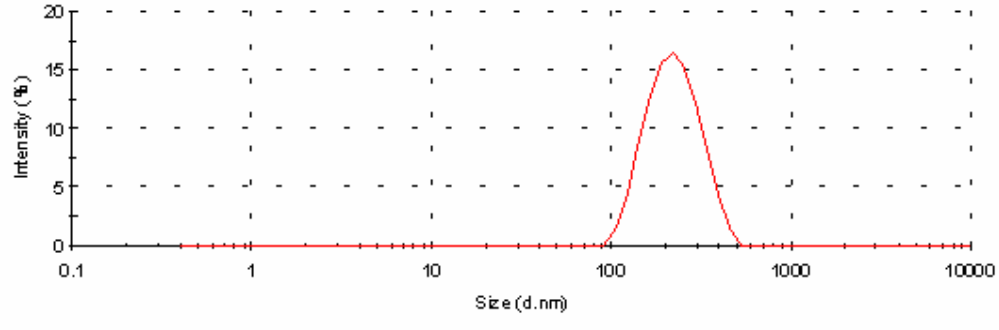

Figure 4.100: Particle size distribution of the regenerated cellulose permeate after 20 hours storage for a 1.0wt% black tea solution ultrafiltered using 30 kDa regenerated cellulose membrane at 1.0 bar transmembrane pressure .

Chapter 5 Conclusions and Recommendations

5.1 Conclusions

The research performed in this study concerned the use of ultrafiltration as a clarification technique for the processing of black tea liquors for ready-to-drink final products. Ultrafiltration produced black tea solutions of significantly increased stability (reduced haze) with realistic operating fluxes. This study focused on characterisation and therefore understanding of foulant – membrane – cleaning agent interactions which will help with future optimisation procedures for black tea ultrafiltration and also other protein / polyphenol containing beverages. This study has examined mainly the performance of two ultrafiltration membrane materials, namely, fluoropolymer and regenerated cellulose for the clarification of black tea liquor. The detailed results represented in chapter 4 are summarized below.

5.1.1 Tea filtration (Fouling) Conditions

5.1.1.1 Concentration

The influence of black tea feed concentration and temperature were investigated for two different membrane materials, FP and RC. Generally, the RC membrane demonstrated a reduced foulant – membrane interaction and thus a reduced overall deposit formation when compared to the FP membrane. However, as a consequence, the membrane selectivity was increased for the RC membrane and mass transfer reduced due to an increased concentration of feed close to the membrane surface.

The importance of feed condition upon filtration performance due to variations in fouling mechanism and cleaning efficiency has been demonstrated.

Concentration polarisation contributes predominantly for the conditions examined, increasing the total resistance of both membranes as the feed concentration was increased. Increasing the feed concentration had no extra effect on deposit formation on the RC membrane, whereas rinsable fouling deposit did increase on the FP membrane surface with increased feed concentration. This suggests that there was a somewhat stronger interaction of fouling species with the FP membrane than with the RC membrane.

Total fouling resistance and membrane rejection were increased upon cooling of the black tea feed. Lower temperature feeds reduced irreversible fouling while increased rinsable fouling and concentration polarisation, suggesting that enhanced aggregation (tea creaming) decreased foulant – membrane interactions.

Preliminary investigations regarding the influence of feed ionic strength and calcium ion content upon filtration performance were investigated. Increasing the ionic strength of the tea solution increased the total fouling resistance (R_F) thus reducing performance, while decreasing the severity of deposition fouling due to an increased concentration polarisation. Addition of calcium to the feed stream (which is known to increase aggregation and creaming within the black tea system) caused a significant increase in irreversible fouling deposition. This could not be removed effectively either by the standard sodium hydroxide cleaning regime adopted, or by the use of a formulated agent in the concentration range studied.

5.1.1.2 Transmembrane pressure (TMP)

Fouling TMP was varied through different cycles on the same membrane, fresh virgin conditioned membranes, and during a single fouling cycle (pressure stepping). The effect of multiple fouling / cleaning cycles was also investigated at constant conditions to understand the significance of repeated cycles on the same membrane.

(i) TMP variation on same membrane

The effect of fouling TMP was investigated on the same FP and RC membranes.

At 1.0 bar TMP and 30 minutes of fouling, the FP and RC membranes had steady state fluxes of 23.0 and 32.1 LMH respectively, rejecting 21% and 27% of tea solids respectively. For both membranes examined, the permeate lightness and yellowness were increased and the haze was significantly reduced. The redness of the FP permeate was also increased.

Initially at 1.0 bar TMP, the FP membrane had a lower steady state flux and a lower rejection of tea solids when compared to the RC membrane. Concentration polarisation was responsible for significantly more of the RC membrane resistance at these initial conditions than for the FP membrane.

Rejection was found to increase for both membranes as the TMP increased.

The RC membrane showed higher total solids rejection ratios than the FP membrane at the same TMP.

The RC membrane had reached a limiting flux by 1.0 bar TMP and the FP membrane appeared to be approaching a limiting flux at 4.0 bar TMP.

The RC membrane resistance was very stable as TMP was increased from cycle to cycle, increasing by approximately 10% from virgin membrane conditions. Multiple operational cycles produced a clean RC membrane that had a similar hydrophilicity to that of a virgin RC membrane.

The cleaned FP membrane resistance was reduced as the membrane was fouled at higher TMP values and the membrane surface became more hydrophilic. However, the membrane's solids rejection ratio and the L*, a* and b* values of the permeate did not change over multiple cycles.

The experimental findings reported here are industrially relevant as they indicate that moderately hydrophobic membranes, with their advantages of chemical and thermal stability, maybe modified by selective adsorption of hydrophilic tea species to give fluxes similar to those seen with more hydrophilic materials. There may therefore be a distinct processing advantage in using moderately hydrophobic polymeric membranes over highly hydrophilic materials for the filtration of tea liquors.

(ii) TMP variation on individual membranes

Increasing the TMP from 1.0 to 4.0 bar with the FP membrane increased the steady state flux from 22 LMH to 25 LMH using fresh conditioned virgin membranes for each TMP. The RC membrane demonstrated a limiting flux, such that increasing the TMP from 1 to 3 bar TMP maintained a flux of 24 LMH for each TMP.

The FP membrane rejected less tea solids (0.31) compared to the RC membrane (0.35) at 1.0 bar TMP. Increasing the TMP of the FP / RC membrane to 4.0 / 3.0 bar significantly increases the membrane rejection to 0.47 and 0.45 respectively.

Although the total tea solids transmission decreased upon increasing the operating TMP, the relative amount of the important theaflavins and caffeine in the clarified tea solids increased.

The RC membrane demonstrated no additional fouling by increasing the operating TMP. Both RC membrane surfaces after fouling (1.0 / 3.0 bar) and cleaning demonstrated no permanent modification to the surface and thus a cleaning protocol that returned pristine membrane surface equal to the virgin conditioned surface.

The FP membrane demonstrated over twice the fouling deposit during 4.0 bar fouling compared to 1.0 bar fouling based on fouling resistance measurements, confirming enhanced fouling at elevated TMP. Both FP membrane surfaces after fouling and cleaning demonstrated a permanent modification to the surface. Either the membrane was not adequately cleaned of tea constituents or was modified during the NaOH cleaning process.

(iii) Multiple fouling / cleaning cycles

Multiple fouling / cleaning cycles were performed using the 30kDa FP membrane, the black tea fouling flux and total tea solids rejection varied insignificantly over the 17 cycles examined. The pure water fluxes after cleaning increased initially for the first few cycles, and then decreased to 91% of the initial virgin membrane flux by cycle 17.

Negatively charged foulant adhered to the virgin conditioned membrane pore wall surface during the black tea filtration run. Subsequently, cleaning of the fouled surface reduced the negative charge such that it lay between the virgin membrane and the fouled membrane. This suggests that either the NaOH cleaning solution was not completely removing the tea foulant from the pore walls or the NaOH was completely removing the foulant and then modifying the membrane polymer. Multiple fouling and cleaning cycles modified the pore wall charge differently to a single cycle such that the surface on the pore walls were less negative when fouled and had a shallower gradient of charge after fouling and cleaning.

(iv) Pressure stepping

A lower transmission of polyphenols occurred during TMP ramping suggesting that increased concentration polarisation was increasing the selectivity of the membrane. Increased concentration at the membrane surface then caused increased adsorption and formation of a cake layer. During high TMP / high concentration polarisation periods the tea constituents (polyphenols / caffeine / proteins) were in a higher concentration environment, consequently increased interactions causing increased aggregation. This phenomenon would enhance tea constituent precipitation and thus adsorption and / or build up of solute at the membrane surface. During the pressure

relaxing period, fouling flux, total tea solids and polyphenolic transmission were lower than those recorded at equal TMP during pressure ramping period. This variation demonstrates that the formation of the cake layer caused a secondary boundary to the membrane which increased the membrane selectivity.

5.1.2 Membrane Cleaning

The optimum cleaning conditions were found to be: 0.5wt% NaOH, 60°C feed temperature, 0.5bar TMP and 1.15ms^{-1} CFV for the FP membrane. All conditions were found to affect membrane flux recovery after each cycle although TMP and NaOH concentration were found to be the most significant in terms of product fouling fluxes and product solids transmission of tea solutions. Note a maximum temperature of 60°C was used in further experiments due to the difficulty of operating at 65°C.

The regenerated cellulose membrane has strict operational pH and temperature limits due to the physical nature of the membrane. Within the current study, cleaning was only optimised based on CFV, all other conditions were maintained constant. The NaOH concentration of 0.01wt% was used to maintain the cleaning pH within operational limits and a slightly lower temperature (45°C) reducing any potential membrane damage. No significant variation in product flux or total tea solids membrane rejection were found with variation in cleaning CFV although turbulent (1.15ms^{-1}) CFV is recommended to ensure maximum removal of any cake layers present.

5.1.3 Surface properties

Black tea clarification was also investigated using the same two ultrafiltration membrane materials, namely regenerated cellulose and fluoropolymer with three different nominal molar mass cut-offs (10, 30 and 100 kg mol^{-1}). Ultrafiltration produced a clarified black ready to drink tea beverage with an increased stability and a significantly reduced haze for all membrane materials tested.

The FP membranes generally showed lower fouling fluxes than the RC membranes, FP10 the lowest steady state flux of 14 LMH (litres m^{-2} h^{-1}) and RC100 the highest of 32 LMH. FP30 provided the highest total tea solids transmission of 73% while FP10 (65%) and FP100 (62.5%) gave the lowest solids transmission of all FP membranes. The RC membranes all gave similar solids transmissions of 69 – 73%. All the RC

membranes and the FP30 membrane performed such that around 90% and 100% of the important total polyphenols and more specifically, total theaflavins were transferred into the permeate respectively. The FP10 membrane gave the lowest transmission of total polyphenols (78%) and also theaflavins (62%). All membranes produced permeates with a higher relative concentration of caffeine than the initial feed solution, 118 – 142% transmission.

These results demonstrate that flux and defined molar mass cut-off are not adequate by themselves to decide upon membrane choice for filtration. Surface science parameters are important to the filtration properties and fouling and cleaning mechanisms.

Increased deposition (FTIR) and increased negative charge (ZP) on the FP membranes caused higher fouling rates (k_J) resulting in lower fouling fluxes. The deposits and negative charge were observed such that FP30 > FP10 > FP100 which corresponds to the increased roughness (R_a) of the FP membranes, FP30 (59 nm), FP10 (27 nm) and FP100 (11 nm). The foulant appears to be more significantly entrapped by rougher surfaces.

The FP membranes were also significantly rougher (R_a) than the RC membranes (3nm) demonstrating why the RC membranes had less deposit and negative charge than the FP membranes. The amount of deposit on the FP membranes corresponds to the hydrophobicity of the surfaces such that FP30 is most hydrophobic and FP100 is the least hydrophobic. This suggests that the foulant – membrane interactions are hydrophobic in nature.

The virgin FP30 membrane displayed an isoelectric point at pH 4.5, the same as that recorded for the tea used in this study. At this pH value, the FP10 membrane had a slightly positive charge and the FP100 displayed a slightly negative charge. Increased solids, polyphenolic, theaflavins and caffeine transmission were apparent through the FP30 membrane. This suggests that the negatively charged molecules (based on negative charge in pores of all fouled membranes) would theoretically pass through FP30 easiest whilst an interaction or repulsion would be more likely with the FP10 and FP100 membranes.

Cake filtration was confirmed as a fouling mechanism for all membranes used in this study. Due to similar surface charge properties, formation of a cake layer might dominate filtration with all RC membranes which was apparent due to similar solids, polyphenolic, theaflavins and caffeine transmissions.

FP100 and RC membranes all had comparatively low negative ZP values which did not vary significantly with varying pH, i.e the membranes did not accept a lot of negative or positive charge. Subsequently all membranes recovered initial PWF values, ZP profiles and chemical nature (as detected by FTIR) after a fouling / cleaning cycle. Generally all the RC membranes demonstrated high fouling fluxes with the least fouling. This might indicate that over longer fouling runs the performance of RC membranes might be superior to the FP membranes which demonstrated increased fouling.

FP10 and FP30 membranes had a negative charge following fouling then cleaning or cleaning of the virgin membrane. This charge was between that of the virgin surface and that of the fouled membrane. This suggests that the action of NaOH cleaning increased the negative charge of the fluoropolymer within the pores primarily, although modification due to foulant interaction cannot be disregarded. It seems most likely that the cleaning solution is removing the majority of the foulant thus reducing the negative charge, and then modifying the fluoropolymer increasing the negative charge within the pores, possibly by adsorption of hydroxyl ions.

There were no significant changes in fouling flux through the FP30 membrane during the second cycle or after initial cleaning. Although FP10 and FP30 demonstrated increases in PWF values following fouling and/or cleaning, the FP100 and all of the RC membranes tested showed no significant variation in PWF through successive fouling & cleaning cycles.

5.1.4 Polyphenol – membrane force measurements

AFM force interaction measurements have been used to investigate the interaction of a model polyphenol present in tea (theaflavin-3-gallate) with a regenerated cellulose ultrafiltration membrane. This study has investigated the influence of multiple (200x) measurements of force curves at different points on the membrane surface. Approach force data to the membrane surface has been analysed in addition to adhesion force measurements that are more usually reported.

The results demonstrate the usefulness of this technique for understanding foulant – membrane – cleaning agent interactions at different stages during a fouling / cleaning cycle. The average adhesion forces of the foulant to the virgin and the F1C1

membrane surface were larger than those seen for the foulant – foulant interactions. Sodium hydroxide cleaning of the virgin conditioned membrane reduced foulant – membrane adhesion compared to that seen for the virgin or F1C1 surface. The uniform narrow distribution of attraction (approach) forces to the fouled and cleaned surfaces helps explain this due to uniformly charged foulant / hydroxyl ions adhered to these membrane surfaces whereas the virgin membrane distribution was very wide demonstrating no charge modification on this surface.
This technique aids understanding of the nature of membrane fouling and cleaning mechanisms.

5.1.5 Physical properties of black tea

5.1.5.1 Untreated black tea

Black tea solution viscosity increases with total tea solids concentration where a more significant step change was observed at 1.5 wt%. Increasing the temperature reduces the viscosity. All the colour parameters, L*, a* and b* increase linearly from 0wt% to 0.2 wt% tea solids, after this concentration, L* become non-linear at 0.6wt%, a* and b* reached a maximum at 0.3wt% and 0.2wt% respectively.

5.1.5.2 Capability of ultrafiltration for black tea clarification

The black ready – to – drink product can be stored for a period of time under fridge conditions (< 5°C). This will effect the nature of the black tea product and it's stability over this period becomes significantly important. For both membrane materials studied the clarified products showed an increase in redness and yellowness when stored for 20 days at 5°C and a slight reduction in lightness. Comparing with the measurements for *Lipton ice tea* for both membranes the lightness and yellowness of the clarified liquor was higher demonstrating a clearer yellow solution. The permeate from the FP membrane demonstrated a redder solution than that of *Lipton's ice tea* whereas the permeate from the RC membrane showed lower redness. Optimising the concentration of the clarified permeate solutions would give desired visual properties based on required colour and reduced haze in the final product for variations in concentration. This would lead to increased total tea solids concentration in the final iced tea (RTD) product. These observations are based on

visual properties and taste must be investigated next, a tea tasting panel would be required for this.

The permeates produced from FP and RC ultrafiltration initially contained little physical haze and measured particulates using a zeta sizer, although after 8 hours particulates were formed in the FP permeate and 20 hours in the RC permeate. These particulates are most likely formed from polyphenol – polyphenol interactions, also involving caffeine and must account for the small amount of haze observed.

5.1.5.3 Overview

Ultrafiltration technology has been successfully demonstrated in ready to drink (RTD) tea processing to yield beverages with reduced levels of haze at commercially viable fluxes. Subsequently the fouling mechanisms have been analysed based on physical and chemical interaction between tea foulant components and different membrane material surfaces. Membrane transport has also been modelled based on flux decline curves confirming the domination of cake filtration fouling mechanisms during black tea ultrafiltration. The application of an atomic fore microscope technique has been suggested and proven a valuable future tool to evaluate individual foulant – membrane force interactions. Optimisation of cleaning conditions have also been investigated to regenerate the ultrafiltration membranes. Numerous techniques to evaluate membrane cleanliness have been utilised to interpret maximum removal of foulant from the membrane surface producing advantageous conditions for multiple fouling and cleaning cycles.

5.2 Recommendations for future work

The work produced in this three year study has demonstrated that flat sheet plate and frame ultrafiltration produces clarified black tea liquor for ready-to-drink purposes. A significant investigation into the mechanisms involved in both fouling and cleaning of fluoropolymer and regenerated cellulose organic membranes have been performed.

For the long term, it would be interesting to investigate aspects relevant for industrial implementation such as scaling up and different module configurations. The plate and frame set up used in this study works very well, although investigations into a tubular system might demonstrate advantages given the turbulent cross-flow possibilities. Capital and running costs would then be a critical factor for this part of the work and upon definite implementation of the process, environmental issues must be evaluated. This will involve considerable amount of investigative and analytical work.

Although a certain amount of work has been investigated regarding the influence of ultrafiltration upon the black tea quality in the final ready-to-drink product, examination into the quality of tea taste would be of considerable value. Use of a qualified tea tasting panel would be required for this aspect of the work.

Tea is a natural product which varies depending on variety and growing conditions. An investigation into how each component separately affects the filtration process would be invaluable. Following this systematic examination into binary and more complicated systems would help understand the intricate nature of fouling and cleaning of individual components. Some very interesting work has already been performed on this by Wu and Bird 2007 for dead end systems, advancement for cross flow ultrafiltration would be of importance.

A great deal of work has already been performed in this study on the surface interactions of foulants and cleaning agents with the membrane surface. Analyses of the hydrophobicity, charge within the pores (Streaming potential) and chemical nature (FTIR) have already been investigated for fouling and cleaning cycles. Also specific

foulant (TF3'G) - membrane force measurements have been performed throughout a full fouling and cleaning cycle on one particular membrane using atomic force microscopy (AFM). These novel measurements were performed towards the end of the study. Further work is required for different tea foulant compounds and different membrane surfaces.

Another possible method for measuring the adhesion and removal of species from the membrane surface is the surface plasmon resonance (SPR) technique.
SPR is a phenomenon which occurs when light is reflected from thin metal films (usually silver or gold). A fraction of the light energy incident at a sharply defined angle can interact with the delocalised electrons in the metal film (plasmon) thus reducing the reflected light intensity. The precise angle of incidence at which this occurs is determined by a number of factors, the principal determinant becomes the refractive index close to the *backside* of the metal film, to which target molecules are immobilised. The interaction partner is then passed over the immobilised molecules. If binding occurs to the immobilised target the local refractive index changes, leading to a change in SPR angle, which can be monitored in real-time by detecting changes in the intensity of the reflected light, represented in Figure5.1. The size of the change in SPR signal is directly proportional to the mass being immobilised and can thus be interpreted crudely in terms of the stoichiometry of the interaction. Signals are easily obtained from sub-microgram quantities of material. (www.astbury.leeds.ac.uk/facil/SPR/spr_intro2004.htm)

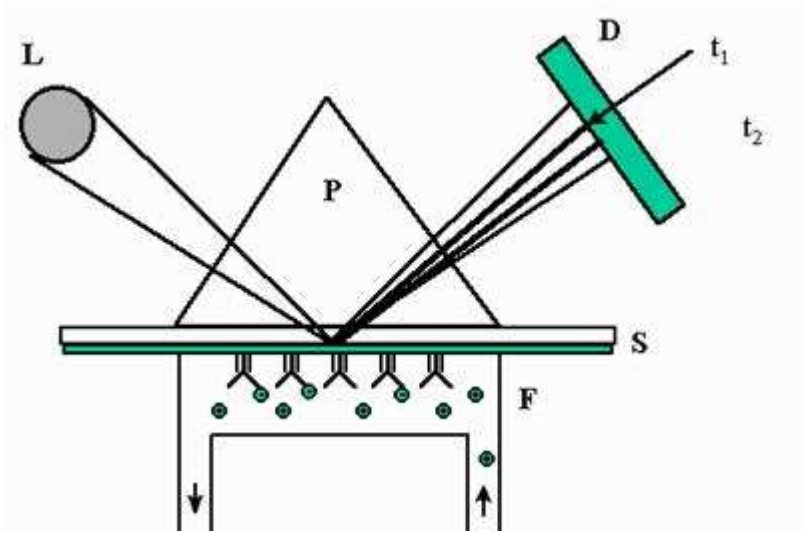

Figure5.1 SPR detection unit.
*(*www.astbury.leeds.ac.uk/facil/SPR/spr_intro2004.htm*)*

Where,

L - light source

D - photodiode array,

P - prism,

S - sensor surface,

F - flow cell.

The two dark lines in the reflected beam projected on to the detector symbolise the light intensity drop following the resonance phenomenon at time = t1 and t2. The line projected at t1 corresponds to the situation before binding of antigens to the antibodies on the surface and t2 is the position of resonance after binding.

Some preliminary work was performed on this technique during the current project. The aim was to immobilise the membrane polymer on the sensor surface and then pass tea solution and model foulants over the polymer surface. Simply placing the whole membrane or the active layer was not possible as this was too thick for any analysis to be made. Following this, an attempt was made to dissolve the active layer of the membrane in a solvent and then precipitate the polymers onto the sensor surface. The fluoropolymer and regenerated cellulose polymer would dissolve in dimethylformamide (DMF) and dimethylacetamide (DMAC) which was too aggressive for the SPR device. Attempts to dilute the solvent with water after the polymers had been dissolved in the pure solvent caused the polymers to precipitate

from the solution. Dissolving of the regenerated cellulose polymer in sodium hydroxide was also attempted to no avail.
A possible future solution to the problem may be to spin coat the membrane material onto the sensor surface.
Once a method is determined to coat the sensor surface with the polymer, this technique will give very interesting data regarding adsorption kinetics to the polymer surface mimicking fouling and also desorption kinetics from the polymer surface during cleaning.

As well as the achieved streaming potential measurements recorded for the pore walls of the membrane, it is also possible to measure the surface charge along the membrane surface. This data would give extra clarification to our current knowledge regarding membrane charge and the effect on membrane – foulant – cleaning agent interactions.

Surface roughness measurements were recorded using AFM to obtain topographical images of the membrane surface. These measurements were performed on 5 x 5μm surface areas which provide details of the surface roughness, i.e. the inherent, fine, closely-spaced irregularities created by the production process. Further information would be useful regarding the surface waviness, i.e. the repeating irregularities with spacing greater than roughness marks that result from the production process. Larger areas are required to make this measurement than can be obtained using AFM. The Wyko profilometer is essentially a white light interferometer which can measure surface waviness as well as surface roughness, image topography in 3D non-destructively (non-contact) as well as do statistical computation of surface data. This added information on the membrane waviness may give further information regarding fluid flow across the membrane surface and possibly enhanced knowledge of foulant adhesion into the more localised surface roughness.

A measure of the mass of tea deposits formed during fouling filtration runs would help identify further the fouling mechanism occurring and how best to clean the membrane surfaces. This could be performed by flushing the fouled surfaces with pure water after fouling runs. This would give a measure of the desorption rate of reversible foulant from the membrane surface. This would not give a measure of the

total deposit on the membrane surface. The total mass of deposit on the membrane surface would have to be calculated by measuring the initial mass of a damp (drip dry) virgin conditioned membrane surface then fouling the membrane and measuring the damp (drip dry) fouled membrane. There would be obvious errors associated with this method including variations in the water content with the virgin conditioned membrane and the fouled membrane.

Researching chemical resistive, high temperature capable ceramic membrane materials would be of interest for black tea filtration. The potential for high temperature filtration may offer advantages of high flux and reduced selectivity such that haze active components such as proteins are still retained by the membrane. Also modification to the pH of the black tea solution may offer advantageous filtration characteristics and, given the increased chemical stability associated with these membranes, a wider range of pH will be possible.

Other membrane materials of interest are woven steel membrane materials as represented in Figure 5.2. These filters can be made from numerous grades of steel and other metals such as aluminium, copper and brass. The twilled Dutch weave is capable of absolute retentions of 4 microns. It may be possible to selectively adsorb species such that the membrane pores sizes may be reduced potentially in the territory of ultrafiltration specifications. Another possibility may be to place two of these membranes on top of each other which may increase the selectivity.

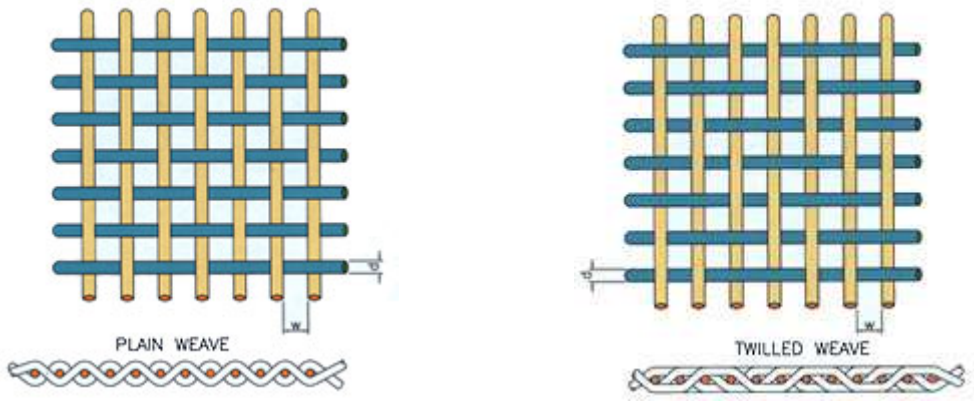

Figure 5.2: Locker Woven Wire Mesh plain and twilled, Dutch weave micro woven filters (www.lockergroup.com/buyersguide/)

Operating the ultrafiltration process below the critical flux conditions (section 2.4.9.10) would be advantageous if possible due to the removal of fouling from the system or significant reduction in fouling and thus reduction in cleaning requirements. Investigation into the criteria required for such a system would involve operating with significantly reduced operating concentrations and increased cross flow velocity. This may then make the operation uneconomical compared with higher concentration feeds.

There are other beverages that contain polyphenols and or proteins such as beer, wine and different fruit juices which form haze active polyphenol / protein aggregates which affect both taste and appearance of the final product. The techniques used and the conclusions found in this study can help tackle these problems for other polyphenol / protein based beverages.

Chapter 6

6.1 References

Aimar, P., Meireles, M. and Sanchez, V. 1990. A contribution to the translation of retention curves into pore size distributions for sieving membranes. *Journal of Membrane Science* **54**, 321 - 338.

Aimar, P. and Sanchez, V. 1986. A novel approach to transfer limiting phenomena during ultrafiltration of macromolecules. *Industrial and Engineering Chemistry Fundamentals* **25**, 789.

Ang, W. S., Lee, S. and Elimelech, M. 2006. Chemical and physical aspects of cleaning of organic-fouled reverse osmosis membranes. *Journal of Membrane Science* **272**, 198 - 210.

Arnot, T. C., Field, R. W. and Koltuniewicz, A. B. 2000. Cross - flow and dead - end microfiltration of oily - water emulsions Part II. Mechanisms and modelling of flux data. *Journal of Membrane Science* **169**, 1 - 15.

Astill, C., Birch, M. R., Dacombe, C., Humphrey, P. and Martin, P. T. 2001. Factors Affecting the caffeine and polyphenol contents of black and green tea infusions. *Journal of Agricultural and Food Chemistry* **49**, 5340 - 5347.

Bacchin, P. 2004. A possible link between critical and limiting flux for colloidal systems: consideration of critical deposit formation along a membrane. *Journal of Membrane Science* **228**, 237 -241.

Balentine, D. A. 1992. Manufacturing and Chemistry of Tea : Phenolic Compounds in food and their effects on health. *Am Chem Soc Symp* **506**, 102 - 116.

Barhate, R. S., Subramanian, R., Nandini, K. E. and Hebbar, H. U. 2003. Processing of honey using polymeric microfiltration and ultrafiltration membranes. *Journal of Food Engineering* **60**, 49 - 54.

Barros, S. T. D. d., Nadrade, C. M. G., Mendes, E. S. and Peres, L. 2003. Study of fouling mechanism in pinapple juice clarification by ultrafiltration. *Journal of Membrane Science* **215**, 213 - 224.

Bartlett, M. 1998. Chemical cleaning of fouled membrane systems. **Doctoral Dissertation, Chemical Engineering Department, University of Bath**,

Bartlett, M., Bird, M. R. and Howell, J. A. 1995. An experimental study for the development of a qualitative membrane cleaning model. *Journal of Membrane Science* **105**, 147 - 157.

Bee, R. D., Izzard, M. J., Harbon, R. S. and Stubbs, J. M. 1987. The morphology of black tea cream. *Food Microstructure* **6**, 47 - 56.

Bird, M. R. and Bartlett, M. 1995. CIP Optimisation for the food industry: Relationship Between Detergent Concentration, Temperature and Cleaning Time. *Food and Bioproducts Processing* **73**, 63 - 70.

Bird, M. R. and Fryer, P. J. 1991. An experimental study of the cleaning of surfaces fouled by whey proteins. *Food and Bioproducts Processing* **69**, 13 - 21.

Blanpain, P., Hermia, J. and Lenoel, M. 1993. Mechanisms governing permeate flux and protein rejection in the microfiltration of beer with a cyclopore membrane. *Journal of Membrane Science* **84**, 37 - 51.

Borneman, Z., Gokmen, V. and Nijhuis, H. H. 2001. Selective removal of polyphenols and brown colour in apple juices using PES/PVP membranes in a

single ultrafiltration process. *Separation and Purification Technology* **22-23**, 53 - 61.

Bowen, W. R., Calvo, J. I. and Hernandez, A. 1995. Steps of membrane blocking in flux decline during protein microfiltration. *Journal of Membrane Science* **101**, 153 - 165.

Bowen, W. R., Doneva, T. A. and Stoton, J. A. G. 2002. Protein deposition during cross-flow membrane filtration: AFM studies and flux loss. *Colloids and Surfaces B: Biointerfaces* **27**, 103 - 113.

Bowen, W. R., Kingdon, R. S. and Saubuni, H. A. M. 1989. Electrically enhanced separation processes: The basis of in situ intermittent electrolytic membrane cleaning (IIEMR) and in situ electrolytic membrane restoration (IEMR). *Journal of Membrane Science* **40**, 219 - 229.

Brujin, I. d., Venegas, A. and Borquez, R. 2002. Influence of crossflow ultrafiltration on membrane fouling and apple juice quality. *Desalination* **148**, 131 - 136.

Capannelli, G., Bottino, A., Gekas, V. and Trägårdh, G. 1990. Protein fouling behaviour of Ultrafiltration membranes prepared with varying degrees of hydrophilicity. *Process Biochemistry International* 221 - 224.

Cartalade, D. and Vernhet, A. 2006. Polar interactions in flavan-3-ol adsorption on solid surfaces. *Journal of Agricultural and Food Chemistry* **54**, 3086 - 3094.

Chai, X., Kobayashi, T. and Fujii, N. 1999. Ultrasound-associated cleaning of polymeric membranes for water treatment. *Separation and Purification Technology* **15**, 139 - 146.

Chan, R. and Chen, V. 2004. Characterization of protein fouling on membranes: opportunities and challenges. *Journal of Membrane Science* **242**, 169 - 188.

Chao, Y. C. and Chiang, B. H. 1999. Cream formation in semifermented tea. *Journal of the Science of Food and Agriculture* **79**, 1767 - 1774.

Charlton, A. J., Baxter, N. J., Khan, M. L., Moir, A. J. G., Haslam, E., Davies, A. P. and Williamson, M. P. 2002. Polyphenol/peptide Binding and precipitation. *Journal of Agricultural and Food Chemistry* **50**, 1593 - 1601.

Charlton, A. J., Davis, A. L., Jones, D. P., Lewis, J. R., Davies, A. P., Haslam, E. and Williamson, M. P. 2000. The self-association of the black tea polyphenol theaflavin and its complexation with caffeine. *Journal of the Chemical Society* **2**, 317 - 322.

Cheryan, M. 1986. Ultrafiltration Handbook. *Technomic Publishing Company*

Cheynier, V. 2005. Polyphenols in foods are more complex than often thought. *American Journal of Clinical Nutrition* **81**, 223S - 229S.

Churaev, N. V., Holdich, R. G., Prokopovich, P. P., Starov, V. M. and Vasin, S. I. 2005. Reversible adsorption inside pores of ultrafiltration membranes. *Journal of Colloid and interface science* **288**, 205 - 212.

Coinceanainn, M. O., Astill, C. and Schumm, S. 2003. Potentiometric, FTIR and NMR studies of the complexation of metas with theaflavin. *The Royal Society of Chemistry* 801 - 807.

Coulson, J. M. and Richardson, J. F. 1998. Chemical Engineering: Fluid Flow, Heat Transfer and Mass Transfer. **Vol 1**, 683.

Coulson, J. M., Richardson, J. F., Backhurst, J. R. and Harker, J. H. 1997. Chemical Engineering: Particle Technology Separation Processes. **Vol 2**, 868 - 901.

Czekaj, P., Lopez, F. and Guell, C. 2000. Membrane fouling during microfiltration of fermented beverages. *Journal of Membrane Science* **166**, 199 - 212.

Daufin, G., Escudier, J.-P., Carrere, H., Berot, S., Fillaudeau, L. and Decloux, M. 2001. Recent and emerging applications of membrane processes in the food and dairy industry. *Food and Bioproducts Processing* **79**, 89 - 102.

Daufin, G., Merin, U., Labbe, J. P., Quemerais, A. and Kerherve, F. L. 1991. Cleaning of inorganic Membranes after whey and milk Ultrafiltration. *Biotechnology and Bioengineering* **38**, 82 - 89.

Duriyabunleng, H., Petmunee, J. and Muangnapoh, C. 2001. Effects of the Ultrasonic waves on microfiltration in plate and frame module. *Journal of Chemical Engineering of Japan* **34**, 985 - 989.

Espinasse, B., Bacchin, P. and Aimar, P. 2002. On an Experimental method to measure critical flux in ultrafiltration. *Desalination* **146**, 91 - 96.

Fernandez-Caceres, P. L., Martin, M. J., Pablos, F. and Gonzalez, A. G. 2001. Differentiation of Tea (Camellia sinensis) varieties and their geographical origin according to their metal content. *Journal of Agricultural and Food Chemistry* **49**, 4775 - 4779.

Field, R. W., Wu, D., Howell, J. A. and Gupta, B. B. 1995. Critical Flux concept for microfiltration fouling. *Journal of Membrane Science* **100**, 259-272.

Gekas, V., Trägårdh, G., Capannelli, C. and Bottino, A. 1990. Correlation of Direct Porosimetric Data and performance of Ultrafiltration membranes. *Process Biochemistry International* 111 - 116.

Gekas, V. and Zhang, W. 1989. Membrane characterization using porosimetry and contact angle measurements: A comparison with experimental ultrafiltration results. *Process Biochemistry International* 159 - 166.

Goosen, M. F. A., Sablani, S. S., Al-Hinai, H., Al-Belushi, S. and Jackson, D. 2004. Fouling of Reverse Osmosis and Ultrafiltration membranes: A Critical Review. *Separation and Science Technology* **39**, 2261 - 2297.

Harbowy, M. E. and Balentine, D. A. 1997. Tea Chemistry. *Critical Reviews in Plant Sciences* **16**, 415 - 480.

Haslam, E. 2003. Thoughts on thearubigins. *Phytochemistry* **64**, 61 - 73.

Hermia, J. 1982. Constant pressure blocking filtration laws. Application to power-law non-newtonian fluids. *Trans. Ind. Chem. Eng* **60**, 183 - 187.

Hlavacek, M. 1995. Break up of oil-in-water emulsions induced by permeation through a microfiltration membrane. *Journal of Membrane Science* **102**, 1 - 7.

Hodgson, P. H., Leslie, G. L., Schneider, R. P., Fane, A. G., Fell, C. J. D. and Marshall, K. C. 1993. Cake resistance and solute rejection in bacterial microfiltration: the role of the extracellular matrix. *Journal of Membrane Science* **79**, 35 - 53.

Hu, Q., Pan, G. and Zhu, J. 2001. Effect of selenium on green tea preservation quality and amino acid composition of tea protein. *Journal of Horticultural Science & Biotechnology* **76**, 344 - 346.

Huisman, I. H., Pradanos, P. and Hernandez, A. 2000. Electrokinetic characterisation of ultrafiltration membranes by streaming potential, electroviscous effect, and salt retention. *Journal of Membrane Science* **178**, 55 - 64.

Iritani, E., Mukai, Y., Tanaka, Y. and Murase, T. 1995. Flux decline behaviour in dead-end microfiltration of protein solutions. *Journal of Membrane Science* **1995**, 181 - 191.

Jhoo, J.-W., Lo, C.-Y., Li, S., Sang, S., W, C. Y., Heinze, T. M. and Ho, C.-T. 2005. Stability of black tea polyphenol, theaflavin, and identification of Theanaphthoquinone as its major radica reaction product. *Journal of Agricultural and Food Chemistry* **53**, 6146 - 6150.

Jobstl, E., Patrick, J., Fairclough, A., Davies, A. P. and Williamson, M. P. 2005. Creaming in Black Tea. *Journal of Agricultural and Food Chemistry* **53**, 7997 - 8002.

Johnson, G., Donnelly, B. J. and Johnson, D. K. 1968. The chemical nature and precursors of clarified apple juice sediment. *Journal of Food Science* **33**, 254 - 257.

Jonsson, C. and Jonsson, A.-S. 1995. Influence of membrane material on the adsorptive fouling of ultrafiltration membranes. *Journal of Membrane Science* **108**, 79 - 87.

Juang, R.-S. and Lin, H.-H. 2004. Flux recovery in the ultrafiltration of suspended solutions with ultrasound. *Journal of Membrane Science* **115**, 115 - 124.

Kaplan, M. C., Jegou, A., Chaufer, B., Rabiller-Baudry, M. and Michalsky, M. C. 2002. Adsorption of lysozyme on membrane material and cleaning with non-ionic surfactant characterized through contact angle measurements. *Desalination* **146**, 149 - 154.

Kim, K.-J., Sun, P., Chen, V., Wiley, D. E. and Fane, A. G. 1993. The cleaning of ultrafiltration membranes fouled by protein. *Journal of Membrane Science* **80**, 241 - 249.

Koltuniewicz, A. B., Field, R. W. and Arnot, T. C. 1995. Cross - flow and dead end microfiltration of oily - water emulsion. Part I: Experimental study and analysis of flux decline. *Journal of Membrane Science* **102**, 193 - 207.

Lee, S. and Elimelech, M. 2006. Relating organic fouling of reverse osmosis membranes to intermolecular adhesion forces. *Environmental Science & Technology* **40**, 980 - 987.

Leite, F. L. and Herrmann, P. S. P. 2005. Application of atomic force spectroscopy (AFS) to studies of ahesion phenomena: a review. *Journal of Adhesion and Science Technology* **19**, 365 - 405.

Leone, M., Zhai, D., Sareth, S., Kitada, S., Reed, J. C. and Pellecchia, M. 2003. Cancer Prevention by tea polyphenols is linked to their direct inhibition of antiapoptotic Bcl-2-Family Proteins. *Cancer Research* **63**, 8118 - 8121.

Li, Q. and Elimelech, M. 2004. Organic fouling and chemical cleaning of nanofiltration membranes: measurements and mechanisms. *Environmental Science & Technology* **38**, 4683 - 4693.

Liang, Y. and Xu, Y. 2001. Effect of pH on cream particle formation and solids extraction yield of black tea. *Food Chemistry* **74**, 155 - 160.

Liang, Y. and Xu, Y. 2003. Effect of extraction temperature on cream and extractability of black tea. *International Journal of Food Science and Technology* **38**, 37 - 45.

Liang[a], Y. and Xu, Y. 2003. Effect of extraction temperature on cream and extractability of black tea. *International Journal of Food Science and Technology* **38**, 37 - 45.

Liang[b], Y., Lu, J., Zhang, L., Wu, S. and Wu, Y. 2003. Estimation of black tea quality by analysis of chemical composition and colour difference of tea infusions. *Food Chemistry* **80**, 283 - 290.

Luczaj, W. and Skrzydlewska, E. 2004. Antioxidant properties of black tea in alcohol intoxication. *Food and Chemical Toxicology* **42**, 2045 - 2051.

Luczaj, W. and Skrzydlewska, E. 2005. Antioxidative properties of black tea. *Preventative Medicine* **40**, 910 - 918.

Lunder, T. L. 1992. Catechins of Green Tea: Antioxidant Activity. *Am Chem Soc Symp (Nestle' Research Centre)* **507**, 114 - 120.

Mangas, J., Suarez, B., Picinelli, A., Moreno, J. and Blanco, D. 1997. Differentiation by phenolic profile of apple juices prepared according to two membrane techniques. *Journal of Agricultural and Food Chemistry* **45**, 4777 - 4784.

Marshall, A. D., Munro, P. A. and Trangardh, G. 1993. The effect of protein fouling in microfiltration and ultrafiltration on permeate flux, protein retention and selectivity - A literature review. *Desalination* **91**, 655 - 108.

Martin, A., martinez, F., malfeito, J., Palacio, L., Pradanos, P. and Hernandez, A. 2003. Zeta potential of membranes as a function of pH Optimization of isoelectric point. *Journal of Membrane Science* **213**, 225 - 230.

Masselin, I., Chasseray, X., Durand-Bourlier, L., Laine, J.-M., Syzaret, P.-Y. and Lemordant, D. 2001. Effect of sonication on polymeric membranes. *Journal of Membrane Science* **181**,

McMurrough, Kelly, R. and Bryne, J. 1991. Effect of the removal of sensitive Proteins and proanthocyanidins on the colloidal stability of lager beer. *Journal of American Society of Brewing Chemists* **50**, 67 - 76.

Meien, O. F. v. and Nobrega, R. 1994. Ultrafiltration model for partial solute rejection in the limiting flux region. *Journal of Membrane Science* **95**, 277 - 287.

Menet, M.-C., Sang, S., Yang, C. S., Ho, C.-T. and Rosen, R. T. 2004. Analysis of Theaflavins and Thearubigins from black tea extract by MALDI-TOF Mass Spectrometry. *Journal of Agricultural and Food Chemistry* **52**, 2455 - 2461.

Metsamuurronen, S., Howell, J. and Nyström, M. 2002. Critical flux in ultrafiltration of myoglobin and baker's yeast. *Journal of Membrane Science* **196**, 13 - 25.

Minh, H., Tran-Ha and Wiley, D. E. 1998. The relationship between membrane cleaning efficiency and water quality. *Journal of Membrane Science* **145**, 99 - 110.

Mohammadi, T., Madaeni, S. S. and Moghaddam, M. K. 2002. Investigation of membrane fouling. *Desalination* **153**, 155 - 160.

Mores, W. D. and Davis, R. H. 2002. Direct observation of membrane cleaning via rapid backpulsing. *Desalination* **146**, 135 - 140.

Mueller, J. and Davis, R. H. 1996. Protein fouling of surface-modified polymeric microfiltration membranes. *Journal of Membrane Science* **116**, 47 - 60.

Mulder, M. 2000. Basic Priniplces of membrane technology. **Second edition**,

Mumin, M. A., Akhter, K. F., Abedin, M. Z. and Hossain, M. Z. 2006. Determination of caffeine in Tea, Coffee and soft drinks by solid phase extraction and high performance iquid chromatography (SPE - HPLC). *Malaysian Journal of Chemistry* **8**, 45 - 51.

Munson-McGee, S. H. 2002. Effect of particle-size and pore-size distribution in cross-flow filtration. *Separation and Purification Technology* **37**, 493-513.

Nikolova, J. D. and Islam, M. A. 1998. Contribution of adsorbed layer resistance to the flux-decline in an ultrafiltration process. *Journal of Membrane Science* **146**, 105-111.

Nyström, M., Pihlajamäki, A. and Ehsani, N. 1994. Characterization of ultrafiltration membranes by simutaneous streaming potential and flux measurements. *Journal of Membrane Science* **87**, 245 - 256.

Palacio, L., Calvo, J. I., pradanos, P., Hernandez, A., Vaisanen, P. and Nyström, M. 1999. Contact angles and external protein adsorption onto UF membranes. *Journal of Membrane Science* **152**, 189 - 201.

Penders[a,] M. H. G., Jones, D. P., Needham, D. and Pelan, E. G. 1998. Mechanistic study of equilibrium and kinetic behaviour of tea cream formation. *Food Hydrocolloids* **12**, 9 - 15.

Penders[b], M. H. G., Scollard, D. J. P., Needham, D., Pelan, E. G. and Davies, A. P. 1998. Some molecular and colloidal aspects of tea cream formation. *Food Hydrocolloids* **12**, 443 - 450.

Persson, A., Jonsson, A.-s. and Zacchi, G. 2003. Transmission of BSA during cross-flow microfiltration: influence of pH and salt concentration. *Journal of Membrane Science* **223**, 11-21.

Persson, K. M., Gekas, V. and Trägårdh, G. 1995. Study of membrane compaction and its influence on ultrafiltration water permeability. *Journal of Membrane Science* **100**, 155-162.

Pihlajamäki, A. 1998. Electrochemical characterisation of filter media properties and their exploitation in enhanced filtration. *Doctoral Dissertation, Lappeenranta University of Technology, Lappeenranta, Finland*

Pradanos, P., Arribas, J. I. and Hernandez, A. 1995. Mass transfer coefficient and retention of PEGs in low pressure cross-flow ultrafiltration through asymmetric membranes. *Journal of Membrane Science* **99**, 1-20.

Pradanos, P., Hernandez, A., Calvo, J. I. and Tejerina, F. 1996. Mechanisms of protein fouling in cross-flow UF through an asymmetric inorganic membrane. *Journal of Membrane Science* **114**, 115 - 126.

Rabiller-Baudry, M., maux, M. L., Chaufer, B. and Begoin, L. 2002. Characterisation of cleaned and fouled membrane by ATR-FTIR and EDX analysis coupled with SEM: application to UF of skimmed milk with a PES membrane. *Desalination* **146**, 123 - 128.

Ripperger, S. and Altmann, J. 2002. Crossflow microfiltration - State of the art. *Separation and Purification Technology* **26**, 19 - 31.

Robinson, C. W., Siegel, M. H., Condemine, A., Fee, C., Fahidy, T. Z. and Glick, B. R. 1993. Pulsed-electric-field crossflow ultrafitration of bovine serum albumin. *Journal of Membrane Science* **80**, 209 - 220.

Satoh, E., ishii, T., Shimizu, Y., Sawamura, S.-i. and Nishimura, M. 2001. Black tea extract, thearubigin fraction, counteracts the effects of botulinum neurotoxins in mice. *Journal of Pharmacology* **132**, 797 -798.

Scharbert, S. and Hofmann, T. 2005. Molecular Definition of Black tea Taste by means of quantitative studies, taste Reconsitution, and omission experiments. *Journal of Agriculture and Food Chemistry* **53**, 5377-5384.

Shallo, H. E., Rao, A., Ericson, A. P. and Thomas, R. L. 2001. Preparation of soy protein concentrated by ultrafiltration. *Journal of Food Science* **66**, 242 - 246.

Shorrock, C. J. and Bird, M. R. 1998. Membrane Cleaning: Chemical Enhanced Removal of Deposits Formed During Yeast Cell Harvesting. *Food and Bioproducts Processing* **76**, 30 - 38.

Siebert, K. J. 1999. Effects of protein-polyphenol interactions on beverage haze, stabilization, and analysis. *Journal of Agricultural and Food Chemistry* **47**, 353 - 362.

Siebert, K. J. 2006. Haze formation in beverages. *Lebensm.-Wiss. U.-Technol* **39**, 987 - 994.

Siebert[a], K. J., Troukhanova, N. V. and Lynn, P. Y. 1996. Nature of Polyphenol - Protein Interaction. *Journal of Agricultural and Food Chemistry* **44**, 80 -85.

Siebert[b], K. J., Carrasco, A. and Lynn, P. Y. 1996. Formation of Protein - Polyphenol Haze in Beverages. *Journnal of Agriculture and Food Chemistry* **44**, 1977 - 2005.

Singh, G. and Song, L. 2005. Quantifying the effect of ionic strength on colloidal fouing potential in membrane filtration. *Journal of Colloid and Interface Science* **284**,

Singleton, V. L. and Rossi(Jr)., J. A. 1965. Colorimetry of Total Phenolics with Phosphomolybdic-Phosphotungstic Acid Reagents *American Journal Enology Viticulture* **16**, 144 - 158.

Song, L. 1998. A new model for the calculation of the limiting flux in ultrafiltration. *Journal of Membrane Science* **144**, 173 - 185.

Song, L., Chen, K. L., Ong, S. L. and Ng, W. J. 2004. A new normalization method for determination of colloidal fouling potential in membrane processes. *Journal of Colloid and Interface Science* **271**, 426 - 433.

Tajchakavit, S., Boye, J. I. and Couture, R. 2001. Effect of processing on post-bottling haze formation in apple juice. *Food Research International* **34**, 415 - 424.

Tang, H. R., Covington, A. D. and Hancock, R. A. 2003. Structure - Activity relationships in the hydrophobic interactions of polyphenols with cellulose and collagen. *Biopolymers* **70**, 403 - 413.

Tanizawa, Y., Abe, T. and Yamada, K. 2007. Back tea stain formed on the surface of tea cups and pots. Part 1 - Study on the chemical composition and structure. *Food Chemistry* **103**, 1 - 7.

Tarabara, V. V., Koyuncu, I. and Wiesner, M. R. 2004. Effect of hydrodynamics and solution ionic strength on permeate flux in cross-flow filtration: direct experimental observation of filter cake cross-sections. *Journal of Membrane Science* **241**, 65 - 78.

Todisco, S., Tallarico, P. and Gupta, B. B. 2002. Mass transfer and polyphenols retention in the clarification of black tea with ceramic membranes. *Innovative Food Science and Emerging Technologies* **3**, 255 - 262.

Tolstoguzov, V. 2002. Thermodynamic Aspects of biopolymer functionality in biological systems, foods, and beverages. *Critical Reviews in Biotechnology* **22**, 89-174.

Tracey, E. M. and Davis, R. H. 1994. Protein fouling of track-etched polycarbonate microfiltration membranes. *Journal of Colloid and Interface Science* **167**, 104 - 116.

Trägårdh, G. 1989. Membrane cleaning. *Desalination* **71**, 325 - 335.

Turker, M. and Hubble, J. 1987. Membrane fouling in a constant-flux ultrafiltration cell. *Journal of Membrane Science* **34**, 267 - 281.

Tzeng, W. C. and Zall, R. R. 1990. Combining polymers with chemical, thermal, and turbulent conditions to clean an Ultrafiltration Membrane Fouled with milk. *Process Biochemistry* 71 - 78.

Unilever 2004. Personal Communication.

Vaisanen, P., Bird, M. R. and Nyström, M. 2002. Treatment of UF membranes with simple and formulated cleaning agents. *Food and Bioproducts Processing* **80**, 98 -108.

Vegte, E. W. v. d. and Hadziioannou, G. 1997. Scanning force microscopy with chemical specificity: an extensive study of chemically specific tip - surface interactions and the chemical imaging of the surface functional groups. *Langmuir* **13**, 4357 - 4368.

Vernhet, A. and Moutounet, M. 2002. Fouling of organic microfiltration membranes by wine constituents: importance, relative impact of wine polysacharides and polyphenols and incidence of membrane properties. *Journal of Membrane Science* **201**, 103 - 122.

Vladisavljevic', G. T., Vukosavljevic', P. and Bukvic', B. 2003. Permeate flux and fouling resistance in ultrafiltration of depectinized apple juice using ceramic membranes. *Journal of Food Engineering* **60**, 241 -247.

Wagner, J. 2001. Membrane filtration handbook, Practical tips and hints. *Osmonics*

Weis, A., Bird, M. R. and Nyström, M. 2003. The chemical cleaning of polymeric UF membranes fouled with spent sulphite liquor over multiple operational cycles. *Journal of Membrane Science* **216**, 67 - 79.

Weis, A., Bird, M. R., Nyström, M. and Wright, C. 2005. The influence of morphology, hydrophobicity and charge upon the long-term performance of ultrafiltration membranes fouled with spent sulphite liquor. *Desalination* **175**, 73 - 85.

Weisburger, J. H. 1997. Tea and Health: a historic perspective. *Cancer Letters* **114**, 315 - 317.

Wu, D. and Bird, M. R. 2007. The foulling and cleaning of ultrafiltration membranes during the filtration of model tea component solutions. *Journal of Food Engineering* **30**, 293 - 323.

Wu, D., Howell, J. A. and Field, R. W. 1999. Critical flux measurement for model colloids. *Journal of Membrane Science* **152**, 89 - 98.

Yamada, K., Abe, T. and Tanizawa, Y. 2007. Black tea stain formed on the surface of tea cups and pots. Part 2 - Study of the structure change caused by aging and calcium addition. *Food Chemistry* **103**, 8 - 14.

Yamada, T., Terashima, T., Okubo, T., Juneja, T. R. and Yokogoshi, H. 2005. Effects of theanine, r-glutamylethylamide, on neurotransmitter release and its relationship with glutamic acid neurotransmission. *Nutritional Neuroscience* **8**, 219 - 226.

Yeh, H. M., Wu, H. P. and Dong, J. F. 2003. Effects of design and operating parameters on the declination of permeate flux for membrane ultrafiltration along hollow-fiber modules. *Journal of Membrane Science* **213**, 33 - 44.

Youn, K.-S., Hong, J.-H., Bae, D.-H., Kim, S.-J. and Kim, S.-D. 2004. Effective Clarifying proces of reconstituted apple juice using membrane filtration with filter-aid pretreatment. *Journal of Membrane Science* **228**, 179 - 186.

Zhang, G. and Liu, X. 2003. Membrane fouling and cleaning in ultrafiltration of wastewater from banknote printing works. *Journal of Membrane Science* **211**, 235 - 249.

Zhang, G. J., Liu, Z. Z., Song, L. F., Hu, J. Y., Ong, S. L. and Ng, W. J. 2004. One-step cleaning method for flux recovery of an ultrafiltration membrane fouled by banknote printing works wastewater. *Desalination* **170**, 271 -280.

Chapter 7 Appendices

7.1 Calibrations

7.1.1 Internal Module Dimensions

Number of channels		
Number	4	
Channel length	0.135	m
Channel Width	0.017	m
Channel height	0.0007	m
Total channel volume	0.000006426	m^3
Total channel cross section area	4.76E-05	m^2
Hydraulic Diameter, dh	0.001344633	m
Effective cross section area	5.68012E-06	m^2

7.1.2 M10 pilot lab-scale factory settings

Generic design: Plate and frame type cross-flow membrane filtration module

Membrane filtration area	0.0336	m2
Module internal volume	0.000057	m3
Rig dead volume	0.0005	m3

Module parts	**Material**
All external steel	Stainless, AISI 304
Internal, product wetted steel	Acid resistant, AISI 316
Support and spacer plates	Polysuphone (PSO)
Permeate hose	silicone
O-ring	Viton

7.1.3 Pressure Gauge

Gauge type - O/N 347015/1 - Inlet to Membranes

Gauge representation bar	Actual representation bar	% diff
0.500	0.528	5.60
1.000	1.030	3.00
1.500	1.525	1.67
2.000	2.026	1.30
2.500	2.539	1.56
3.000	3.040	1.33
3.500	3.552	1.49
4.000	4.047	1.18
4.500	4.546	1.02
5.000	5.050	1.00
5.500	5.560	1.09

Gauge type - O/N 347015/2 - Outlet

Gauge representation bar	Actual representation bar	% diff
0.500	0.508	1.60
1.000	1.001	0.10
1.500	1.508	0.53
2.000	2.000	0.00
2.500	2.505	0.20
3.000	3.020	0.67
3.500	3.520	0.57
4.000	4.030	0.75
4.500	4.509	0.20
5.000	5.080	1.60
5.500	5.509	0.16

Table 7.1: Table showing pressure gauge calibrations

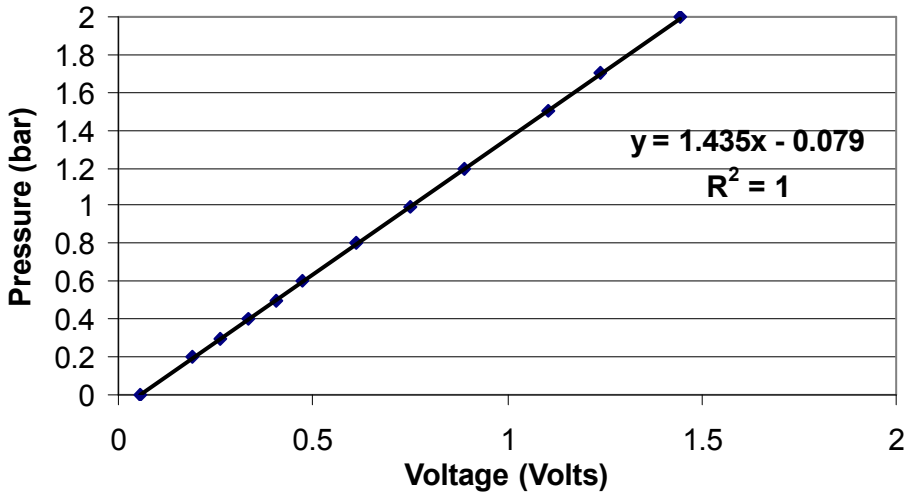

Figure 7.1: Graph to show inlet pressure transducer calibration

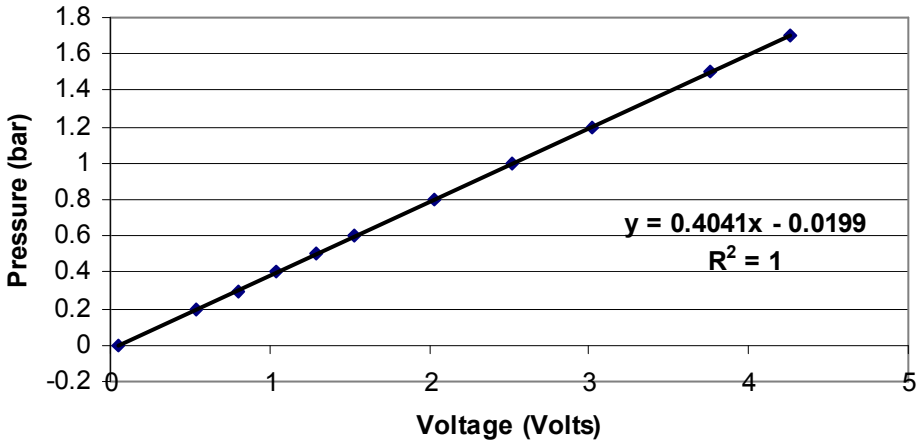

Figure 7.2: Graph to show outlet pressure transducer calibration

7.1.4 Rotameter

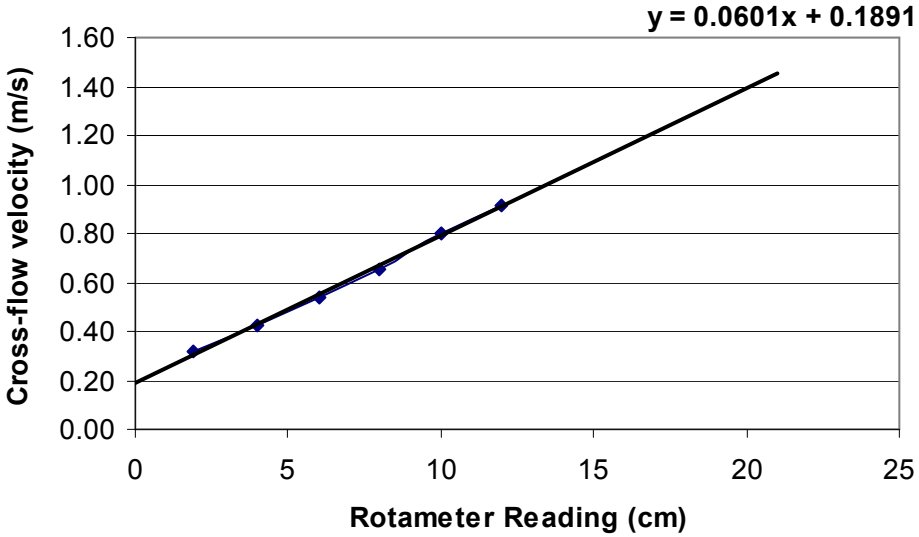

Figure 7.3: Graph to show rotameter reading vs actual flowrate within M10 lab pilot rig.

7.1.5 Haze measurement

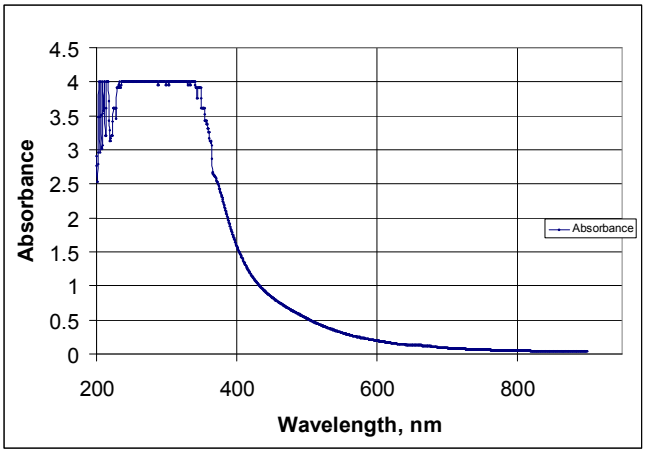

Figure 7.4 Absorbance vs Wavelength for 0.125wt% reconstitute at 80°C for determination of suitable wavelength for haze measurements using a UV-VIS spectrophotometer.

A scan was performed to find the wavelength associated with no absorbance using a very low concentration solution of tea with little or no haze. It was found that at 900nm there was no absorbance. It was therefore decided that any further haze measurements would be analysed and recorded as the absorbance at a wavelength of 900nm.

7.1.6 NaOH wt% vs pH

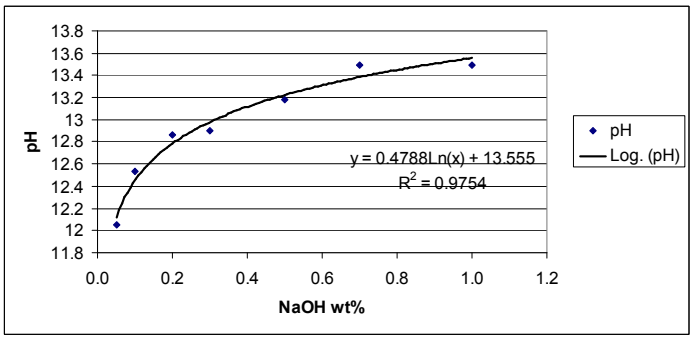

Figure 7.5: Graph to show the relationship between NaOH concentration (wt%) and pH at 30°C when NaOH powder is dissolved in Reverse Osmosis RO water.

7.2 Error Calculations

7.2.1 Tea Fouling (Flux Standard Error)

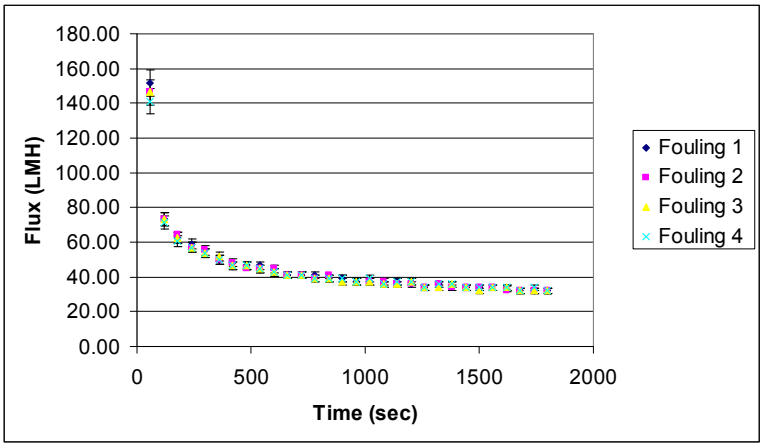

Figure 7.6: Graph to show repeated consistent multiple fouling of regenerated cellulose membrane (1.0wt%, 1.0bar, 0.44m/s, 50°C for 30 mins) where cleaning and RO water characterisation conditions remain constant.

Table 7.2: Raw data and calculations used to determine the error used in all flux data experimentation

	Flux Data													
	Fouling 1	Fouling 2	Fouling 3	Fouling 4	Average	Fouling 1 Error	Fouling 2 Error	Fouling 3 Error	Fouling 4 Error	Largest	% error	Mean	Standard Deviation	% error 2
Time	18/04/2005	19/04/2005	26/04/2005	26/04/2005						Error				
	litres/hr/m2	litres/hr/m2	litres/hr/m2	litres/hr/m2										
60	151.79	146.43	146.43	141.07	146.43	-5.36	0.00	0.00	5.36	5.36	3.7	146.4	4.4	3.0
120	73.21	73.21	73.21	71.43	72.77	-0.45	-0.45	-0.45	1.34	1.34	1.8	72.8	0.9	1.2
180	62.50	64.29	62.50	60.71	62.50	0.00	-1.79	0.00	1.79	1.79	2.9	62.5	1.5	2.3
240	58.93	57.14	57.14	57.14	57.59	-1.34	0.45	0.45	0.45	-1.34	2.3	57.6	0.9	1.6
300	55.36	55.36	53.57	53.57	54.46	-0.89	-0.89	0.89	0.89	0.89	1.6	54.5	1.0	1.9
360	50.00	50.00	51.79	50.00	50.45	0.45	0.45	-1.34	0.45	0.45	0.9	50.4	0.9	1.8
420	48.21	48.21	46.43	46.43	47.32	-0.89	-0.89	0.89	0.89	0.89	1.9	47.3	1.0	2.2
480	46.43	44.64	46.43	46.43	45.98	-0.45	1.34	-0.45	-0.45	1.34	2.9	46.0	0.9	1.9
540	46.43	44.64	44.64	44.64	45.09	-1.34	0.45	0.45	0.45	-1.34	3.0	45.1	0.9	2.0
600	44.64	44.64	42.86	42.86	43.75	-0.89	-0.89	0.89	0.89	0.89	2.0	43.8	1.0	2.4
660	41.07	41.07	41.07	41.07	41.07	0.00	0.00	0.00	0.00	0.00	0.0	41.1	0.0	0.0
720	41.07	41.07	41.07	41.07	41.07	0.00	0.00	0.00	0.00	0.00	0.0	41.1	0.0	0.0
780	41.07	39.29	39.29	39.29	39.73	-1.34	0.45	0.45	0.45	-1.34	3.4	39.7	0.9	2.2
840	39.29	41.07	39.29	39.29	39.73	0.45	-1.34	0.45	0.45	-1.34	3.4	39.7	0.9	2.2
900	39.29		37.50	39.29	38.69	-0.60		1.19	-0.60	1.19	3.1	38.7	1.0	2.7
960	37.50		37.50	37.50	37.50	0.00		0.00	0.00	0.00	0.0	37.5	0.0	0.0
1020	37.50	37.50	37.50	39.29	37.95	0.45	0.45	0.45	-1.34	-1.34	3.5	37.9	0.9	2.4
1080	37.50	37.50	35.71	35.71	36.61	-0.89	-0.89	0.89	0.89	0.89	2.4	36.6	1.0	2.8
1140	37.50	35.71	35.71	37.50	36.61	-0.89	0.89	0.89	-0.89	0.89	2.4	36.6	1.0	2.8
1200	35.71	35.71	37.50	37.50	36.61	0.89	0.89	-0.89	-0.89	-0.89	2.4	36.6	1.0	2.8
1260	33.93	33.93	33.93	33.93	33.93	0.00	0.00	0.00	0.00	0.00	0.0	33.9	0.0	0.0
1320	35.71	35.71	33.93	35.71	35.27	-0.45	-0.45	1.34	-0.45	1.34	3.8	35.3	0.9	2.5
1380	33.93	33.93	35.71	35.71	34.82	0.89	0.89	-0.89	-0.89	-0.89	2.6	34.8	1.0	3.0
1440	33.93	33.93	33.93	33.93	33.93	0.00	0.00	0.00	0.00	0.00	0.0	33.9	0.0	0.0
1500	33.93	33.93	32.14	33.93	33.48	-0.45	-0.45	1.34	-0.45	1.34	4.0	33.5	0.9	2.7
1560		33.93	33.93	33.93	33.93		0.00	0.00	0.00	0.00	0.0	33.9	0.0	0.0
1620	33.04	32.14	33.93	33.93	33.26	0.22	1.12	-0.67	-0.67	1.12	3.4	33.3	0.9	2.6
1680	32.14	32.14	32.14	32.14	32.14	0.00	0.00	0.00	0.00	0.00	0.0	32.1	0.0	0.0
1740	32.14	32.14	32.14	33.93	32.59	0.45	0.45	0.45	-1.34	-1.34	4.1	32.6	0.9	2.7
1800	32.14	32.14	32.14	32.14	32.14	0.00	0.00	0.00	0.00	0.00	0.0	32.1	0.0	0.0

Based on the data shown in Figure 7.6 and calculations performed in Table 7.2, the assumed error for all flux data experimentation was determined based on the % error for the largest difference between average and actual values and the %error 2 based on standard deviation from the median value . Generally % error gave the largest errors ranging from 4.1 – 0% error. It was decided to use a **standard error of 5.0%** for all flux data based on this reproducibility set of experiments.

7.2.2 Solids Concentration

Original concentration	Beaker weight	Beaker and solution	Dried Beaker	Wet weight	dry weight	wt%	Error
wt%	grams	grams	grams	grams	grams		%
2.00	49.6267	62.4445	49.8647	12.818	0.238	1.86	-7.16
1.75	51.2214	63.3330	51.4177	12.112	0.196	1.62	-7.39
1.50	50.6397	62.1880	50.7988	11.548	0.159	1.38	-8.15
1.25	50.8831	63.1825	51.0237	12.299	0.141	1.14	-8.55
1	50.7465	62.5761	50.8545	11.830	0.108	0.91	-8.70
0.75	49.9894	61.7632	50.0690	11.774	0.080	0.68	-9.86
0.50	52.8656	64.2223	52.9166	11.357	0.051	0.45	-10.19

Table 7.3: Demonstrating error when drying known concentration reconstituted tea solutions in oven at 85°C for 48hours

Beaker weight	Beaker and solution	Dried Beaker	Wet weight	dry weight	wt% loss
grams	grams	grams	grams	grams	
50.437	50.6678	50.6483	0.2308	0.2113	91.55
50.4289	50.6936	50.6702	0.2647	0.2413	91.16
49.7344	50.0019	49.9788	0.2675	0.2444	91.36
48.6278	49.4289	49.3614	0.8011	0.7336	91.57
50.64	51.6683	51.5839	1.0283	0.9439	91.79
49.929	50.9091	50.8282	0.9801	0.8992	91.75

Table 7.4 Demonstrating error when drying already spray dried tea powder in oven at 85°C for 48hours.

Table 7.3 shows the difference between known concentration reconstituted tea powder solution and the concentration measured from oven drying at 85°C for 48 hours. As can be seen the error increases from 7 – 10% reduction in measured concentration as the actual concentration reduces. When only freeze-dried tea powder is dried in an oven at under the same conditions a weight loss is also noticed as shown in Table 7.4. This may be because of the tea lights being vaporised from the solution and powder. Another possibility is that water is present in the powder, which is evaporated in the oven, even though care was taken to make measurements at room temperature after drying to avoid any increased errors.

7.2.3 Colour haze with different storage methods

0.7wt%

Actual time	Time from retrieving sample	Temp. °C		L*		a*		b*		Transmittance %		Abs	
			Er(+ / -)%		Er(+ / -)%		Er(+ / -)%		Er(+ / -)%	900nm	Er(+ / -)%	900nm	Er(+ / -)%
A - In Labarotory	00:36:00	35	0.0	17.99	-20.1	26.85	-4.2	30.83	-19.5	50.13	-11.7	0.299	21.1
B - In cold room	01:05:00	35	0.0	20.36	-9.6	27.32	-2.6	34.83	-9.0	52.8	-7.0	0.276	11.7
C - In freezer	01:26:00	34.5	-1.4	19.32	-14.2	26.4	-5.8	33.04	-13.7	49.61	-12.6	0.303	22.7
D - After 1 hour from preparation	01:03:00	35	0.0	22.52	0.0	28.04	0.0	38.29	0.0	56.77	0.0	0.247	0.0

0.5wt%

Actual time	Time from retrieving sample	Temp. °C		L*		a*		b*		Transmittance %		Abs	
			Er(+ / -)%		Er(+ / -)%		Er(+ / -)%		Er(+ / -)%	900nm	Er(+ / -)%	900nm	Er(+ / -)%
A - In Labarotory	00:46:00	35	0	32.31	-10.3	27.71	2.3	53.44	-8.9	66.06	-4.7	0.18	13.2
B - In cold room	01:07:00	35	0.0	34.37	-4.5	27.28	0.7	56.36	-3.9	67.77	-2.3	0.169	6.3
C - In freezer	01:28:00	35	0.0	34.88	-3.1	26.82	-1.0	57.05	-2.8	67.66	-2.4	0.169	6.3
D - After 1 hour from preparation	01:06:00	35	0.0	36	0.0	27.08	0.0	58.67	0.0	69.35	0.0	0.159	0.0

0.25wt%

Actual time	Time from retrieving sample	Temp. °C		L*		a*		b*		Transmittance %		Abs	
			Er(+ / -)%		Er(+ / -)%		Er(+ / -)%		Er(+ / -)%	900nm	Er(+ / -)%	900nm	Er(+ / -)%
A - In Labarotory	00:51:00	35	0	57.78	-1.5	17.28	11.1	64.53	0.4	83.96	1.1	0.074	-8.6
B - In cold room	01:09:00	35	0.0	58.84	0.3	16.45	5.8	64.5	0.4	84.81	2.2	0.071	-12.3
C - In freezer	01:32:00	35	0.0	59.56	1.5	15.54	-0.1	64.15	-0.2	84.53	1.8	0.073	-9.9
D - After 1 hour from preparation	01:07:00	35	0.0	58.67	0.0	15.55	0.0	64.25	0.0	83.01	0.0	0.081	0.0

0.125wt%

Actual time	Time from retrieving sample	Temp. °C		L*		a*		b*		Transmittance %		Abs	
			Er(+ / -)%		Er(+ / -)%		Er(+ / -)%		Er(+ / -)%	900nm	Er(+ / -)%	900nm	Er(+ / -)%
A - In Labarotory	00:55:00	35	0	75.02	0	6.16	26.5	49.44	1.9	92.55	1.8	0.032	-22.0
B - In cold room	01:12:00	35	0.0	75.66	0.6	5.51	13.1	48.68	0.3	92.82	2.1	0.032	-22.0
C - In freezer	01:35:00	35	0.0	75.71	0.6	5.22	7.2	48.62	0.2	92.25	1.5	0.035	-14.6
D - After 1 hour from preparation	01:09:00	35	0.0	75.23	0.0	4.87	0.0	48.52	0.0	90.91	0.0	0.041	0.0

Table 7.5: Colour / haze parameters for 0.7, 0.5, 0.25, 0.125 wt% reconstituted tea samples stored under different conditions for 72 hours comparing with sampling within 1 hour of preparation. All errors are based on percentage change from storage method D.

The colour and haze of four different concentration reconstituted tea solutions was measured after storing under different conditions; A – In Lab, B – In cold room (5°C) and C – In freezer for 48 hours and compared with measuring after 1 hour from sample preparation. All samples were measured at 35°C by warming in a heated water bath. The error shown is the difference between all the different methods and measurement after 1 hour to compare the effect of different storage conditions.
As can clearly be seen storage in the laboratory (about 20°C) has the biggest error or deviation from initial sampling for all concentrations, although freezing the sample shows a bigger error with regard to absorbance (haze) than this at 0.7wt%. Freezing the sample shows larger errors at higher concentrations than lower concentrations when compared with placing the samples in the cold room. This study showed that storage in colder conditions, either in the cold room or freezer maintained colour qualities within 15% of direct sampling. The absorbance measurements were less reliable with deviations of up to 23%. The errors noticed are based largely on concentration also. It was decided for this study to freeze samples as this would enable longer reliable storage periods allowing for potential errors. Future work requires measuring L*a*b* and haze at constant concentration (0.2wt%) as discussed in section 4.1.3 and due to this lower concentrations required should minimise any errors noticed.

7.3 Sample Calculations

7.3.1 Flux measurement

The volumetric permeate flux (J_V) is defined as the volume of permeate (V_P) collected in unit time (t) per membrane area (A_m)

$$J_V = {V_P}/{A_m \times t}$$

Equation 7.1

An example calculation is shown below where 45g or 0.045 Litres (assuming permeate has the same density of water) of permeate (V_P) was collected in 60 seconds (t) through a membrane of area (A_m) 0.0336m2:-

$$J_V = \left[{0.045}/{0.0336 \times 60}\right] = 0.2232 Litres/m^2 s = 80.36 Litres/m^2 s$$

7.3.2 Resistance measurement

The membrane resistance (R_M) can be calculated by knowing the flux of permeate (J_V), the permeate fluid viscosity (μ_P) and the transmembrane pressure (ΔP).

$$R_M = \frac{\Delta P}{\mu_P (J_V)}$$

Equation 7.2

The membrane resistance was calculated either by the gradient of flux data or from individual flux points. Rearranging the equation above gives:-

$$J_V = \left({1}/{R_M \mu_P}\right)\Delta P$$

Equation 7.3

such that plotting J_V vs ΔP gives a gradient of $1/R_m\mu_p$ and by knowing μ enables the calculation of the resistance (R). This method is usually used to calculate the resistance of the membrane which will provide a linear plot such as in Figure 4.2. The resistance can also be calculated using Equation 7.2.

7.3.3 Solids Concentration

The solids concentration was calculated initially when making samples with reconstituted tea powder and RO water measured using a mass balance where:-

Mass of tea powder = M_{tea}

Mass of RO water = M_{RO}

So that the tea weight percentage (Teawt%) was calculated from:-

$$TeaWt\% = \left[\left(\frac{M_{tea}}{M_{RO} + M_{tea}}\right) \times 100\%\right]$$

Equation 7.4

For example, 1.0wt% solution was made up of 40g of tea powder in 3960g of RO water:-

$$TeaWt\% = \left[\left(\frac{40}{3960 + 40}\right) \times 100\%\right] = 1.0wt\%$$

When unknown concentrations of tea solids are obtained such as with permeate samples for UF, the mass of the drying vials were recorded (M_{V0}), the sample added to the vial and the total mass of the vial and sample recorded (M_{VT0}). The vial then dried in the oven using standard conditions (see 3.5.1). After sample drying had finished, the sample was cooled to room temp and the mass of the dried sample in the vial was measured again (M_{VT1}). The total tea solids weight percentage (Tea wt%) of the sample was then recorded using:-

$$TeaWt\% = \left[\left(\frac{M_{VT1} - M_{V0}}{M_{VTO} - M_{VO}}\right) \times 100\%\right]$$

Equation 7.5

For example with a vial of weight, (M_{V0}) - 25.6365g and a sample added making the total mass of the vial and sample recorded (M_{VT0}) – 50.0259g. After drying the dried sample and the vial, (M_{VT1}) was 25.9995g, the Tea wt% was thus calculated as shown below:-

$$TeaWt\% = \left[\left(\frac{25.9995 - 25.6365}{50.0259 - 25.6365}\right) \times 100\%\right] = 1.49wt\%$$

7.3.4 Linear Cross-flow velocity and Reynolds number

Calculation of linear cross flow velocity and Reynolds number

Figure 7.7 shows a schematic of one channel used in cross flow module.

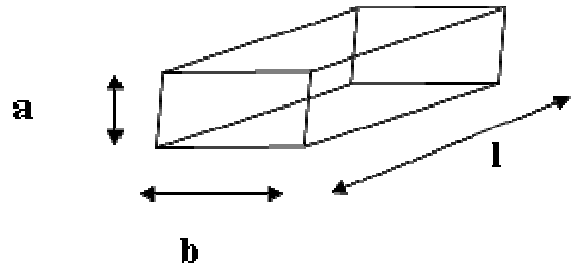

Figure 7.7: Schematic of one channel within cross flow module

The Reynolds number is defined as:-

$$\mathrm{Re} = \frac{du\rho}{\mu}$$

Equation 7.6

where
d – diameter of channel (m)
u – average linear velocity (ms^{-1})
ρ - fluid density (kgm^{-3}) (Nm^{-1})
μ - fluid dynamic viscosity (Nsm^{-2})

When the channel cross section is not circular an equivalent diameter (d_e) of a channel is used. For a rectangular cross section of height (a) and width (b), de is calculated as shown below:-

$$d_e = \frac{2ab}{a+b}$$

Equation 7.7

The linear velocity, u can then b calculated using:-

$$u = \frac{Q}{abN} = \left(\frac{m^3 / s}{m^2} \right)$$

Equation 7.8

Where,
Q – volumetric flowrate (m^3s^{-1})

N – number of channels

For a rectangular channel of height 0.001m and width 0.007m the effective diameter, de can be calculated using Equation 7.7:-

$$d_e = \frac{2 \times 0.0007 \times 0.017}{0.0007 + 0.0017} = 0.00134m$$

When the volumetric flowrate of a 1wt% tea solution is $0.0000213 m^3 s^{-1}$ (1.278 litres min^{-1}) through 4 channels of the same height and width as previously described, the linear velocity can be calculated from Equation 7.8:-

$$u = \frac{0.0000213}{0.0007 \times 0.017 \times 4} = 0.44 ms^{-1}$$

The Reynolds number can then be calculated knowing the linear velocity, u using Equation 7.6, knowing that the viscosity is 0.0005224 Nsm^{-2} and the effective diameter, d_e as calculated above is 0.00175m and assuming a density, ρ is $1000 kgm^{-3}$:-

$$\mathrm{Re} = \frac{0.00134 \times 0.44 \times 1000}{0.0005224} = 1128$$

7.3.5 Total Polyphenol Calculation

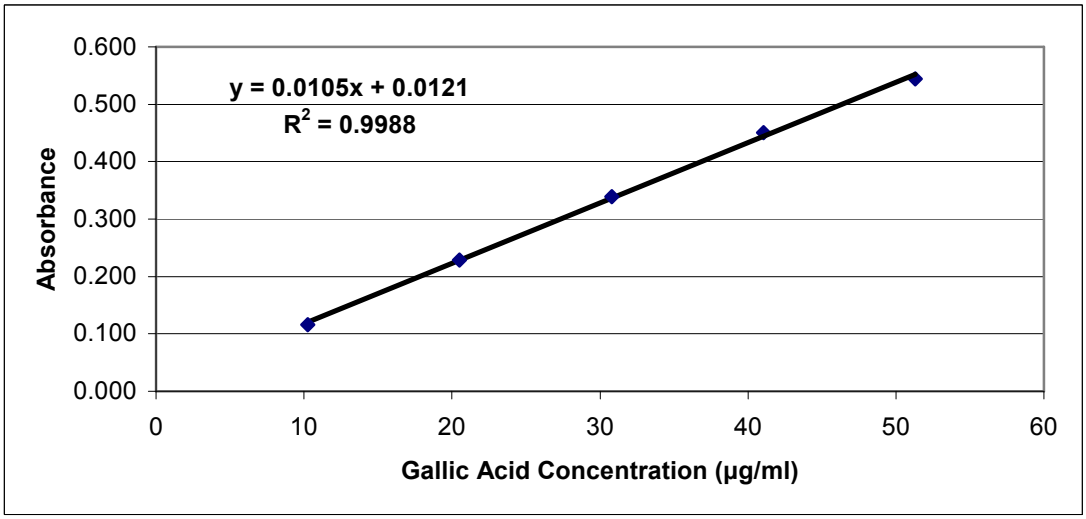

Figure 7.8 Graph to show absorbance gallic acid standard at 765 nm after Folin-Ciocalteu assay.

Once the calibration has been performed as described in section 3.5.4 , a graph similar to Figure 7.8 was produced. Obtaining sample absorbance's (OD_{sample}) of

0.4389 and 0.4455 we could then calculate the total polyphenolic wt% expressed as a percentage of the sample dry matter.

Total Solids = 0.8wt%
ODsample = 0.4422 (average of duplicate measurement)
$OD_{Intercept}$ = 0.0121 (From Figure 7.8)
$Slope_{std}$ = 0.0105 (from Figure 7.8)
The concentration of tea solids in diluted sample is given by M_{conc} below:

$$= \left[\left((0.8wt\% \times 9ml(tea) \times 10) \Big/ (9ml(tea) + 1ml(ACN)) \right) \times \left(0.2ml(tea/ACN) \Big/ (0.2ml(tea/ACN) + 9.8ml(wate \right.$$

=0.144mg/ml

The total polyphenol content, expressed as a percentage by mass on a sample dry matter basis is given by:

$$TP = \left[OD_{sample} + OD_{Intercept} \Big/ Slope_{std} \times M_{conc} \right] \times 100\%$$

Equation 7.9

$$TP = \left[[0.4422 + 0.0121] \Big/ 0.0105 \times 0.144 \right] \times 100 = 30.0\%$$

7.4 CIE LAB derivation

CIELAB values L* a* b* are derived from spectral data (transmission/reflectance) from a spectrophotometer or colour meter by an algorithm.

The calculation is carried out in two stages – L*a*b* are derived from the Tristimulus values X, Y and Z, which have to be calculated from the spectral data.

The C.I.E (Commission Internationale de l'Eclairage) is the international body that oversees and advises on colour measurement and sets the definitions of L*a*b*.

Calculation of Tristimulus X, Y, Z values is done by reflectance of light from the sample or transmission of light through the standard. The human eye contains three types of colour sensor (cells known as "cones") that selectively detect red, green and blue light, and from this information the brain creates a "colour". It is possible to match the colour of any given wavelength of light in a spectrum (Figure 7.9) by mixing different amounts of the three primary colours (red, green and blue), so that the colours appear identical to the human eye. (http://en.wikipedia.org/wiki/CIE_1931_color_space)

Figure 7.9 shows the relative amounts of the primary colours (spectral tristimulus value or colour matching response value) needed to produce an exact colour match by eye at each wavelength.

Red, green and blue are represented by the curves x, y and z respectively.

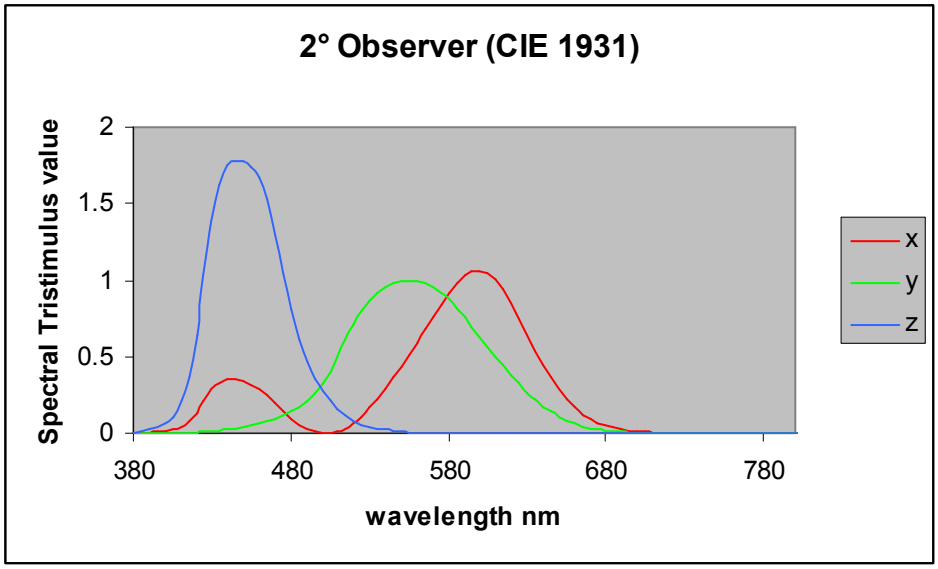

Figure 7.9: 2° Observer spectral tristimulus values (X, Y, Z) vs wavelength. (After http://en.wikipedia.org/wiki/CIE_1931_color_space)

The CIE has used these curves so that spectral data (a plot of strength of reflected or transmitted light from an object at a range of different wavelengths) can be converted into the tristimulus values X Y and Z.

This is done by multiplying the amount of light at each wavelength by the colour matching response value x at that wavelength, and then summing the values to give the tristimulus value X.

The operation is then repeated using the colour matching response values y and z to give the Tristimulus Y and Z values.

X, Y and Z values are fairly hard to understand, so the CIE developed a much easier system to use known as CIELAB.

CIELAB has three parameters, L* a* and b*

L* represents lightness – roughly it goes from 100 (white) to 0 (black)

a* represents colour on a red/green axis – positive a* is red and negative a* is green

b* represents colour on a yellow/blue axis – positive b* is yellow and negative b* is blue where;

$$L^* = 116(Y/Yn)^{1/3}-16$$ **Equation 7.10**

$$a^* = 500[(X/Xn)^{1/3} - (Y/Yn)^{1/3}]$$ **Equation 7.11**

$$b^* = 200[(Y/Yn)^{1/3}-(Z/Zn)^{1/3}]$$ **Equation 7.12**

These terms are limited to X/Xn; Y/Yn; Z/Zn > 0.01

Where X Y and Z are tristimulus values and Xn, Yn, and Zn are tristimulus values for perfect diffuser for illuminant used.

The chroma (C*) of a colour can be worked out using the formula

$$C^* = (a^{*2} + b^{*2})^{1/2}$$ **Equation 7.13**

The higher the value of C*, the more intense the colour is. Values of C* close to 0 indicate a relatively colourless (grey) sample.

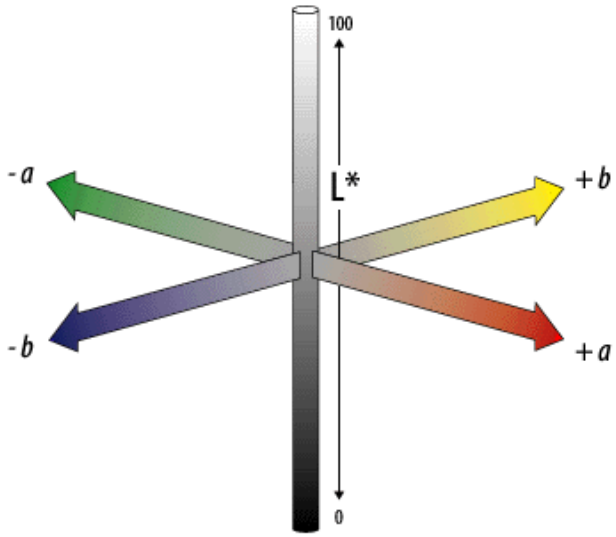

Figure 7.10: CIELAB colour lightness scale represented visually (After http://dba.med.sc.edu/price/irf/Adobe_tg/models/cielab.html).